UC-4
LBL-23992
c.1

Lawrence Berkeley Laboratory

UNIVERSITY OF CALIFORNIA

Materials & Chemical Sciences Division

NOV 6 1987
DOCUMENTS SECTION

Synthesis and Structural Characterization of Transition Metal Oxo (Hydroxo) Siloxides; Reactions of Transition Metal Dialkylamides with Diphenylsilanediol

N.M. Rutherford
(Ph.D. Thesis)

September 1987

For Reference
Not to be taken from this room

LBL-23992
c.1

Prepared for the U.S. Department of Energy under Contract DE-AC03-76SF00098

DISCLAIMER

This document was prepared as an account of work sponsored by the United States Government. While this document is believed to contain correct information, neither the United States Government nor any agency thereof, nor the Regents of the University of California, nor any of their employees, makes any warranty, express or implied, or assumes any legal responsibility for the accuracy, completeness, or usefulness of any information, apparatus, product, or process disclosed, or represents that its use would not infringe privately owned rights. Reference herein to any specific commercial product, process, or service by its trade name, trademark, manufacturer, or otherwise, does not necessarily constitute or imply its endorsement, recommendation, or favoring by the United States Government or any agency thereof, or the Regents of the University of California. The views and opinions of authors expressed herein do not necessarily state or reflect those of the United States Government or any agency thereof or the Regents of the University of California.

LBL-23992

Synthesis and Structural Characterization of Transition Metal Oxo (Hydroxo) Siloxides; Reactions of Transition Metal Dialkylamides with Diphenylsilanediol

Nicole Marie Rutherford

Ph.D. Thesis

Lawrence Berkeley Laboratory
University of California
Berkeley, California 94720

September 1987

This work was supported by the Director, Office of Energy Research, Office of Basic Energy Sciences, Chemical Sciences Division of the U.S. Department of Energy under Contract Number DE-AC03-76SF00098.

Synthesis and Structural Characterization of Transition Metal Oxo (Hydroxo) Siloxides; Reactions of Transition Metal Dialkylamides with Diphenylsilanediol

Nicole Marie Rutherford

Abstract

A systematic approach to the synthesis of molecular metallosiloxanes, compounds heretofore rarely obtainable, was investigated via the reaction of transition metal dialkylamides with diphenylsilanediol.

Reaction of $Ti(NEt_2)_4$ with $Ph_2Si(OH)_2$ yielded the molecular complexes $[H_2NEt_2]_2[Ti_4O_2(OH)_2(OSiPh_2O)_6]$ and $[H_2NEt_2]_2[Ti_4O_2(OH)_2(OSiPh_2O)_5((OSiPh_2)_2O)]$. Both complexes were tetranuclear, with structures containing a Ti_4O_4 cubane bridged diagonally across each face by a silanediolate ligand. A homocondensed form of diphenylsilanediol, $(OSiPh_2)_2O^{2-}$, which contained an Si-O-Si linkage, occurred as one of the six bridging ligands in the latter complex. Titanium dialkylamides derived from other amines similar in basicity to $HNEt_2$, such as $HNMe_2$ and $HNPr^i_2$, also reacted to give polynuclear products, while titanium amides derived from non-basic amines such as $HNPh_2$ unanimously reacted to give a mononuclear complex with homocondensed chelate ligands, $Ti((OSiPh_2)_4O)_2$.

Reaction of the vanadium(V) dialkylamide, $OV(NEt_2)_3$ with $Ph_2Si(OH)_2$ afforded $[H_2NEt_2]_2[V_2O_4(OSiPh_2O)_2]$ and $[H_2NEt_2][VO_2(OSiPh_2)_3O)]$, a bridged dimer and a chelated monomer, respectively. Both compounds have siloxane-type structures in which silicon has been replaced by tetrahedrally coordinated vanadium(V). Reaction of the vanadium(IV) dialkylamide $V(NEt_2)_4$ gave $[Li(THF)_2]_2[VO((OSiPh_2)_2O)_2]$, a vanadium centered spiro structure created by the two chelating six-membered siloxane rings bonded to vanadium.

Infrared studies on the new metallosiloxanes showed that a comparison of the relative intensity of the M-O-Si band with that of an internal reference band allowed differentiation between mononuclear and polynuclear structures. In addition, the appearance of an Si-O-Si infrared band revealed the presence of the homocondensed form of the ligand, while the position of the was band indicative of the extent of ligand polymerization.

The solution molar conductivities of all of the complexes in non-coordinating solvents were anomalously low. Treatment of the complexes with acid removed the dialkylammonium cation to yield the neutral complexes; these were subsequently converted to tetraalkylammonium derivatives which showed the expected conductivities for 2:1 electrolytes.

Silicon-29 MASNMR spectra (see reference 1, Chapter 3)

of the metallosiloxanes revealed a correlation between the average M-O-Si (M = Si, Ti, V) bond angle and the chemical shift, where the bond angle varied with cation hydrogen bonding and with chelate ring size. A marked difference in chemical shift was also observed between silicon atoms in the bidentate bridged- versus the homocondensed chelate-complexes.

Reaction of $Ph_2Si(OH)_2$ with dialkylamides of Cr, Mo, Zr, Si and Al, and with the trimethylsilylamides of Fe and Co gave polymeric products containing M-O-Si structural units.

COMPLETION

1, completion; accomplishment, achievement, fulfillment, realization, fruition; execution, performance; dispatch; consummation, culmination; finish, close, END; terminus (see arrival); issue, outcome (see effect); final, crowning, or finishing touch, epilogue, coup de grâce; fait accompli; feat; missing link, makeweight; PERFECTION; elaboration; exhaustion. See PRODUCTION, SUCCESS.

Acknowledgements

Sincere thanks go to Dick Andersen for his unfailing interest in this project, for his constant inspiration and encouragement, for instilling in all of his students a love of inorganic chemistry, and finally for his sense of humor. Thanks also go to Angy Stacy for her incredible enthusiasm and for opening my eyes to a new area of chemistry.

There are many people who have helped to make my graduate career a challenging one, but special thanks go to Fred Hollander for his guidance through the sometimes bewildering world of crystallography and for his friendship.

The members of the Andersen and Stacy research groups also deserve acknowledgement for providing stimulating discussion and for the enormous amount of help they have given me over the past four years. In particular I wish to thank Joanne Stewart, Carol Burns, Dave Berg, Steve Stults, and Hanno zur Loye for their support and friendship. I also wish to thank Yumi Nakagawa, John Bushweller, Chuck Marlowe Tom Chung and especially Jim Lincoln for making my stay at Berkeley a very memorable and rewarding experience.

Finally, I wish to thank Chris Holmes for his love and companionship, for sharing his knowledge of chemistry with me, and for tirelessly editing this thesis.

Table of Contents

Synthesis and Structural Characterization of Transition Metal Oxo (Hydroxo) Siloxides; Reactions of Transition Metal Dialkylamides with Diphenylsilanediol

Introduction 1

Chapter 1.

Reaction of Titanium Amides With $Ph_2Si(OH)_2$ 13

X-ray Studies 16

Infrared Spectra. 33

Reactivity. 40

Conductivity Studies. 46

Reaction of $Ph_2Si(OH)_2$ with Other Titanium Amides 49

References. 54

Chapter 2.

Reaction of Vanadium Amides with $Ph_2Si(OH)_2$ 56

Vanadium(V) 56

X-ray Studies 60

Infrared Spectra. 75

Reactivity of 3-H_2HEt_2. 80

Conductivity Studies. 84

Reaction of $Ph_2Si(OH)_2$ with Other Vanadium(V) Amides. 85

Vanadium(IV). 86

X-ray Studies 89

Infrared Spectrum 96

Visible Spectrum and Magnetic Susceptibility 97

Reactivity of 5 98

Reaction of $Ph_2Si(OH)_2$ with Other Vanadium(IV) amides 100

Reaction of $Ph_2Si(OH)_2$ with Other Transition Metal Amides 101

Reactions with Aluminum and Silicon Dialkylamides 104

References. 107

Chapter 3.

Silicon-29 MASNMR of Some Metallosiloxanes 109

References. 126

Experimental 127

General 127

X-ray Experimental. 159

References. 179

Appendix I.

Tables of Thermal and Positional Parameters. 182

Figures

Chapter 1.

ORTEP of the anionic unit in $[H_2NEt_2]_2$-$[Ti_4(O)_2(OH)_2(OSiPh_2O)_6]\cdot MeCN$, 1-$H_2NEt_2$. 19

Overall view of the anion $[Ti_4(O)_2$-$(OH)_2(OSiPh_2O)_6]^{2-}$, 1-H_2NEt_2 20

Stereoview of the packing of 1-H_2NEt_2 within the unit cell 21

ORTEP of the anionic unit in $[H_2NEt_2]_2$-$[Ti_4(O)_2(OH)_2(OSiPh_2O)_5((OSiPh_2)_2O)]\cdot PhMe\cdot 2H_2O$, 2-$H_2NEt_2$ 28

Overall view of the anion $[Ti_4(O)_2(OH)_2$-$(OSiPh_2O)_5((OSiPh_2)_2O)]$, 2-$H_2NEt_2$. 29

View of the Ti_4O_4 core in 2-H_2NEt_2 30

Infrared Spectra of $(SiPh_2O)_3$ and $(SiPh_2O)_4$. 35

Infrared Spectra of 1-H_2NEt_2 and 1-OH. 38

Infrared Spectra of 2-H_2NEt_2 and $Ti((OSiPh_2)_4O)_2$ . . 39

Reactivity of 1-H_2NEt_2 and 1-OH. 45

Chapter 2

ORTEP of the anionic portion of $[H_2NEt_2]_2$-$[V_2O_4(OSiPh_2O)_2]$, 3-H_2NEt_2 61

Side-view of 3-H_2NEt_2. 62

ORTEP of the anionic portion of $[H_2NEt_2][VO_2$-$((OSiPh_2)_3O)]$, 4-H_2NEt_2. 67

Side-view of $[VO_2((OSiPh_2)_3O]^-$ 68

ORTEP of the asymmetric unit in 4-H_2NEt_2 74

Infrared Spectra of 3-H_2NEt_2 and 4-H_2NEt_2. 76

Infrared Spectrum of 4-H_2NEt_2 (square plates). . . . 79

Reactivity of 3-H_2NEt_2 83

Infrared Spectrum of 5 88

ORTEP of $[Li(THF)_2]_2[VO(OSiPh_2)_2O)_2]$, 5. 91

Stereoview of 5. 92

Side-view of 5 93

Chapter 3

Relationship between the mean T-O-T angle and ^{29}Si chemical shift in zeolites. 110

^{29}Si MASNMR spectrum of $[H_2NEt_2]_2$-$[Ti_4(O)_2(OH)_2(OSiPh_2O)_6]\cdot MeCN$. 113

^{29}Si MASNMR spectrum of $[H_2NEt_2]_2$-$[Ti_4(O)_2(OH)_2(OSiPh_2O)_5(OSiPh_2O)]\cdot PhMe\cdot 2H_2O$. 116

^{29}Si MASNMR spectrum of $Ti((OSiPh_2)_4O)_2$. 117

^{29}Si MASNMR spectrum of $[H_2NEt_2]_2$-$[V_2O_4(OSiPh_2O)_2]$ 121

^{29}Si MASNMR spectrum of $[H_2NEt_2]$-$[VO_2((OSiPh_2)_3O)]$. 122

Plot of ^{29}Si chemical shift as a function of the average Si-O-Si bond angle. 124

Introduction

Carbon is unique among the elements in its exceptional capacity to form homopolymer chains. The variety of possible combinations of carbon atoms leads to the great diversity of structures and properties exhibited by organic polymers.[1] For a time it was thought that heavier congeners of carbon might also form homopolymer chains,[2] hence silicon was perceived as providing a possible basis for a field of chemistry as broad as organic chemistry. It soon became apparent, however, that because silicon accepts and donates electrons much more readily than does carbon, the homopolymers of silicon were too sensitive to atmospheric oxygen and moisture to enjoy extensive practical use.[3] While polymer chains composed exclusively of silicon have proven to be unstable, polymers in which organic groups frame a primary chain composed of alternate atoms of silicon and oxygen have been shown to have good thermal stability and elasticity.[4] The polyorganosiloxanes, or silicones, comprise an immense group of high molecular weight compounds, both linear and branched, which are important from both scientific and technological points of view.[5]

The development of heterosiloxanes emerged as a way of altering or tailoring the properties of the polymers for specific uses.[6,7] Unlike the polyorganosiloxanes, compounds with the heterosiloxane grouping Si-O-X are found abundantly

in nature and most exhibit very high chemical and thermal stability.[8] Numerous attempts were made to prepare new inorganic polymers, or modified silicones, from the organo-heterosiloxanes of Ge, Sn, Pb, Al, Ga, As, and Sb.[9] The practical success, however, was relatively limited due to the instability of the O-X bond relative to the O-Si bond; for example, most of the heterosiloxanes were sensitive to both oxidation and hydrolysis.

Investigations into heterosiloxanes of the transition metals also arose in response to the technological demands on inorganic polymers.[6,7] The possibility existed that the transition metals would posses the requisite electronic structure to form strong M-O bonds. Transition metal heterosiloxanes, or metallosiloxanes, can be prepared by the use of silanols, metal silanolates, acyloxysilanes, di-siloxanes or alkoxysilanes, where the transition metal may be introduced as a halide, an organometallic compound, as an alkoxy compound or as an oxide.[10] In general two types of products have resulted from these synthetic endeavors: simple metal trialkylsiloxides, and polymeric metallo-siloxanes. The polymeric compounds are summarized in Table I; unfortunately, none have been structurally characterized.

Hydrolysis of the metal trialkylsilyloxides gives compounds $[MO_x(OSiR_3)_{(y-2x)}]_n$ known as metal oxide trialkyl-silyloxides or polyorganosiloxanometalloxanes.[11] These compounds are regarded as intermediate between oligomeric

Table I. Transition Metal Heterosiloxane Polymers

M donor	Si-O donor	properties	product	Ref.
$TiCl_4$	$K(OSiPhMe)_3OK$		$(SiRR'O)_xOTi(OSiRR')_xOTiO(SiRR')_x$	(12)
$Zr(OPr^i)_4$	Ph_2SiCl_2		$[(SiPh_2O)_m\text{-}Zr(OPr^i)_2\text{-}O]_n$	(13)
VCl_4	$Ph_2Si(OH)_2$	sticky polymer	uncharacterized	(14)
$OV(OPr^i)_3$	$Ph_2Si(OH)_2$	insol. polymer	$[(VO)_2(O_2SiPh_2)_3]_n$	(15)
CrO_3	$(Me_2SiO)_3$		$[OSiMe_2]\{CrO_4SiMe_2\}_a[OSiMe_2\}_b$ a,b = 1, 2, 3,...	(10)
$FeCl_3$	$NaOSiPh_2OH$		$[Fe(OSiR_3)(OSiR_2)_2O\}$	(16)
$Co(OAc)_2$	$Me_2Si(OEt)_2$	dark blue powder	$EtO[SiMe_2OCoO]_nAc$	(17)
$CoBr_2$	$R_2Si(ONa)_2$	brittle blue resin	$[SiR_2OCoO\}_n$	(17)
$CoBr_2$	$PhSi(ONa)_3$	insol., infusable	uncharacterized	(17)
$NiCl_2$	$RSi(OH)_2ONa/AlCl_3$	green polymer	uncharacterized	(18)
$CuCl_2$	$Ph_2Si(ONa)_2$	unstable	$[Ph_2SiO]_x[CuO]_y$	(19)

metal trialkylsiloxides and the mineral silicate macromolecules. Bradley and Prevedorou-Demas[20] carried out the hydrolysis of several different metal trialkylsilyloxides in dioxane solution and characterized the resulting metal oxide trialkylsilyloxides by elemental analysis and cryoscopic molecular weight determination in cyclohexane. They demonstrated that an increase in hydrolysis (x) was accompanied by an increase in the number average degree of polymerization (n). Moreover, the variation of n with x showed a characteristic pattern which was interpreted in terms of repeating structural units. Presumably, the polymers were not suitable for X-ray crystallographic study, however a molecular structure was proposed for an octamer described as the lowest polymer formed by hydrolysis of $Ti(OSiMe_3)_4$.[21] An illustration of the proposed octamer is shown in Figure 1.

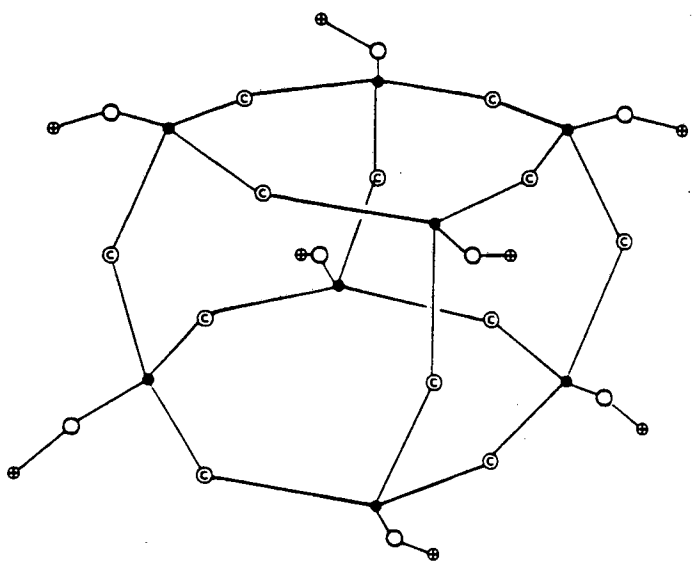

Figure 1. $Ti_8O_{12}(OSiMe_3)_8$ • = Ti; © = oxygen in TiOTi; ⊕ = $SiMe_3$; O = oxygen in TiOSi.

Progress in understanding the properties of heterosiloxanes is expected only from a better understanding of structure and bonding. Since investigations of polymers with irregular compositions only rarely give detailed information, it is necessary to prepare low molecular weight compounds of definite composition; these should contain all the structural units and building blocks which would be involved in the structures of larger molecules and polymers. To this end, we have been interested in the development of a systematic method of preparing molecular metallosiloxane complexes which can be characterized by X-ray crystallography.

Because there are so few complex molecular metallosiloxanes known, we felt it would be a worthwhile effort to approach the synthesis of molecular metallosiloxanes from the standpoint of coordination chemistry. In order to apply such an approach, a simple organosilicon compound that would constitute a "good" ligand needed to be chosen. The silanol Ph_3SiOH forms trialkylsiloxides in a manner similar to the formation of alkoxides from alcohols,[22] but for more complex structures, a bifunctional ligand is necessary. Diphenylsilanediol has several advantageous properties which make it an excellent candidate: It can easily be obtained in pure form as a crystalline solid,[23] and it is more stable than corresponding dialkyl analogues which undergo facile homocondensation by α-hydrogen abstraction.[3] In addition,

there are several possible ways in which $Ph_2Si(OH)_2$ could coordinate to a transition metal, as shown in Figure 2.

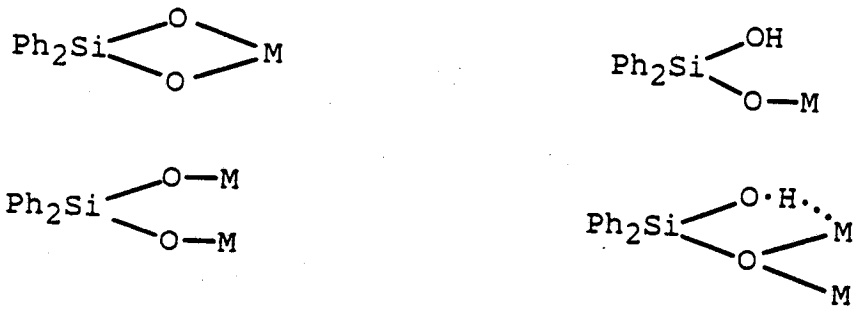

Figure 2. Possible bonding modes for $Ph_2SiO_2^{2-}$.

It is tempting to draw upon the wealth of structural information on organometallic compounds in order to predict the types of compounds which might be formed with $Ph_2Si(OH)_2$. Unfortunately, the formally analogous gem-diols, $R_2C(OH)_2$, are unstable relative to ketones and hence cannot form complexes with transition metals. Since the bonding modes proposed for $Ph_2Si(OH)_2$ are similar to those found for the carboxylate ion RCO_2^-, perhaps carboxylate complexes can be employed as structural models. Polymeric complexes containing carboxylate bridges are known, as are dinuclear, trinuclear and tetranuclear molecular compounds.[24] The wide variety of complexes containing carboxylate bridging groups can be attributed to the versatility of the O-C-O bond angle. Table II gives the O-C-O angles and other relevant structural parameters for binuclear, tri-

nuclear and tetranuclear complexes whose structures have been determined by X-ray crystallography. The variance observed in the O-C-O bond angles allows the carboxylate

Table II. Structural Parameters of Some Polynuclear Carboxylate Bridged Compounds.

Compound	C-O (Å)	O-C-O (°)	M-O-C (°)	M--M (Å)	Ref.
$Cu_2(H_2O)_2(RCO_2)_4$	1.261(2)	124.4(1)	125.2(1)	2.614(2)	(25)
$Cu_2(Quin)_2(RCO_2)4$	1.24	130	-	2.64	(26)
$Cr_2(H_2O)_2(RCO_2)_4$	1.25(2)	123.1(3)	120.4(4)	2.362(1)	(27)
$Ru_3(Ph_3P)_3O(RCO_2)_6$	1.26(3)	126(2)	126(1)	3.329(3)	(28)
$Co_4(RCO_2)_2(MeO)_4$-$(C_5H_7O_2)_4$	1.20(2) 1.31(2)	130(2)	124(1)	2.82(1) 3.02(2)	(29)

ligands to bridge metal-metal distances from 2.11 Å in $Mo_2(MeCO_2)_4$,[30] to 3.02 Å in $Co_4(RCO_2)_2(MeO)_4(C_5H_7O_2)_4$.[29] It is doubtful that $Ph_2Si(OH)_2$ will exhibit such flexibility at the O-Si-O angle. Based on the structures of the silicates[31] and simple siloxanes,[32] one may assume that the silicon in $Ph_2SiO_2^{2-}$ is rigidly tetrahedral. Thus far the only report of a molecular compound where the $Ph_2SiO_2^{2-}$ anion acts as a ligand is one in which titanium is chelated in a tetrahedral fashion.[33] The proposed structure of the compound has not, however, been confirmed by an X-ray crystallographic determination.

Unlike the carboxylate group, $Ph_2Si(OH)_2$ has the

ability to undergo homocondensation in acidic or basic media. Figure 3 illustrates two of the possible bonding modes for a siloxanediolate derived from $Ph_2Si(OH)_2$.

Figure 3. Two bonding modes proposed for a homocondensed derivative of the $Ph_2SiO_2^{2-}$ anion.

The greater number of atoms contained in the siloxanediolate ligand may give it more flexibility than $Ph_2Si(OH)_2$ and allow it to bridge greater distances. Apparently, the only structurally characterized coordination compound which contains the diphenylsiloxanediolate ligand is the chelated, spiro titanium compound $Ti((OSiPh_2)_4O)_2$.[34] As expected, the O-Si-O bond angles in the nine-membered siloxane chelate ring fall within a narrow range of values from 107.3(2) to 110.6(2)°; the Si-O-Si bond angles, however, range in value from 143.8 to 172.5°.[35] Thus, although $Ph_2Si(OH)_2$ may be limited by the tetrahedral angle at Si, the condensed siloxane derivative shows even greater flexibility at the Si-O-Si angles than does RCO_2^- at the O-C-O angle.

The carboxylate ion can at least provide a basis for

predicting the types of bonding which may be found in complexes containing $Ph_2SiO_2^{2-}$, although as was found for the carbon and silicon based homopolymers, strict analogies are rarely validated. Quite often the structures and the stabilities of the inorganic products are affected by additional factors which are not accounted for by a carbon-based model.

Our approach to the synthesis of molecular metallosiloxanes of the first row transition metals, and the main group metals Si and Al with the diolate ligand $Ph_2Si(OH)_2$, is the topic of this thesis.

References

(1) For a general reference on the uses of carbon polymers in industry, see Jones, M. B. E., In "Basic Organic Chemistry", Part 5; Tedder, J. M.; Nechvatal, A.; Jubb, A. H. Eds., John Wiley & Sons: London, 1975; Chapter 8, p 197.

(2) Kipping, F.; Murray, A. J. Chem. Soc. **1929**, 1180; Kipping, F.; Sands, J. J. Chem. Soc. **1921**, 830; **1923**, 2590.

(3) MacDiarmid, A. G. In " New Pathways in Inorganic Chemistry"; Ebsworth, E. A. V.; Maddock, A. G.; Sharpe, A. G., Eds.; University of Cambridge Press: London, 1968; Chapter 8.

(4) Burkhard, C. A.; Rochow, E. G.; Booth, H. S.; Hartt, J. Chem. Rev. **1947**, 41, 97.

(5) Eaborn, C. "Organosilicon Chemistry"; Academic Press: New York, 1960.

(6) Stone, F. G. A.; Graham, W. A. G. "Inorganic Polymers"; Academic Press: New York, 1962.

(7) Lappert, M. F.; Leigh, G. J. "Development in Inorganic Polymer Chemistry"; Elsevier: Amsterdam, 1962.

(8) Wells, A. G. "Structural Inorganic Chemistry", 4th ed.; Oxford University Press: London, 1975; Chapter XXIII.

(9) Schmidbaur, H. Angew. Chem. Int. Ed. Eng. **1965**, 4, 201.

(10) Schindler, F.; Schmidbaur, H. Angew. Chem Int. Ed. Eng. **1967**, 6, 683.

(11) Bradley, D. C. Coord. Chem. Rev. **1967**, 2, 299.

(12) Adrianov, K. A.; Sipyagina, M. A.; Lomonosov M. V. Br. Patent 1 329 180, 1973; Chem. Abstr. **1974**, 80, 37626.

(13) Avilova, T. P.; Bykov, B. T.; Flushchenko, B. Yu.; Marinin, B. P. Vysokomolekul. Soedineniya **1966**, 8, 11; Chem. Abstr. **1966**, 64, 14206.

(14) Chamberlain, M. M.; Kern, G.; Jabs, G. A.; Germanas, K.; Green, A.; Brain, D.; Wayland, B. U.S. Dept. Com., Office Tech. Serv., PB Rept. 152,086, 1960; Chem. Abstr. **1963**, 58, 2508.

(15) Nakaido, Y.; Akikusa, Y.; Otani, S. Kogyo Kagaku Zasshi **1967**, 70, 221.

(16) Sutton, R. A. Br. Patent 978 666, 1964; Chem. Abstr. **1965**, 62, 6650.

(17) Schneider, C.; Berg, G. Makromol. Chem. **1962**, 54, 171.

(18) Andrianov, K. A.; Zhdanov, A. A. Inzvest. Akad. Nauk SSSR, Otdel. Chim. Nauk **1959**, 1590; Chem. Abstr. **1960**, 54, 8687.

(19) Hornbaker, E. D.; Conrad, F. J. Org. Chem. **1959**, 24, 1858.

(20) Bradley, D. C.; Prevedorou-Demas, C. J. Chem. Soc. (London) **1964**, 1580.

(21) Bradley, D. C.; Prevedorou-Demas, C. Can. J. Chem. **1963**, 41, 629.

(22) Bradley, D. C.; Thomas, I. M. J. Chem. Soc. (London) **1959**, 3404.

(23) Diphenylsilanediol is available from Petrarch Systems Inc.

(24) Catterick, J.; Thornton, P. In "Advances in Inorganic Chemistry and Radiochemistry"; Emeleus, H. J., Sharpe, A. G., Eds., Academic Press: New York, 1977; Vol. 20, p 291.

(25) Brown, G. M.; Chidambaram, R. Acta Cryst. Sect. **1973**, B29, 2393.

(26) Tarkhova, T. N.; Ablov, A. V. Kristallografiya **1968**, 13, 611; Chem. Abstr. **1968**, 69, 91018.

(27) Cotton, F. A.; de Boer, B. G.; La Prade, M. D.; Pipal, J. R.; Ucko, D. A. Acta Cryst. Sect. **1971**, B27, 1664.

(28) Cotton, F. A.; Norman, J. G. Inorg. Chim. Acta. **1972**, 6, 411.

(29) Bertrand, J. A.; Hightower, T. C. Inorg. Chem. **1973**, 12, 206.

(30) Lawton, D.; Mason, R. J. Am. Chem. Soc. **1965**, 87, 921.

(31) Baur, W. H.; Kahn, A. A. Acta Cryst. **1971**, B27, 2133.

(32) Braga, D.; Zanotti, G. Acta Cryst., **1980**, B36, 950.

(33) Unny, I. R.; Gopinathan, S.; Gopinathan, C. Ind. J. Chem. **1980**, 19A, 598.

(34) Zeitler, V. A.; Brown, C. A. J. Chem. Soc. **1957**, 79, 4618.

(35) Hursthouse, M. B.; Hossain, M. A. Polyhedron, **1984**, 3, 95.

Chapter 1

Reaction of Titanium Amides with $Ph_2Si(OH)_2$

Following the success achieved with silicone-based polymers, titanium heterosiloxanes were extensively studied because of the high thermal stability of the compounds.[1] Although many of the metallosiloxanes are intractable polymers, the large majority of tractable compounds are derivatives of the monodentate triorganosiloxy ligands, $-OSiR_3$; exceptions include the two spirobicyclotitanium species, $Ti((OSiPh_2)_4O)_2$ and $Ti((OSiPh_2)_2O)_2$. The latter compound was synthesized by Adrianov and coworkers[2] in 1976 by a method analogous to the synthesis of many spirobicyclosiloxanes. Thus, reaction of tetraphenyl disiloxane-1,3-diol with $TiCl_4$ in the presence of pyridine produces $Ti((OSiPh_2)_2O)_2$ (eq. 1). In the absence of pyridine, which acts as an acid acceptor, the main products are cyclosiloxanes. Earlier, Zeitler and Brown[3] had reported the synthesis of $Ti((OSiPh_2)_4O)_2$, prepared by treating diphenylsilanediol with $Ti(OBu^t)_4$ (eq. 2).

$$TiCl_4 + 2\ HOSiPh_2OSiPh_2OH \xrightarrow{4\ py} Ti((OSiPh_2)_2O)_2 + 4\ pyHCl \quad (1)$$

$$Ti(OBu^t)_4 + 2\ Ph_2Si(OH)_2 \longrightarrow Ti((OSiPh_2)_4O)_2 + 4\ {}^tBuOH \quad (2)$$

The synthetic method used by Zeitler is useful because,

unlike the preparations of spirosiloxanes, it does not directly involve the use of metal halides, and hence there are no acidic side products. The synthesis of $Ti((OSiPh_2)_4O)_2$ is similar to the preparation of simple metal trialkylsiloxides, which are often made by exchange reactions between metal alkoxides and silanols (eq. 3).[4]

$$M(OR)_n + x\ R_3SiOH \longrightarrow M(OR)_{n-x}(OSiR_3)_x + x\ ROH \quad (3)$$

A similiar strategy which has been used successfully for the synthesis of metal alkoxides, but which has not been commonly employed to prepare metal siloxides, is ligand exchange with metal dialkylamides (eq. 4).[5] This method has the advantage that when the metal amide is readily available, the generated dialkylamine is volatile and can easily be removed from the reaction mixture.

$$M(NR_2)_x + x\ ROH \longrightarrow M(OR)_x + HNR_2 \quad (4)$$

For the synthesis of new heterosiloxane complexes containing transition metals, it was of interest to use the metal dialkylamide ligand exchange method. Thus, reaction of $Ti(NEt_2)_4$ with 3 molar equivalents of $Ph_2Si(OH)_2$ afforded a mixture of four products. The two principal products, 1 and 2, contained titanium, whereas the two minor products

were shown to be the cyclic siloxanes, $(Ph_2SiO)_3$ and $(Ph_2SiO)_4$. Both **1** and **2** were air-stable and could be separated from one another by their solubility differences. The minor product, **2** (24% yield), was soluble in acetonitrile and hot toluene, while the major product, **1** (54% yield), was soluble only in hot acetonitrile. Both compounds crystallized readily when their solutions were allowed to stand in air at ambient temperature.

Identification of the titanium containing products was achieved by analysis of the infrared spectra. The spectra of the titanium compounds comprised a strong infrared band near 900 cm^{-1} that was absent from the spectra of the siloxanes. Bands in this region have been assigned to the Ti-O-Si stretching mode of titanium trialkylsiloxides.[6] It was intriguing that, except for one additional band at 1053 cm^{-1} in the spectrum of **2**, the infrared spectra of **1** and **2** were virtually identical. Both spectra exhibited a weak O-H band, with the remaining peaks in each characteristic of diphenyl substituted siloxanes: 1588 cm^{-1} (C-C, phenyl); 1426, 1117 cm^{-1} (Si-C); and 744, 716, 702 cm^{-1} (monosubstituted benzene).

The ^1H NMR spectra of **1** and **2** in CD_3CN showed complex multiplets in the aromatic region assignable to the phenyl groups on silicon. In addition, both spectra contained a triplet at δ 0.97 ppm (J = 7) and a quartet at δ 2.78 ppm characteristic of a diethylamino group, and a broad singlet

at δ 2.85 ppm. The methylene quartet was shifted downfield in the spectra of both compounds by approximately 0.3 ppm relative to the parent amide, $Ti(NEt_2)_4$. Because the ^1H NMR of $Ti(NEt_2)_4$ had been measured in benzene, it was not immediately clear whether the change in chemical shift was due to solvent effects or due to a different chemical environment for the methylene protons within the compound. The broad singlet was assigned to hydroxyl protons. For **1**, the ratio of phenyl to hydroxyl to amido protons was 30:1:10, respectively; for **2**, the ratio was 35:1:10.

As diagnostic evidence, the infrared and ^1H NMR data alone were inadequate to characterize **1** and **2** with absolute certainty. One difficulty was that the phenyl:hydroxyl: amido ratios observed in the ^1H NMR spectra could not be reconciled with rational mixed-ligand (amido-siloxy) formulations. Unfortunately, mass spectral data obtained from both chemical ionization (methane) and electron impact ionization (70 eV) methods revealed only low molecular weight ion fragments which were not readily interpretable. Fast atom bombardment mass spectra of **1** and **2**, using a number of different matrices, revealed some higher mass ions; there were, however, very few ion fragments and the pattern was usually obscured by the matrix.

X-ray Studies

Because of the general lack of structural information

on complex titanosiloxanes, and the uncertainty accompanying a fit of our spectroscopic data to a reasonable structure, a single crystal X-ray diffraction study was performed on the major product **1**. The molecular geometry and atom labelling scheme of the anionic portion of **1**-H_2NEt_2* is shown in Figure 1. Figure 2 shows an overall view of the molecule, while Figure 3 shows a stereoview of the packing within the unit cell. Bond distances and angles for both independent molecules are given in Tables I-IV. Unless otherwise specified, the bond distances and angles in the discussion refer to molecule **1**.

The anionic portion of the molecule consists of a tetrahedral array of four titanium atoms intersected by a tetrahedral array of four oxygen atoms to form a Ti_4O_4 cubane. Two of the oxygens at the corners of the cubane are part of triply bridging hydroxyl groups, and two are triply bridging oxo-oxygens. There are six diphenylsiloxy ligands, each bridging two titanium atoms diagonally across each face of the cubane. This appears to be the first structural example of diphenylsilanediol forming a simple bridge in a molecular compound. The complex posseses crystallographic site symmetry C2, and there are two independent halves of the complex molecule and one acetonitrile molecule for each unique crystallographic unit. Two whole molecules of the complex and two molecules of acetonitrile are generated by

---

* **1** will hereafter be referred to as **1**-H_2NEt_2.

the 2-fold axis.

The Ti(1)-O(1), Ti(2)-O(1), and Ti(2)-O(1') bond distances to the triply bridging hydroxyl ligands are 2.140(4), 2.150(3), and 2.159(3) Å, respectively. There appears to be no other structurally characterized examples of titanium bound to a triply bridging hydroxyl group with which to compare these Ti-μ_3O distances, however Ti-O bond lengths to doubly bridging hydroxyls are significantly shorter at values of 1.994(6)-2.023(5) Å in the trinuclear complex $[Ti_3(\mu_3\text{-}O)(\mu_2\text{-}OH)_3(\mu_2\text{-}HCOO)_3(C_5H_5)_3]^+$ [7] and 2.05(1) Å in $[CpTi(OH)]_2C_{10}H_8$.[8] The corresponding Ti(1)-O(2), Ti(1)-O(2'), and Ti(2)-O(2) bond distances, where O(2) and O(2') are the μ_3-oxo oxygens, are 1.968(3), 2.021(3) and 1.965(4) Å, respectively. These values for the Ti-O bond distances are comparable with those found in the trinuclear complex (1.964(5)-1.976(5) Å).[7] The average Ti-O bond distances to the siloxy ligands (1.862(1) Å) are longer than those found in tetrahedrally coordinated $Ti((OSiPh_2)_4O)_2$ (1.777(5)-1.791(5) Å), but shorter than those found in octahedrally coordinated complexes containing diacetylacetonate[9] (1.96-2.07 Å) or dioxalate[10] (2.06, 2.10 Å) ligands. The Si-O bond distances are similar to those found in cyclic siloxanes.[11,12]

The geometry around titanium is distorted octahedral, with O-Ti-O bond angles in the central Ti_4O_4 core spanning the range 74.51(14)-77.20(16)°, and with bond angles around

Figure 1. ORTEP of the anionic unit in $[H_2NEt_2]_2[Ti_4(O)_2(OH)_2(OSiPh_2O)_6]\cdot MeCN$, **1-$H_2NEt_2$**, with phenyl groups removed for clarity.

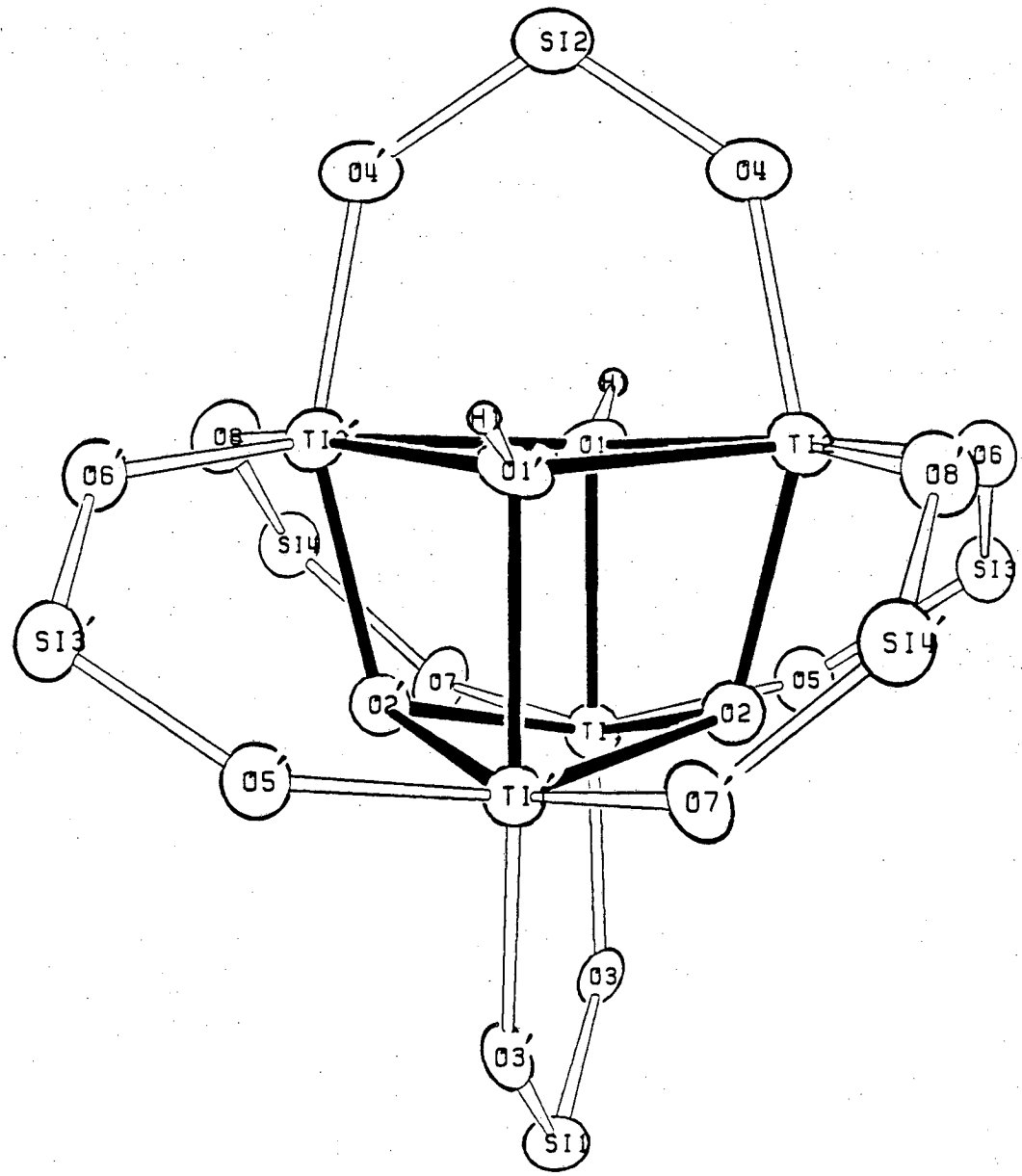

Figure 2. Overall view of the anion $[Ti_4(O)_2(OH)_2(OSiPh_2O)_6]^{2-}$ (thermal ellipsoids at 50% probability level).

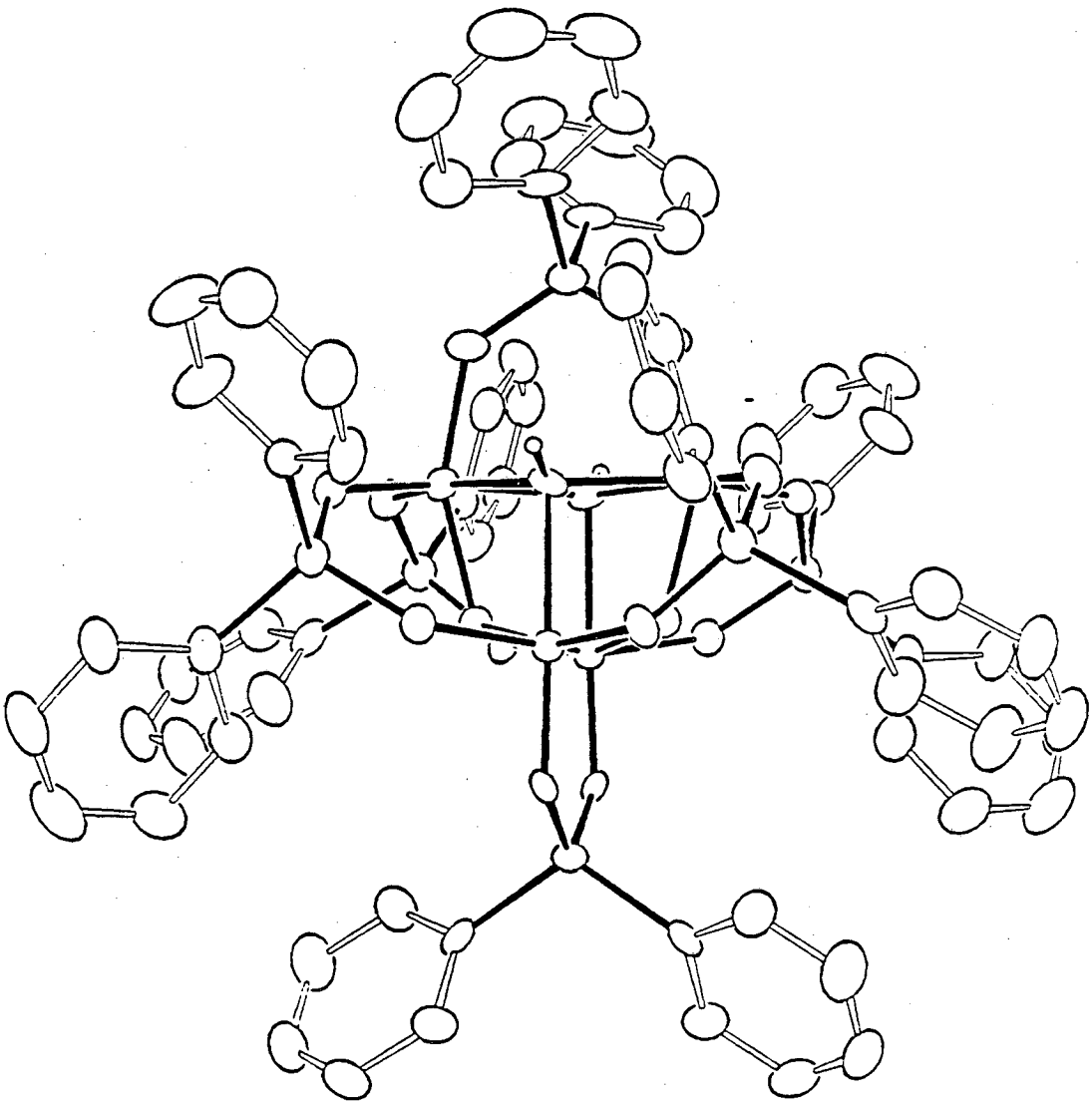

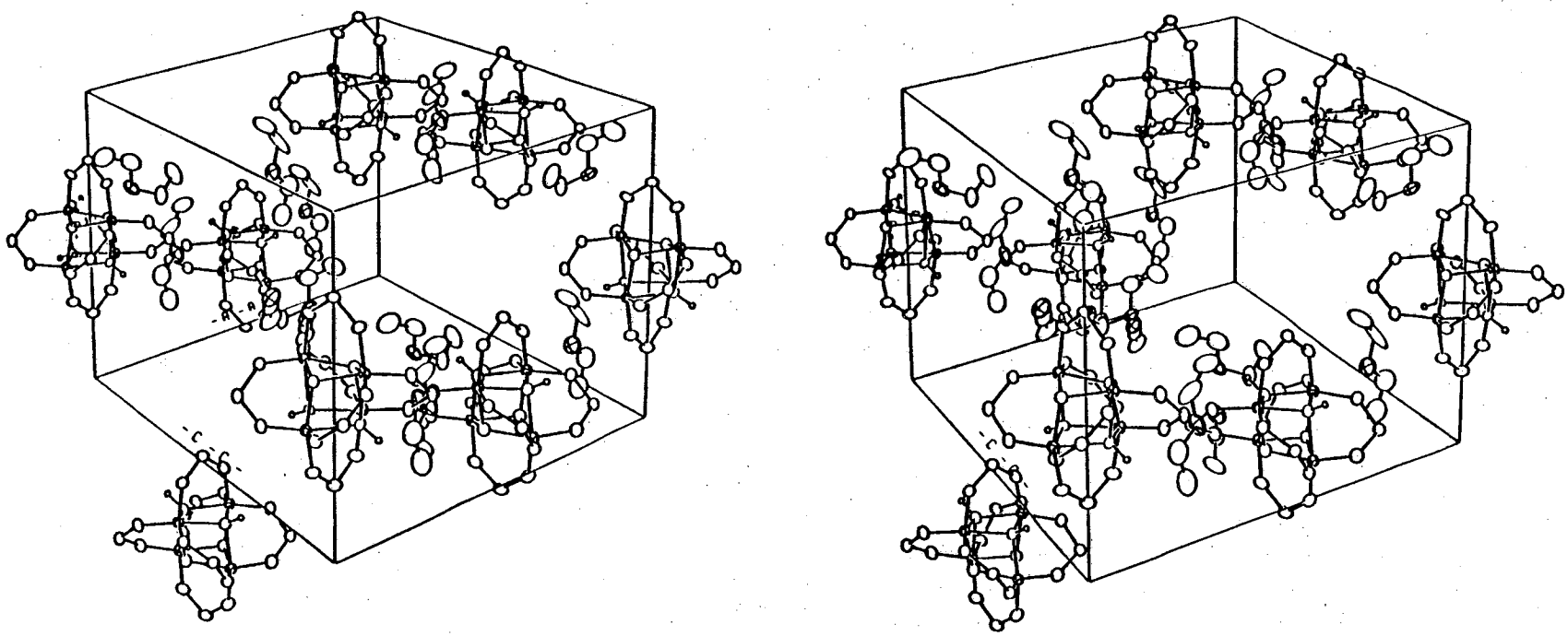

Figure 3. Stereoview of the packing of **1-H_2NEt_2** within the unit cell.

Table I. Selected Bond Lengths (Å) for $[H_2NEt_2]_2[Ti_4(O)_2(OH)_2(OSiPh_2O)_6]\cdot MeCN$

Ti(1)-O(1)	2.140(4)	Ti(2)-O(1)	2.150(3)
-O(2)	1.968(3)	-O(1')	2.159(3)
-O(2')	2.021(3)	-O(2)	1.965(4)
-O(3)	1.875(4)	-O(4)	1.871(4)
-O(5)	1.884(3)	-O(6)	1.836(3)
-O(7)	1.866(3)	-O(8')	1.843(2)
-Ti(1')	3.037(2)*	-Ti(1)	3.195(1)*
-Ti(2')	3.238(1)*	-Ti(2')	3.419(2)*
Si(1)-O(3)	1.637(4)	Si(2)-O(4)	1.622(4)
-C(1)	1.887(6)	-C(7)	1.869(6)
Si(3)-O(5)	1.620(4)	Si(4)-O(7)	1.627(4)
-O(6)	1.647(4)	-O(8')	1.634(4)
-C(13)	1.849(5)	-C(25)	1.875(1)
-C(19)	1.874(5)	-C(31)	1.866(5)
O(1)-H(1)	1.032(3)		

* Non-bonded distances

Table II. Selected Bond Lengths (Å) for $[H_2NEt_2]_2[Ti_4(O)_2(OH)_2(OSiPh_2O)_6]\cdot MeCN$ (Molecule **2**)

Ti(3)-O(9)	2.096(3)	Ti(4)-O(9')	2.106(4)
-O(9')	2.113(4)	-O(10)	2.052(4)
-O(10)	1.995(4)	-O(10')	2.026(4)
-O(11)	1.847(4)	-O(12')	1.833(4)
-O(13)	1.892(3)	-O(14)	1.881(3)
-O(15)	1.877(3)	-O(16')	1.862(3)
-Ti(3')	3.294(2)*	-Ti(3')	3.194(1)*
-Ti(4)	3.230(1)*	-Ti(4')	3.173(2)*
Si(5)-O(11)	1.631(4)	Si(6)-O(12)	1.632(4)
-C(37)	1.871(6)	-C(43)	1.865(6)
Si(7)-O(13)	1.642(4)	Si(8)-O(15)	1.646(4)
-O(14)	1.622(4)	-O(16)	1.623(4)
-C(49)	1.855(5)	-C(61)	1.864(5)
-C(55)	1.870(5)	-C(67)	1.870(5)
O(9)-H(37)	1.082(4)		

* Non-bonded distances

Table III. Selected Bond Angles (deg) for $[H_2NEt_2]_2[Ti_4(O)_2(OH)_2(OSiPh_2O)_6]\cdot MeCN$

O(1)-Ti(1)-O(2)	74.2(1)	O(1)-Ti(2)-O(1')	74.5(1)
-O(2')	75.8(1)	-O(2)	75.7(1)
-O(3)	168.2(1)	-O(4)	84.2(1)
-O(5)	86.0(1)	-O(6)	90.2(1)
-O(7)	89.3(1)	-O(8')	162.4(1)
O(2)-Ti(1)-O(2')	77.2(2)	O(1')-Ti(2)-O(2)	75.6(1)
-O(3)	93.9(1)	-O(4)	85.6(1)
-O(5)	90.2(1)	-O(6)	162.6(1)
-O(7)	161.6(2)	-O(8')	89.0(1)
O(2')-Ti(1)-O(3)	97.9(1)	O(2)-Ti(2)-O(4)	155.4(1)
-O(5)	160.0(2)	-O(6)	92.7(1)
-O(7)	89.8(1)	-O(8')	94.6(2)
O(3)-Ti(1)-O(5)	98.4(2)	O(4)-Ti(2)-O(6)	101.4(2)
-O(7)	100.8(2)	-O(8')	100.9(2)
O(5)-Ti(1)-O(7)	98.3(1)	O(6)-Ti(2)-O(8')	105.1(1)
Ti(1)-O(1)-Ti(2)	97.7(1)	Ti(1)-O(2)-Ti(1')	97.7(1)
-Ti(2')	96.3(1)	-Ti(2)	108.6(2)
-H(1)	109.0(2)	-Ti(2')	108.6(2)
Ti(2)-O(1)-Ti(2')	105.0(1)		
-H(1)	122.3(2)	Ti(1)-O(3)-Si(1)	130.1(2)
Ti(2')-O(1)-H(1)	120.9(2)		
		Ti(2)-O(4)-Si(2)	134.1(2)
Ti(1)-O(5)-Si(3)	133.9(2)		
		Ti(2)-O(6)-Si(3)	130.6(2)
Ti(1)-O(7)-Si(4)	133.6(2)		
		Ti(2)-O(8')-Si(4)	131.2(2)

' Primed atoms are related to the atoms in the asymmetric unit by 2-fold symmetry.

Table IV. Selected Bond Angles (deg) for $[H_2NEt_2]_2[Ti_4(O)_2(OH)_2(OSiPh_2O)_6]\cdot MeCN$ (Molecule **2**)

O(9)-Ti(3)-O(9')	76.2(1)	O(9')-Ti(4)-O(10)	75.6(1)
-O(10)	76.5(1)	-O(10')	75.0(1)
-O(11)	87.7(1)	-O(12')	164.4(2)
-O(13)	163.5(1)	-O(14)	89.6(1)
-O(15)	92.8(1)	-O(16')	87.1(1)
O(9')-Ti(3)-O(10)	76.1(1)	O(10)-Ti(4)-O(10')	75.2(2)
-O(11)	87.0(1)	-O(12')	93.6(2)
-O(13)	90.1(1)	-O(14)	89.3(1)
-O(15)	165.3(2)	-O(16')	160.2(2)
O(10)-Ti(3)-O(11)	159.1(1)	O(10')-Ti(4)-O(12')	91.3(2)
-O(13)	91.5(2)	-O(14)	160.8(2)
-O(15)	92.0(2)	-O(16')	92.3(1)
O(11)-Ti(3)-O(13)	100.9(2)	O(12')-Ti(4)-O(14)	101.1(2)
-O(15)	102.5(2)	-O(16')	102.1(2)
O(13)-Ti(3)-O(15)	98.9(1)	O(14)-Ti(4)-O(16')	99.2(2)
Ti(3)-O(9)-Ti(3')	103.0(1)	Ti(3)-O(10)-Ti(4)	103.0(1)
-Ti(4')	98.9(1)	-Ti(4')	105.2(2)
-H(37)	118.1(2)	Ti(4)-O(10)-Ti(4')	102.2(2)
Ti(3')-O(9)-Ti(4)	99.9(2)		
-H(37)	121.6(2)	Ti(3)-O(11)-Si(5)	133.4(2)
Ti(4')-O(9)-H(37)	111.5(2)		
		Ti(4')-O(12)-Si(6)	132.2(2)
Ti(3)-O(13)-Si(7)	126.2(2)		
		Ti(4)-O(14)-Si(7)	128.3(2)
Ti(3)-O(15)-Si(8)	129.4(2)		
		Ti(4')-O(16)-Si(8)	133.4(2)

'Primed atoms are related to the atoms in the asymmetric unit by 2-fold symmetry.

titanium involving the siloxy ligands close to 100°. The bond angles around oxygen within the cubane core are also near 100°, ranging from 97.74(14)° for Ti(1)-O(1)-Ti(2), to 108.64(17)° for Ti(1)-O(2)-Ti(2').

In cyclic siloxanes the Si-O-Si bond angle is known to be quite flexible with values that vary widely depending on ring size and steric constraints.[12,13] Similarly, a wide variation in Ti-O-Si bond angles are also found. For **1-HNEt$_2$**, the Ti-O-Si bond angles are smaller (130.10(22)-134.06(24)°) than those found in $Ti((OSiPh_2)_4O)_2$ (156.4-173.3°).[14]

Distortion of the Ti_4O_4 cubane is evidenced by the dihedral angle of 74° between the Ti(2),Ti(1),Ti(1') and Ti(2'),Ti(1),Ti(1') planes.

The diethylammonium cation is associated with the anionic titanium tetramer by a hydrogen bond between the amino nitrogen and O(3).

Knowledge of the structure of **1-H$_2$NEt$_2$** provided a basis for assigning the structure of **2**. It was evident from the spectroscopic data that the two compounds were closely related; the primary differences were the appearance of an absorption band at 1053 cm^{-1} in the infrared spectrum of **2**, and a slightly higher ratio of aromatic protons to amino protons in the ^{1}H NMR spectrum. In order to determine exactly which structural features were responsible for the observed differences, a single crystal X-ray diffraction

study was performed on **2**.

An ORTEP diagram of **2-H_2NEt_2*** with the atom labelling scheme is shown in Figure 4, while Figure 5 shows an overall view of the molecule. Selected bond lengths and angles are given in Table V and VI. The structure of the anionic portion of the molecule consists of a Ti_4O_4 core with two of the triply bridging corner positions occupied by hydroxyl groups and two occupied by oxo groups. A drawing of the naked Ti_4O_4 core is shown in Figure 6. There are five bidentate diphenylsiloxy ligands that bridge diagonal titanium atoms on five of the six faces of the distorted Ti_4O_4 cube. The sixth face is bridged by a siloxane linked ligand (Si-O-Si), formed by condensation of two diphenylsilanediol molecules. The molecule posseses a crystallographic 2-fold axis which passes through Si(4) and the siloxane oxygen, O(6), with one half of the complex molecule, one half of a toluene molecule, and one molecule of water per crystallographically independent unit. One whole molecule of the complex, one whole molecule of toluene, and two molecules of water are generated by the 2-fold axis.

There are three types of Ti-O bonds in the molecule, Ti-O(siloxy) (1.854(1) Å (av.)), Ti-O(μ_3-oxo) (1.986(2) Å (av.)), and Ti-O(μ_3-hydroxyl) (2.150(3)-2.214(3) Å). The Ti(2)-O(8) bond distance to the triply bridging hydroxyl

---

* 2 will hereafter be referred to as **2-H_2NEt_2**

Figure 4. ORTEP of the anionic unit in $[H_2NEt_2]_2[Ti_4(O)_2(OH)_2(OSiPh_2O)_5((OSiPh_2)_2O)]\cdot PhMe\cdot 2H_2O$, **2-$H_2NEt_2$**, with phenyl groups removed for clarity.

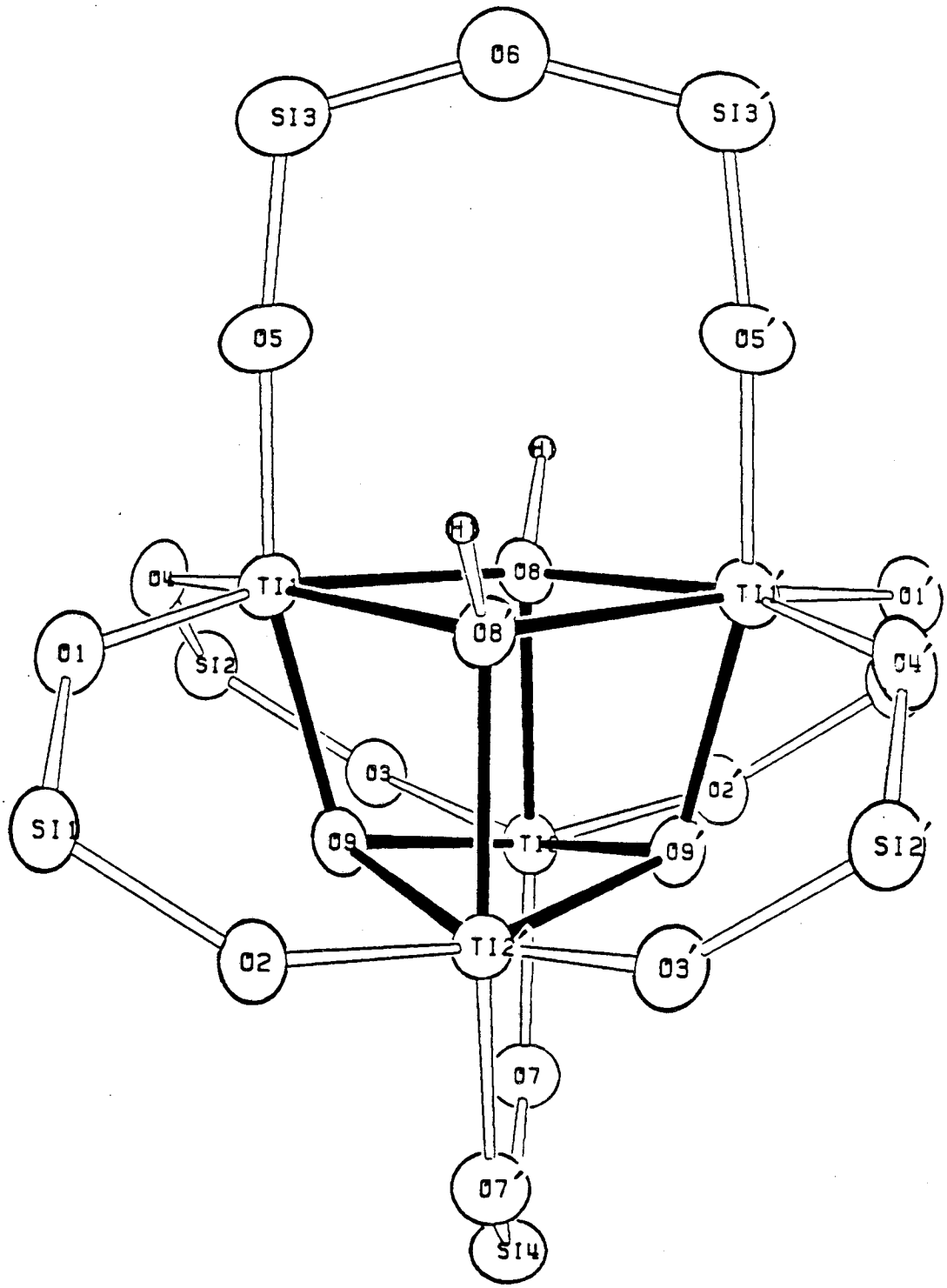

Figure 5. Overall view of the anion $[Ti_4(O)_2(OH)_2(OSiPh_2O)_5((OSiPh_2)_2O)]^{2-}$ (thermal ellipsoids at 50% probability level).

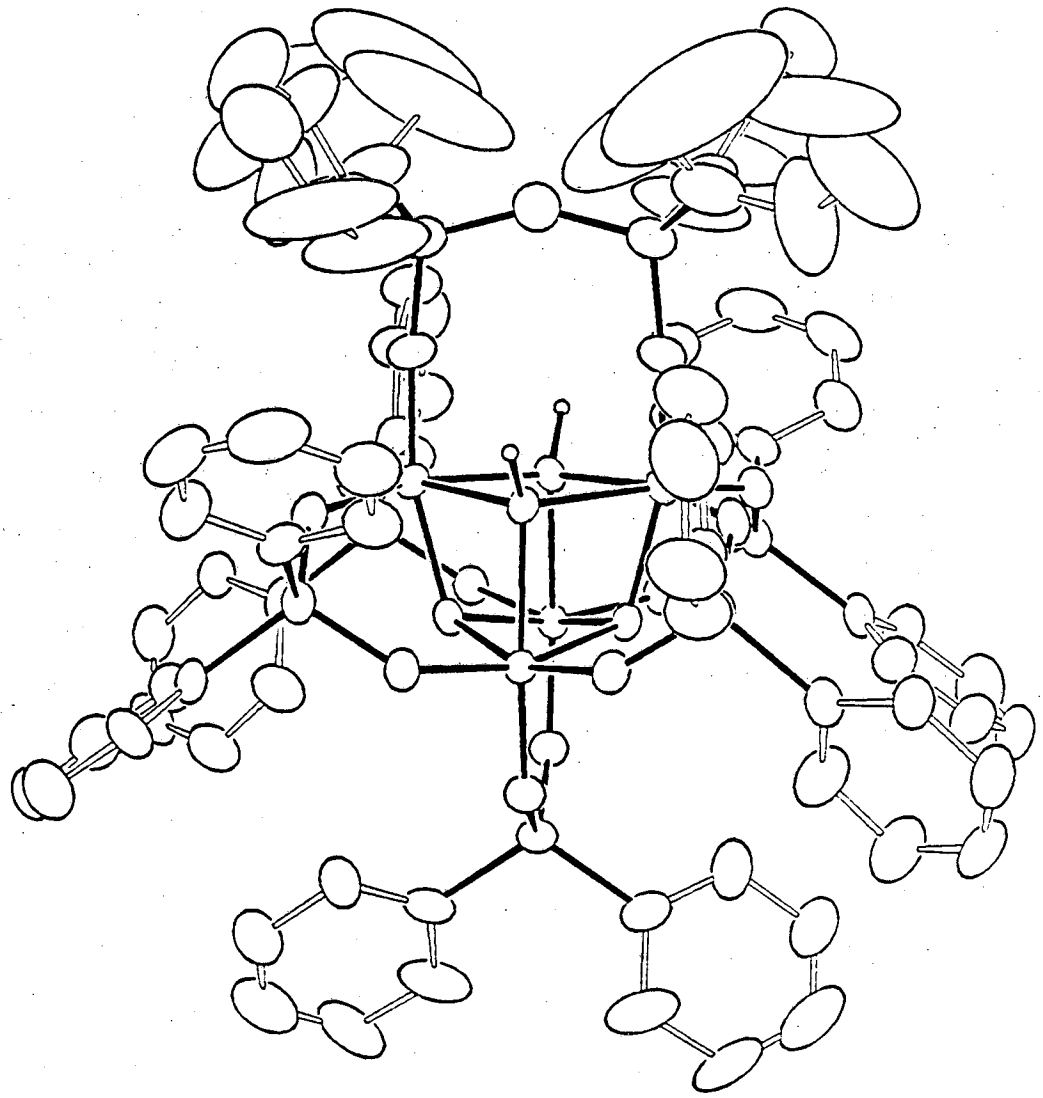

Figure 6. View of the Ti_4O_4 core.

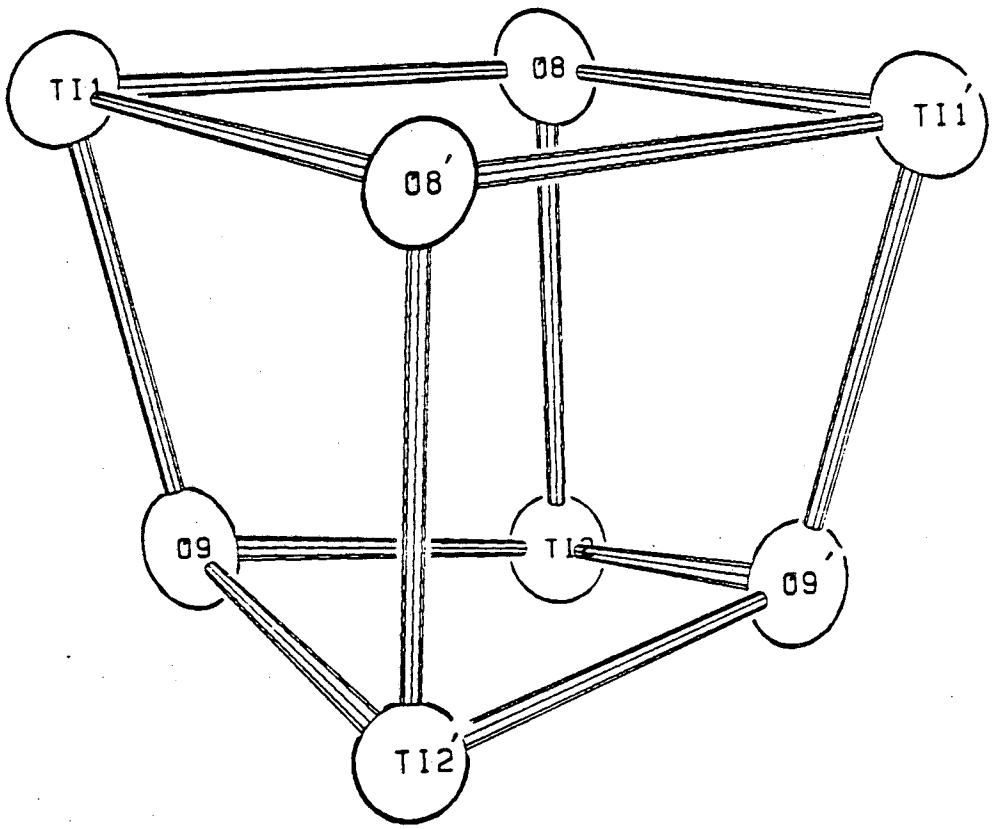

Table V. Selected Bond Lengths (Å) for $[H_2NEt_2]_2[Ti_4(O)_2(OH)_2(OSiPh_2O)_5((OSiPh_2)_2O)]\cdot PhMe\cdot 2H_2O$

Ti(1)-O(1)	1.849(3)	Ti(2)-O(2')	1.861(3)
-O(4)	1.837(3)	-O(3)	1.885(3)
-O(5)	1.845(3)	-O(7)	1.850(3)
-O(8)	2.150(3)	-O(8)	2.214(3)
-O(8')	2.153(3)	-O(9)	1.982(3)
-O(9)	1.995(3)	-O(9')	1.982(3)
-Ti(1')	3.462(2)*	-Ti(1)	3.241(1)*
-Ti(2')	3.234(1)*	-Ti(2')	3.014(2)*
Si(1)-O(1)	1.641(3)	Si(2)-O(3)	1.625(3)
-O(2)	1.632(3)	-O(4)	1.637(3)
-C(1)	1.877(5)	-C(13)	1.868(6)
-C(7)	1.870(7)	-C(19)	1.856(7)
Si(3)-O(5)	1.611(4)	Si(4)-O(7)	1.638(3)
-O(6)	1.614(2)	-C(37)	1.861(5)
-C(25)	1.844(9)		
-C(31)	1.869(3)	O(8)-H(1)	1.130(3)

* Non-bonded distances

Table VI. Selected Bond Angles (deg) for $[H_2NEt_2]_2[Ti_4(O)_2(OH)_2(OSiPh_2O)_5((OSiPh_2)_2O)]\cdot PhMe\cdot 2H_2O$

O(1)-Ti(1)-O(4)	103.2(1)	O(2')-Ti(2)-O(3)	95.4(1)
-O(5)	97.1(1)	-O(7)	100.1(1)
-O(8)	161.8(1)	-O(9)	161.8(1)
-O(8')	91.6(1)	-O(9')	91.3(1)
-O(9)	91.3(1)	O(3)-Ti(2)-O(7)	100.5(1)
O(4)-Ti(1)-O(5)	97.7(1)	-O(9)	91.1(1)
-O(8)	90.7(1)	-O(9')	160.3(1)
-O(8')	161.6(1)	O(7)-Ti(2)-O(9)	95.3(1)
-O(9)	92.2(1)	-O(9')	96.4(1)
O(5)-Ti(1)-O(8)	92.5(1)	O(8)-Ti(2)-O(9)	75.1(1)
-O(8')	91.1(1)	-O(9')	75.3(1)
-O(9)	165.2(1)	O(9)-Ti(2)-O(9)	77.4(1)
O(8)-Ti(1)-O(8')	72.7(1)		
-O(9)	76.3(1)	Ti(1)-O(1)-Si(1)	131.9(2)
O(8')-Ti(1)-O(9)	76.5(1)		
		Ti(2')-O(2)-Si(1)	133.7(2)
Ti(2)-O(3)-Si(2)	134.1(2)		
		Ti(1)-O(4)-Si(2)	132.3(2)
Ti(1)-O(5)-Si(3)	174.6(2)		
		Si(3)-O(6)-Si(3')	149.4(4)
Ti(2)-O(7)-Si(4)	131.3(2)		
		Ti(1)-O(8)-H(1)	113.9(2)
Ti(1)-O(9)-Ti(2)	109.2(1)	-Ti(1')	107.1(1)
-Ti(2')	108.8(1)	-Ti(2)	95.8(1)
Ti(2)-O(9)-Ti(2')	99.0(1)	H(1)-O(8)-Ti(1')	108.5(2)
		H(1)-O(8)-Ti(2)	132.7(2)
		Ti(1')-O(8)-Ti(2)	96.6(1)

' Primed atoms are related to the atoms in the asymmetric unit by two-fold symmetry.

group (2.214(3) Å) is significantly longer than the other Ti-μ_3-OH bond lengths found in **2-H_2NEt_2** or in **1-H_2NEt_2**. No lengthening or shortening is observed in the Ti(1)-O(5) bond length in the unique ligand relative to the other Ti-O(siloxy) distances. Non-bonded distances between Ti atoms (3.014(2)-3.462(2) Å) in **2-H_2NEt_2** are very close to those found in **1-H_2NEt_2**.

As in **1-H_2NEt_2**, the geometry around titanium in **2-H_2NEt_2** is distorted octahedral, such that within the Ti_4O_4 core the O-Ti-O bond angles are compressed to values between 72.7(1) and 77.4(1)°. There are two types of Ti-O-Si bond angles, those around the normal siloxy ligand oxygen atoms with an average value of 132.7(1)°, and the nearly linear Ti(1)-O(5)-Si(3) bond angle of 174.6(2)° at the unique bridge. Because of the flexible nature of the Si-O-Si bond, it is of interest that the Si(3)-O(6)-Si(3') bond angle (149.4(4)°) lies between the values found for Si-O-Si bond angles in $(OSiPh_2)_3$ (131.9°),[11] and in $(OSiPh_2)_4$ (167.8(5)-153.7(4)°).[12]

The diethylammonium cations are well-behaved and contain the expected dimensions.[15] A hydrogen bond exists between the donor oxygen of the water molecule and an acceptor oxygen, O(3), of the titanium tetramer.

Infrared Spectra

The analysis of infrared spectra has always ranked high

in the study of siloxanes because the spectra are of considerable value in identification and quantitative analysis. There have been a number of studies examining the infrared spectra of disubstituted cyclosiloxanes, and as a result, most of the prominent absorption bands have been unambiguously assigned.[16,17] An excellent example of the value of infrared spectroscopy in providing fundamental information is found in the diphenyl substituted cyclosiloxanes: the cyclic trimer and the cyclic tetramer can be differentiated solely by the position of the Si-O-Si infrared band.[16] Thus, even though their physical properties are nearly identical, $(Ph_2SiO)_3$ is observed to have a strong absorption at 1018 cm^{-1}, whereas $(Ph_2SiO)_4$ exhibits a strong band at 1096 cm^{-1} (Figure 7).

The most striking evidence of a structural difference between **1-H_2NEt_2** and **2-H_2NEt_2** was an absorption band observed at 1053 cm^{-1} in the infrared spectrum of **2-H_2NEt_2**. $Ti((OSiPh_2)_4O)_2$ also contains an absorption doublet (1091, 1053 cm^{-1}) in the same region. Absorptions in this region (1100-1000 cm^{-1}) have been assigned to the Si-O-Si configuration.[9] When the infrared spectra and structures of the two titanosiloxanes are considered along with the diphenylcyclosiloxanes, a useful correlation can be made, viz., that as the Si-O-Si bond angle increases, the Si-O-Si infrared band shifts to higher energy. Table VII gives

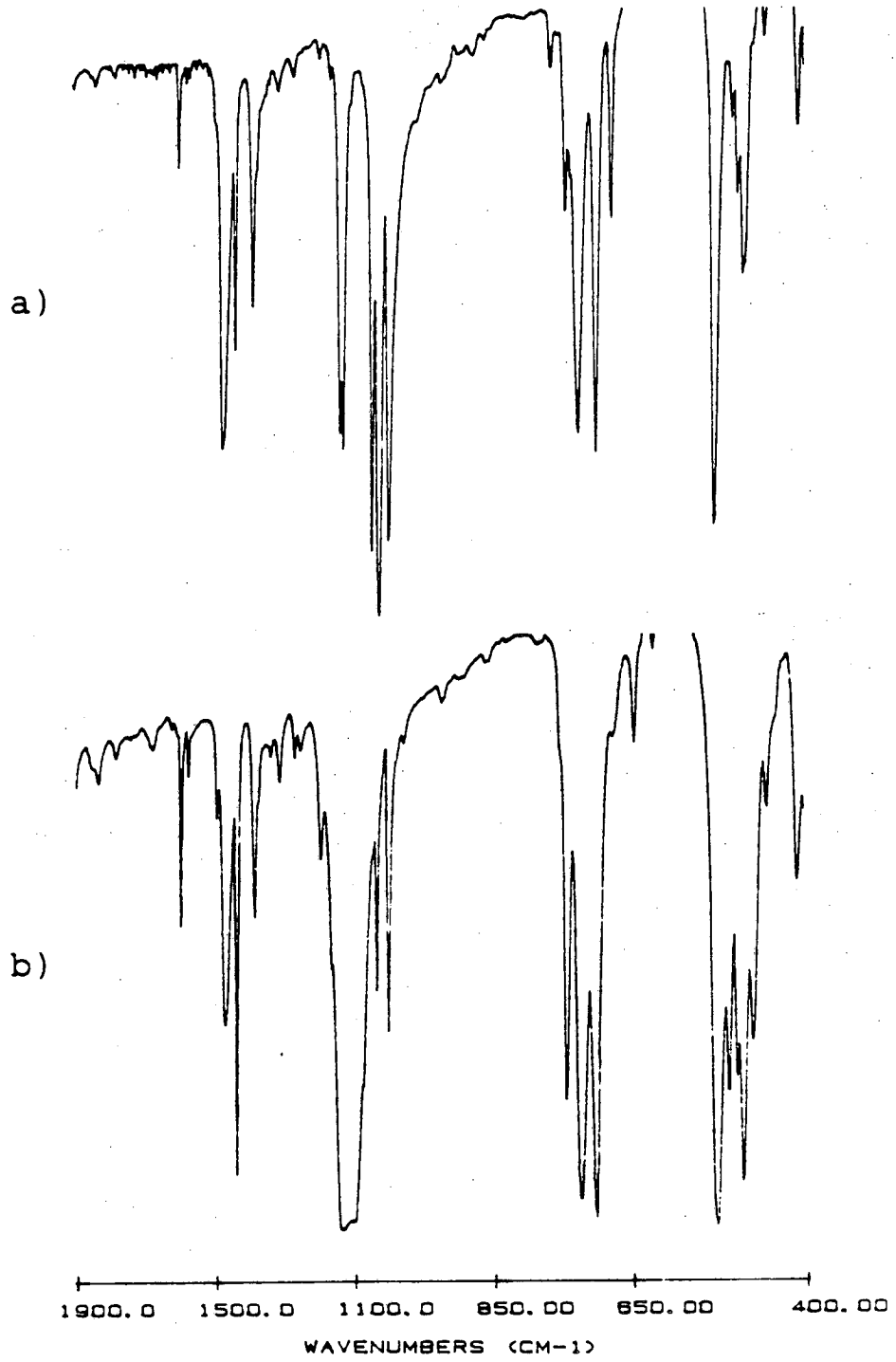

Figure 7. Infrared spectra of a) $(Ph_2SiO)_3$ and b) $(Ph_2SiO)_4$ in Nujol mulls.

Si-O-Si bond angles and infrared absorption frequencies for the compounds considered.

Table VII. Correlation between Infrared Frequency and Bond Angle in some Siloxanes and Metallosiloxanes.

Si-O-Si	angle (°)	frequency (cm^{-1})
cyclic trimer $(SiPh_2O)_3$	136[a]	1018[c]
$Ti((OSiPh_2)_4O)_2$	143[b]	1054[c]
2-H_2NEt_2	149[c]	1053[c]
cyclic tetramer $(SiPh_2O)_3$	156[d] 167	1096[c]
$Ti((OSiPh_2)_4O)_2$	172[b]	1091[c]

[a] ref. 8. [b] ref. 11. [c] this work. [d] ref 9.

The correlation of the Si-O-Si bond angle with the Si-O-Si stretching vibration is of considerable value for identification of siloxane ligands, and can be employed in predicting the structures of new titanosiloxanes. Once the position of the Si-O-Si infrared band is known, the siloxane bond angle can be estimated, and the extent of condensation in the ligands can be deduced. Conversely, although neither the X-ray crystal structure nor the full infrared spectrum of $Ti((OSiPh_2)_2O)_2$ have been reported, it is expected that the angles around oxygen in the siloxane units should be near 130° and the Si-O-Si infrared absorption near 1018 cm^{-1}.

Another prominant feature in the infrared spectra of **1-H_2NEt_2** and **2-H_2NEt_2** was the very intense and broad Ti-O-Si band at approximately 890 cm^{-1}; undoubtably the intensity of this band is due to the large number of Ti-O-Si bonds per mole of compound. In Figure 8 and 9 note that the height of the Ti-O-Si band is large relative to the Si-C absorption band at 1124 cm^{-1}. For comparison, the Ti-O-Si band in the spectrum of $Ti((OSiPh_2)_4O)_2$, which contains only four Ti-O-Si bonds per mole, is of the same relative intensity as the 1124 cm^{-1} band.

The broadness of the Ti-O-Si peak in the spectra of **1-H_2NEt_2** and **2-H_2NEt_2**, and the lack of any additional peaks relative to $Ti((OSiPh_2)_4O)_2$, suggested that the Ti-O-Ti absorption occurred in the same region, and was obscured by the intense Ti-O-Si band. Zeitler and Brown[6] postulated that infrared bands at 820 and 763 cm^{-1} observed for a condensed butoxy ester of titanium were Ti-O-Ti bands; neither band was present in the parent titanium ester, and both fall in a region where rutile (TiO_2) shows almost complete absorption (Table VIII). For **1-H_2NEt_2** and **2-H_2NEt_2** no bands were present in the spectra near 762 cm^{-1}, however there was a shoulder on the Ti-O-Si peak in both compounds that may be due to the Ti-O-Ti absorption.

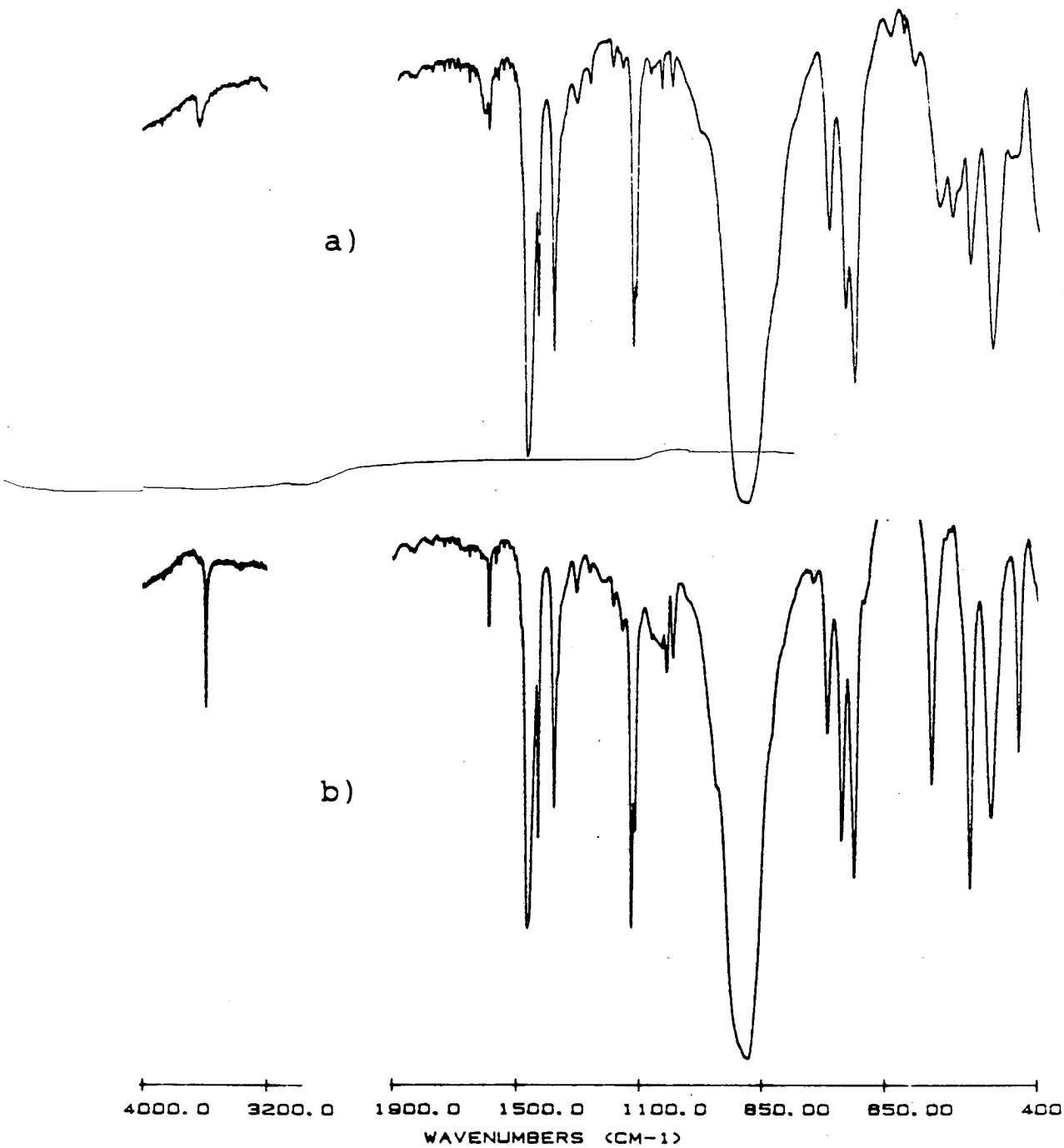

Figure 8. Infrared spectra of a) **1-H_2NEt_2** and b) **1-OH** in Nujol mulls.

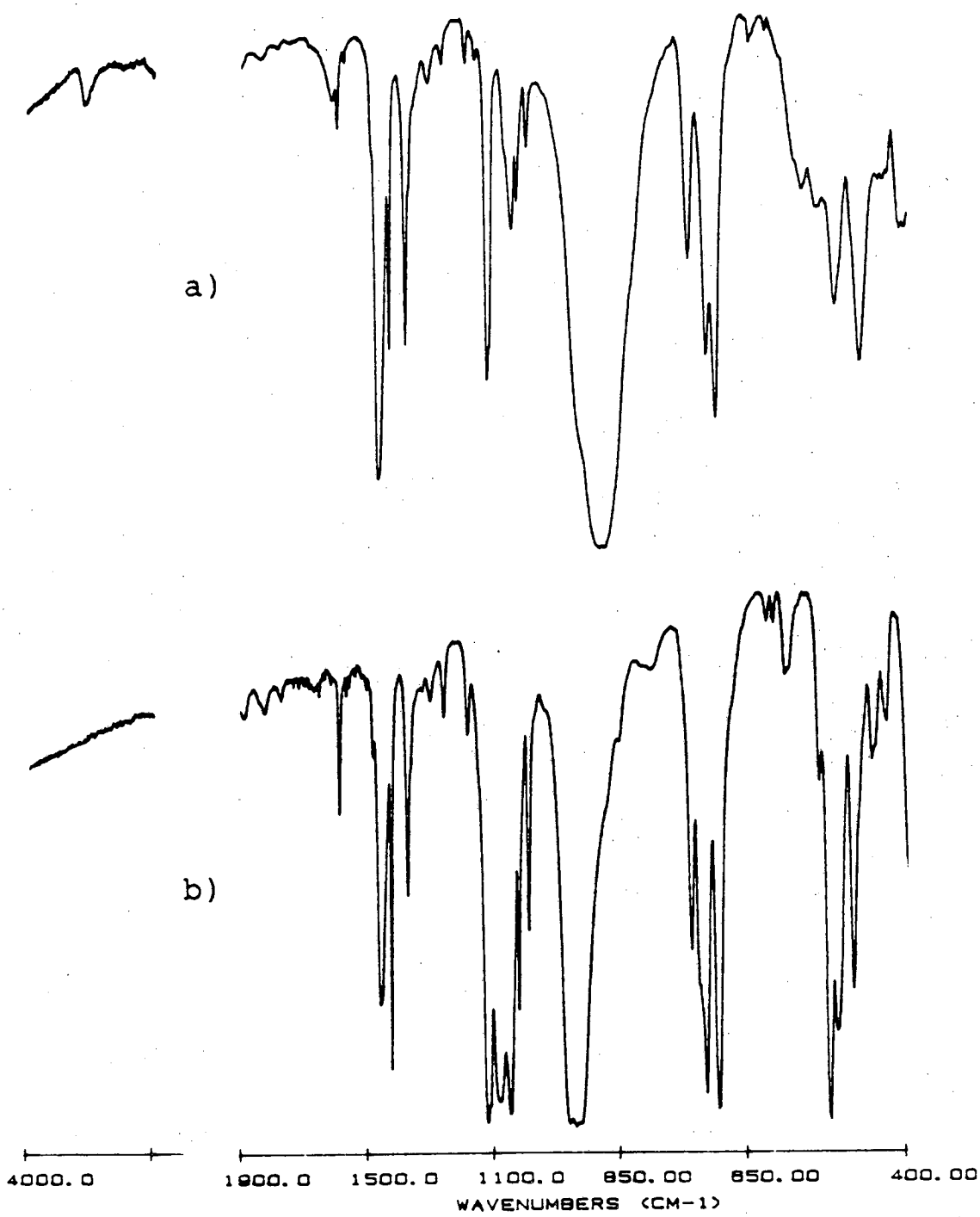

Figure 9. Infrared spectra of a) **2-H_2NEt_2** and b) $Ti((OSiPh_2)_4O)_2$ in Nujol mulls.

Table VIII. Comparison of Ti-O-M Stretching Frequencies (cm^{-1}) in some Ti(IV) Compounds

Compound	Ti-O-Ti	Ti-O-Si
condensed butoxytitanium	820, 763	---
TiO_2, rutile	900-667	---
$[Ti_3(\mu_3\text{-}O)(\mu\text{-}OH)(\mu\text{-}HCOO)_3Cp_3]^+$	825, 759	---
$Ti(OPh_3)_4$	---	926
$Ti((OSiPh_2)_4O)_2$	---	925
1-H_2NEt_2	(?) 827(sh)	889
2-H_2NEt_2	(?) 841(sh)	885

Reactivity of 1-H_2NEt_2

We were interested in exploring the reactivity of 1-H_2NEt_2 especially with regard to reactivity at the hydroxo- and oxo-sites. It was envisaged that if the hydroxyl hydrogens were acidic, they might react with an alkylhydroperoxide according to Scheme I.

Scheme I.

$$R_3COOH + H\text{-}O\text{-}M \longrightarrow R_3COOH_2^+ + {}^-O\text{-}M$$

$$R_3COOH_2^+ \longrightarrow R_3CO^+ + H_2O$$

$$R_3CO^+ + {}^-O\text{-}M \longrightarrow R_3CO\text{-}O\text{-}M$$

Such a mechanism may be responsible for the proposed exchange of alkoxide ligands for alkylhydroperoxide in

titanium tartrates during asymmetric epoxidations;[18] one of the few examples of reaction between a well-characterized metal complex and a peroxide in nonaqueous media. Unfortunately, mixtures of **1-H_2NEt_2** and ^tBuOOH or H_2O_2 in toluene failed to react and **1-H_2NEt_2** was recovered unchanged.

An additional type of reactivity which we investigated was the reaction of **1-H_2NEt_2** with trialkyl derivatives of aluminum. Organoaluminums are very reactive with protonic acids; nearly all Al-C bonds react quantitatively with water and alcohols to form compounds with Al-O bonds.[19] Aluminum alkyls are also very strong electron acceptors, and reactions of AlR_3 with compounds containing active lone pairs often leads to formation of coordination complexes.[20] Treatment of **1-H_2NEt_2** with aluminum alkyls gave a mixture of uncharacterizable products in the form of black and brown glassy solids. The solids were very soluble in both dichloromethane and toluene but could not be induced to precipitate or crystallize from solution upon cooling. Such solubility properties were consistent with degradation of the cubane structure resulting in the formation of polymers.

The lack of the desired reactivity prompted us to postulate that the hydroxyl protons were either not sufficiently acidic, or were perhaps not sterically accessible and that destructive side reactions were more favorable. It was also found that both **1-H_2NEt_2** and **2-H_2NEt_2** were resistant to boiling water, did not exchange hydrogen with D_2O,

and did not undergo direct cation exchange with tetra-alkylammonium halides or hydroxides, $[Ph_3P]_2NCl$, or Ph_4PBr.

It was hoped that protonation of **1-H_2NEt_2** would yield a hydrocarbon or toluene soluble neutral complex containing reactive hydroxyl groups. Addition of CH_3COOH to **1-H_2NEt_2** gave no reaction. However, addition of a stronger acid, CF_3COOH, to **1-H_2NEt_2** gave the tris(μ_3-hydroxo) monoanion, $[H_2NEt_2][Ti_4O(OH)_3(OSiPh_2O)_6]$. An attempt to completely protonate the complex under more vigorous conditions by heating **1-H_2NEt_2** in refluxing acetonitrile with an excess of CF_3COOH gave instead the spiro titanium compound $Ti((OSiPh_2)_4O)_2$. Finally, reaction of **1-H_2NEt_2** with para-toluenesulfonic acid gave the neutral complex $Ti_4(OH)_4(OSiPh_2)_6$, **1-OH**, in good yield; unfortunately, the white microcrystalline powder was sparingly soluble only in chlorinated solvents.

The ^1H NMR spectrum of **1-OH** revealed the absence of diethylammonium protons and an increase in the area of the OH resonance at δ 1.90 ppm. The neutral compound **1-OH** was also characterized by a sharp peak in the infrared spectrum at 3585 cm^{-1} associated with the hydroxyl groups. Other than a dramatic increase in the intensity of the O-H band, the infrared spectrum of **1-OH** remained unchanged from that of **1-H_2NEt_2**.

A mixture of **1-OH** and ^tBuOOH or $AlEt_3$ gave only unreacted starting material. Although the insolubility of

1-OH may have been a factor, the lack of reactivity was somewhat surprising in light of an apparent reaction of **1-OH** with methanol in refluxing acetonitrile. The product of this reaction, a white solid which was soluble in toluene and dichloromethane, did not exhibit any peaks in the ^1H NMR spectrum attributable to a methyl group, thus overruling simple O-Me for O-H exchange. Attempts to crystallize the white solid and characterize it further were not successful. Reaction of butanol with **1-OH** at ambient temperature gave a similar white solid which was soluble in toluene but could not be induced to crystallize. It was likely that some rearrangement or decomposition of the cubane structure was occurring since reaction of **1-OH** with isopropanol in acetonitrile for 5 days afforded $Ti((OSiPh_2)_4O)_2$ and a small amount of an uncharacterized white solid. Apparently, Ti-O(Si) bonds were being broken, with concomitant formation of the alkoxide. The alkoxide, so formed, could then react with the silanol in a manner similar to that shown in eq. (5).

$$Ti(OBu^t)_4 + 2\ Ph_2Si(OH)_2 \longrightarrow Ti((OSiPh_2)_4O)_2 + 4\ Bu^tOH \quad (5)$$

Although **1-H_2NEt_2** did not undergo direct cation exchange with tetraalkylammonium halides or hydroxides, **1-OH** reacted cleanly with 2 molar equivalents of tetramethylam-

monium hydroxide to yield the dianion, $[NMe_4]_2[Ti_4(O)_2(OH)_2(OSiPh_2O)_6]$, **1-NMe$_4$**. Unlike the $H_2NEt_2^+$ analogue, this colorless, crystalline compound was moderately soluble in polar solvents. The infrared spectrum of **1-NMe$_4$** is nearly identical to that of **1-H$_2$NEt$_2$**. The monoanion, $[NMe_4][Ti_4O(OH)_3(OSiPh_2O)_6]$, was prepared as a crystalline powder from **1-OH** and 1 molar equivalent of Me_4NOH. A summary of the reactivity found for **1-H$_2$NEt$_2$** and its derivatives is given in Figure 10.

Figure 10. Reactivity of **1-H_2NEt_2** and **1-OH**

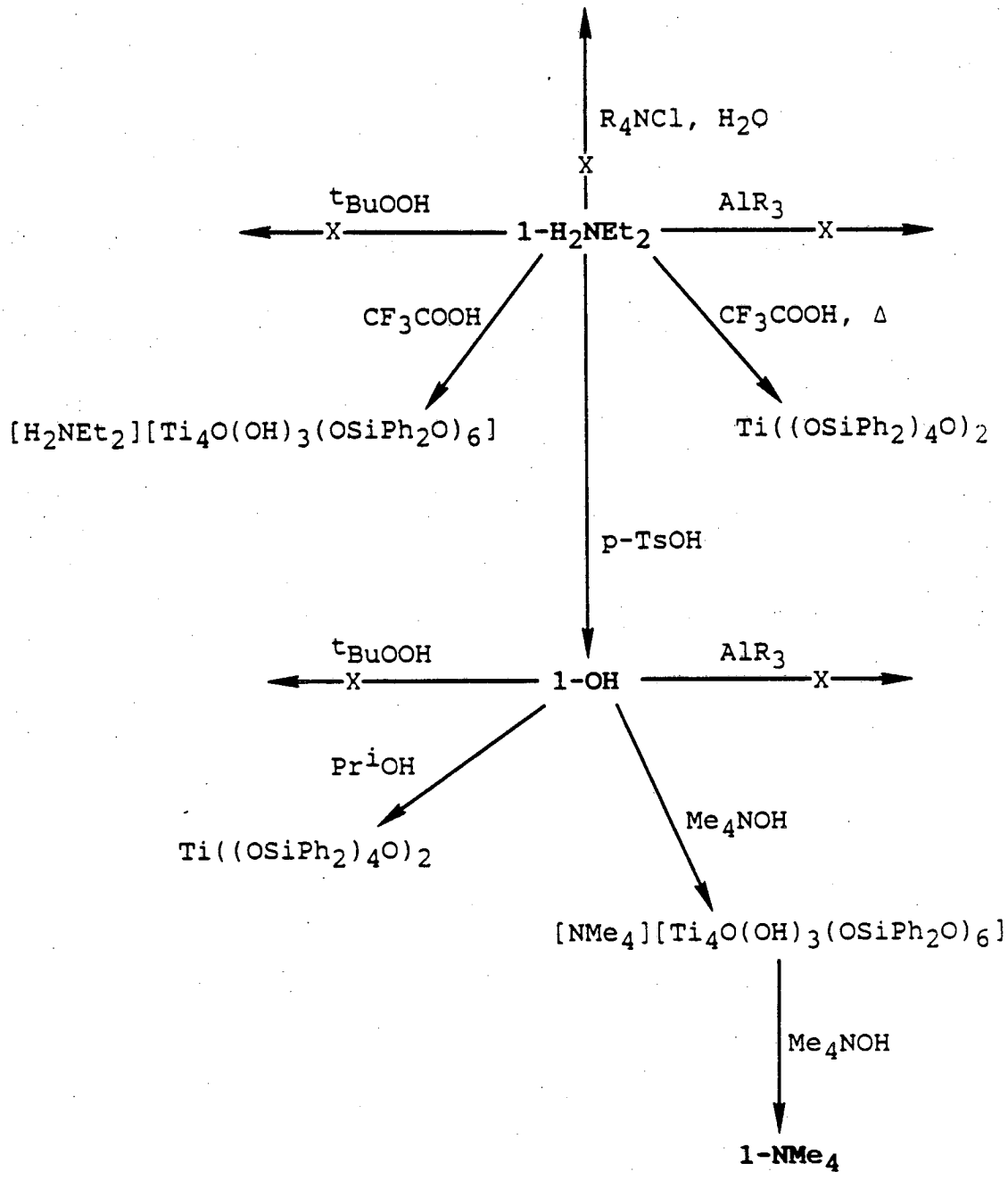

Conductivity Studies

One important method of characterizing ionic substances is the determination of the ability of their solutions to conduct an electric current. Since all of the compounds synthesized thus far, except **1-OH**, were ionic an attempt was made to measure their molar conductivities. Nitromethane was chosen as an appropriate solvent since all of the compounds were soluble in that solvent, and since it is the most widely used solvent for determination of conductivity due to its relatively low donor capacity. An average Λm value for 2:1 electrolytes in nitromethane is 167 $ohm^{-1}cm^2mole^{-1}$ for concentrations ca. 10^{-3} M.[21] Conductivity measurements were also made in acetonitrile although it is generally considered to have a somewhat higher coordinating power. Unfortunately, estimation of acceptable Λ_m values for 2:1 electrolytes in acetonitrile is difficult. Values as low as 145, and as high as 336 $ohm^{-1}cm^2mole^{-1}$ have been reported; a realistic range is probably 220-300 $ohm^{-1}cm^2mole^{-1}$ for concentration ca. 10^{-3} M.[21]

Because the molecular structures of both **1-H_2NEt_2** and **2-H_2NEt_2** were known and no unusual close contacts were found, it was suprising that the molar conductivity measured at 10^{-3} M for **1-H_2NEt_2** was 56 $ohm^{-1}cm^2mole^{-1}$ in nitromethane, and 130 $ohm^{-1}cm^2mole^{-1}$ in acetonitrile. The values found for **2-H_2NEt_2** were comparable, being 62 $ohm^{-1}cm^2mole^{-1}$

in nitromethane and 142 $ohm^{-1}cm^2mole^{-1}$ in acetonitrile. Each of these values was too low for a 2:1 electrolyte, and more nearly approximated the behavior of a 1:1 electrolyte. In acetone, a 2:1 electrolyte is expected to have an average molar conductivity of about 180 $ohm^{-1}cm^2mole^{-1}$.[21] For 1-H_2NEt_2 in acetone at 10^{-3} M, Λ_m = 64 $ohm^{-1}cm^2mole^{-1}$ and for 2, Λ_m = 91 $ohm^{-1}cm^2mole^{-1}$.

Low conductivity values are often attributed to formation of ion-pairs caused by Coulomb forces between oppositely charged ions, or to low ion mobilities. The best method for reducing ion-pairing effects was to measure the conductivity over a concentration range governed by the solubility limit at one extreme and approach of infinite dilution at the other. Comparisons of the data would be most valid for systems in which a series of complex anions were balanced by the same non-complex cation.[21] Unfortunately, there were apparently no other reports of conductivity studies on complex diethylammonium salts with which we could compare our data. Table IX gives the conductivity of 1-H_2NEt_2 and 2-H_2NEt_2 in nitromethane over a concentration range of 10^{-3}-10^{-5} M.

Although the conductivity values appeared to be slowly approaching ideal behaviour for 2:1 electrolytes as the solutions became more dilute, the apparent ion pairing was not eliminated. We assumed that low cation mobilities were not the cause for the irregular conductivity values because

Table IX. Molar Conductivity in Nitromethane

	Λ_m (mho·cm^2·mol^{-1})	
concentration, M	**1-H_2NEt_2**	**2-H_2NEt_2**
1×10^{-3}	53	54
1×10^{-4}	71	66
2×10^{-5}	91	71
1×10^{-5}	86	90

the molar conductivity of H_2NEt_2Cl (Λ_m = 47.9, 10^{-3} M) in acetonitrile showed that while it was also lower than the value expected for a 1:1 electrolyte, the conductivity of Et_4NCl (Λ_m = 185.6, 10^{-3} M) was at the higher end of the 1:1 range for tetraalkylammonium salts. According to Witschonke and Kraus[22] in a study of di-n-butylammonium salts, the low conductivity values of partially substituted ammonium ion salts are understandable if it is assumed that the active hydrogen atom in the ammonium ion interacts with the negative ion through non-Coulombic forces. As a result of the interaction, which may take the form of a strong hydrogen bond, the energy of the ion pairs is greatly increased over what it would be due to Coulombic forces alone. The net result is a decrease in the conductivity of solutions of the salt.

Many studies have been done on the conductivity of complex tetraalkylammonium salts and in general, these salts have been found to be well-behaved.[23,24] For **1-NMe_4**, the

molar conductivity fell within the 2:1 electrolyte range expected for acetonitrile as solvent, and values were only slightly lower than expected in nitromethane. Table X gives the experimental molar conductivities for all of the compounds, including the monoanions, in $ohm^{-1}cm^2mole^{-1}$ ca. 10^{-3} M.

Table X. Molar Conductivity in Nitromethane at 10^{-3} M.

Compound	Λ_m (mho cm^2 mol^{-1})
$[H_2NEt_2]Cl$	48
1-H_2NEt_2	53
2-H_2NEt_2	54
$[H_2NEt_2][Ti_4O(OH)_3(OSiPh_2O)_6]$	12
$[NMe_4]Cl$	107
1-NMe_4	127
$[NMe_4][Ti_4O(OH)_3(OSiPh_2O)_6]$	74

Reaction of $Ph_2Si(OH)_2$ with other Titanium Amides

A greater number of homoleptic amides are known for titanium than for any other transition metal. Accordingly, several other titanium amides were prepared in order to determine the effect of different amide ligands on the resulting products. For example, reaction of $Ti(NMe_2)_4$ with

$Ph_2Si(OH)_2$ gave polynuclear products similar to **1-H_2NEt_2** and **2-H_2NEt_2**. In this case, separation of the two titanium products was difficult because of the near insolubility of both compounds. However, repeated extraction of crude **1-H_2NMe_2** with hot toluene did yield a small amount of a white crystalline powder, identified by ^1H NMR, IR and elemental analysis as **2-H_2NMe_2**.

Attempts were made to synthesize the sterically bulky diisopropylamide from $TiCl_4$ and $LiNPr^i_2$ according to the method of Airoldi and Bradley.[25] The final product, however, was always contaminated with significant amounts of chloride. A mass spectrum of the yellow, crystalline solid gave a parent ion at 383 indicative of $ClTi(NPr^i_2)_3$. Reaction of $Ph_2Si(OH)_2$ with $ClTi(NPr^i_2)_3$ gave $H_2NPr^i_2Cl$ and a small amount of a white crystalline powder tenatively identified as **1-$H_2NPr^i_2$**, based on the infrared and ^1H NMR spectra. Although **1-$H_2NPr^i_2$** was not completely purified due to the similar solubility of the chloride salt, we could obtain no evidence of any condensed titanosiloxane species from examination of the infrared spectrum.

In contrast to the titanium dialkylamides, reaction of $Ti(NPh_2)_4$ with diphenylsilanediol gave the monomeric spiro titanium complex, $Ti((OSiPh_2)_4O)_2$. Moreover, under the reaction conditions used to synthesize **1-H_2NEt_2** and **2-H_2NEt_2**, $HNEt_2$ alone deprotonated $Ph_2Si(OH)_2$ to give cyclic siloxanes, whereas no reaction occurred between $HNPh_2$ and

$Ph_2Si(OH)_2$. It was apparent from these results that the more basic dialkylamines were capable of taking part in the overall reaction while the diarylamine was not. A possible series of reactions leading to formation of polynuclear products is: (1) nucleophilic attack by the silandiol on the titanium dialkylamide to form a Ti-O-Si bond and the free amine, (2) deprotonation of a terminal Si-OH by the free amine to give a bound silanolate anion, (3) attack by the anion on another relatively electropositive titanium atom to form a bridged species, and (4) attendant formation of oxo and hydroxo bridges from water generated <u>in situ</u> by condensation of free $Ph_2Si(OH)_2$. Scheme II illustrates the process.

Scheme II.

$$L_xTi\text{-}NEt_2 + HO\text{-}SiPh_2OH \longrightarrow L_xTi\text{-}OSiPh_2OH + HNEt_2$$

$$L_xTi\text{-}OSiPh_2OH + HNEt_2 \longrightarrow L_xTi\text{-}OSiPh_2O^- + H_2NEt_2^+$$

$$L_xTiOSiPh_2O^- + TiL_x \longrightarrow L_xTi\text{-}OSiPh_2O\text{-}TiL_x^-$$

$$TiL_x + H_2O \longrightarrow TiL_{x-1}(OH) + HL$$

The actual mechanism was undoubtably more complex, with many steps involving protonation or exchange of a proton, processes that were approximately equal in energy. It appeared, however, that the basicity of the amine relative to the disilanol was the key to this reaction. Thus, with relatively basic amines such as $HNMe_2$, $HNEt_2$, and $HNPr^i_2$,

polynuclear products were formed, usually with simple siloxy bridges. Conversely, with non-basic amines such as $HNPh_2$, or with alcohols (see eq. 2), products were mononuclear with chelating condensed siloxane ligands. Table XI lists the free amines and alcohols along with their pKa's.

Table XI. pK_a Values for Selected Amines and Alcohols

compound	pK_a*†
Me_2NH	10.7
Et_2NH	10.9
$Pr^i{}_2NH$	10.9
Ph_2NH	0.80
Pr^iOH	-2.00

* pK_a's refer to the conjugate acid of the compounds listed.
† ref. 26

It was of some interest to block one coordination site on the metal atom in order to discover whether lower nuclearity complexes could be obtained. Cyclopentadienide ligands on "titanocene" were found to be stable to hydrolysis during formation of the hydroxide.[8] Unfortunately, only **1-H_2NEt_2** could be isolated from the reaction of the heteroleptic amide $CpTi(NEt_2)_3$ with $Ph_2Si(OH)_2$. This result was presumed to be due to protonation with subsequent loss of the Cp ligands. No attempts were made to investigate this approach further.

In summary, we have demonstrated that titanium dialkylamides afforded a convenient entry into molecular Ti-O-Si systems. Infrared spectra combined with X-ray crystallographic data on the titanosiloxane products have allowed us to make some powerful correlations between spectroscopy and structural fact which should aid in the characterization of new metallosiloxanes.

References

(1) (a) Stone, F. G. A.; Graham, W. A. G. "Inorganic Polymers"; Academic Press: New York, 1962. (b) Lappert, M. F.; Leigh, G. J. "Development in Inorganic Polymer Chemistry"; Elsevier: Amsterdam, 1962. (c) Adrianov, K. A. "Metalorganic Polymers" (Polymer Reviews Vol. 8); Interscience: New York, 1965.

(2) Adrianov, K. A.; Kurasheva, N. A.; Kuteinikova, L. I. Zh. Obshch. Khim. **1976**, 46, 1497.

(3) Zeitler, V. A.; Brown, C. A. J. Chem. Soc. **1957**, 79, 4618.

(4) Bradley, D. C.; Thomas, I. M. J. Chem. Soc. (London) **1959**, 3404.

(5) Bradley, D. C.; Mehrotra, R. C.; Gaur, D. P. "Metal Alkoxides"; Academic Press: London, 1978; Chapter 2, p. 36.

(6) Zeitler, V. A.; Brown, C. A. J. Am. Chem. Soc. **1957**, 61, 1174.

(7) Döppert, K.; Thewalt, U. J. Organomet. Chem. **1986**, 301, 41.

(8) Guggenberger, L. J.; Tebbe, F. N. J. Am. Chem. Soc. **1976**, 98, 4137.

(9) Smith, G. D.; Caughlan, C. N.; Campbell, J. A. Inorg. Chem. **1972**, 11, 2989.

(10) van de Velde, G. M. H.; Harkema, S.; Gellings, P. J. Inorg. Nucl. Chem. Lett. **1973**, 9, 1169.

(11) Bokii, N. G.; Zakharova, G. N.; Struchkov, Yu. T. Zh. Strukt. Khim. **1972**, 13(2), 291.

(12) Braga, D.; Zanotti, G. Acta Cryst. **1980**, B36, 950.

(13) Steinfink, H.; Post B.; Fankuchen I. Acta Cryst. **1955**, 8, 420.

(14) Hursthouse, M. B.; Hossain, M. A. Polyhedron **1984**, 3, 95.

(15) Lazarini, F. Acta Cryst. **1987**, C43, 637.

(16) Young, C. W.; Servais, P. C.; Currie, C. C.; Hunter, M. J. J Am. Chem. Soc. **1958**, 70, 3758.

(17) Wright, N.; Hunter, M. J. J. Am. Chem. Soc. **1947**, 69, 803.

(18) Williams, I. D.; Pedersen, S. F.; Sharpless, K. B.; Lippard, S. J. J. Am. Chem. Soc. **1984**, 106, 6430.

(19) Cotton, F. A.; Wilkinson, G. "Advanced Inorganic Chemistry", 4th ed.; John Wiley & Sons: New York, 1980; Chapter 10.

(20) Coates, G. E.; Green, M. L. H.; Wade, K. "Organometallic Compounds"; Methuen: London, 1967; Vol. 1, Chapter III.

(21) Geary, W. J. Coord. Chem. Rev. **1971**, 7, 81.

(22) Witschonke, C. R.; Kraus, C. A. J. Am. Chem. Soc. **1947**, 69, 2472.

(23) Goodgame, D. M. L.; Goodgame, M.; Weeks, M. J. J. Chem. Soc. A **1967**, 1676.

(24) Young, J. F.; Gillard, R. D.; Wilkinson, G. J. Chem. Soc. **1964**, 5176.

(25) Airoldi, C.; Bradley, D. C. Inorg. Nucl. Chem. Lett. **1975**, 11, 155.

(26) Streitweiser Jr., A.; Heathcock, C. H. "Organic Chemistry"; Macmillan: New York, 1981; App. IV, p 1197.

Chapter 2

Reaction of Vanadium Amides with $Ph_2Si(OH)_2$

Although a majority of the reports on complex transition metal siloxanes concern titanium, there is every indication that vanadium could also form complex heterosiloxanes. Like the simple titanium trialkylsiloxides, the triorganosilyl vanadates are well known and can be synthesized by at least eight different routes.[1] Fewer reports of vanadium(IV) trialkylsiloxides have been described. Complex polymers containing the structural unit V-O-Si are reported to form by reaction of VCl_4 with diphenylsilanediol,[2] and a crystalline polymer was prepared from the reaction of vanadyl(tris)isopropoxide with $Ph_2Si(OH)_2$.[3] None of these materials have been structurally characterized.

Vanadium(V)

As described in Chapter 1, the interaction of a silanediol with titanium dialkylamides provided a convenient route to complex metallosiloxanes. It was of interest to discover the types of compounds which could be formed by similar reactions with other transition metals. Moving across the first row transition series to the d^1 metals gave us the opportunity to work with several different oxidation states.

For organometallic compounds of vanadium, the most common oxidation states are the +4 and +5 states; of these, the dialkylamides of the pentavalent state are the most stable. Since there are no known homoleptic vanadium(V) dialkylamides, it was necessary to begin with a heteroleptic complex. Thus reaction of 2.25 molar equivalents of $Ph_2Si(OH)_2$ with $OV(NEt_2)_3$ afforded a small amount of cyclic siloxanes (both $(Ph_2SiO)_3$ and $(Ph_2SiO)_4$), and two vanadium containing products. Of the latter two, the minor product **4** (2% yield) was soluble in toluene and polar solvents and was isolated from the major product **3** (29% yield) by extraction with warm toluene. Both **3** and **4** were colorless, air-stable materials and both crystallized readily.

The ^1H NMR spectrum of **3** in CD_3CN comprised a complex and ill-defined multiplet in the aromatic region and two broad singlets at δ 2.80 and 1.06 ppm. Although the insolubility of **3** allowed for weak signals and undoubtably contributed to the poor resolution, the chemical shifts and the area ratio of the two broad singlets were consistent with the quartet and triplet found previously for the alkyl protons of a diethylammonium group. The ratio of aromatic to alkyl protons was 1:1, that is, one diphenylsubstituted siloxy group per diethylammonium group. This fact severely limited the number of diphenylsiloxy groups that could be bound to vanadium because of the improbability of a very highly charged anion.

A comparison of the infrared spectra of **1-H_2NEt_2** and **2-H_2NEt_2** with that of **3** revealed few similarities aside from the appearance of the characteristic bands of diphenyl substituted silicon. Instead of a single broad M-O-Si band, the spectrum of **3** contained four separate bands in the infrared region between 1000 and 850 cm^{-1}. The lower frequency bands at 878 and 913 cm^{-1} were assigned to the V-O-Si stretching mode by reasoning that the higher frequency bands at 948 and 997 cm^{-1} were more consistent with the frequencies reported for V=O species.[4] We were unable to adequately assign the two remaining bands at 639 and 610 cm^{-1}. The consequences of the infrared analysis were two-fold: First, the complex appeared to be a polynuclear siloxy-bridged structure (the possibility of a chelating diphenyldisiloxide was considered unlikely), and second, it appeared to contain vanadyl groups. Based on this interpretation of the spectroscopic evidence, the structure of **3** was postulated as shown.

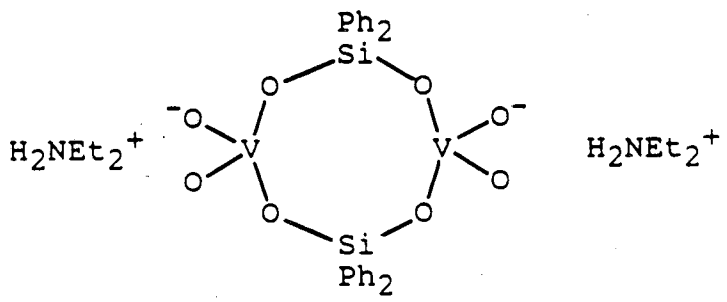

The ^1H NMR spectrum of **4** was similar to those of the previous metallosiloxanes with the exception that the methylene and methyl resonances in **4** were sharp and well-defined and occurred at δ 2.98 and 1.22 ppm, respectively. The ratio of aromatic protons to diethylammonium alkyl protons was 3:1, allowing three diphenylsiloxy groups per diethylammonium cation. The high solubility of **4** not only aided solution spectroscopy, but also provided some qualitative evidence for the presence of siloxane ligands. In **2-H_2NEt_2**, the presence of one siloxane ligand out of a total of six bridging ligands significantly increased its solubility relative to **1-H_2NEt_2**.

The infrared spectrum of **4** exhibited three peaks in the M-O-Si and V=O region. Again, the low frequency peaks at 878 and 920 cm^{-1} were strongest and were assigned to the V-O-Si stretching vibrations; the band observed at 957 cm^{-1} was assigned to V=O. The infrared spectrum of **4** differed from that of **3** in that two strong, sharp peaks appeared in the Si-O-Si region at 1090 and 1087 cm^{-1}. These peaks corresponded well with the 1096 cm^{-1} band in the spectrum of $(SiPh_2O)_4$, suggesting a siloxane bridge or ring in the structure of **4** containing at least three diphenylsiloxy groups. A comparison of the spectroscopic data collected on all of the metallosiloxanes led to the conclusion that the structural relationship between the two products in each reaction was similar. Therefore, the structure of **4** was

postulated as shown.

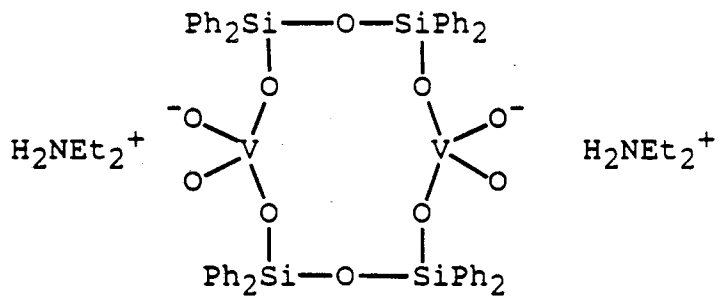

X-ray Studies

It was important to continue to verify our predictions, especially of new structural types, with X-ray crystallography. Hence, a single crystal X-ray diffraction study was first performed on **3**.

The crystal structure of **3-H_2NEt_2*** consists of the packing of discrete dimeric molecules. The complex possesses crystallographic site symmetry C2, and there is one half of the complex molecule per crystallographically independent unit. One whole molecule of the complex is generated by the 2-fold axis. The anionic portion of the molecule consists of two vanadium atoms bridged by two diphenylsiloxy ligands to form an eight-membered ring in an extended chair conformation. In addition, each vanadium is ligated by two terminal oxygen atoms. An ORTEP drawing of the anionic portion of the complex is given Figure 1. A side view of

---

* **3** will hereafter be referred to as **3-H_2NEt_2**.

Figure 1. An ORTEP drawing of the anionic portion of **3-H_2NEt_2**. The atomic labeling scheme in one crystallographically independent half of the molecule is defined.

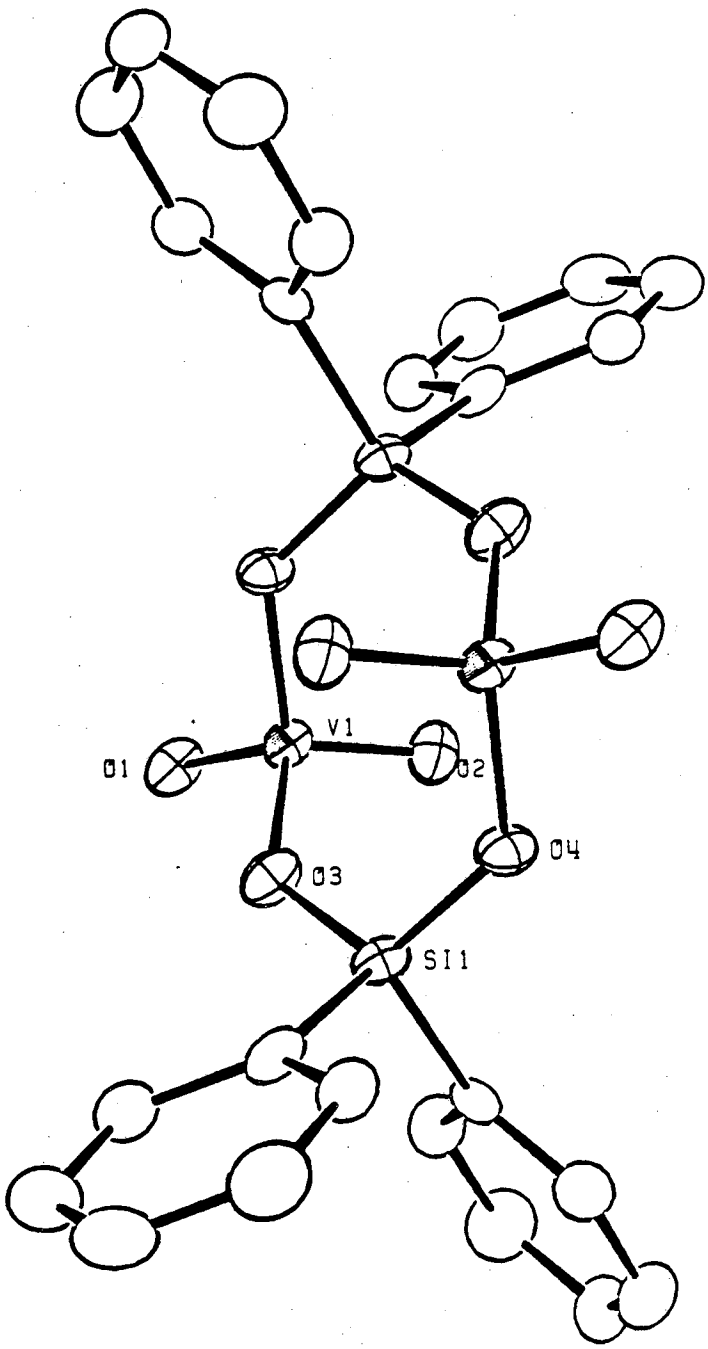

Figure 2. A side view of **3-H_2NEt_2** showing the extended chair conformation of the 8-membered $V_2Si_2O_4$ ring.

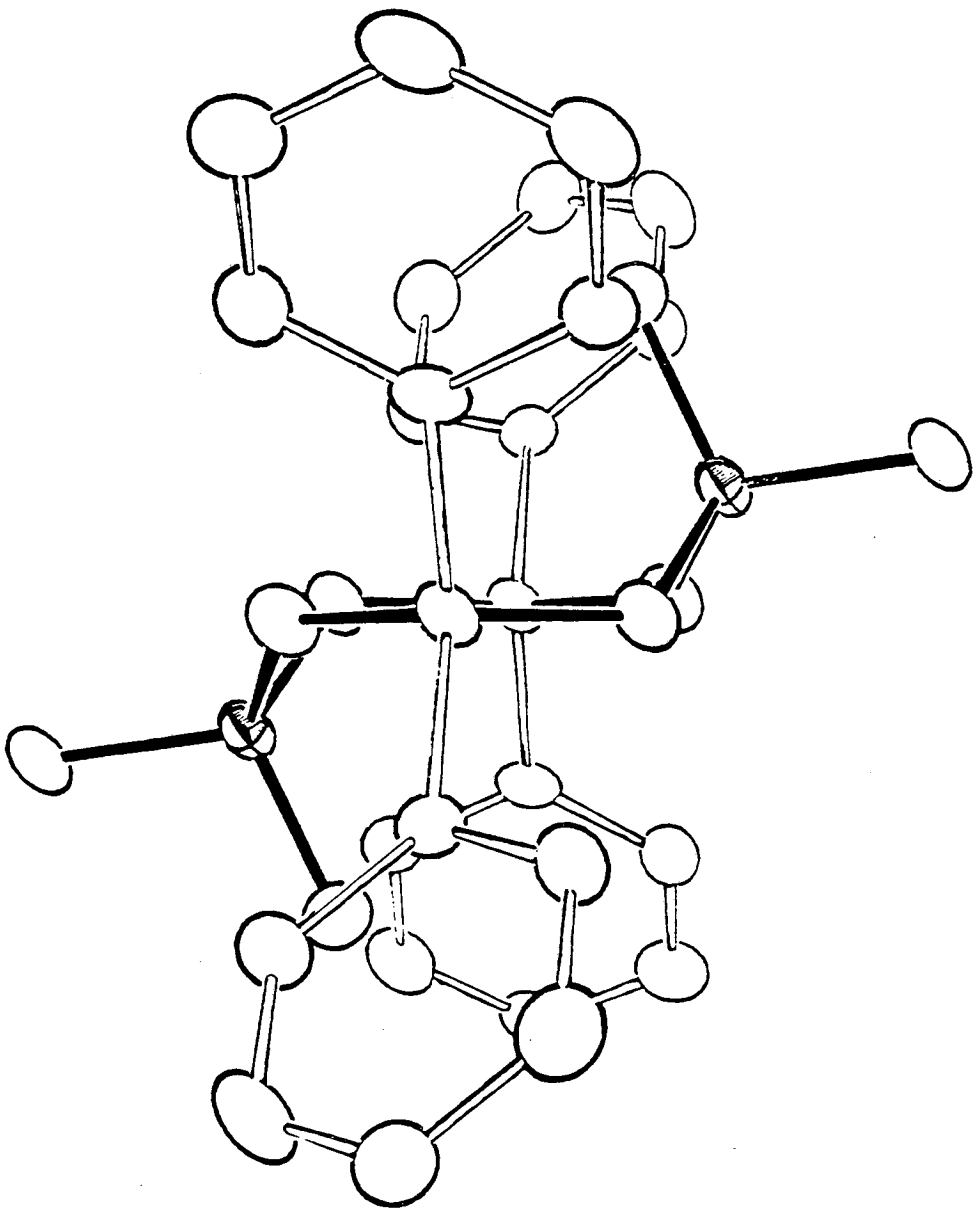

the molecule showing the conformation of the the ring is shown in Figure 2.

A selected set of interatomic distances and angles is given in Table I and II, respectively. The O(1) and O(2) bonding distances to V(1) are 1.643(2) and 1.611(2) Å, respectively. Comparison with the sum of the ionic radii[5] (1.99 Å) for V^{5+} and O^{2-} suggests a bond order approaching two for the V-O linkages in the VO_2 group. Similar V-O bond distances are found in octahedrally coordinated $[NH_4]$-$[O_2V(ox)_2]\cdot 2H_2O$ (1.648(2), 1.635(2) Å)[6] and in the trigonal bipyramidal environment of VO_2(Pic)(HMPT) (1.600(5), 1.606(5) Å).[7] The average V-O(Si) bond distance of 1.814(1) Å is short in comparison to chelate ligand V-O(C) bond distances of 1.980(2) and 2.000(4) Å found in the oxalate[5] and the py-2-carboxylate (Pic)[6] complexes, respectively. We consider the V-O(Si) distances in **3-H_2NEt_2** to indicate very strong bonds; the small V-O-Si bond angles (to be discussed below) do not, however, support O→V π-bonding. The Si-O bond distances are comparable to those found in cyclic siloxanes.[9] The non-bonded distance between equivalent vanadium atoms is 4.158(1) Å; the largest distance spanned by the diphenyldisiloxy bridge yet observed.

The rigorous tetrahedral geometry around vanadium is evidenced by an average O-V-O bond angle of 109.47(4)°. Four coordination is unusual for V^{5+}; the only other

Table I. Selected Bond Lengths (Å) for $[H_2NEt_2]_2$-$[V_2O_4(OSiPh_2O)_2]$

V(1)-O(1)	1.643(2)	Si(1)-O(3)	1.626(2)
-O(2)	1.611(2)	-O(4)	1.635(2)
-O(3)	1.805(2)	-C(1)	1.859(3)
-O(4)	1.823(2)	-C(7)	1.869(3)
-V(1')	4.158(1)•		
		O(1)-H(23)	1.864(2)*
N(1)-C(13)	1.474(6)	-H(24)	1.908(2)*
-C(15)	1.473(6)		

• Non-bonded distances. * Hydrogen bond.

Table II. Selected Bond Angles (deg) for $[H_2NEt_2]_2$-$[V_2O_4(OSiPh_2O)_2]$

O(1)-V(1)-O(2)	107.3(1)	O(3)-Si(1)-O(4)	112.4(1)
-O(3)	110.4(1)	-C(1)	110.3(1)
-O(4)	109.8(1)	-C(7)	108.9(1)
O(2)-V(1)-O(3)	110.6(1)	O(4)-Si(1)-C(1)	108.2(1)
-O(4)	109.6(1)	-C(7)	108.8(1)
O(3)-V(1)-O(4)	109.1(1)	C(1)-Si(1)-C(7)	108.3(1)
V(1)-O(3)-Si(1)	135.9(1)	C(13)-N(1)-C(15)	115.7(1)
		-H(23)	107.8(3)
V(1)-O(4)-Si(1)	130.8(1)	-H(24)	108.5(3)
		C(15)-N(1)-H(23)	108.5(4)
		-H(24)	108.5(3)
		H(23)-N(1)-H(24)	107.6(2)

dioxovanadium(V) complex that has been found to have a tetrahedral structure is KVO_3.[8] In **3-H_2NEt_2** the average V-O-Si bond angle of 133.34(2)° is comparable to the values for M-O-Si bond angles found in **1-H_2NEt_2**, but smaller than the Si-O-Si angle of 142.5° found in $(Me_2SiO)_4$, also a puckered eight-membered ring. The O-Si-O bond angle in **3-H_2NEt_2** is 112.4(1)°, slightly larger than the expected tetrahedral value commonly found in cyclic siloxanes. Although the deviation from ideality is small, it may indicate that some strain is involved in bridging the nearly 4 Å V···V distance.

The bond lengths and angles within the equivalent $[H_2N(C_2H_5)_2]^+$ cations are in agreement with the values found in **1-H_2NEt_2** and **2-H_2NEt_2**. Each cation is bonded to the anionic complex by two hydrogen bonds, N(1)-H(23)···O(1) (2.835 Å), and N(1)-H(24)···O(1) (2.859 Å).

With the determination of the structure of **3-H_2NEt_2**, the predicted stoichiometry was confirmed. Confident that the X-ray crystal structure of **4** would again prove the predictive strength of our infrared analysis, an attempt was made to grow X-ray quality crystals. Unlike the relative ease accompanying crystallization of the previous three metallosiloxanes, growing single crystals of **4** proved to be a tricky task. The only crystals suitable for X-ray crystallography were those that grew in the original acetonitrile filtrate derived from purification of **3-H_2NEt_2**.

These crystals were clear, rectangular blocks that remained unclouded after removal of the solvent. Upon recrystallization however, crystals with a different morphology were formed. The new crystals were square platelets which usually contained small, star-shaped cracks in the center; during drying these crystals turned opaque. Changing the solvent of crystallization did not result in the formation of any of the original rectangular crystals. Ultimately it was necessary to repeat the preparation of **3-H_2NEt_2** and **4** several times in order to obtain a rectangular shaped crystal of **4** that could be used for a structure determination.

The crystal consists of diethylammonium cations and monomeric vanadosiloxane anions. There are two independent molecules in the asymmetric unit loosely connected through a series of hydrogen bonds. Unless otherwise specified, the bond distances and angles in the discussion refer to molecule **1**. An ORTEP drawing of the overall geometry of the anion is shown in Figure 3. Selected bond distances and angles for molecule **1** are presented in Tables III and V, respectively; those for molecule **2** are given in Tables IV and VI, respectively. The coordination geometry at vanadium is tetrahedral with the chelating siloxanediolate ligand occupying two sites, and two terminal oxygen atoms occupying the remaining two sites. The bond lengths in **4-H_2NEt_2*** have

---

* **4** will hereafter be referred to as **4-H_2NEt_2**.

Figure 3. ORTEP drawing of the anionic portion of $[H_2NEt_2]$-$[VO_2((OSiPh_2)_3O)]$ showing the atom numbering scheme

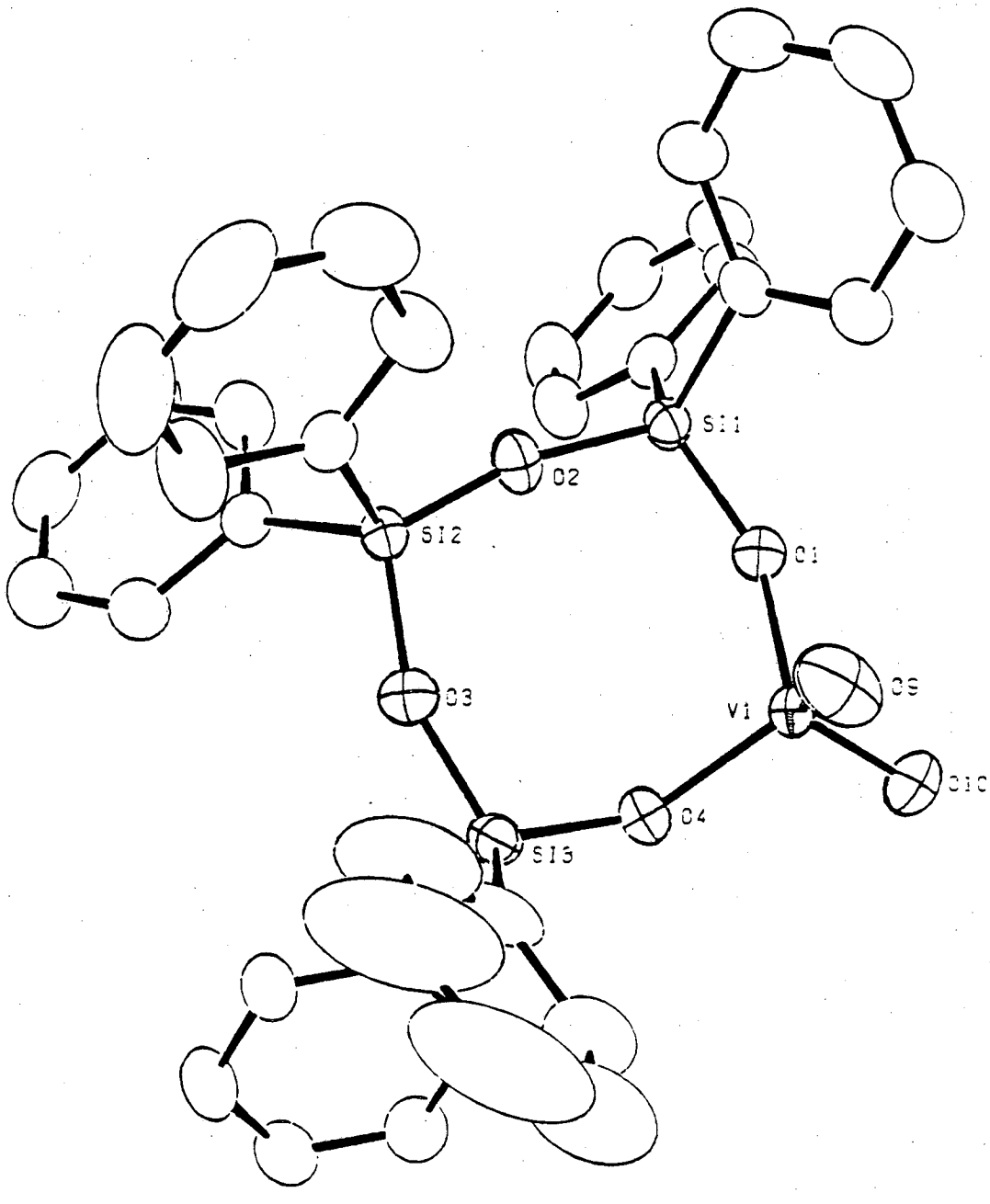

Figure 4. Side view of $VO_2((OSiPh_2)_3O)^-$ with 50% probability thermal elipsoids

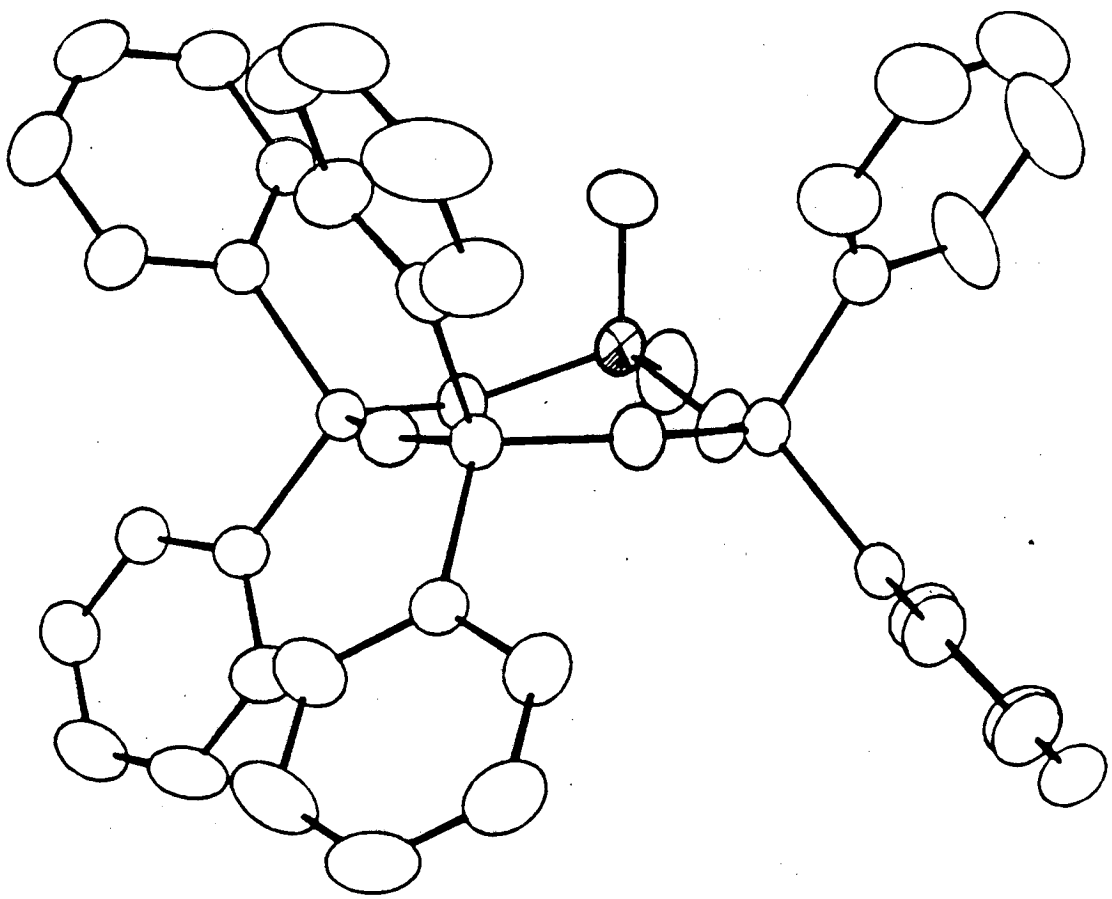

values similar to those observed in **3-H_2NEt_2**; the average V-O(Si) bond distance is 1.807(1) Å, and the bond distance to the terminal oxygens are 1.617(3) and 1.621(3) Å to O(9) and O(10) respectively. The Si-O bond distances are comparable to those found in the parent siloxane rings.[9] Although Hursthouse[10] found a slight tendency toward lengthening of the Si-O distances next to Ti-O bonds in $Ti((OSiPh_2)_4O)_2$, no lengthening of the Si-O bonds nearest vanadium is observed. Curiously, it is the Si-O bonds twice removed from the V-O bonds which are longest, 1.624(3) Å between Si(1) and O(2), and 1.623(2) Å between Si(3) and O(3).

The conformation of the eight-membered VSi_3O_4 ring in both molecules **1** and **2** are nearly planar with the largest deviation from the least squares plane being 0.7 Å for V(1) in molecule **1** and 0.2 Å for V(2) in molecule **2**. The dihedral angle between the V(1), O(1), O(4) and Si(1), Si(2), Si(3) planes is 40°. A side-on view of the ring in **4-H_2NEt_2** is shown in Figure 4. In the parent siloxane, $(Ph_2SiO)_4$, the Si_4O_4 ring is somewhat closer to planarity, with the maximum deviation from the root-mean-square plane being 0.1 Å.[9]

In **4-H_2NEt_2** the Si(1)-O(2)-Si(2) bond angle is 164.6(1)°, while the Si(2)-O(3)-Si(3) bond angle is smaller at a value of 156.6(2)°. The Si-O-Si bond angles are comparable with those found in octaphenylcyclotetrasiloxane (from 152.8 to 167.8°).[9] It has been found that the Si-O-

Table III. Selected Bond Lengths (Å) for $[H_2NEt_2][VO_2((OSiPh_2)_3O)]$

V(1)-O(1)	1.810(2)	Si(1)-O(1)	1.614(2)
-O(4)	1.804(2)	-O(2)	1.624(3)
-O(9)	1.617(3)	-C(1)	1.867(3)
-O(10)	1.621(3)	-C(7)	1.873(3)
Si(2)-O(2)	1.612(3)	Si(3)-O(3)	1.623(2)
-O(3)	1.617(2)	-O(4)	1.620(3)
-C(13)	1.857(3)	-C(25)	1.861(3)
-C(19)	1.855(4)	-C(31)	1.851(4)
N(1)-C(73)	1.475(5)	O(9)-H(58)	1.830(2)*
-C(75)	1.497(6)		
-H(57)	0.949(3)	O(10)-H'(70)	1.817(2)*
-H(58)	0.949(3)		
		H(57)-O'(11)	1.890(2)*

' Primed atoms belong to molecule **2**. * Indicates a hydrogen bond.

Table IV. Selected Bond Lengths (Å) for $[H_2NEt_2][VO_2-((OSiPh_2)_3O)]$ (Molecule **2**)

V(2)-O(5)	1.794(2)	Si(4)-O(5)	1.606(2)
-O(8)	1.791(3)	-O(6)	1.625(3)
-O(11)	1.654(2)	-C(37)	1.858(4)
-O(12)	1.599(3)	-C(43)	1.862(3)
Si(5)-O(6)	1.613(3)	Si(6)-O(7)	1.623(2)
-O(7)	1.609(2)	-O(8)	1.614(3)
-C(49)	1.857(3)	-C(61)	1.856(3)
-C(55)	1.854(4)	-C(67)	1.861(4)
N(2)-C(77)	1.485(5)	O(11)-H(69)	1.825(2)*
-C(79)	1.494(6)	-H'(57)	1.890(2)*
-H(69)	0.952(3)		
-H(70)	0.954(3)		

' Primed atoms belong to molecule **1**. * Indicates a hydrogen bond.

Table V. Selected Bond Angles (deg) for $[H_2NEt_2][VO_2-((OSiPh_2)_3O)]$

O(1)-V(1)-O(4)	109.4(1)	O(1)-Si(1)-O(2)	110.2(1)
-O(9)	109.4(1)	-C(1)	110.1(1)
-O(10)	109.7(1)	-C(7)	109.7(1)
O(4)-V(1)-O(9)	109.6(1)		
-O(10)	109.5(1)	O(2)-Si(2)-O(3)	112.1(1)
O(9)-V(1)-O(10)	109.2(1)	-C(13)	109.0(1)
		-C(19)	108.8(1)
O(3)-Si(3)-O(4)	111.8(1)		
-C(25)	109.9(1)	V(1)-O(1)-Si(1)	142.4(2)
-C(31)	107.5(2)		
		Si(1)-O(2)-Si(2)	164.6(1)
Si(2)-O(3)-Si(3)	156.6(2)		
		Si(3)-O(4)-V(1)	140.7(1)

Table VI. Selected Bond Angles (deg) for $[H_2NEt_2][VO_2-((OSiPh_2)_3O)]$ (Molecule 2)

O(5)-V(2)-O(8)	109.0(1)	O(5)-Si(4)-(O6)	110.5(1)
-O(11)	111.1(1)	-C(37)	111.0(1)
-O(12)	110.8(1)	-C(43)	108.4(1)
O(8)-V(2)-O(11)	109.1(1)		
-O(12)	109.9(1)	O(7)-Si(6)-O(8)	110.5(1)
O(11)-V(2)-O(12)	106.8(1)	-C(61)	109.0(1)
		-C(67)	106.8(1)
O(6)-Si(5)-O(7)	111.5(1)		
-C(49)	109.6(1)	V(2)-O(5)-Si(4)	158.5(2)
-C(55)	109.4(1)		
		Si(4)-O(6)-Si(5)	159.3(1)
Si(5)-O(7)-Si(6)	160.0(2)		
		Si(6)-O(8)-V(2)	151.3(2)

Si bond angles in planar, or nearly planar, cyclotetrasiloxanes are larger than those found in compounds with puckered rings, e.g. in $(Me_2SiO)_4$ from 142 to 145°.[11] In **4-H_2NEt_2** the V-O-Si bond angles are smaller than the Si-O-Si angles because the vanadium atom, with no bulky phenyl groups to accomodate, is not forced to lie in the plane of the oxygen and silicon atoms. For molecule **1**, where the vanadium atom is well out of the plane of the ring, the V-O-Si bond angles are 140.7(1) and 142.4(2)°. In molecule **2** the vanadium atom is almost lying in the plane and the V-O-Si bond angles are correspondingly larger at values of 151.8(1) and 158.5(2)°.

It should be noted that the rigorous tetrahedral geometry around vanadium - an unusual geometry for the +5 oxidation state - make it an ideal replacement for silicon in siloxane-type structures.

The diethylammonium cations are well-behaved and contain dimensions which are expected for them.[12] Hydrogen bonds exist between N(1) and O(9), O(10) and N(2), N(2) and O(11), and O(11) and N(1). An ORTEP diagram of the asymmetric unit, including hydrogen bonding, is shown in Figure 5.

Figure 5. ORTEP drawing of the asymmetric unit in **4-H_2NEt_2**

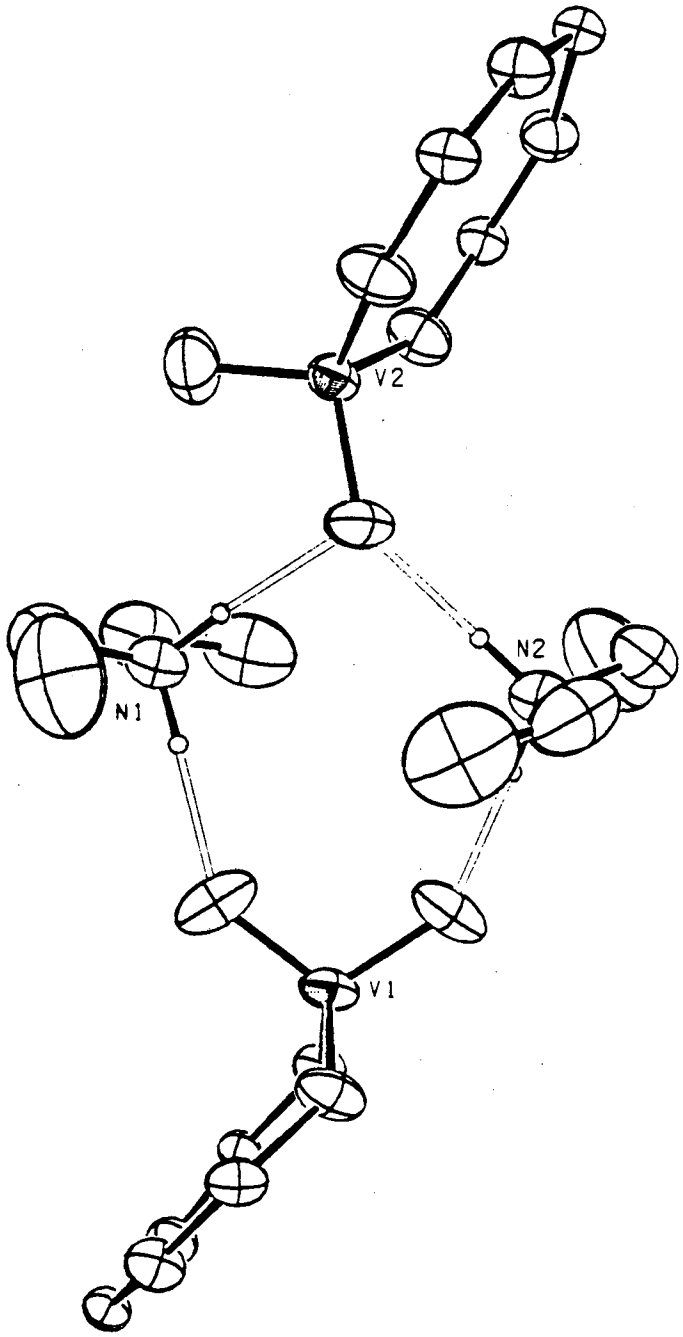

Infrared Spectra

The X-ray crystal structure determination of **4-H_2NEt_2** revealed that the compound was monomeric, not dimeric as had been predicted. Based as it was on infrared data correlated with previous polynuclear structures, it was easy to understand why our prediction had been wrong. It seemed there might be no way to distinguish mononuclear compounds from polynuclear ones, aside from an X-ray crystallographic determination of the structure. Luckily, our predictive misstep led to the discovery that the infrared spectra of the metallosiloxanes contained another piece of structural information whose significance had not been previously realized.

Earlier, it had been found that the infrared band due to the M-O-Si stretching mode was very intense in the polynuclear compounds. In addition, as illustrated in Chapter 1, Figure 8, the monomeric compound $Ti((OSiPh_2)_4O)_2$ has an M-O-Si infrared band of equal intensity to that of a distinctive Si-C band at 1124 cm^{-1}, a useful internal reference band. The monomeric vanadosiloxane, **4-H_2NEt_2**, was observed to have a V-O-Si absorption band which was also the same intensity as that of the internal reference band (Figure 6).

From these comparisons came the realization that the relative intensity of the M-O-Si band was indicative of nuclearity. Thus, a mononuclear metallosiloxane would have

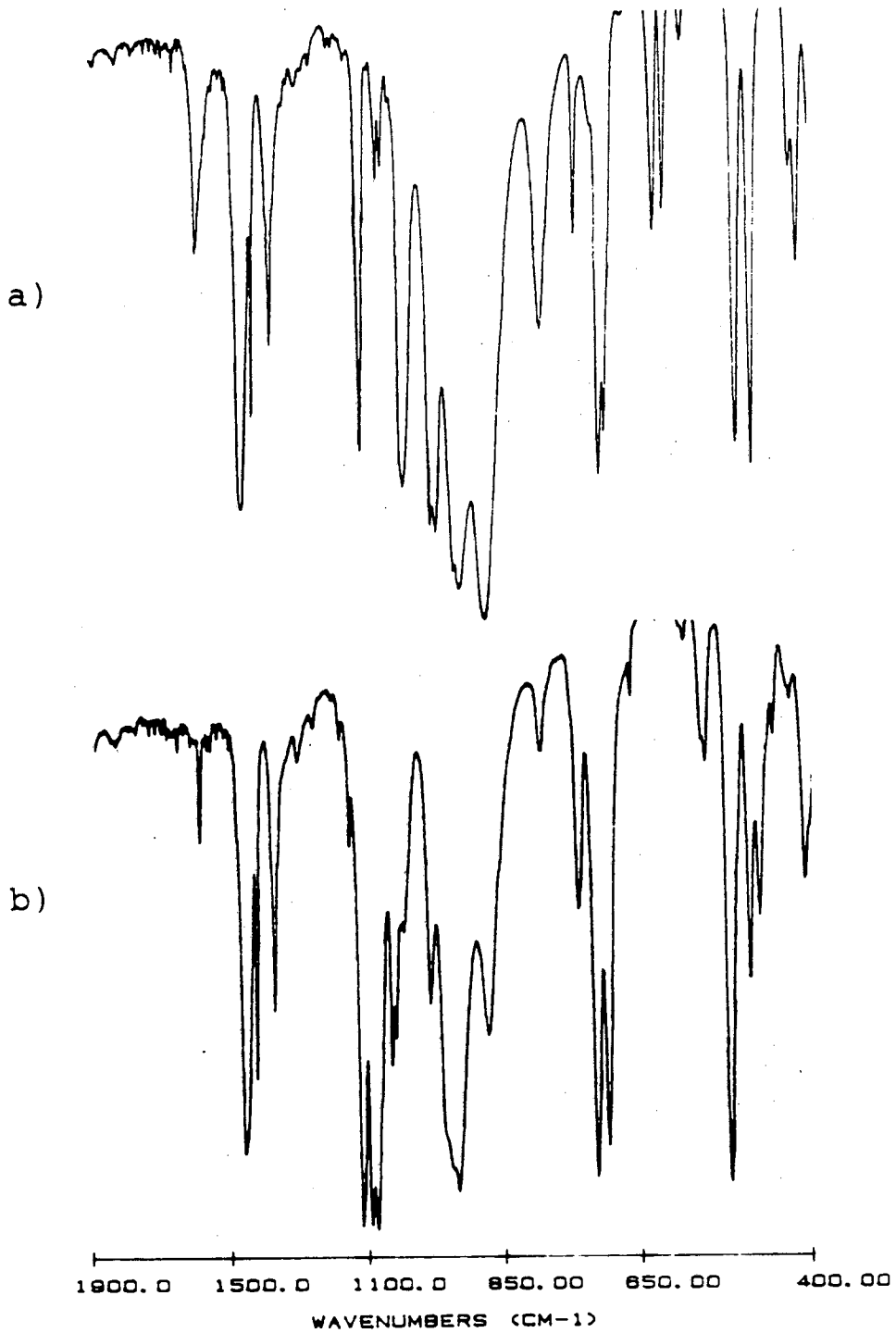

Figure 6. Infrared Spectra of a) **3-H_2NEt_2** and b) **4-H_2NEt_2** (rectangular crystals) in Nujol mulls.

an M-O-Si band which was less than, or the same height as, the internal reference band (1124 cm^{-1}). This axiom depends on the absence of any chelating diphenylsiloxy ligands - a relatively safe assumption since no compounds with this ligand configuration have been isolated. It follows that a polynuclear compound, even a dinuclear one such as **3-H_2NEt_2**, would have an M-O-Si band of greater intensity than the Si-C reference band (Figure 6). Because of the many structural variations which were possible, dinuclear compounds could not be discerned from tri- or tetranuclear. The ability to differentiate mononuclear from polynuclear compounds, however, provided us with an additional structural handle.

Characterization of the metallosiloxane complexes depended heavily on the information which could be obtained from the infrared spectrum. For this reason, some effort was made to correlate the assignments made previously with structural facts. In **3-H_2NEt_2** and **4-H_2NEt_2** the infrared region between 850 and 1100 cm^{-1} contained a profusion of bands; not only did V-O-Si and Si-O-Si configurations absorb in this region, but the cis-dioxo group, O=V=O, exhibited absorptions there as well. Two absorptions were expected for a cis-dioxo group, one at approximately 950 cm^{-1} and another at approximately 900 cm^{-1}, based on the infrared spectra of trigonal bipyramidal and octahedral structures.[13] The bands assigned to V=O in **3-H_2NEt_2** (948, 997 cm^{-1}) and **4-H_2NEt_2** (957 cm^{-1}) corresponded well with the higher energy

band for cis-dioxo groups, however the lower energy band was more difficult to identify since it apparently overlaps with the V-O-Si band.

Table VII shows again the correlation between the Si-O-Si bond angles and siloxane absorption bands of compounds whose structures are known, with the addition of **4-H_2NEt_2**. The frequency of the siloxane stretching band and the Si-O-Si bond angles of **4-H_2NEt_2** fit in nicely with the cyclic siloxane tetramer.

Table VII. Correlation between Infrared Frequency and Bond Angle for some Siloxanes and Metallosiloxanes

Si-O-Si	angle (°)	frequency (cm^{-1})
cyclic trimer $(SiPh_2O)_3$	136[a]	1018[c]
$Ti((OSiPh_2)_4O)_2$	143[b]	1054[c]
2-H_2NEt_2	149[c]	1053[c]
4-H_2NEt_2	156[c] 165	1087[c] 1090[c]
cyclic tetramer $(SiPh_2O)_3$	156[d] 167	1096[c]
$Ti((OSiPh_2)_4O)_2$	172[b]	1091[c]

a) ref. 9b. b) ref. 14. c) this work d) ref. 9a.

After the observation that two different crystal types existed for **4-H_2NEt_2**, it was found that the two types of crystals exhibited different infrared spectra. Figure 7

shows that the infrared spectrum of the square crystals revealed lower energy Si-O-Si absorption bands (1067, 1047 cm^{-1}) relative to those found in the spectrum of the structurally characterized, rectangular crystals (1090, 1087 cm^{-1}). In addition, only one band at 920 cm^{-1} appeared in the spectrum of the square, opaque crystals while the same region consisted of several bands (957, 920, 878 cm^{-1}) in the infrared spectrum of the rectangular crystals.

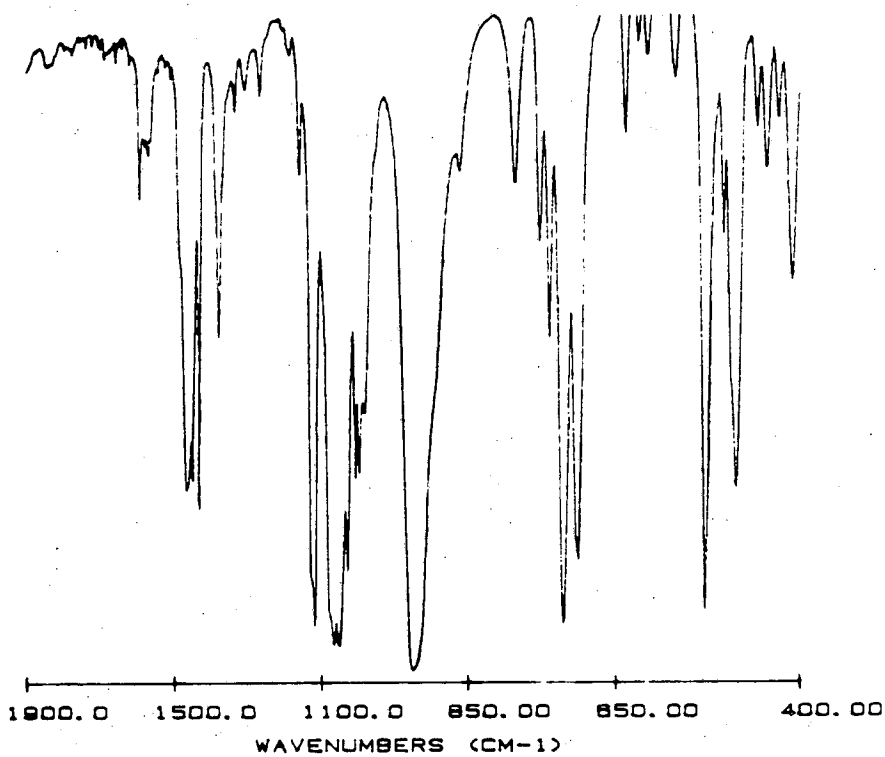

Figure 7. Infrared spectrum of **4-H_2NEt_2** (square plates) in Nujol mull.

The fact that the ^1H NMR spectra of both crystal types were identical and that they both analyzed for $[H_2NEt_2][VO_2((OSiPh_2)_3O)]$ suggested the presence of two polymorphs of **4-H_2NEt_2**. The shift of the Si-O-Si infrared bands to lower energy in the uncharacterized polymorph implied a crystal packing arrangement that increased the puckering of the eight-membered VSi_3O_4 ring while decreasing the Si-O-Si bond angles. The parent siloxane, octaphenylcyclotetrasiloxane, exhibits three different solvent-free polymorphs, one triclinic (mp 200-201°), and two monoclinic (mp 200-201°, 188°) forms; the cyclic trimer exists in two crystalline forms.[14] Similar observations were reported by Zeitler and Brown[15] where rhombic crystals of $Ti((OSiPh_2)_4O)_2$ were transformed to square plates after recrystallization. Although the infrared spectra of both crystal types were reported to be identical, they had different melting points. Because of the known polymorphism of both the diphenyl-substituted cyclic trimer and the tetramer, it was not unlikely that **4-H_2NEt_2** was also polymorphic; the observations made by Zeitler indicated that this phenomenon, common to cyclosiloxanes, may also be common to cyclic metallosiloxanes.

<u>Reactivity of 3-H_2NEt_2</u>

The reactivity of **1-H_2NEt_2** and **2-H_2NEt_2** was shown to be mainly limited to protonation and formation of tetraalkyl-

ammonium salts. Much the same reactivity was found for the vanadium(V) complexes. Thus, reaction of **3-H_2NEt_2** with p-toluenesulfonic acid afforded the neutral dimer **3-OH** as an insoluble, orange powder. Because of its insolubility, our assumption that the orange powder was indeed $V_2O_2(OH)_2$-$(OSiPh_2O)_2$ could not be confirmed by ^1H NMR spectroscopy or X-ray crystallography. The low volatility of the compound precluded mass spectroscopy as a possible avenue of characterization. Therefore, indirect evidence of the identity of **3-OH** was gained by reconversion of the orange powder to **3-H_2NEt_2** by addition of a stoichiometric amount of $HNEt_2$.

Tetraalkylammonium salts of **3-H_2NEt_2** were prepared by reaction of the neutral complex with tetraalkylammonium halides such as Me_4NCl or Et_4NCl. The use of Me_4NOH, which successfully converted **1-OH** to a Me_4N^+ salt, apparently led to degradation of **3-OH**. This result, along with the observation that the orange color of **3-OH** turned brownish-green if allowed to stand in air, led to the conclusion that **3-OH** was somewhat moisture sensitive.

n-Butyllithium was added to **3-OH** with the hope of forming the lithium salt, $Li_2[V_2O_4(OSiPh_2O)_2]$. Though the latter compound was not a product of the reaction, a few pale blue crystals were isolated suggesting the formation of a vanadium(IV) complex. The apparent reduction was intriguing, but the yield of the blue compound was so low that further efforts in this direction were not pursued.

Reaction of **3-OH** with alcohols (MeOH, Pr^iOH) gave reaction products which were not characterized due to their insolubility or intractable nature.

Transformation of **3-H_2NEt_2** to a trimethylsiloxy derivative was achieved by reaction with Me_3SiCl. The product, a colorless oil, was characterized by its ^1H NMR spectrum.

Just as with **1-H_2NEt_2**, the simple bridged structure of **3-H_2NEt_2** was degraded by reaction with alkyl aluminums and no reaction occurred with ^tBuOOH or H_2O_2. The dimer **3-H_2NEt_2** was also unreactive toward methylating agents such as MeI or Me_2SO_4. A summary of the reactivity found for **3-H_2NEt_2** is given in Figure 8.

Figure 8. Reactions of **3-H_2NEt_2**

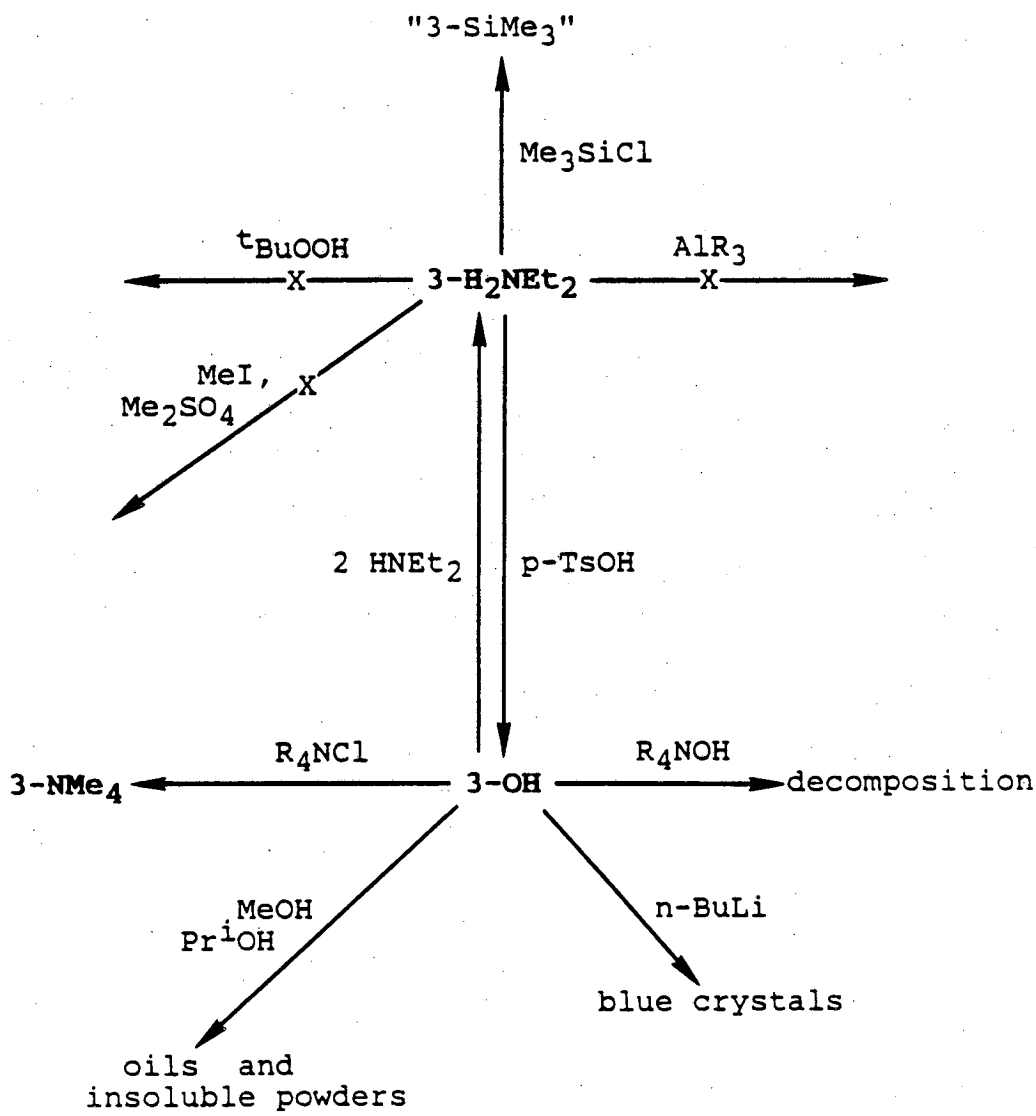

Conductivity Studies

The conductivity data for **4-H_2NEt_2** was consistent with that found for the titanium complexes; the low solubility of **3-H_2NEt_2** prevented the preparation of a 10^{-3} M solution. As before, Λ_m values were approximately half of the expected values for both 2:1 and 1:1 electrolytes. For **3-H_2NEt_2**, conversion to the tetraalkylammonium complex led to conductivity data in satisfactory agreement with the suggested ranges for 2:1 electrolytes. Table VIII lists the molar conductivity for all of the compounds synthesized thus far.

Table VIII. Molar conductivity in Nitromethane at 10^{-3} M.

Compound	Λ_m (mho cm^2 mol^{-1})
$[H_2NEt_2]Cl$	48
1-H_2NEt_2	53
2-H_2NEt_2	54
$[H_2NEt_2][Ti_4O(OH)_3(OSiPh_2O)_6]$	12
3-H_2NEt_2	insol.
4-H_2NEt_2	34
$[NMe_4]Cl$	107
1-NMe_4	127
$[NMe_4][Ti_4O(OH)_3(OSiPh_2O)_6]$	74
3-NMe_4	141

Reaction of $Ph_2Si(OH)_2$ with other Vanadium Amides

For the system described in Chapter 1, the relative basicity of the dialkylamine or alcohol originating from the titanium starting material had a pronounced effect on the structure of the final product. It was of interest to do a parallel study with vanadium to discover what effect the previous conditions would have on the structures of the products. It had already been shown with $OV(NEt_2)_3$ that the vanadium system was quite unlike that of titanium. The presence of a basic amine, $HNEt_2$, did not appear to encourage high nuclearity structures in the vanadium products.

Unfortunately, reaction of $OV(OEt)_3$ with $Ph_2Si(OH)_2$ gave an insoluble solid which could not be successfully characterized, hence precluding any structural studies. This result was not entirely unexpected since Nakaido et al.[3] had earlier synthesized an insoluble vanadium siloxide from the reaction of $OV(OPr^i)_3$ with $Ph_2Si(OH)_2$. It was proposed that the compound was a polymer with the formulation,

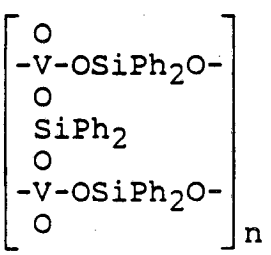

The infrared spectrum of our insoluble vanadosiloxane was similar, but not identical to, that of the compound prepared by Nakaido.

Vanadium(IV)

After the disappointing events with the vanadyl alkoxide, we were eager to address the vanadium(IV) system. Synthesis of tetrakis(diethylamido)vanadium(IV) was not a trivial matter however. The method used most frequently was one developed by Alyea and Bradley[16] that involved disproportionation of the vanadium(III) product formed from reaction of VCl_3 and $LiNEt_2$. Understandably, this reaction is characterized by very low yields. It was essential to our task that gram quantities of $V(NEt_2)_4$ be prepared by a straightforward method. Inadvertantly, it was found that reaction of $OVCl_3$ with five equivalents of $LiNEt_2$ produced $V(NEt_2)_4$ in 8% yield when air was rigorously excluded from the reaction. The highest yield of product, however, was obtained when the amide was derived from $V(OBu^t)_4$ by reaction with an excess of $LiNEt_2$. Unfortunately, this preparation resulted in the isolation of a product that was contaminated by $LiOBu^t$. Repeated filtration reduced the contaminant, but did not completely remove it.

Before continuing on with the impure $V(NEt)_4$, we carried out a model study with $LiOPr^i$ contaminated $Ti(NEt_2)_4$ which had been prepared from $Ti(OPr^i)_4$ and $LiNEt_2$. Reaction of the contaminated titanium dialkylamide with $Ph_2Si(OH)_2$ afforded **1-H_2NEt_2** upon work-up. That the $LiOPr^i$ contaminant had some effect was reflected by the absence of an isolable amount of **2-H_2NEt_2** from the reaction mixture. Based on

these results the decision was made to attempt a reaction using the contaminated vanadium dialkylamide as a starting material.

The mixture of impure $V(NEt_2)_4$ and three equivalents of $Ph_2Si(OH)_2$ afforded a pale blue vanadium compound, 5, along with the ubiquitous cyclic siloxanes. Purification of 5 was achieved by repeated washing with ether. The ^1H NMR spectrum of the compound in CD_3CN revealed a broad, featureless multiplet in the aromatic region and two broad singlets at δ 3.61 and 1.77 ppm. The latter two peaks corresponded to the positions of the two resonances found for pure THF in CD_3CN. Because of the likely paramagnetism of 5, the possibility existed that some resonances in the ^1H NMR spectrum might be dramatically shifted or broadened, hence the absence of any resonances attributable to dialkylammonium protons. The absence of dialkylammonium cations in 5 was confirmed, however, by elemental analysis for C, H, and N, as nitrogen was not detected in the sample.

Previously synthesized metallosiloxanes had not exhibited parent ions in their mass spectra, but because of the low melting point and high solubility of 5, it was hoped that mass spectroscopy might reveal some structural information. Unfortunately, the mass spectrum was characterized by two independent parent ions: one at 792 corresponding to $(SiPh_2O)_4$, and another at 596 corresponding to $(SiPh_2O)_3$.

With four metallosiloxanes structurally characterized

and with specific absorption bands in their infrared spectra correlated with known structural features, we possessed a wealth of information which could be drawn upon for the characterization of 5. Beginning with the most dominant feature in the infrared spectum, the M-O-Si band, it was noted that the intensity of the V-O-Si band was equivalent to that of the internal reference band at 1124 cm^{-1}, (Figure 9) suggesting a mononuclear structure. Absorption bands

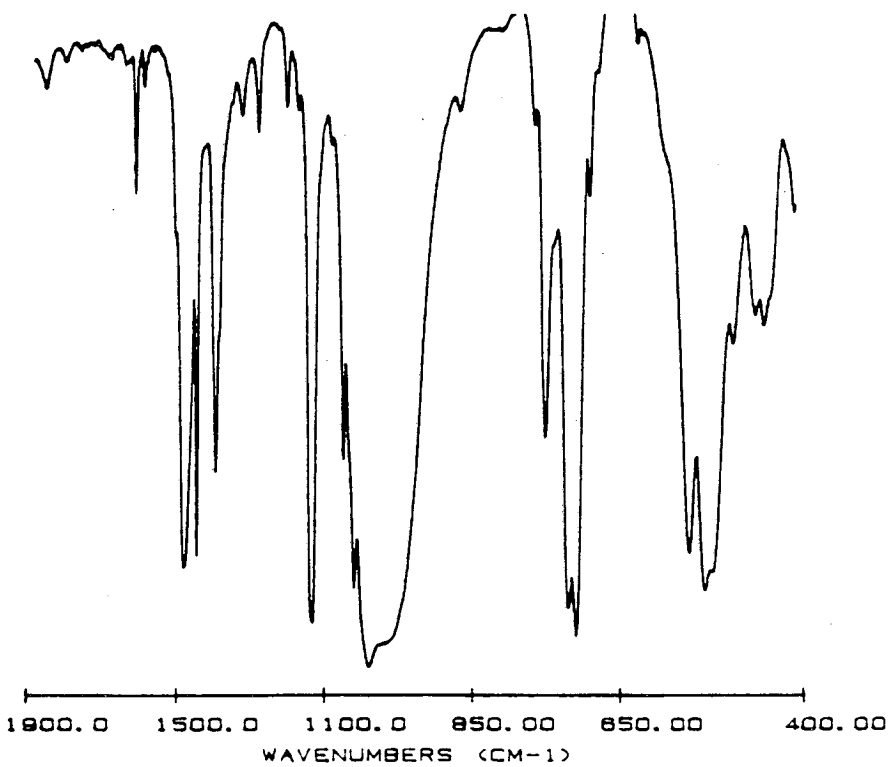

Figure 9. Infrared Spectrum of 5 in Nujol mull.

in the Si-O-Si region appeared at 1025 and 997 cm^{-1} corresponding to the 1018 cm^{-1} peak of hexaphenyl cyclosiloxane. On the basis of these two observations the compound was believed to have two five-membered cyclic siloxane ligands containing two diphenylsiloxy groups per cyclic ring, with each ring chelated to a central vanadium atom. The structural formula as postulated is illustrated below.

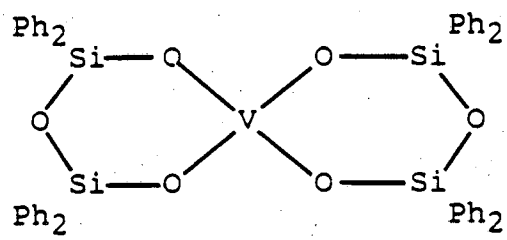

X-ray Studies

In order to confirm, or refute, the postulate that 5 was indeed $[V(OSiPh_2)_2O)_2]$, a single crystal X-ray diffraction study was performed. The atom numbering scheme is shown in Figure 10, while the actual stoichiometry and structure of the complex is shown in Figure 11. The molecular structure consists of two chelating five-membered siloxane ligands bonded to a central VO^{2+} moiety. The four oxygen atoms bound to vanadium are also bound to two $Li(THF)_2$ groups. A selected set of bond distances and bond angles are given in Tables IX and X, respectively. The V-O distances appear to be of two types: V-O(2) and V-O(3) at

1.954(8) and 1.969(8) Å, respectively, and V-O(1) and V-O(4) at 2.029(8) and 2.017(8) Å, respectively. The former two are comparable with the average V-O(C) bond distance in $VO(acac)_2$ at a value of 1.97 Å.[17] Because of the relatively large error associated with the bond distances in the structure of **5**, it is probable that the appearance of two types of V-O(siloxy) bond distances is not chemically meaningful. The V(1)-O(7) vanadyl bond distance in **5** is 1.543(9) Å, compared to 1.56 Å in $OV(acac)_2$. The V=O bond distance found in **5** is at the short end of the range found for V=O bonds in oxovanadium (IV) compounds which vary from 1.56 to 1.67 Å.[18] The shortest Si-O distances are 1.56(1) and 1.59(1) for Si(1)-O(1) and Si(4)-O(4) respectively, where O(1) and O(4) are involved in the long bond distances to vanadium. In general, the Si-O bonds adjacent to the V-O bonds are shorter at an average value of 1.586(5) Å, than those twice removed from the vanadium atoms (average 1.642(4) Å). Hursthouse[10] observed longer bond distances for Si-O bonds adjacent to Ti-O bonds in $Ti((OSiPh_2)_4O)_2$.

The coordination polyhedron around vanadium in **5** is approximately square pyramidal with angles around vanadium involving the siloxane ligands ranging from 79.6(3)-89.3(3)°. The average O(7)-V-O(Si) angle is 107.0(8)°. The angles around Li(1) and Li(2) vary widely with the O(1)-Li(1)-O(4) and O(2)-Li(2)-O(3) bond angles being the

Figure 10. An ORTEP drawing of $[Li(THF)_2]_2[VO((OSiPh_2)_2O)_2]$ with $Li(THF)_2$ groups removed for clarity.

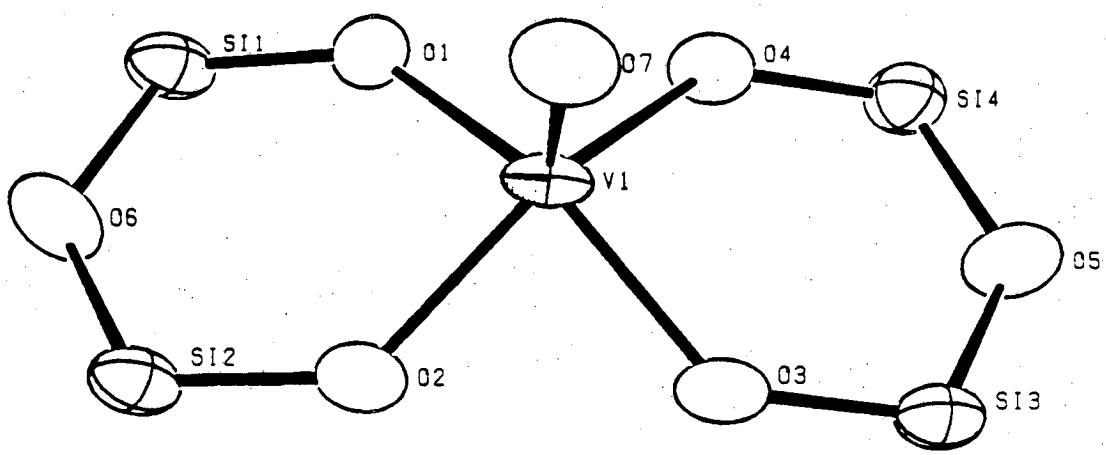

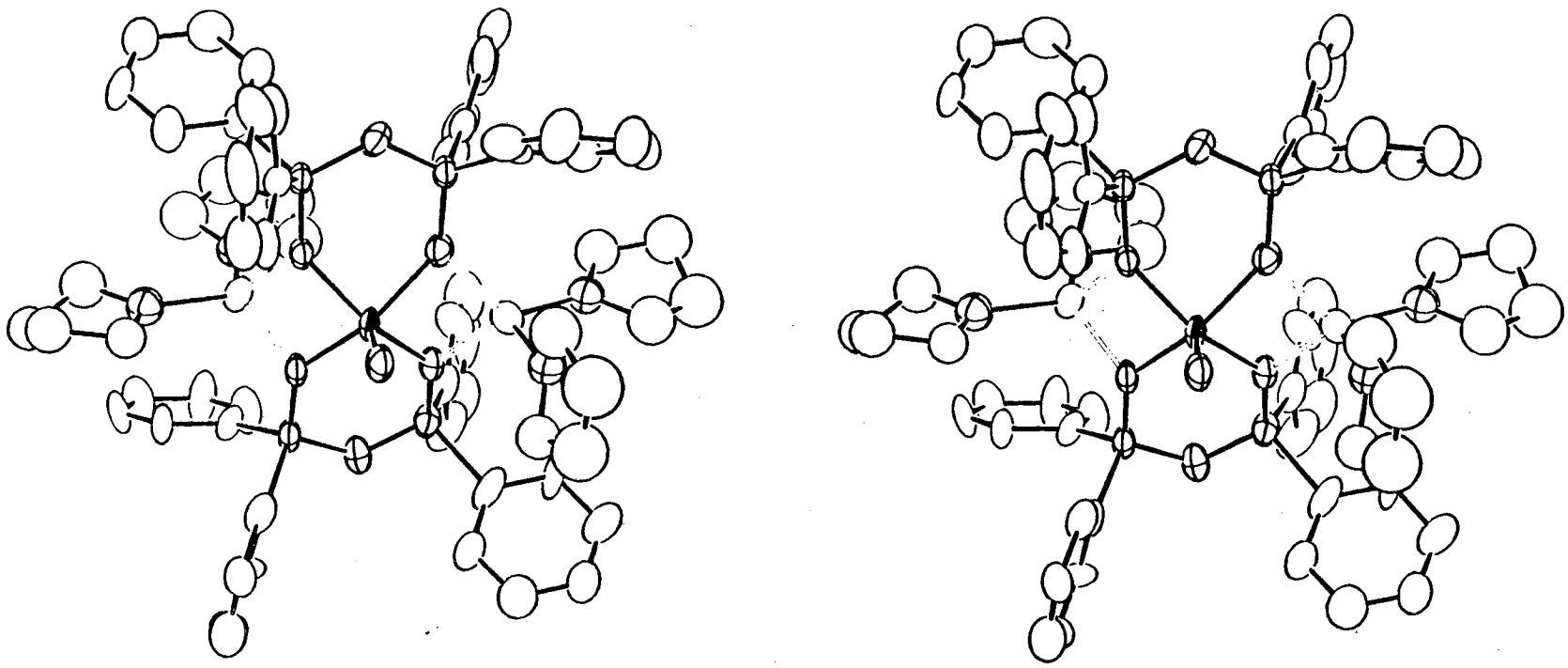

Figure 11. A stereoview of $[Li(THF)_2]_2[VO((OSiPh_2)_2O)_2]$.

Figure 12. A side on view of **5** showing the displacement of the vanadium atom relative to the chelate rings.

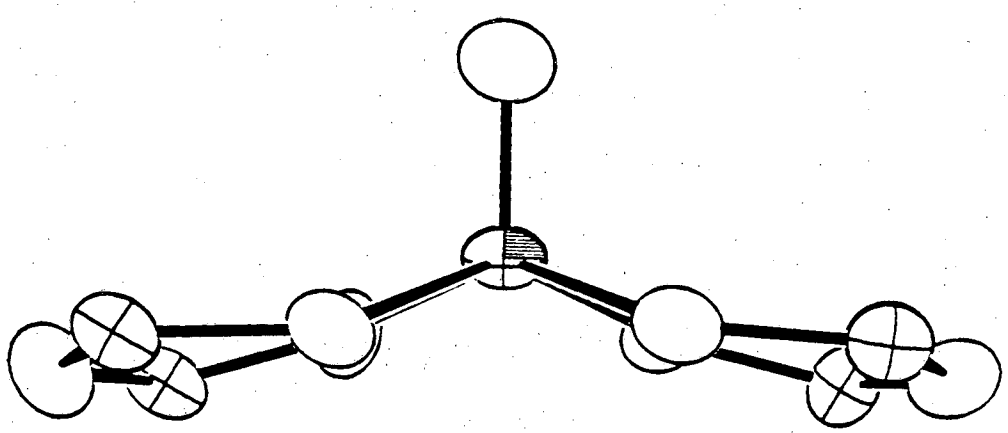

Table IX. Selected Bond Lengths (Å) for $[Li(THF)_2]_2$-$[VO((OSiPh_2)_2O)_2]$

V(1)-O(1)	2.029(8)	Si(1)-O(1)	1.56(1)
-O(2)	1.954(8)	-O(6)	1.627(9)
-O(3)	1.969(8)	-C(1)	1.92(1)
-O(4)	2.017(8)	-C(7)	1.89(1)
-O(7)	1.543(9)		
		Si(3)-O(3)	1.593(9)
Si(2)-O(2)	1.606(9)	-O(5)	1.652(9)
-O(6)	1.627(9)	-C(25)	1.84(1)
-C(13)	1.85(1)	-C(31)	1.89(1)
-C(19)	1.87(1)		
		Si(4)-O(4)	1.59(1)
Li(1)-O(1)	1.96(3)	-O(5)	1.652(9)
-O(4)	1.95(2)	-C(37)	1.90(1)
-O(10)	1.96(3)	-C(43)	1.89(2)
-O(11)	1.95(2)		
		Li(2)-O(2)	1.87(3)
		-O(3)	1.91(3)
		-O(8)	1.96(2)
		-O(9)	1.96(2)

Table X. Selected Bond Angles (deg) for $[Li(THF)_2]_2$-$[VO((OSiPh_2)_2O)_2]$

O(1)-V(1)-O(2)	88.6(3)	O(1)-Si(1)-O(6)	112.9(5)
-O(3)	147.0(4)	-C(1)	110.0(6)
-O(4)	79.6(3)	-C(7)	110.9(6)
-O(7)	107.3(4)		
O(2)-V(1)-O(3)	82.9(3)	O(2)-Si(2)-O(6)	111.4(5)
-O(4)	144.9(4)	-C(13)	112.9(6)
-O(7)	107.2(4)	-C(19)	111.4(6)
O(3)-V(1)-O(4)	89.3(3)		
-O(7)	105.7(4)	O(3)-Si(3)-O(5)	111.6(5)
O(4)-V(1)-O(7)	107.8(4)	-C(25)	110.8(6)
		-C(31)	111.6(6)
O(4)-Si(4)-O(5)	113.3(5)		
-C(37)	111.5(6)	V(1)-O(1)-Si(1)	137.1(5)
-C(43)	109.4(6)		
		V(1)-O(2)-Si(2)	134.2(5)
V(1)-O(3)-Si(3)	135.6(5)		
		V(1)-O(4)-Si(4)	135.8(5)
Si(3)-O(5)-Si(4)	129.1(6)		
		Si(1)-O(6)-Si(2)	127.9(6)

smallest at 83.1(10) and 86.7(10)°, respectively, in both sets. As in all vanadyl(IV) complexes, the vanadium atom lies out of the plane of the chelate rings, in this case by 0.4 Å (Figure 12). The chelate rings are nearly coplaner as evidenced by a dihedral angle of 17°.

Infrared Spectrum

Examination of the solid state structure of 5 revealed that lithium from the $LiOBu^t$ contaminant had been incorporated into the structure of the final product, apparently taking the place of the more familiar cation $H_2NEt_2^+$.

Another surprising feature of the molecular structure was the presence of the oxovanadium(IV) entity, VO^{2+}. Although a blue color has often been considered as an indication of a VO^{2+} species, in fact, vanadyl(IV) complexes range in color from green to maroon and such a conclusion based on the color of the complex was unwarranted. The most significant piece of evidence for the existence of a multiple V-O bond is generally the observation of a relatively pure and energetic metal oxygen stretching vibration which is present with some variation in frequency in all vanadyl(IV) complexes. In Table XI the V=O stretching frequencies are recorded for compounds whose V-O distances have been measured. It is seen that there is a rough correlation between increasing bond length and decreasing frequency. Based on this bond length-stretching frequency

correlation, the V=O absorption in the spectrum of **5** would occur near 996 cm^{-1}, putting it near the edge of the band

Table XI. Bond Lengths and V-O Stretching Frequencies for some Oxovanadium Compounds[a]

Compound	V-O (Å)	V-O stretch (cm^{-1})
$VOCl_3$	1.56	1035
$VO(acac)_2$	1.56	996
V_2O_5	1.58	1020
$[VO(NCS)_4(H_2O]^{2+}$	1.62	982, 963
$V_2O_4(2H_2O)$	1.65	968

a. From ref 18.

assigned to V-O-Si, and nearly on top of the band assigned to Si-O-Si. We were confident in our assignment of the Si-O-Si band, and it was therefore assumed that the V=O and V-O-Si bands were overlapping to form the single broad band centered at 969 cm^{-1}, thus precluding identification of the complex as an oxovanadium(IV) species.

Visible Spectrum and Magnetic Susceptibility

As is commonly found for oxovanadium(IV) species, there were three low intensity absorption bands between 8300-28,600 cm^{-1} observed in the optical spectrum of **5**. Band I occurred at 12,800 cm^{-1}, II occurred at 16,400 cm^{-1}, and III

at 25,000 cm^{-1}. Valek and coworkers[19] have carried out a single-crystal spectroscopic analysis of OV(acac) and have assigned band I as $a^1(d_{x^2-y^2}) \rightarrow b_1(d_{xz}), b_2(d_{yz})$; band II as $b_1(d_{x^2-y^2}) \rightarrow b_2(d_{xy})$; and band III as $a_1(d_{x^2-y^2}) \rightarrow a_1(d_{z^2})$ in agreement with the assignment scheme of Ballhausen and Gray.[20] The structural similarities between 5 and OV(acac)[17] suggest a similar assignment of the peaks in the optical spectrum of 5.

The normal magnetic moment expected for the vanadyl(IV) complexes when the orbital contribution is completely quenched, as it is expected to be by the low symmetry fields, is 1.73 BM. Most of the measured values fall on or close to this ideal value.[18] The measured magnetic susceptibility of 5 was consistent with other vanadyl complexes at a value of 1.79 BM.

Reactivity of 5

Reaction of 5 with either CF_3COOH or H_2O decomposed the vanadosiloxane such that cyclic siloxanes were the only products isolated upon recrystallization of the crude reaction mixture. Interestingly, in the reaction with H_2O, the infrared spectrum of the crude product exhibited peaks at 884 and 851 cm^{-1}, which although somewhat low in frequency, still fell within an acceptable range for V-O-Si stretching vibrations. An Si-O-Si absorption band at 1079 cm^{-1} was also observed corresponding to approximately an

eight-membered ring. Upon recrystallization from acetonitrile, however, the infrared spectrum of the colorless crystals which were isolated contained bands attributable to $(SiPh_2O)_4$ at 1096 cm^{-1}, and $(SiPh_2O)_3$ at 1018 cm^{-1}, with no bands observed in the V-O-Si region. The appearance of the infrared bands at 884 and 851 cm^{-1} was hence attributed to impurities.

Reaction of 5 with H_2O_2 afforded a toluene soluble product which recrystallized from hot hexane as colorless crystals. Surprisingly, the infrared spectrum of the crystals was identical to that of the crude product formed in the reaction of 5 with water. Moreover, reaction of 5 with ^tBuOOH afforded a similar crystalline product from hexane, again with a similar infrared spectrum, but with a broad infrared band of moderate intensity centered at 863 cm^{-1} instead of the two separate peaks observed in the previous two spectra.

The ^1H NMR of the ^tBuOOH product contained a sharp singlet at δ 0.09 ppm consistent with coordination of a ^tBuO- group to vanadium, but the low melting point (91 °C) of the compound was not characteristic of the vanadosiloxanes which had been structurally characterized.

Referring back to the reaction of 5 with water, we were now uncertain whether the disappearance of the bands at 884 and 851 cm^{-1} were due to purification, or due to decomposition of a vanadium complex. The mass spectrum (E.I.) of the

^{t}BuOOH product revealed parent ions for both the cyclic tetramer and the cyclic trimer - an uniformative result since a similar fragmentation pattern was also found for the parent molecule, **5**.

It was probable that only X-ray crystallography could reveal the true structure, but in the absence of such data several conclusions could still be drawn. Based on the infrared data it appeared that the products obtained from reaction of **5** with H_2O, H_2O_2, and ^{t}BuOOH were all the same compound. Further, it could be assumed that the infrared bands in the region between 900 and 850 cm^{-1} were due to a combination of V-O-V and V-O-Si absorption bands which appeared lower in frequency simply because of the mass effect of vanadium versus silicon on vibration.[21]

The rationalizations given above, in conjunction with the infrared data on the Si-O-Si region stated previously, led us to postulate the structure shown below.

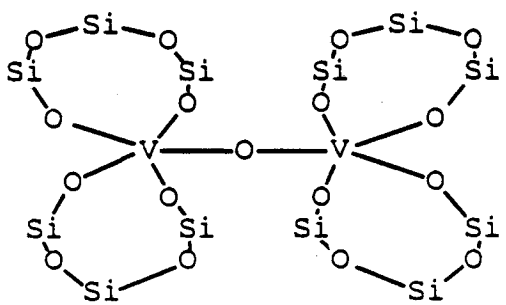

Reaction of $Ph_2Si(OH)_2$ with other Vanadium(IV) Amides

If, as in the titanium system, the basicity of the leaving amine were a dominant factor in the formation of **5**,

it seemed probable that the reaction of $V(NMe_2)_4$ with $Ph_2Si(OH)_2$ would yield a complex similar to 5. Fortunately, $V(NMe_2)_4$ could be made in satisfactory amounts by reaction of $OVCl_3$ with $LiNMe_2$, thus avoiding contamination of the final product with lithium alkoxides.

When $Ph_2Si(OH)_2$ was combined with $V(NMe_2)_4$, a blue green solution was formed. Unlike the earlier reaction with $V(NEt_2)_4$, however, the only crystalline products obtained were cyclic siloxanes.

As stated in the sections on titanium and on vanadium (V), it was desirable to react $Ph_2Si(OH)_2$ with a metal alkoxide which was similar to the metal dialkylamide in order to observe the changes wrought by the alcoholic by-products. Thus, reaction of $V(OBu^t)_4$ with $Ph_2Si(OH)_2$ afforded a tan powder whose infrared spectrum contained bands in the Si-O-Si region at 1121 cm^{-1}, indicative of six-membered rings. Unfortunately, the powder could not be characterized or purified futher because of its insolublility.

<u>Reaction of $Ph_2Si(OH)_2$ with other Transition Metal Amides</u>

The discovery of several new metallosiloxanes and the elucidation of their unusual structures led us to view the rest of the first transition series with anticipation. The differences in behavior observed between titanium and vanadium, however, served as a reminder of our ignorance

with respect to the mechanism of the reaction which had produced **1-4-H_2NEt_2** and 5. Because of the methodolgy that had been chosen, an additional difficulty lay in the lack of homoleptic transition metal dialkylamides beyond chromium, although the trimethylsilylamides of first row transition metals from iron through nickel were known.[22]

Previous reports describing the heterosiloxanes of chromium usually concerned the element in the hexavalent state.[2,23] Schmidbaur[1] reacted octamethylcyclotetrasiloxane and CrO_3 to give a yellow silicon oil described as most probably dimeric with an eight-membered ring structure.

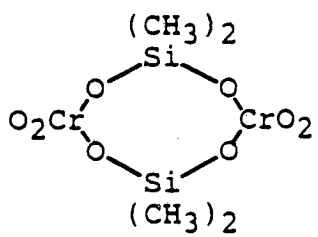

This same structure was also postulated for a corresponding sulfate[1] and is remarkably similar to the structure of 3-**H_2NEt_2**.

As of yet, no heterosiloxanes of manganese are known, although several attempts have been made to prepare $R_3SiOMnO_3$ from $(Me3Si)_2O$ and Mn_2O_7.[1]

A number of low molecular weight heterosiloxanes of trivalent iron are known.[24,25] Polyheterosiloxanes containing the Fe-O-Si structural unit were reportedly produced

from anhydrous $FeCl_3$ and $PhSi(OH)_2ONa$.[26] Preparation of polyferrosiloxanes by treatment of $R_2Si(OH)ONa$ or $RSi(OH)_2ONa$ with FeX_3 was described in a patent; the compounds, which contained structural units $Fe(OSiR_3)$-$OSiR_2$-$OSiR_2$-O-, were not characterized further.[27]

Little is known about heterosiloxanes of cobalt and nickel. Dimeric cobalt trialkylsiloxides have been synthesized[1] and, from the metal acetates, a number of polymers having Co-O-Si and Ni-O-Si structural units have been prepared.[28] The reaction of diorgansilanolates with $CoBr_2$ also leads to cobaltosiloxane polymers of this type.[28]

The rarity of molecular metallosiloxanes has undermined efforts to understand the structural details of the polymeric materials. Though we endeavored to improve this situation, we were apprehensive that many of the previous preparations using $Ph_2Si(OH)_2$ or its monosodium salt had resulted in the isolation of non-crystalline polymers. The route to molecular metallosiloxanes <u>via</u> transition metal dialkylamides had been validated for both vanadium and titanium however, and we hoped it would continue to be a viable method. Unfortunately, the reaction of $Ph_2Si(OH)_2$ with later transition metal dialkylamides did not lead to isolation of any molecular compounds, although many polymeric materials containing the M-O-Si structural unit were formed. Table XII summarizes these reactions.

Table XII. Summary of Late Transition Metal Amide and Alkoxide Reaction Products.

Metal Amide	Equivalents of $Ph_2Si(OH)_2$ added	Product Color	Product Properties
$Cr(NMe_2)_4$	3	green	sol.† glassy solid
$Cr(NEt_2)_4$	1, 2	brown	insoluble solid
$Cr(NEt_2)_4$	3	green	sol.† glassy solid
$Cr\ (NPr^i{}_2)_3$	2.25, 3	green	glassy solid
$Cr(OBu^t)_4$	3	brown	sol.† glassy solid
$Fe[N(SiMe_3)_2]_3$	2.25	yellow	h.c. sol. oil
$\{Co[N(SiMe_3)_2]_2\}_2$	1	purple	sol.† glassy solid
$Zr(NEt_2)_4$	2, 3	white	insoluble solid
$Zr(OBu^t)_4$	3	white	sol.† glassy solid
$Mo(NMe_2)_4$	2	brown	sol.† glassy solid

† Soluble in ether, toluene, THF, CH_2Cl_2, and CH_3CN to give viscous solutions.

Reaction of $Ph_2Si(OH)_2$ with Aluminum and Silicon Dialkylamides

The most suitable elements for modifying a siloxane skeleton by inclusion of heteroatoms are the neighbors of silicon in the periodic table; thus aluminosiloxanes have been among the most numerous compounds encountered in heterosiloxane chemistry. Much of the interest in aluminosiloxanes is due to their relation to the purely inorganic aluminosilicates. In an effort to understand the structures

of the aluminosilicate macromolecules, several of the early X-ray crystallographic structures of heterosiloxanes were concerned with the simple aluminosiloxanes.[29] Recently Interrante and Williams[30] reported that the careful co-hydrolysis of aluminum alkoxides with silicon acetates afforded complexes such as $[Al(acac)(OR)_{2-n}]_x[OSiR_3]_n$ which were useful as precursors for ceramic coatings.

The recent surge of interest in ceramics has also encouraged new research in the area of polysiloxanes. Efforts have been made to synthesize polyorganosiloxane units of definite composition with specific properties, or with size constraints, which could eventually be polymerized in subsequent steps to produce a tailor-made ceramic material.[31] In this approach, the preparation of appropriate polysiloxane units has proven to be a synthetic challenge since there are few known polyorganosiloxanes which are tractable enough to be structurally characterized.[9,11,32]

Unfortunately, none of our reactions with aluminum or silicon dialkylamides produced isolable molecular compounds other than cyclic tetrasiloxanes and trisiloxanes. Table XIII summarizes our results.

Table XIII. Summary of Main Group Dialkylamide Reaction Products.

Metal Amide	Equivalents of $Ph_2Si(OH)_2$ added	Product Color	Product Properties
$[Al(NMe_2)_3]_2$	0.5, 1	colorless	insol. glassy solid
$[Al(NEt_2)_3]_2$	2.25	colorless	insol. glassy solid
$Si(NEt_2)_4$	3	colorless	$(SiPh_2O)_4$, $(SiPh_2O)_3$
$HSi(NEt_2)_3$	2.25	colorless	$(SiPh_2O)_4$, $(SiPh_2O)_3$

References

(1) Schindler, F.; Schmidbaur, H. Angew. Chem. Int. Ed. Eng. **1967**, 6(8), 683.

(2) Chamberlain, M. M.; Dern, G.; Jabs, G.J A.; Germanas, D.; Green, A.; Brain, K.; Wayland, B. B. US Dept. Commerce, Office Techn. Serv., PB Rep. 152086 (1950); Chem. Abstr. **1963**, 58, 2508.

(3) Nakaido, Y.; Akikusa, Y.; Otani, S. Kogyo Kagaku Zasshi **1967**, 70(2), 221.

(4) Vuletić, N.; Djordjević, C. J. Chem. Soc. Dalton **1973**, 1137.

(5) Pauling, L. "The Nature of the Chemical Bond", 3rd ed.; Cornell University Press: Ithaca, N.Y., 1960.

(6) Scheidt, W. R.; Tsai, C.; Hoard, J. L. J. Am. Chem. Soc. **1971**, 93, 3867.

(7) Mimoun, H.; Saussine, L.; Daire, E.; Postel, M.; Fischer, J.; Weiss, R. J. Am. Chem. Soc. **1983**, 105, 3101.

(8) Evans, H. T. Jr. Z. Krist. **1960**, 114, 257; Chem. Abstr. **1961**, 55, 1135.

(9) (a) Hossain, M. A. ; Hursthouse, M. B.; Malik, K. M. A. Acta Cryst. **1979**, B35, 522. Braga, D.; Zanotti, G. Acta. Cryst. **1980**, B36, 950. (b) Bokii, N. G.; Zakharova, G. N.; Struchkov, Yu. T. Zh. Strukt. Khim. **1972**, 13, 291.

(10) Hursthouse, M. B.; Hossain, M. A. Polyhedron **1984**, 3, 95.

(11) Steinfink, H.; Post B.; Fankuchen, I. Acta Cryst. **1955**, 8, 420.

(12) Lazarini, F. Acta Cryst. **1987**, C43, 637.

(13) Griffith, W. P.; Wickins, T. D. J. Chem. Soc. (A) **1968**, 400.

(14) Hyde, J. F.; Frevel, L. K.; Nutting, H. S.; Petrie, P.S.; Purcell M. A. J. Am. Chem. Soc. **1947**, 69, 488.

(15) Zeitler, V. A.; Brown, C. A. J. Chem. Soc. **1957**, 79, 4618.

(16) Alyea, E. C.; Bradley, D. C.; Lappert, M. F.; Sanger, A. T. Chem. Comm. **1969**, 1064.

(17) Dodge, R. P.; Templeton, D. H.; Zalkin, A. J. Chem. Phys. **1961**, 35, 55.

(18) Selbin, J. Chem. Rev. **1965**, 65, 153.

(19) Valek, M. H.; Yeranos, W. A.; Basu, G.; Hon, P. K.; Belford, T. L. J. Mol. Spectrosc. **1971**, 37, 228.

(20) Ballhausen, D. J.; Gray, H. B. Inorg. Chem. **1962**, 1, 111.

(21) Pavia, D. L.; Lampman, G. M.; Kriz, G. S. "Introduction to Spectroscopy"; Saunders College: Philadelphia, 1979; Chapter 2.

(22) Lappert, M. F.; Power, P. P.; Sanger, A. R.; Srivastava, R. C. "Metal and Metalloid Amides"; Ellis Horwood Limited: Chichester, 1980; Chapter 8.

(23) Magomedov, G. I.; Paushkin, Ya. M.; Kirilina, N. I.; Sheludyakov, B. D. G.; Forlov, E. G.; Frenkel, A. S. Dokl. Akad. Nauk. SSSR **1978**, 241, 853; Chem. Abstr. **1978**, 89, 197674.

(24) Schmidbaur, H. Angew. Chem. Int. Ed. Eng. **1963**, 2, 94.

(25) Schmidbaur, H.; Schmidt, M. J. Am. Chem. Soc. **1962**, 84, 3600

(26) Andrianov, K. A.; Ganina, T. N.; Sokolov, N. N. Vysokomolekul. Soedineniya **1962**, 4, 678; Chem Abstr. **1963**, 58, 9239.

(27) Distillers Co. Ltd. Br. Patent 978 666, 1962; Chem Abstr. **1965**, 62, 6650.

(28) Schneider, C.; Berg, G. Makromol. Chem. **1962**, 54, 171.

(29) Wheatley, P. J. J. Chem. Soc. (London) **1963**, 2562; 3200.

(30) Interrante, L. V.; Williams, A. G. Polym. Prep. **1984**, 25, 13.

(31) Mainz, V. V. J. Am. Chem. Soc. **1985**, 107, 8262.

(32) Hossain, M. A.; Hursthouse, M. B.; Malik, K. M. A. Acta Cryst. **1979**, B35, 2258.

Chapter 3

Silicon-29 MASNMR of some Metallosiloxanes[1]

Since 1980, there has been considerable interest in using solid state silicon-29 NMR spectroscopy with "magic-angle" sample spinning (MAS) to investigate the structures of a wide variety of silicate and aluminosilicate materials.[2,3] The interest is due to the sensitivity of the ^{29}Si isotopic shift (δ) to the environment of silicon in tetrahedral (T) sites of zeolitic structures.

During the past few years, as the data bank of ^{29}Si shift values has grown, various correlations have been presented to assist in the interpretation of the observed spectra. For example, a correlation exists between chemical shift (δ) and the mean of the four T-O-T angles (θ) that define a central tetrahedral site in silicates and aluminosilicates.[4,5] Figure 1 presents a least squares treatment of spectroscopic and structural data of the zeolites.[5] A linear correlation is observed between θ and δ according to equation (1).

$$(\delta/\text{ppm from TMS}) = -25.44 - 0.5793\ (\theta/\text{deg}) \qquad (1)$$

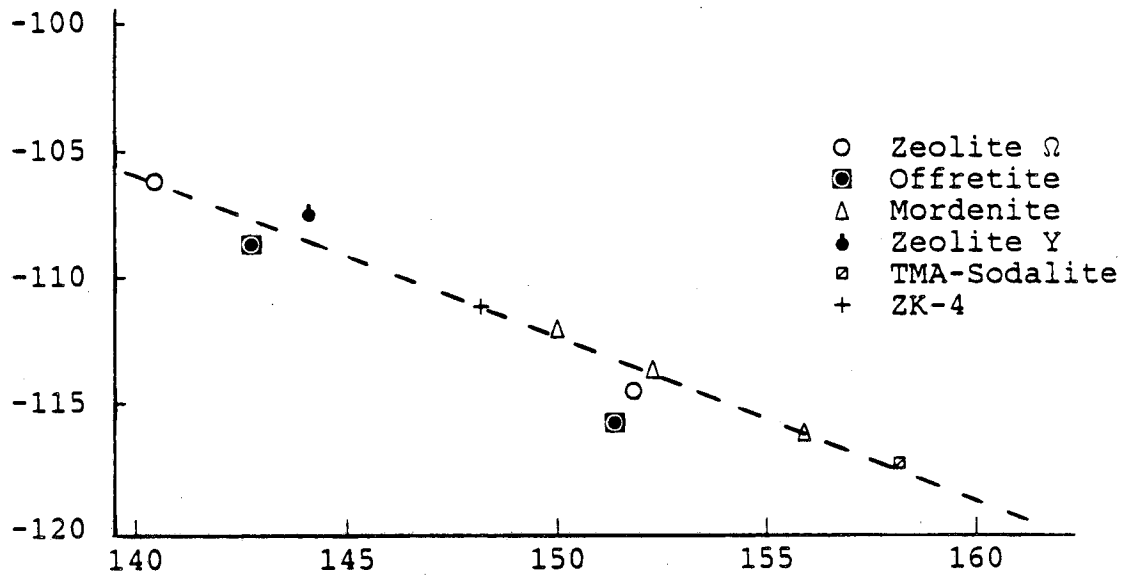

Figure 1. Relationship between the mean T-O-T angle and ^{29}Si chemical shift for the $Si(OSi)_4$ signals in zeolites.[5]

Grimmer and Radeglia[6] have also shown a correlation between Si-O bond length and δ (^{29}Si) according to equation (2).

$$\overline{d\ Si\text{-}O}\ (nm) = 0.1697 + 8.4 \times 10^{-5}\ \bar{\delta}\ (ppm) \qquad (2)$$

From this relationship it follows that a decrease in the mean Si-O bond length corresponds to a high field shift of the isotropic mean values of the chemical shift.

The best correlation between experiment and prediction in silicon-29 NMR thus far is that based on group electronegativities.[7] Janes and Oldfield[8] have utilized this approach with a total of 99 sites in 51 different minerals with a mean agreement between experimental and predicted

chemical shift of 1.96 ppm. Although the δ/EN correlation has thus far only been applied to silicates and aluminosilicates, the calculation of group electronegativities may provide a method to account for different ligand types rather than being strictly limited to SiO_4 and $Si(OAl)_n$-$(OSi)_{4-n}$ tetrahedra.

Unfortunately, because of their current restrictions none of the above correlations can be directly extended to **1-4-H_2NEt_2** or other similar molecular metallosiloxanes. Since there have been no comparable reports on the silicon-29 MASNMR of molecular metallosiloxanes or polysiloxanes which would allow us to predict the chemical shift of each unique silicon atom in the spectra of **1-4-H_2NEt_2**, an effort was made to interpret the observed signals by applying the general chemical shift trends that were common to most of the chemical shift-physical parameter correlations.

Both Lippmaa[9] and Janes[8] have observed a correlation between cation-framework oxygen interactions and silicon-29 chemical shifts; they apparently disagree, however, as to the direction of the shift. Janes and Oldfield[8] have stated that increased shielding was observed for overbonded (more electronegative) oxygen, while Lippmaa et al.[9] has reported that decreasing cation size or the presence of acidic protons results in a downfield shift. It would appear that a downfield shift is more likely since in the solution spectra of a series of related silanes[10], δ moves downfield

as an increasing positive charge develops on Si (Table I).

Table I. Variation of δ (^{29}Si) with Increasing Electron-withdrawing Ability of Substituents[a]

compound	δ (^{29}Si)[b]
Me_3SiOMe	17.2
$Me_3SiOCOCH_3$	21.5
$Me_3SIOCOCF_3$	34.2
$Me_3SiOSO_2CF_3$	46.6
Me_3SiOSO_2F	52

a from ref 10. b ppm from external Me_4Si.

A comparison of chemical shift trends in solution and solid state spectra has been demonstrated to be valid based on the observation that chemical shifts do not change appreciably in the spectra of compounds measured by each of the two methods.[2,9]

For **1-H_2NEt_2** there are eight crystallographically inequivalent silicon atoms contained in two independent molecules in the ratio of 2:2:1:1:2:2:1:1. As the silicon-29 MASNMR spectrum in Figure 2 shows however, only six peaks could be resolved from the broad signal centered at δ -41.0 ppm. Coincidental equivalence of silicon atoms in similar chemical environments undoubtably accounts for the difference between the predicted (8) and observed (6) number of peaks. An obvious way to group the silicon atoms

Figure 2. ^{29}Si MASNMR Spectrum of $[H_2NEt_2]_2[Ti_4O_2(OH)_2(OSiPh_2O)_6]\cdot CH_3CN$ in ppm relative to $[Si_8O_{12}](OCH_3)_8$ at 12.5 ppm.

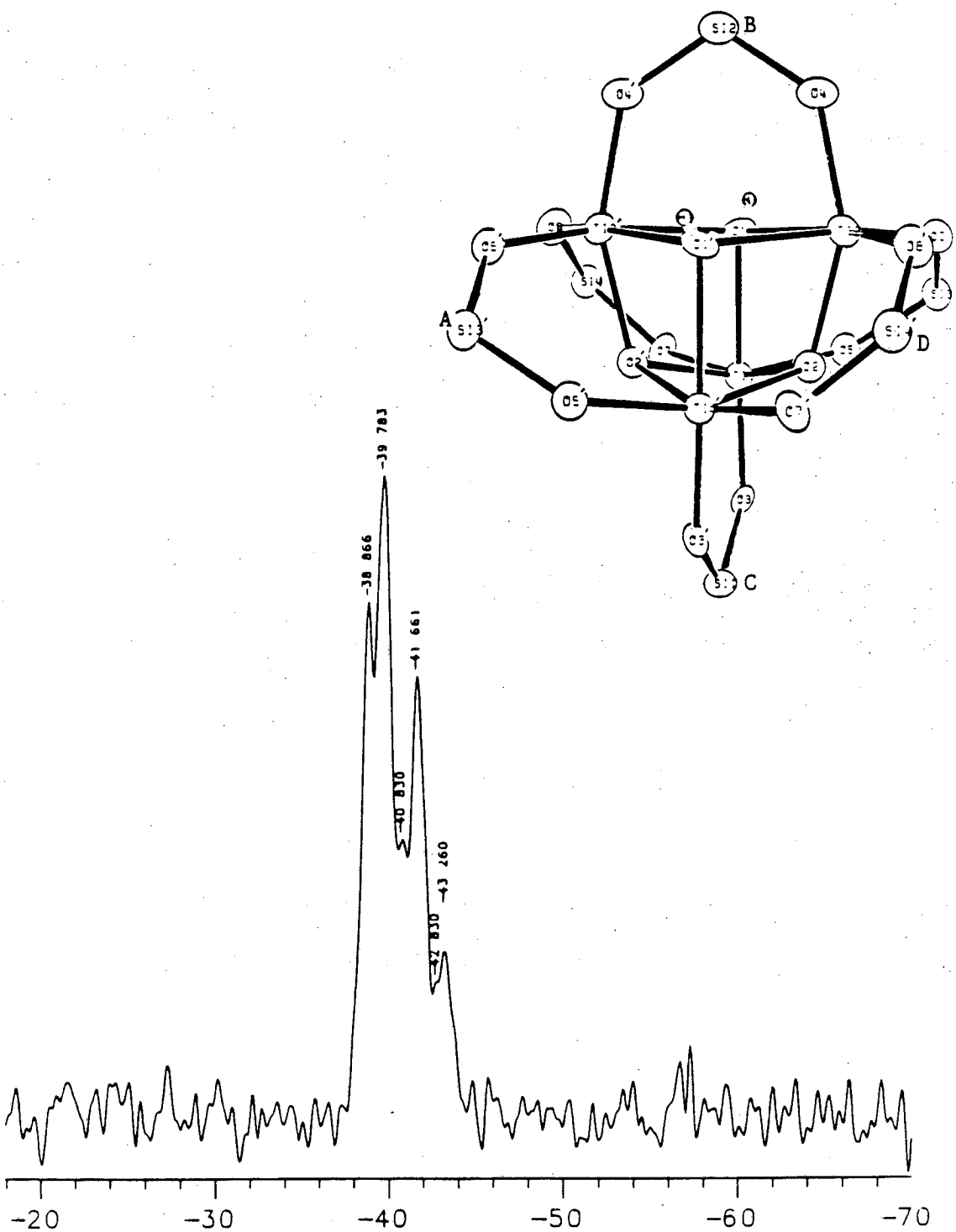

is according to their relative proximity to the diethylammonium cations. Thus, A, A',C and D' are all bonded to oxygens involved in hydrogen bonding with the cation, while B, B', C'and D are bonded to two-coordinate oxygen atoms. Since we have differentiated the silicon atoms which are in similar chemical environments but are located in crystallographically independent molecules by primed letters, it follows that A and A' can logically be considered coincidentally equivalent. If C and D' are grouped together, and B, B', C' and D are taken to be independent of one another, we can then predict six groups in the ratio of 4:3:1:1:1:2. Rearranging the groups to fit the observed area ratios, we make the assignments listed in Table II.

Table II. Assignments of δ (^{29}Si) for **1-H_2NEt_2**

chemical shift (ppm)†	Si atom (area)
-38.9	C, D' (3)
-39.8	A, A' (4)
-40.8	C' (1)
-41.7	D (2)
-42.8	B (1)
-43.3	B' (1)

† Relative to the largest peak in the $Si(CH_3)_3$ region of $[Si_8O_{12}](OCH_3)_8$.[11]

In accordance with the observations made by Lippmaa and coworkers[9], we are able to assign the downfield resonances

to the silicon atoms which are affected most by cationic interactions and the farthest upfield resonance to the silicon atom located farthest from the cations.

Interestingly, the silicon-29 MASNMR spectrum of **2-H_2NEt_2** reveals a single peak at δ -40.0 ppm with $w_{1/2}$ equal to 197 Hz (Figure 3). In the crystal there are four inequivalent silicon atoms in the ratio of 2:2:2:1. No interactions of the siloxy-oxygen atoms with the cation exist, although Si(2) is bonded to an oxygen that is involved in hydrogen bonding with a water molecule. Two structural features which are expected to set Si(3) apart are the Si(3)-Si(3') interaction and the nearly linear Ti(1)-O(5)-Si(3) bond angle. Nevertheless, the chemical environment for each Si atom is similar, and given the line width relative to the expected chemical shift difference, we are forced to conclude that all of the silicon atoms are coincidentally equivalent.

For **1-NMe_4**, where no interaction of the anionic complex with the tetraalkylammonium cations is expected to occur, we also observed a single line in the ^{29}Si NMR spectrum at δ -42.0 ppm, with $w_{1/2}$ = 191 Hz. The complex is expected to be structurally similar to **1-H_2NEt_2** and should contain at least four unique silicon atoms, although the chemical shift difference between them may be small. The X-ray crystal structure of **1-NMe_4** has not yet been determined. The apparent equivalence, or small chemical shift difference, of

Figure 3. ^{29}Si MASNMR Spectrum of a) $[H_2NEt_2]_2[Ti_4O_2(OH)_2(OSiPh_2O)_5((OSiPh_2)_2O)]\cdot PhMe\cdot 2H_2O$ in ppm relative to $[Si_8O_{12}](OCH_3)_8$ at 12.5 ppm.

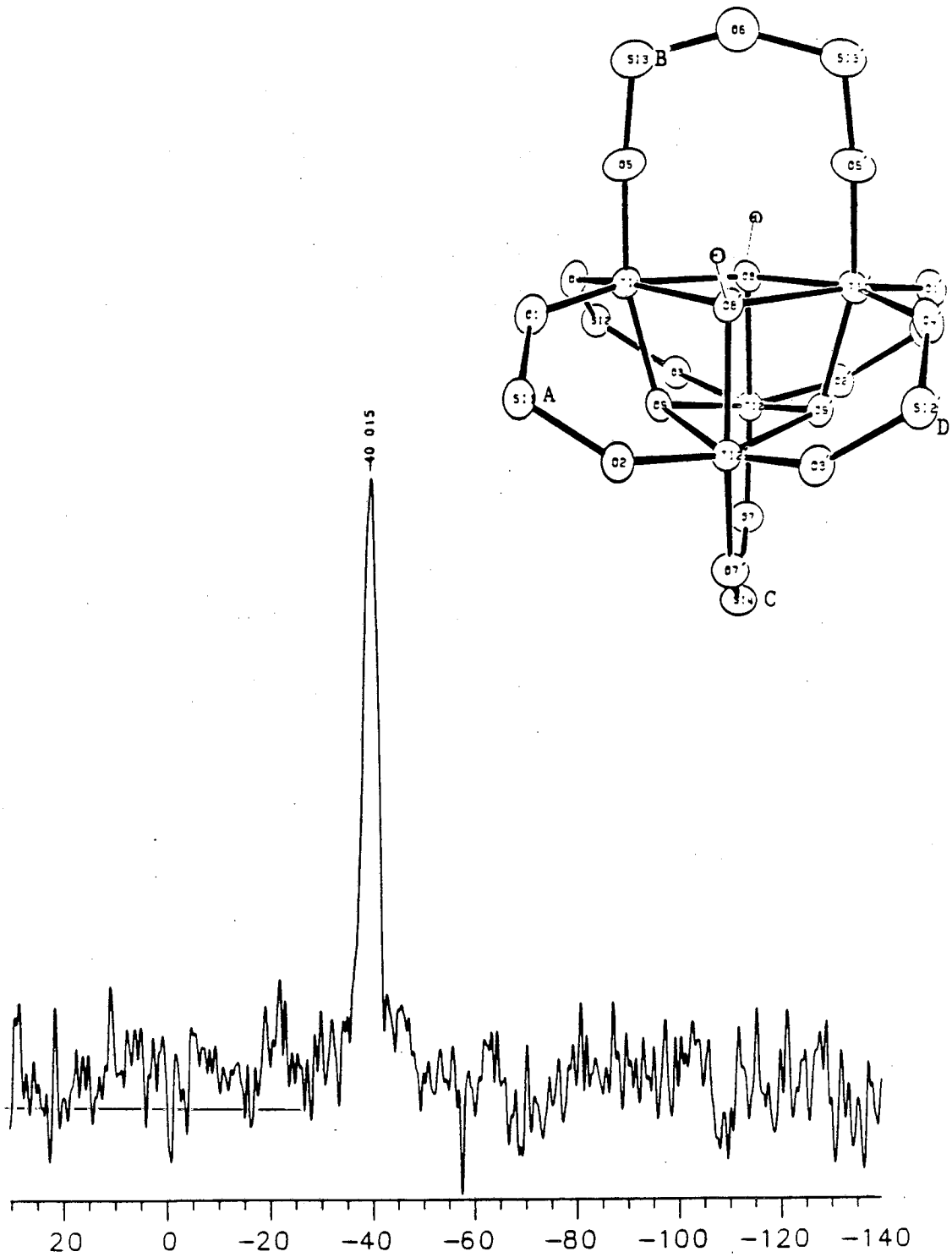

Figure 4. ^{29}Si MASNMR Spectrum of $Ti((OSiPh_2)_4O)_2$ in ppm relative to $[Si_8O_{12}](OCH_3)_8$ at 12.5 ppm.

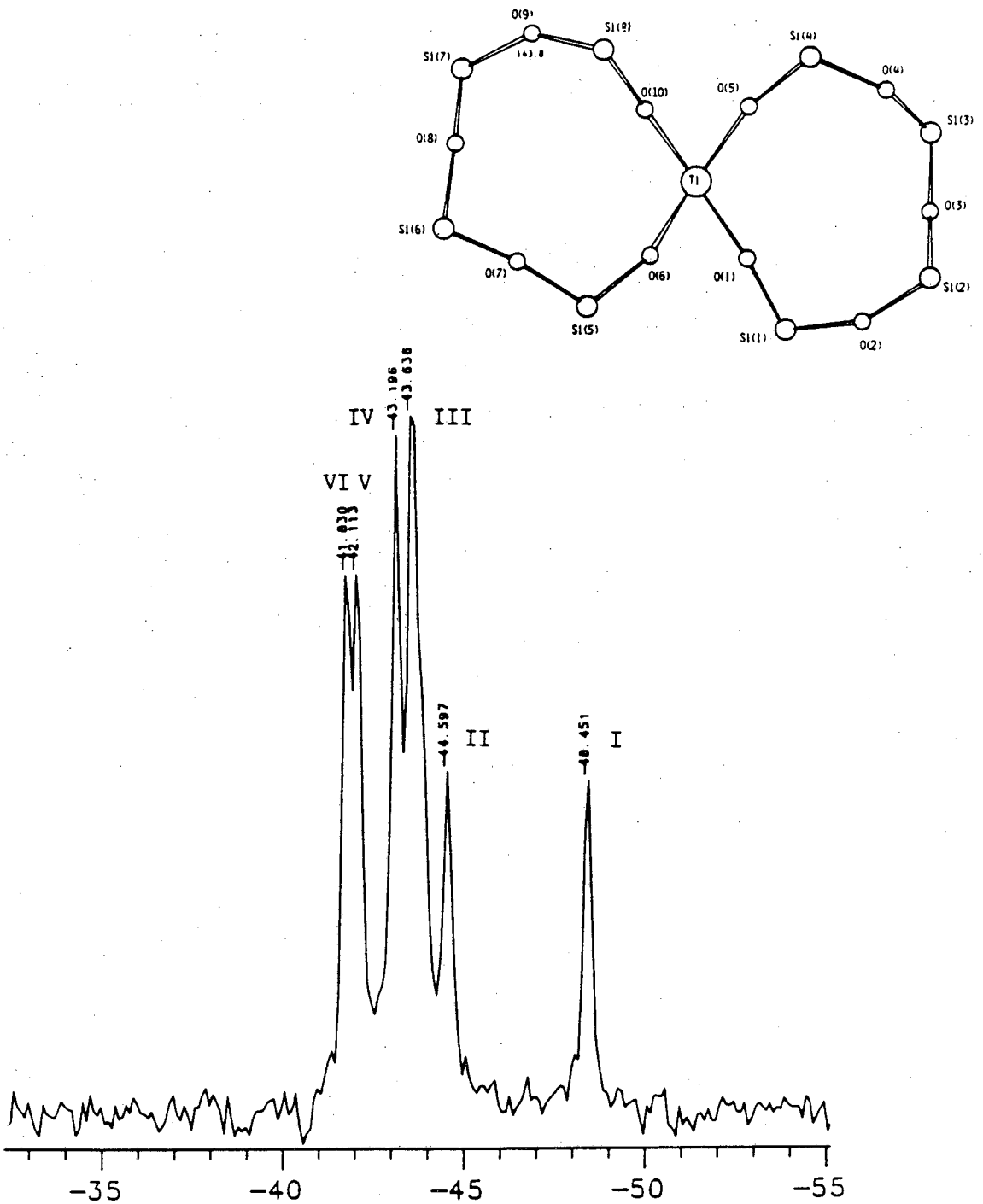

the silicon atoms in **2-H_2NEt_2** and **1-NMe_4** is perhaps disturbing, for it indicates that the ^{29}Si chemical shift is not very sensitive to the crystallographic environment of the silicon in the metallosiloxane complexes, but rather, sensitive only to the local environment around each silicon.

Given the apparent lack of sensitivity we were surprised to find that the spectrum of $Ti((OSiPh_2)_4O)_2$ contained six well-defined peaks (I-VI, Figure 4) in an apparent ratio of 1:1:2:2:1:1. In the crystal there are eight unique silicon atoms.[12] Since there are no hydrogen bonds or unusual close contacts to justify separation of the peaks, the Si-O-M angles and the relative proximity of each silicon to the titanium atom can form the basis for assigning the observed peaks to a given silicon atom; the Si-O-Si angles within $Ti((OSiPh_2)_4O)_2$ vary from 143.8 to 172.5°, and the Ti-O-Si angles vary from 156.4 to 173.3°.[12] Based on the correlations made for the silicates,[4] large Si-O-Si angles should result in an upfield shift. Opposing the upfield shift, in aluminosilicates, is a downfield shift which accompanies substitution of silicon by less electronegative heteroatoms such as aluminum.[5] Although the reason for the downfield shift for $Si(OAl)_n(OSi)_{4-n}$ is not clear, we postulate that substitution of silicon with titanium would have a similar effect on δ (^{29}Si) <u>when the M-O-Si angle is large</u>. Hursthouse[12] has proposed that the large (i.e.→180°) Ti-O-Si bond angles in $Ti((OSiPh_2)_4O)_2$ imply

O→Ti π-bonding. If such π-bonding were present, the strong Ti-O bond may leave the adjacent silicon atom less electron rich than if it were next to another Si-O group, consequently deshielding the silicon atom and shifting δ downfield. Table III shows a distribution of the inequivalent silicon atoms into six different classes based on a balance between bond angle and heteroatom shift criteria. It now becomes possible to rationalize the appearence of a single resonance in the spectrum of **2-H_2NEt_2**. For Si(3) the large M-O-Si angle acts to move δ upfield, while O→Ti π-bonding

Table III. Classification of Inequivalent Silicon Atoms in $Ti((OSiPh_2)_4O)_2$

class		bonded to oxygen adjacent to Ti	average Si-O-M angle of bonded oxygens
I	Si(6)	no	167
II	Si(5)	yes	164
III	Si(1), Si(8)	yes	162, 158
IV	Si(7), Si(2)	no	153, 154
V	Si(4)	yes	155
VI	Si(3)	no	151

acts to move δ by an approximately equal amount downfield. Thus, there is no overall change in δ and overlap of the signals from inequivalent silicon atoms is the observed result.

In the vanadosiloxanes, the spectrum of **3-H_2NEt_2** exhibits one peak corresponding to one type of silicon in the crystal structure. Figure 5 shows that the single resonance occurs at -35.2 ppm with $w_{1/2}$ = 95 Hz, well downfield of the silicon resonances in the titanosiloxanes. The spectrum of **4-H_2NEt_2** is more complex (Figure 6), containing two strong signals and several unresolved, low-intensity signals. The X-ray crystal structure of **4-H_2NEt_2** reveals an asymmetric unit with two independent molecules containing a total of six inequivalent silicon atoms. Based on the same two criteria that were used to assign the spectrum of $Ti((OSiPh)_4O)_2$, the peaks in **4-H_2NEt_2** were tenatively assigned: δ -44.6 ppm to Si(2), δ -43.1 ppm to Si(5), the two doublets centered at δ -40.7 and -40.2 ppm to Si(4) and Si(6), respectively, and the two doublets centered at δ -37.6 and -36.6 ppm to Si(1) and Si(3), respectively. The interpretation of the spectrum of **4-H_2NEt_2** is complicated by the possibility of polymorphism, making assignment of the observed chemical shifts based on Si-O-Si bond angle an uncertain task at best. However, if the structure of the unknown polymorph contains smaller angles around oxygen (see infrared discussion in Chapter 2) a slight downfield shift should be observed in δ (^{29}Si). With this model, the doubling of the four peaks centered at δ -40.7, -40.2, -37.6 and -36.6 ppm can be understood in terms of a small change

Figure 5. ^{29}Si MASNMR Spectrum of $[H_2NEt_2]_2[V_2O_4(OSiPh_2O)_2]$ in ppm relative to $[Si_8O_{12}](OCH_3)_8$ at 12.5 ppm.

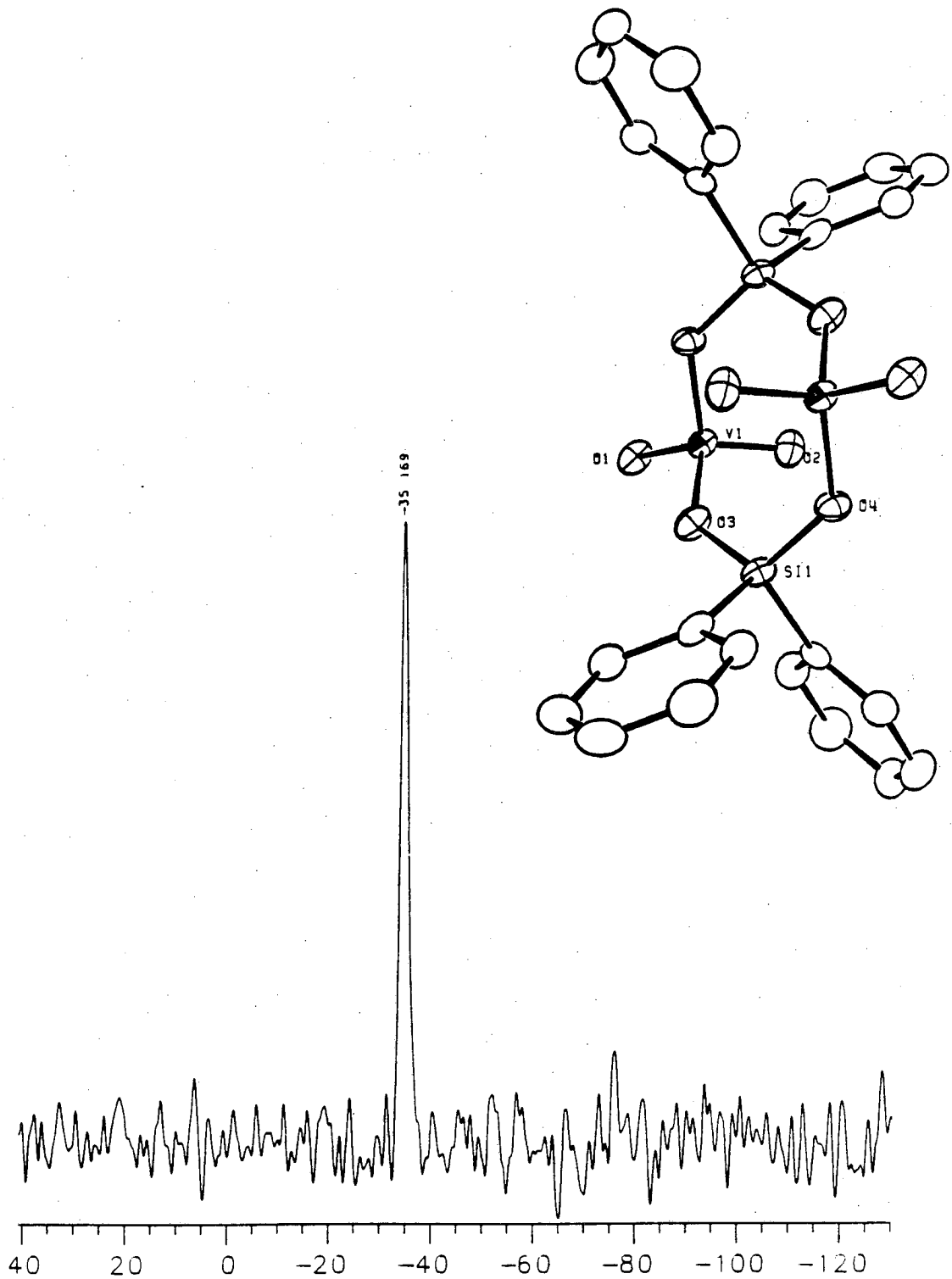

Figure 6. ^{29}Si MASNMR Spectrum of $[H_2NEt_2][VO_2((OSiPh_2)_3O)]$ in ppm relative to $[Si_8O_{12}](OCH_3)_8$ at 12.5 ppm.

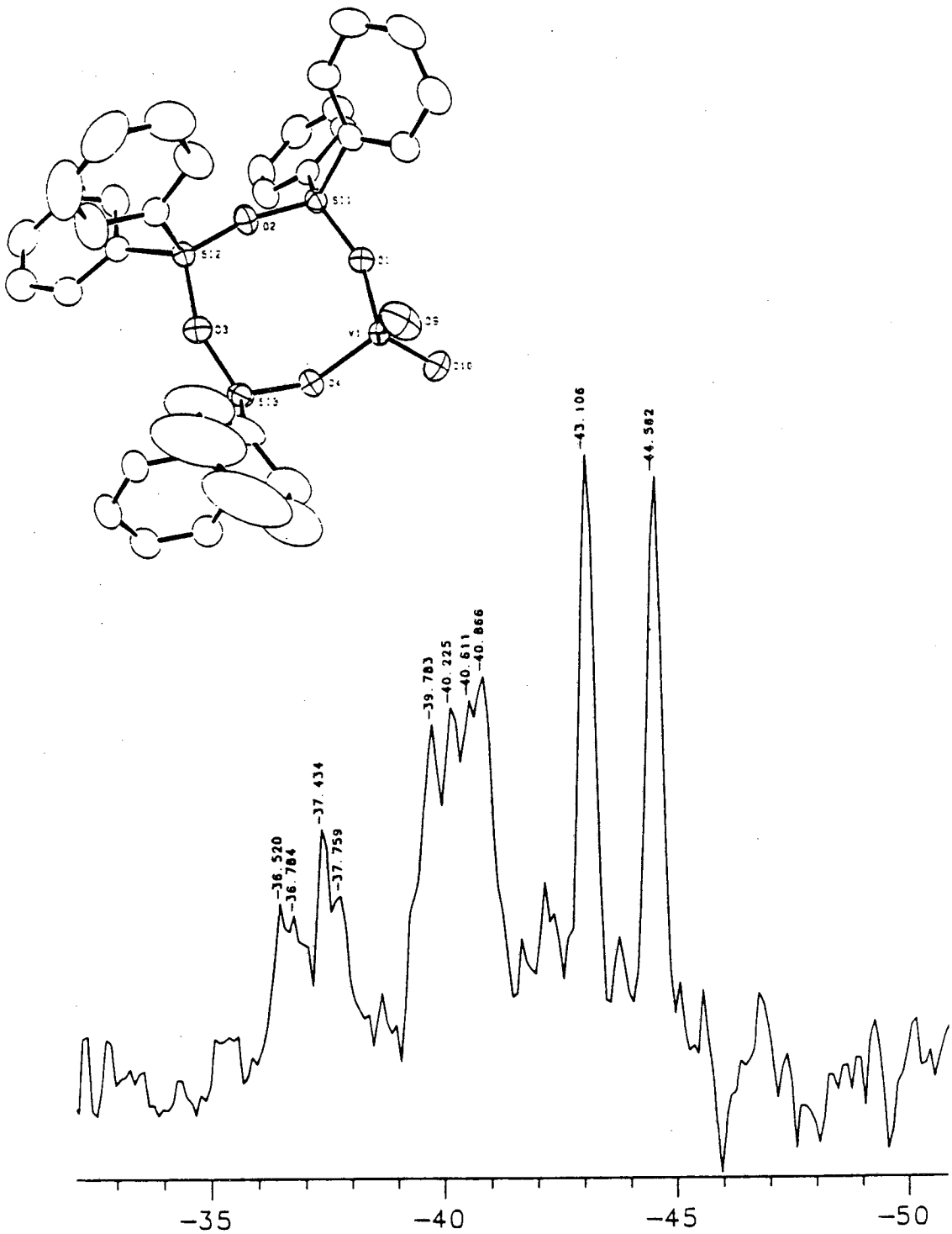

in the M-O-Si angles around neighboring oxygen atoms for Si(1), Si(3), Si(4) and Si(6) with no significant change in the oxygen bond angles near Si(2) and Si(5). The small shift differences observed for the silicon atoms closest to vanadium indicates that most of the distortion from the known structure involves a decrease in the V-O-Si bond angles, resulting in greater displacement of the vanadium atom from the Si_3O_4 plane.

A plot of the chemical shift data versus the average M-O-Si (M = Si, Ti, V) bond angle, θ, is given in Figure 7. Although there is an obvious correlation between the two parameters, the data for the bridged compounds (**1-H_2NEt_2**, **3-H_2NEt_2**) do not fall on the same line as those for the chelated compounds (**4-H_2NEt_2** and $Ti((OSiPh_2)_4O)_2$). It is reassuring, however, that the assignments made for **1-H_2NEt_2**, which were based solely on cation interactions, also show that an increase in θ is accompanied by an upfield shift of δ.

For the siloxane chelates there appears to be two slightly overlapping shift ranges which correspond to the size of the siloxane rings: -36.5 to -44.5 ppm, eight-membered ring; -41.5 to -48.5 ppm, ten-membered ring. Because we have obtained ^{29}Si MASNMR data on only two structurally characterized examples, it is impossible to say whether or not the observed shift ranges will prove viable for deducing ring size in similar complexes. Unfortunately,

Figure 7. A plot of chemical shift, δ (^{29}Si), as a function of the average Si-$O_{a,b}$-Si bond angle, (θ), where O_a and O_b are O_a-Si-O_b.

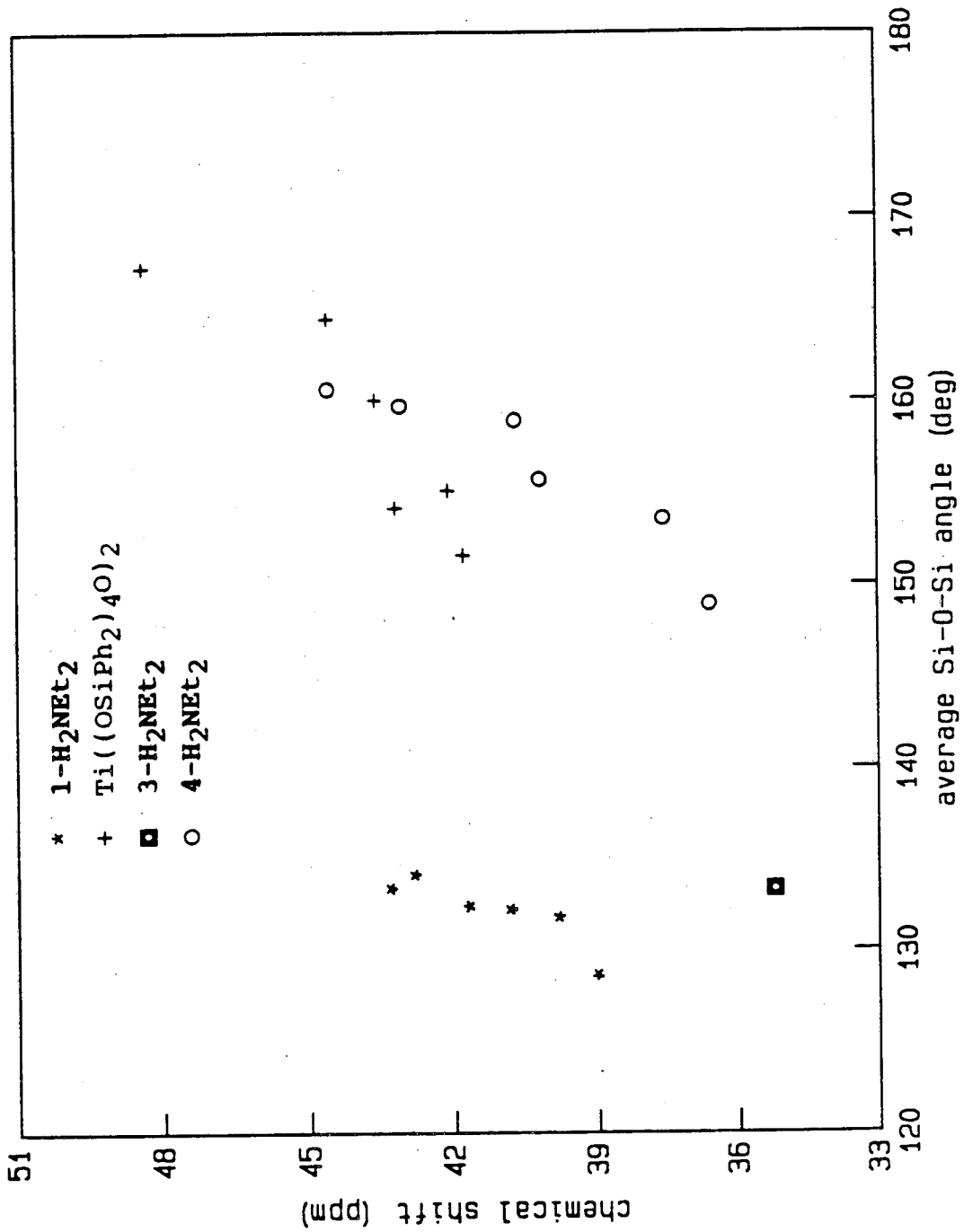

we have not found any comparable NMR data on the cyclic tri- and tetra-siloxanes which could support or refute these qualitative observations.

In conclusion, we find that intermolecular forces (hydrogen bonding) appear to affect the ^{29}Si chemical shift by about the same magnitude (3-5 ppm) as intramolecular forces (π-bonding). We have observed that δ (^{29}Si) is shifted upfield for silicon atoms involved in large Si-O-M bond angles, and downfield by an approximately equal amount when M = Ti, V. Measurement of the silicon-29 MASNMR of other complex metallosiloxanes will be necessary before reliable chemical shift trends can be offered, and before this technique can be used to accurately predict structure in the absence of crystallographic data.

References

(1) All spectra were recorded by Dr. V. V. Mainz, Department of Chemistry and Materials Research Laboratory, University of Illinois, Urbana, Illinois.

(2) Lippmaa, E.; Magi, M.; Samoson, A. ; Engelhardt, G.; Grimmer, A. R. J. Am. Chem. Soc. **1980**, 102, 4889.

(3) Lippmaa, E.; Magi, M.; Samoson, A.; Tarmak, M.; Engelhardt, G. J. Am. Chem. Soc. **1981**, 103, 4992.

(4) Grimmer, A. R.; Von Lampe, F.; Tarmak, M.; Lippmaa, E. Chem. Phys. Lett. **1983**, 97, 185.

(5) Thomas, J. M.; Klinowski, J.; Ramdas, S.; Hunter, B. K.; Tennakoon, D. T. B. Chem. Phys. Lett. **1983**, 102, 158.

(6) Grimmer, A. R.; Radeglia, G. Chem. Phys. Lett. **1984** 106, 262.

(7) Ernst, C. R.; Spialter, L.; Buell, G. R.; White, D. L. J. Am. Chem. Soc. **1974**, 96, 5375.

(8) Janes, N.; Oldfield, E. J. Am. Chem. Soc. **1985**, 107, 6769.

(9) Lippmaa E. T.; Alla, M. A.; Pehk, T. J.; Engelhardt, G. J. Am. Chem. Soc. **1978**, 100, 1929.

(10) Olah, G. A.; Field, L. D. Organometallics **1982**, 1, 1485.

(11) Mainz, V. V. J. Am. Chem. Soc. **1985**, 107, 8262.

(12) Hursthouse, M. B.; Hossain, M. A. Polyhedron **1984**, 3, 95.

Experimental

General

Infrared spectra were recorded on a Nicolet 5DXFTIR spectrophotometer as Nujol mulls between CsI windows or as neat liquids (thin film) between KBr windows. Low resolution mass spectra (electron impact) were taken on an AEI MS 12 mass spectrometer. High resolution mass spectra (fast atom bombardment) were taken on a Kratos MS 50 mass spectrometer. ^{1}H (250.8 or 201.9 MHz) and ^{13}C (50.8 MHz) NMR spectra were measured on the UCB 250 or 200 superconducting FT instruments. ^{1}H NMR data are presented as follows: chemical shift on the δ scale (relative to C_6D_6 as 7.15 ppm, $CDCl_3$ as 7.24 ppm, Me_2CO as 2.05 ppm, or CD_3CN as 1.93 ppm) (multiplicity, number of protons, coupling constants in Hertz). ^{13}C NMR data are presented as follows: chemical shift on the δ scale (relative to C_6D_6 as 128.0 ppm). ^{29}Si MASNMR spectra were recorded by Dr. V. V. Mainz, Department of Chemistry and Materials Research Laboratory, University of Illinois, Urbana, Illinois. ^{29}Si MASNMR data are presented as follows: chemical shift on the δ scale (relative to $[Si_8O_{12}](OCH_3)_8$ as 12.5 ppm). Melting points and boiling points are uncorrected. The optical spectra were measured on a Perkin-Elmer Lambda 9 UV-VIS-NIR spectrophotometer. Elemental analysis were performed by the Microanalytical Laboratory, operated by the College of Chemistry, University of California, Berkeley. Magnetic susceptibility

measurements were performed by D. Berg on an S.H.E. Corp. model 905 SQUID magnetometer at two field strengths (5, 40 kG) for each temperature. Conductivities were measured with a Barnstead conductivity bridge, model PM-70CB at 25 °C. The cell constant was determined by use of a standard aqueous solution of potassium chloride.

All work was conducted under an inert atmosphere (N_2) using standard Schlenk techniques, or in an inert atmosphere glovebox. Pentane, hexane, THF, diethyl ether, dichloromethane and toluene were distilled from Na/benzophenone immediately prior to use. Deuterated benzene for NMR studies was distilled from molten potassium and stored over sodium. Spectrograde acetonitrile and nitromethane for conductivity studies were stored over 3 Å sieves and used without further purification. Diethylamine and diisopropylamine were distilled from barium oxide and stored over 3 Å sieves. t-Butanol was dried over $Mg(OBu^t)_2$, prepared by refluxing Mg turnings in t-BuOH with a small amount of dibromoethane, for 48 hours prior to use. Anhydrous ethanol was stored over BaO. Zirconium tetrachloride was purified by sublimation. Lithium aluminum hydride was purified by Sohxlet extraction with diethyl ether. Trimethylamine hydrochloride was dried by allowing it to stand in warm air above a drying oven for 4 days, then grinding it to a fine powder and heating it on a hot water bath under dynamic vacuum for an additional day. The complexes $LiOBu^{t}$1,

$[Al(NMe_2)_3]_2$[2], and CuCl[3], were prepared according to literature methods, and J. Stewart supplied the $NaNPh_2$. All other materials were obtained from commercial suppliers and used without further purification.

Starting Materials

$AlH_3 \cdot NMe_3$. Trimethylamine alane was prepared according to the method of Ruff and Hawthorne[4] with the following modifications: In a drybox, a sample of finely ground $LiAlH_4$ (1.50 g, 39.5 mmol) was added to anhydrous Me_3NHCl (3.10 g, 32.4 mmol) in a 200 mL flask. Upon mixing, the two solids liberated heat. The mixture was removed from the drybox and cooled to -70 °C. Diethyl ether (80 mL) was slowly added to the flask, then the solution was allowed to warm to room temperature with stirring. As the reaction mixture warmed, hydrogen was evolved. After stirring for 17 h, the mixture was filtered, and the clear filtrate was evaporated to dryness under reduced pressure. The white residue was sublimed (60 °C/0.2 mm) to yield colorless crystals (1.8 g, 51%), mp 74-75 °C (lit.[4], 76 °C). IR (Nujol) 1785 vbrs, 1623vbrs, 1461brs, 1405m, 1377s, 1250s, 1222m, 1004brs, 980-480 vbrs cm^{-1}.

$[Al(NEt_2)_3]_2$. To $AlH_3 \cdot NMe_3$ (1.80 g, 20.2 mmol) at -60 °C was added $HNEt_2$ (ca. 50 mL, 483 mmol). The mixture was

allowed to warm slowly to room temperature with stirring and hydrogen was evolved. After heating to reflux for 20 h, the cloudy white solution was evaporated to a viscous liquid under reduced pressure and dried by heating to 70 °C under dynamic vacuum to leave a solid white residue. The residue was extracted with ether (3 x 20 mL) and the combined extracts were concentrated to ca. 5 mL and cooled to -10 °C. The resultant colorless crystals were collected and dried under reduced pressure. A second crop of crystals was obtained by concentrating the mother liquor to ca. 1 mL and cooling to -10 °C. The total yield was 1.5 g, 15%, mp 167-168 °C[5]. IR (Nujol) 1461s, 1377s, 1342m, 1285m, 1257w, 1187s, 1159s, 1131m, 1103m, 1068m, 1040m, 1019s, 1004m, 906m, 892m, 850m, 786s, 723w, 667m, 646m, 625s, 583m, 477m, 407s cm^{-1}. ^1H NMR (C_6D_6): δ 1.06 (t, 12, J = 7), 1.17 (t, 24, J = 7), 3.01 (q, 8, J = 7), 3.10 (q, 16, J = 7). Anal. calcd for $C_{12}H_{30}N_3Al$: C, 59.2; H, 12.4; N, 17.3. Found: C, 57.0; H, 12.0; N, 16.5.

$BrSi(NEt_2)_3$. A solution of $SiBr_4$ (4.8 mL, 39 mmol) in toluene (8 mL) was added dropwise to a suspension of $Mg(NEt_2)_2$, prepared from Bu_2Mg (186 mL, 131 mmol) and $HNEt_2$ (30.0 mL, 290 mmol), in toluene (100 mL). The mixture was refluxed for 2.5 h to give a clear, bright yellow, viscous solution. Toluene was evaporated under reduced pressure to give a viscous orange residue. The residue was distilled

(115 °C/0.18 mm) to give a pale yellow liquid (11.31 g, 90%). ^{1}H NMR (C_6D_6): δ 0.95 (t, 6, J = 7), 1.15 (t, 3, J = 7), 2.95 (q, 6, J = 7).

$Si(NEt_2)_4$ and $HSi(NEt_2)_3$. Addition of $Mg(NEt_2)_2$, prepared from Bu_2Mg (49.5 mL, 34.9 mmol) and $HNEt_2$ (7.3 mL, 70 mmol), to neat $BrSi(NEt_2)_3$ (11.3 g, 34.9 mmol) gave a paste. The mixture was heated under nitrogen at 150 °C for 7 h, then cooled to room temperature and the residue was extracted twice with diethyl ether (ca. 20 mL). The diethyl ether was evaporated under reduced pressure, and distillation of the residue gave a continuous fraction that boiled in the range 80-120 °C/0.18 mm (4.00 g). The liquid was carefully redistilled to yield two fractions: (a) $HSi(NEt_2)_3$ (1.6 g, 19%), bp 55 °C/0.09 mm (lit.[6], 62-65 °C/1 mm). IR (thin film) 2108 brm, 1461m, 1377s, 1342m, 1293m, 1208s, 1180s, 1103m, 1075w, 1053m, 1025s, 934s, 906m, 842vbrs, 794m, 681m, 625w, 505m cm^{-1}. ^{1}H NMR (C_6D_6): δ 1.03 (t, 18, J = 7), 2.90 (q, 12, J = 7), 4.61 (s, 1). MS: (E.I.) 245 M^+, 173 $(M-NEt_2)^+$; and **$Si(NEt_2)_4$** (1.6 g, 15%), bp 90 °C/0.09 mm (lit.[7], 156-158 °C/14 mm). IR (thin film) 1461m, 1377s, 1342m, 1293m, 1201s, 1173s, 1103m, 1075w, 1054m, 1025s, 927s, 794m, 780m, 688s, 519m, 505m cm^{-1}. ^{1}H NMR (C_6D_6): δ 1.05 (t, 24, J = 7), 2.94 (q, 16, J = 7). MS: (E.I.) 316 M^+, 244 $(M-NEt_2)^+$. Anal. Calcd for $C_{16}H_{40}N_4Si$: C, 60.7; H, 12.7; N, 17.7. Found : C, 61.0; H, 12.7; N, 17.3.

$Ti(NMe_2)_4$. $LiNMe_2$ was generated by dropwise addition of 43.0 mL of n-butyllithium (2.55 M in hexane, 109 mmol) to a solution of $HNMe_2$ (ca. 40 mL, 603 mmol) at -70 °C in diethyl ether (250 mL). The solution was allowed to warm slowly to room temperature. After stirring for 1 h, the diethyl ether was evaporated and replaced by an equal amount of hexane. The solution was cooled to 0 °C and $TiCl_4$ (2.9 mL, 26 mmol) was added dropwise. After warming to room temperature, the mixture was stirred 4 h. Finally, the solution was heated to reflux for 2 h, allowed to cool and settle, and was filtered. The filtrate was evaporated under reduced pressure to afford a dark yellow oil. Distillation gave the product as a mobile yellow liquid (3.4 g, 60%), bp 60 °C/0.1 mm (lit.[8], 50 °C/0.05). IR (thin film) 1454s, 1264m, 1138m, 1053s, 941m, 864m, 603w, 582m, 519m cm^{-1}. ^1H NMR (C_6D_6): δ 3.03 (s). Incomplete reaction was observed if the heating to reflux step was omitted.

$Ti(NEt_2)_4$. A solution of $TiCl_4$ (2.0 mL, 18 mmol) in pentane (8 mL) was added dropwise to a suspension of $LiNEt_2$, prepared from n-BuLi (91 mmol) and $HNEt_2$ (9.5 mL, 91 mmol), in pentane (125 mL) at 0 °C . The mixture was warmed to room temperature and stirred 18 h. After settling, the yellow solution was filtered and the solvent was evaporated to give a yellowish brown liquid. Distillation gave the

product as a mobile yellow liquid (3.8 g, 61%), bp 120 °C/0.2 mm (lit.[8], 112 °C/0.1 mm). IR (thin film) 1450m, 1370s, 1360s, 1285w, 1190s, 1160s, 1100m, 1070m, 1050m, 1010s, 890s, 800s, 620s cm^{-1}. 1H NMR (C_6D_6): δ 1.12 (t, 24, J = 7), 3.57 (q, 16, J = 7). $^{13}C\{^1H\}$ NMR (C_6D_6): δ 15.61, 45.35. MS: (E.I.) 355 $(M-H)^+$. At times, the reaction mixture turned black after addition of $TiCl_4$. When this occurred, normal short path distillation was difficult because of excessive foaming. A special distillation apparatus was constructed using two vertical reflux condensers before the distillation path. This allowed a sufficient volume for the foaming to occur without it entering the vacuum line. When reflux began, the foaming subsided, and the $Ti(NEt_2)_4$ could be collected cleanly. The cause of the black coloration is not known.

$Ti(NPh_2)_4$. A solution of $TiCl_4$ (2.3 mL, 21 mmol) in pentane (50 mL) was added dropwise to a solution of $NaNPh_2$ (22.1 g, 116 mmol) in a mixture of THF (50 mL) and pentane (100 mL), at 0 °C. The mixture was allowed to warm to room temperature and stirred 18 h. After settling, the mixture was filtered, and the filtrate was evaporated to yield a red solid. The solid was recrystallized from diethyl ether to give red microcrystals (1.9 g, 13%), mp 186-187 °C (lit.[9], 190 °C).

$Ti(OBu^t)_4$. A solution of t-butanol (5.5 mL, 59 mmol) in pentane (10 mL) was added dropwise to a solution of $Ti(NEt_2)_4$ (4.96 g, 14.8 mmol) in pentane (20 mL) at 0 °C. The mixture was stirred for 12 h, then the solvent was removed under reduced pressure to yield a white residue. Distillation of the residue gave the product as a colorless liquid (3.9 g, 78%), bp 66 °C/0.1 mm (lit.[10], 107-108 °C/10 mm). ^1H NMR (C_6D_6): δ 1.37 (s). MS: (E.I.) 325 $(M-CH_3)^+$, 252 $(M-CH_3-OBu^t)^+$, 179 $(M-CH_3-2OBu^t)^+$. Anal. Calcd for $C_{16}H_{36}O_4Ti$: C, 56.5; H, 10.6. Found: C, 56.5; H, 10.3.

$Zr(NEt_2)_4$. To a suspension of $LiNEt_2$, prepared from n-BuLi (193 mmol) and $HNEt_2$ (20.2 mL, 193 mmol), in pentane (125 mL) was added $ZrCl_4$ (11.3 g, 48.3 mmol) from a dry addition tube over a period of 6 h. The mixture was stirred for an additional 18 h. After settling, the pale yellow solution was filtered and the solvent was removed under reduced pressure to yield a yellow liquid. Distillation gave the product as a colorless to pale yellow liquid (6.1 g, 33%), bp 115 °C/0.09 mm (lit.[8], 120 °C/0.1 mm). ^1H NMR (C_6D_6): δ 1.08 (t, 24, J = 7), 3.24 (q, 16, J = 7). $^{13}C\{^1H\}$ NMR (C_6D_6): δ 16.27, 43.63. Anal. Calcd for $C_{16}H_{40}N_4Zr$: C, 50.6; H, 10.6; N, 14.7. Found: C, 50.8; H, 10.8; N, 14.6.

$V(OBu^t)_4$. To a solution of $LiOBu^t$ (9.00 g, 112 mmol) in a mixture of hexane (125 mL) and THF (50 mL) was added $VCl_3 \cdot 3THF$ (10.5 g, 28.1 mmol) over a 2-hour period. A fuschia colored precipitate formed. The mixture was stirred for 1 h, then CuCl (2.77 g, 28.1 mmol) was added quickly from a dry addition tube. The mixture was heated to reflux for 3 h during which time the solution turned deep blue. The solution was cooled to room temperature, allowed to settle, and the solution was filtered. The filtrate was evaporated under reduced pressure, and the residue was distilled affording a mobile blue liquid (8.5 g, 88%), bp 89 °C/0.1 mm (lit.[11], 60-70*/0.1 mm). IR (thin film) 1600brw, 1468m, 1443m, 1384m, 1363s, 1229m, 1173s, 941vbrs, 786s, 610brs, 477brm cm^{-1}. UV (nm, pentane) λ 720, 850 (sh) (Ref.[12], UV (nm, cyclohexane) λ 719, 915 (sh)).

$OV(NEt_2)_3$. To a suspension of $LiNEt_2$, prepared from n-BuLi (128 mmol) and $HNEt_2$ (13.4 mL, 128 mmol), in pentane (150 mL) was added dropwise at 0 °C a solution of $OVCl_3$ (2.7 mL, 29 mmol) in pentane (8 mL). The resultant dark green solution was stirred for 17 h, then allowed to settle for 6 h. The solution was filtered, and oxygen was bubbled through the filtrate until its color was completely red (ca. 20 min). The red solution was filtered and the solvent was evaporated to yield a mobile red liquid (2.7 g, 34%). IR

---

* bath temperature

(thin film) 1600brw, 1461m, 1443m, 1370m, 1342m, 1187m,1152m, 1060m, 1004s, 892s, 786m, 617m, 505brw cm^{-1}. ^1H NMR (C_6D_6): δ 1.13 (t, 18, J = 7), 3.62 (q, 12, J = 7) (Ref.[13], ^1H NMR (CCl_4, 33 °C): δ 1.15 (t), 3.68 (q)). MS: 283 M^+, 268 $(M-CH_3)^+$, 209 $(M-NEt_2-2H)^+$. Distillation led to substantial thermal decomposition; ca. 5% yield of $OV(NEt_2)_3$ was recovered, bp 120 °C/0.1 mm (lit.[13], 121 °C/0.01 mm).

$OV(OEt)_3$. Method 1. To a solution of $OVCl_3$ (2.8 mL, 30 mmol) in toluene (125 mL) was added dropwise 5.7 mL anhydrous EtOH (99 mmol). During addition, the solution changed from dark red to light yellow to dark brown. After stirring for 3 h, ammonia gas was passed over the solution until a grey-green color persisted. The solution was stirred under nitrogen for an additional 0.5 h, and then filtered. The filtrate was evaporated under reduced pressure to yield the product as a yellow oil (ca. 0.5 g, 8%). ^1H NMR (C_6D_6): δ 1.28 (t, 9, J = 7), 4.80 (q, 6, J = 7).

Method 2. To a solution of EtOH (6.30 mL, 107 mmol) in hexane (25 mL) at 0 °C was added dropwise a solution of $OV(NEt_2)_3$ (9.20 g, 32.5 mmol) in hexane (125 mL). The reaction mixture turned brown and cloudy and a black sticky oil formed on the sides of the flask. After stirring at room temperature 1 h, ca. 25 mL of the solvent was distilled to remove diethylamine. After cooling to room temperature,

the mixture was filtered and the solvent was evaporated under reduced pressure to yield a red-brown residue. The residue was distilled to give the product as a yellow liquid (3.9 g, 60%), bp 95 °C/0.15 mm (lit.[14], bp 108 °C/26 mm).

$V(NEt_2)_4$. Method 1. Transmetallation. $VOCl_3$ (8.2 mL, 87 mmol) was added dropwise to $LiNEt_2$ (290 mmol) in hexane (125 mL) at -20 °C. The solution was slowly brought to room temperature and stirred for 18 h. The mixture was allowed to settle overnight, filtered, and the solvent was removed under reduced pressure to give a dark forest green oil. Initial distillation of the extremely viscous oil was difficult because of violent bumping. A second distillation proceeded smoothly and gave the compound as a viscous green liquid (2.8 g, 9.5%), bp 140 °C/0.1 mm (lit.[12], 90 °C/0.001 mm).

Method 2. Alkoxide-Amide Exchange. A solution of $V(OBu^t)_4$ (8.47 g, 24.6 mmol) in pentane (45 mL) was added over a period of 20 min to $LiNEt_2$ (123 mmol) in hexane (125 mL) at 0 °C. After warming to room temperature and stirring for 5 h, the mixture was allowed to settle for 24 hours at 0 °C. The solution was filtered while cold through a one inch plug of dry celite situated on a glass frit outfitted for operation under an inert atmosphere. The solution was concentrated to half of its original volume and filtered again through fresh celite. The solvent was removed under

g, 28.0 mmol) from a dry addition tube over a 2-hour period. A fuschia precipitate formed. The mixture was stirred for an hour, then CuCl (3.00 g, 27.9 mmol) was added quickly from a dry addition tube. The mixture was heated to reflux for 3 h during which time the solution turned royal blue. After cooling to room temperature and settling, the solution was filtered and the filtrate was evaporated under reduced pressure. Distillation of the residue afforded a dark blue liquid (7.71 g, 80%), bp 92 °C/0.1 mm (lit.[15], 66 °C*/2.7 mm). UV (nm, pentane) λ 635, 730(sh) (Ref.[15], UV (nm, cyclohexane) λ 634, 730 (sh)).

$Cr(NMe_2)_4$. A solution of $Cr(OBu^t)_4$ (3.01 g, 8.73 mmol) in pentane (25 mL) was added over a period of 10 min to $LiNMe_2$ (43.7 mmol) in hexane (75 mL) at 0 °C. After warming to room temperature and stirring for 5 h, the mixture was allowed to settle for 24 hours at 0 °C. The solution was filtered while cold through a one inch plug of dry celite situated on a glass frit outfitted for operation under an inert atmosphere. The solution was concentrated to half its original volume and was filtered again through fresh celite. The solvent was removed under reduced pressure and toluene (30 mL) was added to the residue. The mixture was allowed to settle at 0 °C for 2 h, and the above procedure for filtration was repeated. The filtrate was evaporated under

---

* bath temperature

reduced pressure to yield the product as a green liquid (1.4 g, 72%). MS: 228 M^+, 185 $(M-N(CH_3)(CH_2))^+$. UV (nm, pentane) λ 715.

$Cr(NEt_2)_4$. A solution of $Cr(OBu^t)_4$ (19.5 g, 56.6 mmol) in pentane (45 mL) was added over a period of 20 min to $LiNEt_2$, prepared from n-BuLi (141 mL, 283 mmol) and $HNEt_2$ (30.0 mL, 283 mmol), in hexane (125 mL) at 0 °C. After warming to room temperature and stirring for 5 h, the mixture was allowed to settle for 24 hours at 0 °C. The solution was filtered while cold through a one inch plug of dry celite situated on a glass frit outfitted for operation under an inert atmosphere. The solution was concentrated to half its original volume and was filtered again through fresh celite. The solvent was removed under reduced pressure and toluene (50 mL) was added to the residue. The mixture was allowed to settle at 0 °C for 2 h, and the above procedure for filtration was repeated. The filtrate was evaporated under reduced pressure to yield a dark green viscous liquid (16 g, 80%). MS: 340 M^+, 268 $(M-NEt_2)^+$. UV (nm, pentane) λ 740. The compound decomposes upon distillation (Ref.[16], bp 40-60 °C*/ 0.001 mm; UV (nm, cyclohexane) λ 730).

$Cr(NPr^i{}_2)_3$. To a solution of $HNPr^i{}_2$ (6.2 mL, 44 mmol) in hexane (125 mL) was added dropwise 11.0 mL of n-BuLi (3.98 M

---

* temperature at which $Cr(NEt_2)_3$ disproportionates to $Cr(NEt_2)_4$

reduced pressure to yield the product as a green liquid (1.4 g, 72%). MS: 228 M^+, 185 $(M-N(CH_3)(CH_2))^+$. UV (nm, pentane) λ 715.

$Cr(NEt_2)_4$. A solution of $Cr(OBu^t)_4$ (19.5 g, 56.6 mmol) in pentane (45 mL) was added over a period of 20 min to $LiNEt_2$, prepared from n-BuLi (141 mL, 283 mmol) and $HNEt_2$ (30.0 mL, 283 mmol), in hexane (125 mL) at 0 °C. After warming to room temperature and stirring for 5 h, the mixture was allowed to settle for 24 hours at 0 °C. The solution was filtered while cold through a one inch plug of dry celite situated on a glass frit outfitted for operation under an inert atmosphere. The solution was concentrated to half its original volume and was filtered again through fresh celite. The solvent was removed under reduced pressure and toluene (50 mL) was added to the residue. The mixture was allowed to settle at 0 °C for 2 h, and the above procedure for filtration was repeated. The filtrate was evaporated under reduced pressure to yield a dark green viscous liquid (16 g, 80%). MS: 340 M^+, 268 $(M-NEt_2)^+$. UV (nm, pentane) λ 740. The compound decomposes upon distillation (Ref.[16], bp 40-60 °C*/ 0.001 mm; UV (nm, cyclohexane) λ 730).

$Cr(NPr^i{}_2)_3$. To a solution of $HNPr^i{}_2$ (6.2 mL, 44 mmol) in hexane (125 mL) was added dropwise 11.0 mL of n-BuLi (3.98 M

---

* temperature at which disproportionation occurs

in hexane, 44.1 mmol) at 0 °C. The milk white solution was stirred for 8 h at room temperature. The $CrCl_3 \cdot 3THF$ (5.00 g, 13.4 mmol) was added slowly from a dry addition tube over a period of 45 min at 0 °C. During addition the mixture turned dark reddish brown. The solution was allowed to warm to room temperature and stirred 6 h. After settling, the mixture was filtered, and the solvent was evaporated to give a dark colored solid. The solid was sublimed (100 °C/0.18 mm) to yield dark maroon crystals[17] (2.5 g, 53%). IR (Nujol) 2593w, 1356w, 1335m, 1314w, 1257w, 1187m, 1166s, 1145m, 1117w, 1103s, 997brw, 955w, 934brm, 913m, 850m, 821m, 723w, 610w, 547m, 526w, 484w, 449w.

Reactions and Products

Reaction of $[Al(NMe_2)_3]_2$ with one molar equivalent of $Ph_2Si(OH)_2$. To a solution of $[Al(NMe_2)_3]_2$ (2.20 g, 14.6 mmol) in THF (50 mL) was added dropwise $Ph_2Si(OH)_2$ (3.20 g, 14.6 mmol) dissolved in a minimum amount of THF (ca. 15 mL). After stirring for 10 h, the solvent was evaporated under reduced pressure to give a glassy white solid (4.3 g). The solid was insoluble in diethyl ether, acetonitrile, CH_2Cl_2, toluene, hydrocarbons, ethyl acetate and water, and it was characterized only by its infrared spectrum (Nujol): 3654brvw, 1588w, 1426m, 1124s, 1046brm, 1011brm, 955brm, 744m, 709brs, 519m cm^{-1}.

Reaction of $[Al(NMe_2)_3]_2$ with 2.25 molar equivalents of $Ph_2Si(OH)_2$. To a solution of $[Al(NMe_2)_3]_2$ (1.40 g, 9.14 mmol) in diethyl ether (50 mL) was added dropwise $Ph_2Si(OH)_2$ (4.40 g, 20.3 mmol) dissolved in a minimum amount of THF. A white precipitate formed immediately. The mixture was stirred 17 h and then the solvent was removed by evaporation. The white residue was washed with warm diethyl ether (3 x 50 mL), and dried thoroughly under reduced pressure. The white, glassy solid (3.6 g) was insoluble in diethyl ether, CH_3CN, toluene, CH_2Cl_2, and hydrocarbons, and it was characterized only by its infrared spectrum (Nujol): 3655brvw, 1588m, 1426s, 1124s, 950vbrs, 744m, 716s, 702s, 625m, 610m,561m, 519s, 484m, 435m cm^{-1}.

Reaction of $[Al(NEt_2)_3]_2$ with $Ph_2Si(OH)_2$. To a solution of $[Al(NEt_2)_3]_2$ (1.00 g, 2.05 mmol) in diethyl ether (50 mL) was added dropwise $Ph_2Si(OH)_2$ (2.04 g, 9.43 mmol) dissolved in a minimum amount of THF (ca. 15 mL). A white precipitate formed immediately. The mixture was stirred 14 h and then was filtered. The solid residue was washed with warm diethyl ether (40 mL), and dried thoroughly under reduced pressure to yield a glassy white powder (1.8 g). The solid was soluble in THF and CH_2Cl_2, however repeated attempts at crystallization from these solvents were not successful. The compound did not melt or discolor below 330 °C, and it was insoluble in CH_3CN, acetone, toluene and diethyl ether. IR

(Nujol) 3606w, 1588m, 1426s, 1124w, 1187w, 1117s, 1004vbrs, 843w, 744m, 709brs, 618m, 562m, 519s, 484m, 428w cm^{-1}.

Reaction of $Si(NEt_2)_4$ with $Ph_2Si(OH)_2$. To a solution of $Si(NEt_2)_4$ (1.60 g, 5.06 mmol) in diethyl ether (25 mL) was added dropwise $Ph_2Si(OH)_2$ (3.28 g, 15.2 mmol) dissolved in a minimum amount of THF. After stirring for 17 h, the solvent was evaporated to dryness. The resulting white residue was extracted with pentane (10 mL) and vacuum dried to give a white powder. An infrared spectrum taken of the powder was identical to the infrared spectrum of $Ph_2Si(OH)_2$. The powder and the pentane filtrate were recombined, the pentane was evaporated under reduced presure and THF (20 mL) was added. The mixture was heated to reflux for 5 h, then the solvent was evaporated to afford a gummy residue. The residue was extracted with pentane (10 mL) and dried under reduced pressure. The hardened residue was washed with acetonitrile (20 mL), the mixture was filtered and the resulting powder was vacuum dried. The white powder was identified as a mixture of cyclotetra- and cyclotrisiloxane by its infrared spectrum[18] (Nujol): 1961w, 1890w, 1827w, 1771w, 1588m, 1426m, 1124s, 1096s, 1039m, 1018m, 997m, 744m, 723m, 695s, 674w, 526s, 491m, 407w cm^{-1}.

Reaction of $HSi(NEt_2)_3$ with $Ph_2Si(OH)_2$. To a solution of $HSi(NEt_2)_3$ (1.02 g, 4.15 mmol) in diethyl ether (25 ml) was

added dropwise $Ph_2Si(OH)_2$ (2.02 g, 9.33 mmol) dissolved in a minimum amount of THF. The mixture was stirred 17 h, then the solvent was evaporated to yield a white sticky residue. The residue was washed with pentane (10 mL) and dried under reduced pressure. The resulting white solid was extracted with hot diethyl ether (20 mL) and the extract was set aside. The remaining solid was crystallized from hot acetonitrile to give $(Ph_2SiO)_4$. Upon cooling to room temperature, the diethyl ether extract deposited colorless crystals of $(Ph_2SiO)_4$.

$[Ti_4O_2(OH)_2(OSiPh_2O)_6][H_2NMe_2]_2$, 1-$H_2NMe_2$ and **$[Ti_4O_2(OH)_2(OSiPh_2O)_5((OSiPh_2)_2O)][H_2NMe_2]$, 2-$H_2NMe_2$**. To a solution of $Ti(NMe_2)_4$ (1.07 g, 4.77 mmol) in diethyl ether (50 mL) was added dropwise $Ph_2Si(OH)_2$ (3.10 g, 14.3 mmol) dissolved in a minimum amount of THF. During addition, a gummy precipitate formed. The initial gum dissolved after ca. 5 min to give a white precipitate. After stirring for 10 h, the mixture was allowed to settle. The pale yellow supernatant was filtered from the white precipitate and set aside. The precipitate was washed with hot toluene (4 x 25 mL) and vacuum dried. Crystallization of the precipitate from boiling acetonitrile afforded **1-H_2NMe_2** as colorless crystals (0.52 g, 27%), mp 295 °C (dec). IR (Nujol) 3610w, 1588w, 1426m, 1124m, 1117m, 875brs, 744m, 716m, 695s, 558w, 543w, 512m, 470m, 429w, 400brm cm^{-1}. ^1H NMR (CD_3CN): δ

2.32 (s, 12), 3.40 (s, 2), 6.85-7.62 (m, 60). Anal. Calcd for $C_{76}H_{78}N_2O_{16}Si_6Ti_4$: C, 55.8; H, 4.81; N, 1.71. Found: C, 55.3; H, 4.63; N, 1.70.

The above filtrate and toluene washings were combined and the solvent was evaporated to dryness. The resulting residue was washed with warm diethyl ether (2 x 25 mL) and crystallized from acetonitrile to give **2-H_2NMe_2** as colorless crystals (0.40 g, 9%), mp 296-298 °C. IR (Nujol) 3620w, 1620w, 1588w, 1426m, 1300w, 1257w, 1187w, 1124s, 1117s, 1065w, 1040m, 1025m, 997w, 880brvs, 744m, 716s, 702s, 570w, 502m, 477m, 428w, 402w cm^{-1}. ^1H NMR (CD_3CN): δ 2.32 (s, 12), 4.60 (s,2), 6.85-7.62 (m, 80). Anal. Calcd for $C_{89}H_{86}N_2O_{17}Si_7Ti_4$: C, 58.0; H, 4.70; N, 1.52. Found: C, 57.0; H, 4.64; N, 1.53.

$[Ti_4O_2(OH)_2(OSiPh_2O)_6][H_2NEt_2]_2$, 1-$H_2NEt_2$ and **$[Ti_4O_2(OH)_2(OSiPh_2O)_5((OSiPh_2)_2O)][H_2NEt_2]_2$, 2-$H_2NEt_2$.** To a solution of $Ti(NEt_2)_4$ (1.99 g, 5.94 mmol) in diethyl ether (50 mL) was added dropwise $Ph_2Si(OH)_2$ (3.85 g, 17.8 mmol) dissolved in a minimum amount of THF (ca. 20 mL). A gummy precipitate formed. With vigorous stirring the precipitate quickly became powdery. After stirring for 6 h, the mixture was allowed to settle. The pale yellow supernatant was filtered from the white precipitate and set aside. The latter precipitate was washed with warm toluene (2 x 25 mL) and vacuum dried. Crystallization from boiling acetonitrile

afforded **1-H_2NEt_2** as colorless crystals (1.4 g, 54%), mp 300 °C (dec). IR (Nujol) 3620w, 1616w, 1588w, 1426m, 1307w, 1257w, 1187w, 1117m, 1025w, 997w, 878brvs, 744m, 716m, 702s, 639w, 603w, 569m, 540m, 512m, 470s, 435w cm^{-1}. ^1H NMR (CD_3CN): δ 0.97 (t, 12, J = 7), 2.78 (q, 8, J = 7), 2.85 (s, 2), 6.81-7.62 (m, 60). ^{29}Si MASNMR: δ -43.3, -42.8, -41.7, -40.8, -39.8, -38.9. FABMS: 1533 $(M-2C_6H_5)^+$. Anal. Calcd for $C_{80}H_{82}N_2O_{16}Si_6Ti_4$: C, 56.9; H, 4.89; N, 1.66. Found: C, 57.1; H, 5.01, N, 1.67.

The above filtrate and toluene washings were combined and the solvent was evaporated to dryness. The resulting residue was washed with warm diethyl ether (2 x 25 mL) and crystallized from boiling toluene to give **2-H_2NEt_2** (0.75 g, 24%) as pale yellow crystals, mp 298-300 °C. IR (Nujol) 3620w, 1616w, 1588w, 1426m, 1307w, 1257w, 1187w, 1117s, 1053m, 1025w, 997w, 885brvs, 744m, 716m, 702s, 646w, 561w, 547w, 512m, 477m, 428w cm^{-1}. ^1H NMR (CD_3CN): δ 0.97 (t, 12, J = 7), 2.78 (q, 8, J = 7), 2.85 (s, 2), 6.80-7.65 (m, 80). ^{29}Si MASNMR: δ -40.0. FABMS: 1859 $(M-2C_6H_5)^+$. Anal. Calcd for $C_{92}H_{96}N_2O_{17}Si_7Ti_4$: C, 58.5; H, 5.12; N, 1.48. Found: C, 58.7; H, 5.11; N, 1.33.

$Ti((OSiPh_2)_4O)_2$. The diol, $Ph_2Si(OH)_2$, (3.13 g, 14.5 mmol) was added from a dry addition tube to a solution of $Ti(OBu^t)_4$ (1.64 g, 4.83 mmol) in diethyl ether (50 mL). The reaction mixture was heated to reflux for 3 h. Subsequent

cooling and evaporation of the solvent gave a crude product as a solid foam. The foam was crystallized from hot acetone to give colorless crystals (2.5 g, 35%), mp 295-298 °C (lit.[19], 297-303 °C). IR (Nujol) 1588m, 1426s, 1307w, 1264w, 1187w, 1124s, 1089s, 1060s, 1025m, 997m, 920brs, 871vw, 744m, 716s, 695s, 625w, 610w, 589w, 540w, 526s, 505m, 484m, 456w, 435w cm^{-1}. ^{29}Si MASNMR: δ -48.4, -44.6, -43.6, -43.2, -42.1, -41.8. MS: (E.I.) 1666 M^+, 1589 $(M-C_6H_5)^+$, 1511 $(M-2C_6H_5)^+$.

$[Ti_4O(OH)_3(OSiPh_2O)_6][H_2NEt_2]$. To a solution of 1-$H_2NEt_2$ (1.0 g. 0.60 mmol) in acetonitrile (50 mL) was added CF_3COOH (0.5 ml, 6.7 mmol). A white precipitate formed immediately. The mixture was stirred for 18 h, then allowed to settle, and was filtered. The resulting white solid was washed with warm toluene (20 mL) and vacuum dried. Crystallization from THF at 10 °C gave the product as colorless crystals (300 mg, 60%), mp 250 °C (dec.). IR (Nujol) 3620m, 1616w, 1588w, 1426m, 1307w, 1257w, 1187w, 1117m, 1025w, 997w, 878brvs, 744m, 716m, 702s, 639w, 603w, 569m, 540m, 512m, 470m cm^{-1}. ^1H NMR (CD_3CN): δ 1.20 (t, 6, J=7), 2.89 (q, 4, J=7), 4.14 (s, 3), 7.30 (m, 60). FABMS: 1543 $(M - H_2NEt_2)^-$. Anal. Calcd for $C_{76}H_{74}NO_{16}Si_6Ti_4$: C, 56.45; H, 4.64; N, 0.87. Found: C, 55.42; H, 4.64; N, 1.09.

Reaction of $Ti(NPh_2)_4$ with $Ph_2Si(OH)_2$. To a solution of $Ti(NPh_2)_4$ (1.94 g, 2.69 mmol) in a mixture of diethyl ether

(50 mL) and pentane (5 mL) was added $Ph_2Si(OH)_2$ (1.74 g, 8.04 mmol) dissolved in a minimum amount of THF (ca. 15 mL). The solution was heated to reflux for 1 h, then the solvent was evaporated under reduced pressure. The residue was crystallized from acetone to yield colorless crystals of $Ti((OSiPh_2)_4O)_2$ (1.5, 33%), mp 295-296 °C. The infrared spectrum was identical to the compound as prepared by the method of Zeitler and Brown.[19]

Reaction of 1-H_2NEt_2 with CF_3COOH. To a suspension of 1-H_2NEt_2 (750 mg, 4.43 mmol) in acetonitrile (50 mL) was added rapidly CF_3COOH (1.0 mL, 13 mmol) via syringe. The mixture was heated to reflux for 1 h. The solvent was evaporated to dryness and the residue was crystallized from acetone to yield colorless crystals of $Ti((OSiPh_2)_4O)_2$ (100 mg, 60%), mp 295-296 °C.

$Ti_4(OH)_4(OSiPh_2O)_6$, 1-OH. To a suspension of **1-H_2NEt_2** (444 mg, 0.263 mmol) in acetonitrile (50 mL) was added a solution of p-toluenesulfonic acid (100 mg, 0.526 mmol) dissolved in acetonitrile (10 mL). A fine white precipitate formed immediately. After stirring for 9 h at room temperature, the mixture was allowed to settle, then filtered. The residue was dried under reduced pressure to give a white solid (185 mg, 46%), mp 270 °C (dec). IR (Nujol) 3585s, 1588m, 1667w, 1426s, 1307w, 1264w, 1187w, 1159w, 1124s,

1117s, 1068w, 1039w, 1011w, 997w, 878brs, 765w, 744m, 723s, 702s, 681w, 646w, 617w, 575m, 512s, 477m, 435m cm^{-1}. ^1H NMR ($CDCl_3$): δ 1.90 (s, 4), 7.20 (m, 60). Anal. Calcd for $C_{72}H_{64}O_{16}Si_6Ti_4$: C, 56.0; H, 4.19. Found: C, 55.6; H, 4.13.

$[Ti_4O(OH)_3(OSiPh_2O)_6][NMe_4]$. To a suspension of $Ti(OH)_4(OSiPh_2O)_6$ (0.50 g, 0.32 mmol) in acetonitrile (25 mL) was added $Me_4N(OH)$ (0.03 g, 0.32 mmol) that had been dried thoroughly by heating gently under reduced pressure. The mixture was stirred vigorously for 0.5 h, during which time the solution turned clear. The solvent was evaporated until precipitation ocurred. The precipitate was then redissolved and the solution was cooled slowly to 10 °C. The resulting colorless crystals were isolated and dried under reduced pressure (0.48 g, 100%), mp. IR (Nujol) 3599m, 1588w, 1426m, 1307w, 1264w, 1208w, 1187w, 1117s, 1032w, 1011w, 997w, 948w, 885brvs, 744m, 723m, 702s, 639w, 568m, 540w, 512m, 477m, 435w cm^{-1}. ^1H NMR (CD_3CN): δ 3.05 (s, 12), 7.50 (m, 60). Anal. Calcd for $C_{76}H_{75}N_{O16}Si_6Ti$: C, 56.4; H, 4.67; N, 0.86. Found: C, 55.9; H, 4.73; N, 0.96.

$[Ti_4O_2(OH)_2(OSiPh_2O)_6][NMe_4]_2$, 1-$NMe_4$. To a suspension of $Ti_4(OH)_4(OSiPh_2O)_6$ (300 mg, 0.194 mmol) in acetonitrile (50 mL) was added $(CH_3)_4NOH\cdot 5H_2O$ (70 mg, 0.39 mmol). After stirring for 5 min most of the $Ti_4(OH)_4(OSiPh_2O)_6$ had

dissolved leaving a cloudy solution. After an additional hour of stirring at ambient temperature, the solvent was evaporated under reduced pressure to give a white, crystalline solid (200 mg, 63%). The compound did not melt below 320 °C. IR (Nujol) 3599w, 1588w, 1482m, 1426m, 1307w, 1264w, 1208w, 1187w, 1117s, 1032w, 1011w, 997w, 948w, 885brvs, 744m, 723m, 702s, 681w, 639w, 568m, 540w, 512m, 477m, 435w cm^{-1}. ^1H NMR ($(CD_3)_2CO$): δ 3.28 (s, 24), 7.25 (m, 60). ^{29}Si MASNMR: δ -42.0. Anal. Calcd for $C_{80}H_{86}N_2O_{16}Si_6Ti_4$: C, 56.8; H, 5.12; N, 1.66. Found: C, 56.2; H, 5.05; N, 1.77.

Reaction of $Zr(NEt_2)_4$ with $Ph_2Si(OH)_2$. To a solution of $Zr(NEt_2)_4$ (2.27 g, 6.00 mmol) was added dropwise $Ph_2Si(OH)_2$ (2.58 g, 12.0 mmol) dissolved in a minimum amount of THF (ca. 15 mL). A thick white precipitate formed. After stirring for 10 h, the mixture was filtered and the filtrate was discarded. The remaining white, glassy solid was insoluble in diethyl ether, toluene, acetonitrile and hydrocarbons and it was characterized only by its infrared spectrum (Nujol): 3490brw, 1588w, 1426m, 1124m, 960vbrs, 744m, 716m, 695m, 512brm cm^{-1}.

$[V_2O_4(OSiPh_2O)_2][H_2NEt_2]_2$, 3-$H_2NEt_2$ and **$[VO_2((OSiPh_2)_3O)][H_2NEt_2]$, 4-$H_2NEt_2$.** To a solution of $OV(NEt_2)_3$ (1.34 g, 4.73 mmol) in diethyl ether (50 mL) was

added dropwise $Ph_2Si(OH)_2$ (2.28 g, 10.6 mmol) dissolved in a minimum amount of THF (ca. 15 mL). A tan precipitate formed. After stirring for 12 h at room temperature, the mixture was filtered and the filtrate was set aside. The tan precipitate was washed with warm toluene until the washings appeared colorless, and the remaining solid was crystallized from boiling acetonitrile to give **3-H_2NEt_2** as colorless crystals (500 mg, 29%), mp 175 °C (dec). IR (Nujol) 1588m, 1426m, 1117m, 1068w, 1053w, 997m, 962m, 948m, 913s, 878s, 744m, 716m, 695m, 639m, 610m, 589w, 512m, 484m, 435w, 421m cm^{-1}. ^1H NMR (CD_3CN): δ 1.05 (t, 12, J = 7), 2.80 (q, 8, J = 7), 6.80-7.35 (m, 20). ^{29}Si MASNMR: δ -35.2. FABMS: 693 M^-. Anal. Calcd for $C_{32}H_{44}N_2O_8Si_2V_2$: C, 51.7; H, 5.93; N, 3.77. Found: C, 51.7; H, 5.93; N, 3.76.

The above filtrate and toluene washings were combined and the solvent was evaporated to dryness. The residue was washed with warm diethyl ether (3 x 25 mL), and crystallized from acetonitrile at 10 °C to give **4-H_2NEt_2** as pale yellow crystals (71 mg, 2%), mp 165-166 °C. IR (Nujol) 1588m, 1426m, 1117, 1090s, 1087s, 1068m, 1053m, 957m, 920 brs, 878m, 744m, 723s, 702s, 568m, 526s, 505m, 484m. ^1H NMR (CD_3CN): δ 1.05 (t, 6, J = 7), 2.78 (q, 4, J = 7), 7.45 (m, 30). ^{29}Si MASNMR: δ -44.5, -43.1, -40.9, -40.6, -40.2, -39.8, -37.8, -37.4, -36.8, -36.5. Anal. Calcd for $C_{40}H_{42}NO_6Si_3V$: C, 62.4; H, 5.76; N, 1.82. Found: C, 62.5; H, 5.55; N, 1.83.

$V_2O_2(OH)_2(OSiPh_2O)_2$, 3-OH. To a suspension of **2-H_2NEt_2** (1.50 g, 2.02 mmol) in acetonitrile (50 mL) was added a solution of p-toluenesulfonic acid (767 mg, 4.04 mmol) in acetonitrile (10 mL). Within 1 min an orange precipitate formed. The mixture was stirred 12 h, and then filtered to give an orange solid (1.1 g, 92%). The compound discolors at 150 °C but does not melt below 250 °C. IR (Nujol) 3550w, 1588w, 1426m, 1124m, 1047w, 1027w, 1007m, 997m, 920brvs, 878brm, 744w, 723m, 695m, 639w, 618w, 568w, 515m cm^{-1}. Anal. Calcd for $C_{24}H_{22}O_8Si_2V_2$: C, 48.3; H, 3.69. Found: C, 48.6; H, 3.80. The compound was insoluble in acetonitrile, acetone, toluene, diethyl ether, hydrocarbons, THF and CH_2Cl_2.

$[V_2O_4(OSiPh_2O)_2][NMe_4]_2$, 3-$NMe_4$. To a stirred suspension of $V_2O_2(OH)_2(OSiPh_2O)_2$ (100 mg, 0.168 mmol) in acetonitrile (50 mL) was added $(CH_3)_4NOH\cdot 5H_2O$ (61 mg, 0.34 mmol). After 15 min, most of the $V_2O_2(OH)_2(OSiPh_2O)_2$ had dissolved. The mixture was stirred for an additional 6 h at ambient temperature, filtered, and the supernatant was evaporated under reduced pressure to yield a crystalline, tan powder (50 mg, 44%), mp 191-192 °C. IR (Nujol) 1588w, 1482m, 1426m, 1124m, 1039w, 1011m, 997m, 920vbrvs, 744w, 716m, 695m, 617w, 532w, 512m, 441w cm^{-1}. ^1H NMR (CD_3CN): δ 3.10 (s, 24), 7.40 (m, 20). Anal. Calcd for $C_{32}H_{44}N_2O_8Si_2V_2$: C, 51.7; H, 5.97; N, 3.77. Found: C, 51.1; H, 6.10; N, 4.08.

$[VO((OSiPh_2)_2O)_2][Li(THF)_2]_2$, 5. Diphenylsilanediol (17.8 g, 82.5 mmol) was dissolved in a minimum amount of THF (ca. 50 mL) and added dropwise to a solution of undistilled $V(NEt_2)_4$ (9.33 g, 27.4 mmol), prepared by the alkoxide-amide exchange method, in diethyl ether (200 mL). The color changed during addition from green to red-brown to green-brown. After the mixture had stirred 12 h at room temperature, the solvent was evaporated to give a solid, brown foam. The foam was washed with warm diethyl ether until the washings appeared colorless. The remaining blue powder was crystallized from THF to give **5** as light blue crystals (6.6 g, 23%), mp 145-146 °C. IR (Nujol) 1588m, 1567w, 1426s, 1335w, 1304w, 1264w, 1159w, 1124s, 1117s, 1046m, 1032s, 1007s, 969vbrs, 890m, 754w, 723m, 716s, 744s, 702s, 547brs, 526brs, 507brs, 441m cm^{-1}. Anal. Calcd for $C_{56}H_{56}Li_2O_9Si_4V$: C, 64.4; H, 6.08; Li, 1.16. Found: C, 64.2; H, 5.95; Li, 1.19. The suceptibility of **5** was measured over the range 6-280 K and showed Curie-Weiss Law behaviour (θ = -0.1°) with an average μ_{eff} = 1.79 BM independent of temperature.

Reaction of 5 with ^{t}BuOOH. To a solution of $[VO((OSiPh_2)_2O)_2][Li(THF)_2]_2$ (0.40 g, 0.38 mmol) in toluene was added an excess of ^{t}BuOOH. The blue solution immediately turned cloudy white. After allowing it to settle overnight, the solution was filtered and the solvent

was removed under reduced pressure to yield a sticky white precipitate. The precipitate was very soluble in ether, chloroform, water, and alcohols, and only sparingly soluble in cold hydrocarbon solvents. Colorless crystals formed upon cooling of a solution of the precipitate in boiling hexane. The spectroscopic data, however, was not sufficient to characterize the complex, and its identity remains unknown. mp. 89-90 °C. IR (Nujol) 3198brm, 1588w, 1426s, 1124s, 1082brs, 1025m, 997w, 885brm, 864brm, 850brm, 744m, 716s, 695s, 512s, 484m, 463w, 407w. ^{1}H NMR (C_6D_6): δ 0.09 (s, 2), 3.21 (s,1), 7.34-7.67 (m, 12). Anal. found: C, 67.4; H, 5.43.

Reaction of $V(NMe_2)_4$ with $Ph_2Si(OH)_2$. To a solution of $V(NMe_2)_4$ (1.99 g, 8.77 mmol) in diethyl ether (50 mL) was added dropwise $Ph_2Si(OH)_2$ (5.68 g, 26.3 mmol) dissolved in a minimum amount of THF. The solution changed from green to blue-green. After stirring for 20 h, the solvent was removed under reduced pressure to give a brownish-green, solid foam. The foam was dissolved in ca. 30 mL of acetonitrile and cooled to 10 °C. The resultant colorless crystals were isolated and identified as a mixture of hexaphenylcyclotrisiloxane and octaphenylcyclotetrasiloxane by their infrared spectrum. No discrete products containing vanadium could be isolated from the remaining viscous residue.

Reaction of $V(OBu^t)_4$ with $Ph_2Si(OH)_2$. To a solution of $V(OBu^t)_4$ (2.31 g, 6.73 mmol) in diethyl ether (50 mL) was slowly added $Ph_2Si(OH)_2$ (4.36 g, 20.2 mmol) from a dry addition tube . After stirring for 4 h, the light green precipitate that had formed was allowed to settle, and the mixture was filtered. Concentration of the filtrate gave a brown oil which was discarded. The light green powder (ca. 1.00 g) was insoluble in diethyl ether, THF, toluene, and acetonitrile and it was characterized only by its infrared spectrum (Nujol): 1595w, 1433m, 1121s, 1018m, 890s, 718s, 699s, 523s. The light green powder is apparently air sensitive, darkening to red-brown if left overnight in air.

Reaction of $OV(OEt)_3$ with $Ph_2Si(OH)_2$. To a solution of $OV(OEt)_3$ (3.94 g, 19.5 mmol) in diethyl ether (75 mL) was added dropwise $Ph_2Si(OH)_2$ (9.49 g, 43.9 mmol) dissolved in a minimum amount of THF (ca. 30 mL). A precipitate immediately formed. After stirring for 5 h, the solvent was evaporated under reduced pressure and the resulting residue was washed with warm diethyl ether (3 x 25 mL) to give a light green solid. The solid was insoluble in diethyl ether, toluene, acetonitrile, CH_2Cl_2, and THF and it was characterized only by its infrared spectrum (Nujol): 1588w, 1426m, 1124s, 1046m, 997s, 927brvs, 744w, 723m, 695m, 512m cm^{-1}.

Reaction of $Cr(NMe_2)_4$ with $Ph_2Si(OH)_2$. To a solution of $Cr(NMe_2)_4$ (1.44 g, 6.32 mmol) in diethyl ether (50 mL) was added dropwise $Ph_2Si(OH)_2$ (4.10 g, 19.0 mmol) dissolved in a minimum amount of THF (ca. 20 mL). A blue-green precipitate formed. After stirring for 10 h, the precipitate had dissolved and the clear, green solution was evaporated to dryness. The resulting solid foam was dissolved in diethyl ether (ca. 30 mL) and cooled to 10 °C. The colorless crystals which formed were isolated and identified as $(Ph_2SiO)_3$ by their infrared spectrum. Further cooling of the diethyl ether filtrate did not produce any other solids. Evaporation of the diethyl ether gave a sticky, blue-green residue that was very soluble in toluene, diethyl ether, CH_2Cl_2 or acetonitrile to give viscous solutions that could not be crystallized.

Reaction of $Cr(NEt_2)_4$ with $Ph_2Si(OH)_2$. To a solution of $Cr(NEt_2)_4$ (1.62 g, 4.77 mmol) in diethyl ether (50 mL) was added dropwise $Ph_2Si(OH)_2$ (3.08 g, 14.2 mmol) dissolved in a minimum amount of THF. The solution changed from green to murky brown. After stirring for 16 h, the solvent was removed by evaporation. The resulting solid foam was dissolved in diethyl ether (ca. 30 mL) and cooled to 10 °C. The colorless crystals which formed were isolated and identified as $(Ph_2SiO)_4$ by their infrared spectrum. Further cooling of the diethyl ether filtrate did not produce any

other solids. Evaporation of the diethyl ether gave a sticky, dark green residue that was very soluble in toluene, diethyl ether, CH_2Cl_2 or acetonitrile to give viscous solutions that could not be induced to crystallize.

Reaction of $Cr(NPr^i_2)_3$ with $Ph_2Si(OH)_2$. To a solution of $Cr(NPr^i_2)_3$ (1.50 g, 4.25 mmol) in diethyl ether (40 mL) was added dropwise $Ph_2Si(OH)_2$ (2.79 g, 12.9 mmol) dissolved in a minimum amount of THF (ca. 15 mL). The solution turned blue-grey and a light colored precipitate formed. After stirring for 16 h, the solvent was removed by evaporation. The resulting solid foam was washed with diethyl ether (3 x 10 mL) and dried under reduced pressure. The resulting pale green powder was soluble in toluene, CH_2Cl_2, and THF. The compound decomposed without melting above 300 °C. IR (Nujol) 3585brw, 1588w, 1426m, 1124s, 1037m, 1012m, 987brm, 924brm, 744m, 715s, 702s, 527brm cm^{-1}. Repeated attempts to crystallize the compound were unsuccessful.

Reaction of $Cr(OBu^t)_4$ with $Ph_2Si(OH)_2$. To a solution of $Cr(OBu^t)_4$ (2.65 g, 7.79 mmol) in diethyl ether (50 mL) was added dropwise $Ph_2Si(OH)_2$ (4.99 g, 23.1 mmol) dissolved in a minumum amount of THF (ca. 25 mL). The color of the solution gradually changed from dark blue to dark brown. After stirring for 18 h at room temperature, the mixture was heated to reflux for 1 h. The solvent was evaporated under

reduced pressure to give a sticky oil. Diethyl ether (20 mL) was added and the resulting dark solution was cooled to -10 °C. Subsequent filtration afforded a small amount of crystalline $(Ph_2SiO)_3$. Evaporation of the filtrate gave a sticky, brown residue which was very soluble in toluene, diethyl ether, THF, CH_2Cl_2, or acetonitrile to give viscous solutions that could not be induced to crystallize.

X-Ray Experimental

$[HNEt_2]_2[Ti_4O_2(OH)_2(OSiPh_2O)_6]\cdot CH_3CN$

Colorless crystals of the compound were obtained by slow cooling from a hot acetonitrile solution. A crystal of approximate dimensions 0.30 x 0.22 x 0.10 mm was mounted on a glass fiber with Davcon "5-minute" epoxy. Preliminary precession photographs indicated monoclinic (2/m) Laue symmetry, and yielded preliminary cell dimensions.

The crystal for data collection was then transferred to an Enraf-Nonius CAD4 automated diffractometer[7], cooled to -110(±2) °C in a cold nitrogen stream, and centered in the beam. Automatic peak search and indexing yielded a body centered cell, and confirmed the Laue symmetry. Accurate cell dimensions and the orientation matrix were determined from a least-squares fit to the setting angles of the unresolved MoKα components of 24 symmetry related reflections with 2θ between 22 and 29 degrees. The results are given in Table I along with parameters for data collection.

The 5780 raw intensity data were converted to structure factor amplitudes and their esds by correction for scan speed, background, Lorentz and polarization effects.[8-10] Analysis of the azimuthal scan[11] data showed no variation in intensity so that an absorption correction was unwarranted. Rejection of systematically absent data as well as redundant

data gave a set of 5650 unique data which were used to solve and refine the structure.

The positions of the titanium and silicon atoms were determined using MULTAN. The remaining atom positions were found by standard Fourier and least-squares techniques. In a difference Fourier map calculated following refinement of all non-hydrogen atoms with anisotropic thermal parameters, peaks corresponding to the expected positions of many of the hydrogen atoms were found. Hydrogen atoms were included in the structure factor calculations in their expected positions based on idealized bonding geometry but were not refined in least-squares.

The final residuals for 1001 variables refined against the 4666 data for which $F^2>3\sigma(F^2)$ were R = 2.95%, Rw = 3.68% and GOF = 1.534. The R value for all 5650 data was 5.17%.

The quantity minimized by the least-squares program was $\Sigma w(/F_o/-/F_c/)^2$, where w is the weight of a given observation. The p-factor[12], used to reduce the weight of intense reflections was set to 0.03 throughout refinement. The analytical forms for the scattering factor tables for the neutral atoms[13] were used and all non-hydrogen scattering factors were corrected for both the real and imaginary components of anomolous dispersion[14].

Inspection of the residuals ordered in ranges of sin θ/l, $/F_o/$, and parity and value of the individual indexes showed no unusual features or trends. There was no evidence

of secondary extinction in the low angle, high intensity data. The largest peak in the final difference Fourier map had an electron density of 0.392 e^-/A^3.

Table I.

Crystal Data (-110 °C) for
$[HNEt_2]_2[Ti_4O_2(OH)_2(OSiPh_2O)_6]\cdot CH_3CN$

Space Group	I2/m
a, Å	23.678(6)
b, Å	14.611(3)
c, Å	26.449(6)
β, deg	115.44(2)
V, $Å^3$	8261
Z	4
fw	1732.67
ρ (calc.) g/cm^3	1.39
μ (calc.) 1/cm	5.15
radiation	MoKα (λ = 0.71073Å)
monochrometer	highly oriented graphite
scan range, type	$3° \leq 2\theta \leq 45°$, θ-2θ
scan speed, deg/min	0.84-6.7, variable
scan width, deg	$\theta = 0.55 + 0.35 \tan\theta$
unique reflections	5650
reflections, $F_o^2 > 3\sigma(F_o^2)$	4665
R, %	2.95
R_w, %	3.68
GOF	1.53

$[HNEt_2]_2[Ti_4O_2(OH)_2(OSiPh_2O)_5((OSiPh_2)_2O)]\cdot C_7H_8\cdot 2H_2O$

Colorless crystals of the compound were obtained by slow evaporation from a toluene solution. A crystal of approximate dimensions 0.55 x 0.30 x 0.31 mm was mounted on a glass fiber with Davcon "5-minute" epoxy. Preliminary precession photographs indicated possible orthorhombic (mmm) Laue symmetry, and yielded preliminary cell dimensions. Systematic absences suggested C-centering.

The crystal for data collection was transferred to an Enraf-Nonius CAD4 automated diffractometer[7] and centered in the beam. It was cooled to -110(±2) °C by a cold nitrogen stream and the temperature was monitored by a thermocouple upstream of the crystal that had been previously calibrated against another thermocouple at the crystal location. Automatic peak search and indexing yielded a hexagonal cell. Accurate cell dimensions and the orientation matrix were determined from a least-squares fit to the setting angles of the unresolved MoKα components of 24 symmetry related reflections with 2θ between 23 and 31 degrees. The results are given in Table II along with parameters for data collection.

The 3741 raw intensity data were converted to structure factor amplitudes and their esds by correction for scan speed, background, Lorentz and polarization effects.[8-10] Inspection of the intensity standards showed a slow isotro-

pic decrease of 3.4% of the original intensity. The data were corrected for this decay. Analysis of the azimuthal scan[11] data showed no variation in intensity so that an absorption correction was unwarranted. After rejection of systematically absent data, averaging of redundant data gave a set of 3607 unique data.

The positions of the titanium and silicon atoms were determined using MULTAN. The remaining atom positions were found by standard Fourier and least-squares techniques. During the course of refinement, disorder was observed in the toluene molecule of solvation. The disorder of the toluene was modeled using two half occupancy methyl groups. In a difference Fourier map calculated following refinement of all non-hydrogen atoms with anisotropic thermal parameters, peaks corresponding to the expected positions of many of the hydrogen atoms were found. Hydrogen atoms were included in the structure factor calculations in their expected positions based on idealized bonding geometry but were not refined in least-squares.

The final residuals for 598 variables refined against the 3150 data for which $F^2>3\sigma(F^2)$ were R = 4.19%, Rw = 5.42% and GOF = 2.058. The R value for all 3607 data was 5.17%.

The quantity minimized by the least-squares program was $\Sigma w(/F_o/-/F_c/)^2$, where w is the weight of a given observation. The p-factor[12], used to reduce the weight of intense reflections was set to 0.03 throughout refinement. The

analytical forms for the scattering factor tables for the neutral atoms[13] were used and all non-hydrogen scattering factors were corrected for both the real and imaginary components of anomolous dispersion[14].

Inspection of the residuals ordered in ranges of sin θ/l, $/F_o/$, and parity and value of the individual indexes showed no unusual features or trends. There was no evidence of secondary extinction in the low angle, high intensity data. The largest peak in the final difference Fourier map had an electron density of 0.72 e^-/A^3 associated with Si(3).

Table II.

Crystal Data (-110 °C) for
$[HNEt_2]_2[Ti_4O_2(OH)_2(OSiPh_2O)_5((OSiPh_2)_2O)]\cdot C_7H_8\cdot 2H_2O$

Space Group	$P3_221$
a, Å	21.297(2)
c, Å	19.337(2)
V, $Å^3$	7596
Z	3
fw	2018.17
ρ (calc.) g/cm^3	1.32
μ (calc.) 1/cm	4.64
radiation	MoKα (λ = 0.71073Å)
monochrometer	highly oriented graphite
scan range, type	3° ≤ 2θ ≤ 45°, θ-2θ
scan speed, deg/min	0.84-6.7, variable
scan width, deg	θ = 0.55 + 0.35 tanθ
unique reflections	3728
reflections, $F_o^2>3\sigma(F_o^2)$	3150
R, %	4.19
R_w, %	5.42
GOF	2.06

$\underline{[HNEt_2]_2[V_2O_2(OPh_2SiO)_2]}$

Colorless crystals of the compound were obtained by slow cooling from a hot acetonitrile solution. A crystal of approximate dimensions 0.35 x 0.30 x 0.10 mm was mounted on a glass fiber with Davcon "5-minute" epoxy. Preliminary precession photographs indicated monoclinic (2/m) Laue symmetry, and yielded preliminary cell dimensions. Inspection of the h0l and 0k0 zones showed systematic absences 0k0, k = 2n+1; h0l, l= 2n+1 consistent only with the space group $P2_1/c$.

The crystal for data collection was transferred to an Enraf-Nonius CAD4 automated diffractometer[7] and centered in the beam. Automatic peak search and indexing yielded the same unit cell as found in the photographs, and confirmed the Laue symmetry. Accurate cell dimensions and the orientation matrix were determined from a least-squares fit to the setting angles of the unresolved MoKα components of 24 symmetry related reflections with 2θ between 27 and 29 degrees. The results are given in Table III along with parameters for data collection.

The 2593 raw intensity data were converted to structure factor amplitudes and their esds by correction for scan speed, background, Lorentz and polarization effects[8-10]. Analysis of the azimuthal scan data showed no variation in intensity so that an absorption correction was unwarranted.

Rejection of systematically absent data as well as redundant data gave a set of 2305 unique data. An additional 259 reflections were rejected whose w*del^2 were unusually large. During data collection, these reflections were flagged for deviating from their calculated positions and were collected just prior to redetermination of the orientation matrix. The remaining 2046 reflections were used in refinement.

The positions of V(1) and Si(1) were found using a three-dimensional Patterson synthesis. The remaining atom positions were found by standard Fourier and least-squares techniques. In a difference Fourier map calculated following refinement of all non-hydrogen atoms with anisotropic thermal parameters, peaks corresponding to the expected positions of many of the hydrogen atoms were found. Hydrogen atoms were included in the structure factor calculations in their expected positions based on idealized bonding geometry but were not refined in least-squares.

The final residuals for 208 variables refined against the 1716 data for which $F^2>3\sigma(F^2)$ were R = 5.39%, Rw = 8.52% and GOF = 3.614. The R value for all 2046 data was 6.99%.

The quantity minimized by the least-squares program was $\Sigma w(/F_o/-/F_c/)^2$, where w is the weight of a given observation. The p-factor[12], used to reduce the weight of intense reflections was set to 0.03 throughout refinement. The analytical forms for the scattering factor tables for the neutral atoms[13] were used and all non-hydrogen scattering

factors were corrected for both the real and imaginary components of anomolous dispersion.[14]

Inspection of the residuals ordered in ranges of sin θ/λ, $/F_o/$, and parity and value of the individual indexes showed no unusual features or trends. There was no evidence of secondary extinction in the low angle, high intensity data. The largest peak in the final difference Fourier map had an electron density of 0.661 e^-/A^3 near C(15).

Table III.

Crystal Data (-110 °C) for $[HNEt_2]_2[V_2O_2(OPh_2SiO)_2]$

Space Group	$P2_1/c$
a, Å	12.569(3)
b, Å	17.227(5)
c, Å	8.488(1)
β, deg	105.29
V, $Å^3$	1773
Z	4
fw	747.77
ρ (calc.) g/cm^3	1.39
μ (calc.) 1/cm	6.71
radiation	MoKα (λ = 0.71073Å)
monochrometer	highly oriented graphite
scan range, type	$3° \leq 2\theta \leq 45°$, θ-2θ
scan speed, deg/min	0.84-6.7, variable
scan width, deg	$\theta = 0.55 + 0.35 \tan\theta$
unique reflections	2305
reflections, $F_o^2 > 3\sigma(F_o^2)$	1716
R, %	5.39
R_w, %	8.52
GOF	3.61

$[HNEt_2][VO_2((OSiPh_2)_3O)]$

Colorless crystals of the compound were obtained by slow evaporation of an acetonitrile solution. A crystal was mounted on a glass fiber with Davcon "5-minute" epoxy. Preliminary precession photographs indicated triclinic Laue symmetry, and yielded preliminary cell dimensions.

The crystal for data collection was transferred to an Enraf-Nonius CAD4 automated diffractometer[7] and centered in the beam. The compound undergoes a phase transition when cooled below -40 °C, therefore the temperature was set at -35 °C. Automatic peak search and indexing yielded the same unit cell as found in the photographs, and confirmed the Laue symmetry. There were no systematic absences, and the space group $P\bar{1}$ was confirmed by solution and refinement of the structure.

Accurate cell dimensions and the orientation matrix were determined from a least-squares fit to the setting angles of the unresolved MoKα components of 24 symmetry related reflections with 2θ between 23 and 26 degrees. The results are given in Table IV along with parameters for data collection.

The 10710 raw intensity data were converted to structure factor amplitudes and their esds by correction for scan speed, background, Lorentz and polarization effects.[8-10] Analysis of the azimuthal scan[11] data showed no variation in

intensity so that an absorption correction was unwarranted. Rejection of redundant data gave a set of 10335 unique data which were used to solve and refine the structure.

Solution of the structure by Patterson synthesis was hindered by extensive overlapping, and by the original assumption that the molecule was a dimer. The positions of the vanadium and silicon atoms were found using MULTAN. The remaining atoms were found and refined using standard Fourier and least-squares techniques. All carbon atoms were refined anisotropically except C(50), C(5)1, C(53), C(5)4 and C(81)-C(84) located in a disordered phenyl ring. In a difference Fourier map calculated following refinement of all non-hydrogen atoms with anisotropic thermal parameters, peaks corresponding to the expected positions of many of the hydrogen atoms were found. Hydrogen atoms were included in the structure factor calculations in their expected positions based on idealized bonding geometry but were not refined in least-squares.

The final residuals for 915 variables refined against the 7486 data for which $F^2>3\sigma(F^2)$ were R = 3.7%, Rw = 5.1% and GOF = 2.159. The R value for all 10335 data was 9.7%.

The quantity minimized by the least-squares program was $\Sigma w(/F_O/-/F_C/)^2$, where w is the weight of a given observation. The p-factor[12], used to reduce the weight of intense reflections was set to 0.03 throughout refinement. The analytical forms for the scattering factor tables for the

neutral atoms[13] were used and all non-hydrogen scattering factors were corrected for both the real and imaginary components of anomolous dispersion[14].

Inspection of the residuals ordered in ranges of sin θ/λ, $/F_o/$, and parity and value of the individual indexes showed no unusual features or trends. There was no evidence of secondary extinction in the low angle, high intensity data. The largest peak in the final difference Fourier map had an electron density of 0.439 e^-/A^3 near C(52).

Table IV.

Crystal Data (-35 °C) for $[HNEt_2][VO_2((OSiPh_2)_3O)]$

Space Group	$P\bar{1}$
a, Å	11.136(1)
b, Å	19.296(2)
c, Å	19.577(2)
α, deg	75.773(1)
β, deg	77.290(1)
γ, deg	82.462(1)
V, $Å^3$	3964
Z	2
fw	766.97
ρ (calc.) g/cm^3	1.29
μ (calc.) 1/cm	3.98
radiation	MoKα (λ = 0.71073Å)
monochrometer	highly oriented graphite
scan range, type	$3° \leq 2\theta \leq 45°$, θ-2θ
scan speed, deg/min	0.84-6.7, variable
scan width, deg	$\theta = 0.55 + 0.35 \tan\theta$
unique reflections	10335
reflections, $F_o^2 > 3\sigma(F_o^2)$	7486
R, %	3.7
R_w, %	5.1
GOF	2.16

<u>$[Li(THF)_2]_2[VO((OSiPh_2)_2O)_2]\cdot 2THF$</u>

Pale blue crystals of the compound were obtained by slow cooling from a THF solution. A crystal of approximate dimensions 0.30 x 0.35 x 0.25 mm was mounted on a glass fiber with Superglue under a flow of cold nitrogen to prevent solvent evaporation.

The crystal for data collection was then quickly transferred to an Enraf-Nonius CAD4 automated diffractometer[7], cooled to -110(±2) °C and centered in the beam. Automatic peak search and indexing yielded a monoclinic cell. Inspection of h0l reflections showed systematic absences h0l, h+l 2n+1 consistent with an n-glide. Accurate cell dimensions and the orientation matrix were determined from a least-squares fit to the setting angles of the unresolved MoKα components of 24 symmetry related reflections with 2θ between 20 and 29 degrees. The results are given in Table V along with parameters for data collection.

The 5014 raw intensity data were converted to structure factor amplitudes and their esds by correction for scan speed, background, Lorentz and polarization effects.[8-10] Analysis of the azimuthal scan[11] data showed no variation in intensity so that an absorption correction was unwarranted. Rejection of systematically absent data as well as redundant data gave a set of 4603 unique data. An additional 10 reflections were rejected during final refinement whose

w*del^2 were unusually large. During data collection, these reflections were flagged for deviating from their calculated positions and were collected just prior to redetermination of the orientation matrix.

Solution of the structure was hindered by a strong pseudo mirror plane in an otherwise noncentrosymmetric structure. The positions of the vanadium and three of the silicon atoms were determined by MULTAN. The rest of the atom positions were found by standard Fourier and least-squares techniques. During the course of refinement, two types of disorder were observed. The first occurred in a THF molecule bound to Li(1). The disorder was best modeled using two partial occupancy carbon atoms, C(50) and C(50'), at 0.55 and 0.45 respectively. The second type appeared to be disorder between occupancy and non-occupancy. This disorder was modeled by assigning half occupancy to all of the atoms in that THF molecule. All atoms were refined anisotropically except for the oxygen and carbon atoms of the six THF molecules.

The final residuals for 681 variables refined against the 3290 data for which $F^2>3\sigma(F^2)$ were R = 8.16%, Rw = 10.1% and GOF = 3.36. The R value for all 4603 data was 17.0%.

The quantity minimized by the least-squares program was $\Sigma w(/F_o/-/F_c/)^2$, where w is the weight of a given observation. The p-factor[12], used to reduce the weight of intense reflections was set to 0.04 in the final stages of refine-

ment. The analytical forms for the scattering factor tables for the neutral atoms[13] were used and all non-hydrogen scattering factors were corrected for both the real and imaginary components of anomolous dispersion[14].

Inspection of the residuals ordered in ranges of sin θ/l, $/F_o/$, and parity and value of the individual indexes showed no unusual features or trends. There was no evidence of secondary extinction in the low angle, high intensity data. The largest peak in the final difference Fourier map had an electron density of 0.719 e^-/A^3 near C(70).

Table V.

Crystal Data (-110 °C) for
$[Li(THF)_2]_2[VO((OSiPh_2)_2O)_2]\cdot 2THF$

Space group	Pn
a, Å	21.447(7)
b, Å	16.215(4)
c, Å	10.319(3)
β, deg	100.53(2)
V, $Å^3$	3528
Z	4
fw	1338.66
ρ (calcd.) g/cm^3	2.52
μ (calcd.) 1/cm	5.19
radiation	MoKα (λ = 0.71073 Å)
monochrometer	highly ordered graphite
scan range, type	3° ≤ 2θ ≤ 45°, θ-2θ
scan speed, deg/min	0.84-6.7, variable
scan width, deg	θ = 0.55 + 0.35 tan θ
unique reflections	4603
reflections, $F_o^2>3\sigma(F_o^2)$	3290
R, %	8.16
Rw, %	10.1
GOF	3.36

References

(1) Kamienski, C. W.; Lewis, D. H. J. Org. Chem. **1965**, 30, 3498.

(2) Ruff, J. K. J. Am. Chem. Soc. **1961**, 83, 2835.

(3) Keller, R. N.; Wycoff, H. D. In "Inorganic Syntheses"; Fernelius, W. C., Ed.; McGraw-Hill: London, 1946; Vol. 2, p 1.

(4) Ruff, J. K.; Hawthorne, M. F. J. Chem. Soc. **1960**, 82, 2141.

(5) Kovar, R. A.; Ashby, E. C. Inorg. Chem. **1971**, 10(5), 893.

(6) Pike, R. A.; Schank, R. L. J. Org. Chem. **1962**, 27, 2190.

(7) Breederveld, H.; Watermann, H. I. Research Correspondance, Suppl. 1 to Research (London) **1953**, 6.

(8) Bradley, D. C.; Thomas, I. M. J. Chem. Soc. **1960**, 3857.

(9) Dermer, Von O. C.; Fernelius, W. C. Z. Anorg. Allg. Chem. **1935**, 221, 83.

(10) Bradley, D. C.; Mehrotra, R. C.; Wardlaw, W. J. Chem. Soc. **1952**, 4204.

(11) Bradley, D. C.; Mehta, M. L. Can. J. Chem. **1962**, 40, 1183.

(12) Alyea, E. C.; Bradley, D. C. J. Chem. Soc. (A) **1969**, 2330.

(13) Choukroun, R.; Gervais, D. Inorg. Chim. Acta. **1978**, 27, 163.

(14) Prandtl, W.; Hess, L. Z. anorg. Chem. **1913**, 82, 103.

(15) Alyea, E. C.; Basi, J. S.; Bradley, D. C.; Chisholm, M. H. J. Chem. Soc. (A) **1971**, 772.

(16) Basi, J. S.; Bradley, D. C.; Chisholm, M. H. J. Chem. Soc. (A) **1971**, 1433.

(17) Alyea, E. C.; Basi, J. C.; Bradley, D. C.; Chisholm, M. H. Chem. Comm. **1968**, 495.

(18) Young, C. W.; Servais, P. C.; Currie, C. C.; Hunter, M. J. J. Am. Chem. Soc. **1948**, 70, 3758.

(19) Zeitler, V. A.; Brown, C. A. J. Chem. Soc. **1957**, 79, 4618.

(20) Instrumentation at the University of California Chemistry Department X-ray Crystallographic Facility (CHEXRAY) consists of two Enraf-Nonius CAD-4 diffractometers, one controlled by a DEC PDP 8/a with an RKO5 disk and the other by a DEC PDP 8/e with an RLO1 disk. Both use Enraf-Nonius software as described in the CAD4 Operation Manual, Enraf-Nonius, Delft, Nov. 1977, updated Jan. 1980.

(21) Calculations were performed on DEC Microvax II using locally modified Nonius-SDP[3] software operating under Micro-VMS operating system.

(22) Structure Determination Package User's Guide, 1985, B. A. Frenz and Associates, Inc., College Station, Texas 77840.

(23) The data reduction formulae are:

$$F_o^2 = \frac{\omega}{Lp}(C-2B) \qquad \sigma_o(F_o^2) = \frac{\omega}{Lp}(C + 4B)^{1/2}$$

$$F_o = \sqrt{F_o^2} \qquad \sigma_o(F) = \sqrt{F_o^2 + \sigma_o(F_o^2)} - F_o$$

where C is the total count in the scan, B the sum of the two background counts, ω is the scan speed used in deg/min, and

$$\frac{1}{Lp} = \frac{\sin 2\theta\,(1 + \cos^2 2\theta_m)}{1 + \cos^2 2\theta_m - \sin^2 2\theta}$$

is the correction for Lorentz and polarization effects for a reflection with scattering angle 2θ and radiation monochromatized with a 50% perfect single-crystal monochrometer with scattering angle $2\theta_m$.

(24) Reflections used for azimuthal scans were located near $\upsilon = 90°$ and the intensities were measured at 10° increments of rotation of the crystal about the diffraction vector.

(25) $$R = \frac{\Sigma//F_o/ - /F_c//}{\Sigma/F_o/} \qquad wR = \left\{\frac{\Sigma w(/F_o/ - /F_c/)^2}{\Sigma wF_o^2}\right\}^{1/2}$$

$$GOF = \left\{\frac{\Sigma w(/F_o/ - /F_c/)^2}{(n_o - n_v)}\right\}^{1/2}$$

where n_o is the number of observations, n_v the number of variable parameters, and the weights w are given by

$$w = \frac{1}{\sigma^2(F_o)} \quad , \quad \sigma(F_o^2) = \sqrt{\sigma(F_o^2(F_o'^2) + (pF^2)^2}$$

where $\sigma 2(F_o)$ is calculated as above from $\sigma(F_o^2)$ and where p is the factor used to lower the weight of intense reflections.

(26) Cromer, D. T.; Waber, J. T. "International Tables for X-ray Crystallography"; The Kynoch Press: Birmingham, England, 1974; Vol. IV, Table 2.2B.

(27) Cromer, D. T., ibid., Table 2.3.1.

Appendix I

Tables of Thermal and Positional Parameters

Table I. Positional Parameters and Their Estimated Standard Deviations for $[H_2NEt_2]_2[Ti_4O_2(OH)_2(OSiPh_2O)_6]\cdot CH_3CN$

Atom	x	y	z	B(Å^2)
TI1	0.52899(7)	-0.072	0.06356(6)	1.43(4)
TI2	0.42630(7)	0.0832(1)	-0.00367(6)	1.54(4)
TI3	0.07163(7)	0.1692(1)	0.00440(6)	1.50(4)
TI4	-0.02898(7)	0.3236(1)	-0.06645(6)	1.60(4)
SI1	0.500	-0.2623(3)	0.000	1.59(8)
SI2	0.500	0.2713(3)	0.000	1.93(9)
SI3	0.4327(1)	0.0063(2)	0.1104(1)	1.65(6)
SI4	0.6677(1)	0.0130(2)	0.1238(1)	1.79(6)
SI5	0.000	-0.0166(3)	0.000	1.84(8)
SI6	0.000	0.5125(3)	0.000	1.91(8)
SI7	0.0566(1)	0.2302(2)	-0.1152(1)	1.65(6)
SI8	0.1705(1)	0.2537(2)	0.1197(1)	1.63(6)
O1	0.5236(2)	0.0768(4)	0.0546(2)	1.4(1)
O2	0.4459(2)	-0.0455(4)	-0.0029(2)	1.2(1)
O3	0.5217(2)	-0.1966(4)	0.0561(2)	1.3(1)
O4	0.4424(3)	0.2101(5)	-0.0015(2)	2.2(2)
O5	0.4913(3)	-0.0541(4)	0.1127(2)	1.8(1)
O6	0.4035(3)	0.0724(4)	0.0543(2)	1.8(1)
O7	0.6127(2)	-0.0584(4)	0.1166(2)	1.6(1)
O8	0.6478(3)	0.0779(5)	0.0681(2)	2.0(1)
O9	0.0228(3)	0.1836(4)	0.0548(2)	1.8(1)
O10	0.0532(3)	0.3050(5)	0.0027(2)	2.3(2)
O11	0.0586(2)	0.0464(4)	0.0031(2)	1.5(1)
O12	0.0272(3)	0.4505(5)	0.0560(3)	2.5(2)
O13	0.0971(2)	0.1838(5)	-0.0535(2)	1.7(1)
O14	0.0140(2)	0.3146(4)	-0.1113(2)	1.5(1)
O15	0.1494(2)	0.1848(5)	0.0657(2)	1.8(1)
O16	0.1096(3)	0.3070(5)	0.1198(2)	2.3(2)
N1	0.4787(2)	0.8639(4)	0.2457(2)	4.0(2)
N2	0.7742(2)	0.1584(4)	0.0006(2)	3.9(1)
N3	0.9745(2)	0.2725(4)	0.3269(2)	3.2(1)
C1	0.4312(2)	-0.3359(4)	-0.0081(2)	1.9(1)
C2	0.4392(3)	-0.4137(5)	0.0239(2)	2.5(1)
C3	0.3872(3)	-0.4651(5)	0.0193(3)	3.2(2)
C4	0.3289(3)	-0.4394(5)	-0.0171(3)	3.2(2)
C5	0.3200(3)	-0.3628(5)	-0.0504(3)	3.4(2)
C6	0.3714(3)	-0.3120(4)	-0.0451(2)	2.4(1)
C7	0.5287(3)	0.3428(4)	0.0657(2)	2.5(1)
C8	0.5006(3)	0.3358(5)	0.1024(2)	2.9(2)
C9	0.5235(3)	0.3898(6)	0.1512(3)	4.6(2)
C10	0.5724(4)	0.4471(5)	0.1633(3)	4.4(2)
C11	0.6002(3)	0.4537(5)	0.1278(3)	4.2(2)
C12	0.5790(3)	0.4016(5)	0.0792(3)	3.2(2)
C13	0.3722(2)	-0.0758(4)	0.1084(2)	2.0(1)

Table I. Positional Parameters and Their Estimated Standard Deviations (cont.)

Atom	x	y	z	B(Å^2)
C14	0.3398(3)	-0.0723(5)	0.1419(2)	2.9(1)
C15	0.2999(3)	-0.1404(6)	0.1413(3)	3.8(2)
C16	0.2908(3)	-0.2173(6)	0.1069(3)	4.3(2)
C17	0.3204(3)	-0.2215(5)	0.0727(3)	3.5(2)
C18	0.3602(3)	-0.1520(5)	0.0731(2)	2.6(1)
C19	0.4618(2)	0.0847(4)	0.1726(2)	2.1(1)
C20	0.4234(3)	0.1514(5)	0.1789(2)	3.2(2)
C21	0.4466(3)	0.2130(5)	0.2247(3)	4.1(2)
C22	0.5068(3)	0.2055(5)	0.2631(3)	3.7(2)
C23	0.5453(3)	0.1413(6)	0.2581(3)	4.3(2)
C24	0.5223(2)	0.0803(5)	0.2127(2)	3.0(2)
C25	0.7395(2)	-0.0500(4)	0.1318(2)	2.0(1)
C26	0.7994(3)	-0.0377(5)	0.1741(2)	2.9(2)
C27	0.8502(3)	-0.0841(5)	0.1742(3)	3.5(2)
C28	0.8428(3)	-0.1432(6)	0.1321(3)	3.8(2)
C29	0.7847(3)	-0.1571(6)	0.0902(3)	4.2(2)
C30	0.7337(3)	-0.1113(5)	0.0898(2)	3.3(2)
C31	0.6824(2)	0.0889(4)	0.1852(2)	1.9(1)
C32	0.7122(3)	0.0552(5)	0.2404(2)	2.6(2)
C33	0.7243(3)	0.1100(5)	0.2858(2)	3.1(2)
C34	0.7053(3)	0.2005(5)	0.2788(2)	3.3(2)
C35	0.6741(3)	0.2349(5)	0.2247(3)	3.3(2)
C36	0.6636(2)	0.1792(5)	0.1793(2)	2.5(1)
C37	-0.0308(2)	-0.0912(4)	-0.0628(2)	2.1(1)
C38	0.0052(3)	-0.1592(5)	-0.0708(2)	3.1(2)
C39	-0.0187(3)	-0.2198(5)	-0.1151(3)	4.2(2)
C40	-0.0795(3)	-0.2121(5)	-0.1536(3)	4.6(2)
C41	-0.1168(4)	-0.1441(7)	-0.1476(3)	5.4(2)
C42	-0.0932(3)	-0.0842(5)	-0.1032(3)	3.7(2)
C43	-0.0632(3)	0.5840(5)	0.0042(2)	2.9(2)
C44	-0.0873(3)	0.5625(7)	0.0410(3)	5.4(2)
C45	-0.1350(4)	0.616(1)	0.0446(3)	9.6(3)
C46	-0.1566(4)	0.6888(7)	0.0088(4)	9.0(3)
C47	-0.1340(4)	0.7103(6)	-0.0277(4)	7.1(3)
C48	-0.0872(3)	0.6607(5)	-0.0300(4)	4.8(2)
C49	0.0062(2)	0.1398(4)	-0.1619(2)	1.9(1)
C50	-0.0568(3)	0.1558(5)	-0.1980(2)	2.7(2)
C51	-0.0961(3)	0.0874(5)	-0.2304(3)	3.5(2)
C52	-0.0726(3)	-0.0001(5)	-0.2281(3)	3.5(2)
C53	-0.0114(3)	-0.0173(5)	-0.1938(3)	3.8(2)
C54	0.0274(3)	0.0500(5)	-0.1609(3)	3.1(2)
C55	0.1165(2)	0.2745(4)	-0.1373(2)	2.0(1)
C56	0.1254(2)	0.3661(5)	-0.1408(2)	3.1(2)
C57	0.1736(3)	0.4014(5)	-0.1524(3)	3.9(2)

Table I. Positional Parameters and Their Estimated Standard Deviations (cont.)

Atom	x	y	z	$B(Å^2)$
C58	0.2156(3)	0.3406(6)	-0.1578(3)	4.0(2)
C59	0.2074(3)	0.2493(5)	-0.1556(2)	3.3(2)
C60	0.1579(2)	0.2168(5)	-0.1458(2)	2.4(1)
C61	0.2125(2)	0.1852(4)	0.1845(2)	2.0(1)
C62	0.2339(3)	0.2237(5)	0.2378(2)	2.8(2)
C63	0.2655(3)	0.1720(5)	0.2854(2)	3.5(2)
C64	0.2776(3)	0.0827(6)	0.2828(3)	3.8(2)
C65	0.2591(4)	0.0432(5)	0.2312(3)	4.5(2)
C66	0.2266(3)	0.0933(5)	0.1826(2)	3.7(2)
C67	0.2247(2)	0.3446(4)	0.1161(2)	1.6(1)
C68	0.2016(3)	0.4277(5)	0.0913(3)	3.1(2)
C69	0.2406(3)	0.4964(5)	0.0876(3)	3.9(2)
C70	0.3042(3)	0.4806(5)	0.1101(3)	3.9(2)
C71	0.3278(3)	0.3995(5)	0.1344(3)	3.5(2)
C72	0.2890(3)	0.3317(5)	0.1386(2)	3.0(2)
C73	0.4396(3)	0.9737(6)	0.3017(3)	4.8(2)
C74	0.4616(3)	0.9111(5)	0.2705(3)	3.5(2)
C75	0.7580(4)	0.0622(8)	-0.0044(4)	7.6(3)
C76	0.8022(3)	-0.0039(6)	-0.0082(3)	5.5(2)
C77	0.7239(4)	0.2177(7)	0.0010(3)	6.1(3)
C78	0.7411(4)	0.3079(7)	0.0073(3)	6.0(3)
C79	0.9081(3)	0.3053(5)	0.2928(3)	3.4(2)
C80	0.9833(4)	0.1789(6)	0.3120(3)	5.4(2)
C81	1.0487(4)	0.1517(7)	0.3371(3)	6.3(3)
C82	0.8609(3)	0.2523(7)	0.3035(3)	5.3(2)

Anisotropically refined atoms are given in the form of the isotropic equivalent thermal parameter defined as:

$$(4/3) * [a^2*B(1,1) + b^2*B(2,2) + c^2*B(3,3) + ab(\cos gamma)*B(1,2)$$

$$+ ac(\cos beta)*B(1,3) + bc(\cos alpha)*B(2,3)]$$

Table I. Positional Parameters and Their Estimated Standard Deviations (cont.)

Atom	x	y	z	B(A^2)
H1	0.4813	-0.4309	0.0500	4.0**
H2	0.3943	-0.5202	0.0417	5.0**
H3	0.2941	-0.4745	-0.0187	5.0**
H4	0.2777	-0.3454	-0.0767	5.0**
H5	0.3661	-0.2584	-0.0684	4.0**
H6	0.4654	0.2938	0.0942	5.0**
H7	0.5033	0.3896	0.1768	6.0**
H8	0.5883	0.4822	0.1985	7.0**
H9	0.6369	0.4906	0.1392	6.0**
H10	0.6001	0.4045	0.0552	5.0**
H11	0.3457	-0.0196	0.1664	5.0**
H12	0.2764	-0.1347	0.1635	5.0**
H13	0.2632	-0.2650	0.1082	6.0**
H14	0.3131	-0.2739	0.0478	5.0**
H15	0.3798	-0.1547	0.0477	5.0**
H16	0.3789	0.1541	0.1517	5.0**
H17	0.4205	0.2621	0.2269	6.0**
H18	0.5211	0.2436	0.2955	6.0**
H19	0.5891	0.1388	0.2856	6.0**
H20	0.5494	0.0336	0.2089	5.0**
H21	0.8048	0.0060	0.2039	5.0**
H22	0.8910	-0.0761	0.2047	5.0**
H23	0.8789	-0.1729	0.1315	6.0**
H24	0.7796	-0.2007	0.0606	6.0**
H25	0.6925	-0.1216	0.0594	5.0**
H26	0.7237	-0.0095	0.2463	4.0**
H27	0.7471	0.0831	0.3234	5.0**
H28	0.7131	0.2388	0.3106	6.0**
H29	0.6614	0.2980	0.2191	6.0**
H30	0.5407	0.2025	0.1422	5.0**
H31	0.0492	-0.1635	-0.0445	5.0**
H32	0.0070	-0.2707	-0.1189	6.0**
H33	-0.0956	-0.2543	-0.1830	6.0**
H34	-0.1605	-0.1340	-0.1771	7.0**
H35	-0.1199	-0.0390	-0.0964	6.0**
H36	-0.0713	0.5105	0.0642	7.0**
H37	-0.1565	0.6118	0.0682	9.0**
H38	-0.1798	0.7399	0.0123	9.0**
H39	-0.1530	0.7620	-0.0552	9.0**
H40	-0.0707	0.6734	-0.0589	7.0**
H41	-0.0731	0.2176	-0.1997	5.0**
H42	-0.1393	0.1016	-0.2559	5.0**
H43	-0.0999	-0.0498	-0.2501	5.0**
H44	0.0050	-0.0783	-0.1938	6.0**

Table I. Positional Parameters and Their Estimated Standard Deviations (cont.)

Atom	x	y	z	B(Å^2)
H45	0.0710	0.0364	-0.1362	5.0**
H46	0.0973	0.4103	-0.1349	5.0**
H47	0.1780	0.4669	-0.1574	6.0**
H48	0.2515	0.3650	-0.1631	6.0**
H49	0.2358	0.2072	-0.1620	5.0**
H50	0.1517	0.1511	-0.1453	4.0**
H51	0.2249	0.2897	0.2397	5.0**
H52	0.2807	0.2016	0.3218	5.0**
H53	0.2985	0.0473	0.3166	6.0**
H54	0.2705	-0.0208	0.2295	6.0**
H55	0.2140	0.0616	0.1466	5.0**
H56	0.1572	0.4372	0.0756	5.0**
H57	0.2227	0.5552	0.0700	6.0**
H58	0.3323	0.5283	0.1102	6.0**
H59	0.3725	0.3899	0.1480	5.0**
H60	0.3076	0.2739	0.1579	5.0**
H61	0.7197	0.0506	-0.0345	8.0**
H62	0.7543	0.0433	0.0302	8.0**
H63	0.7879	-0.0665	-0.0099	8.0**
H64	0.8078	0.0071	-0.0413	8.0**
H65	0.8424	-0.0002	0.0234	8.0**
H66	0.7118	0.2016	0.0306	8.0**
H67	0.6860	0.2134	-0.0337	8.0**
H68	0.7085	0.3469	0.0064	8.0**
H69	0.7770	0.3155	0.0430	8.0**
H70	0.7512	0.3273	-0.0213	8.0**
H71	0.8985	0.3041	0.2535	4.0**
H72	0.9056	0.3691	0.3023	4.0**
H73	0.8197	0.2733	0.2819	7.0**
H74	0.8627	0.1883	0.2933	7.0**
H75	0.8698	0.2538	0.3421	7.0**
H76	0.9687	0.1743	0.2715	8.0**
H77	0.9600	0.1362	0.3225	8.0**
H78	1.0555	0.0912	0.3278	7.0**
H79	1.0739	0.1929	0.3269	7.0**
H80	1.0653	0.1546	0.3779	7.0**

** -- Atoms included but not refined.

Table Ia. Table of General Temperature Factor Expressions - B's for $[H_2NEt_2]_2[Ti_4O_2(OH)_2(OSiPh_2O)_6]\cdot CH_3CN$

Name	B(1,1)	B(2,2)	B(3,3)	B(1,2)	B(1,3)	B(2,3)	Beqv
TI1	1.41(3)	1.36(4)	1.43(3)	0.04(3)	0.60(2)	0.07(3)	1.37(2)
TI2	1.53(3)	1.50(4)	1.44(3)	0.21(3)	0.65(2)	0.01(3)	1.49(2)
TI3	1.45(3)	1.57(4)	1.51(3)	-0.02(3)	0.62(2)	-0.01(3)	1.52(2)
TI4	1.43(3)	1.64(4)	1.76(3)	0.06(3)	0.83(2)	0.11(3)	1.55(2)
SI1	1.70(7)	1.14(9)	2.05(8)	0	0.83(5)	0	1.62(5)
SI2	2.53(8)	1.39(9)	1.92(8)	0	1.08(6)	0	1.90(5)
SI3	1.51(5)	2.02(7)	1.33(5)	-0.01(5)	0.68(4)	-0.19(5)	1.60(3)
SI4	1.31(5)	2.11(7)	1.51(5)	-0.05(5)	0.33(4)	0.05(5)	1.74(4)
SI5	1.81(7)	1.5(1)	1.92(8)	0	0.73(6)	0	1.77(5)
SI6	1.78(7)	1.4(1)	2.86(8)	0	1.42(5)	0	1.67(5)
SI7	1.49(5)	1.72(7)	1.66(5)	0.14(5)	0.85(4)	0.18(5)	1.56(3)
SI8	1.41(5)	1.79(7)	1.69(5)	0.07(5)	0.61(4)	-0.15(5)	1.65(3)
O1	1.7(1)	1.1(2)	1.3(1)	-0.3(1)	0.38(9)	0.2(1)	1.45(8)
O2	1.6(1)	1.5(2)	1.1(1)	-0.0(1)	0.63(9)	0.0(1)	1.36(8)
O3	1.2(1)	1.4(2)	1.8(1)	-0.4(1)	0.92(9)	-0.2(1)	1.38(8)
O4	2.5(1)	1.3(2)	2.6(1)	-0.1(1)	1.2(1)	-0.2(1)	2.15(9)
O5	1.5(1)	1.9(2)	1.5(1)	0.2(1)	0.61(9)	0.3(1)	1.65(8)
O6	1.8(1)	1.8(2)	1.8(1)	0.1(1)	1.07(9)	0.1(1)	1.70(8)
O7	1.3(1)	2.1(2)	1.6(1)	-0.1(1)	0.58(9)	0.6(1)	1.70(8)
O8	1.5(1)	2.3(2)	1.7(1)	-0.3(1)	0.4(1)	0.1(1)	1.95(9)
O9	1.2(1)	1.8(2)	1.8(1)	-0.1(1)	0.73(9)	-0.1(1)	1.56(8)
O10	1.7(1)	2.0(2)	2.5(1)	0.2(1)	1.0(1)	-0.2(1)	2.06(9)
O11	1.3(1)	1.8(2)	1.6(1)	0.3(1)	0.68(9)	0.4(1)	1.56(8)

Table Ia. Table of General Temperature Factor Expressions - B's (cont.)

Name	B(1,1)	B(2,2)	B(3,3)	B(1,2)	B(1,3)	B(2,3)	Beqv
O12	2.8(1)	1.9(2)	2.1(1)	-0.6(1)	1.1(1)	-0.2(1)	2.23(9)
O13	1.5(1)	1.8(2)	1.8(1)	0.0(1)	0.71(9)	-0.1(1)	1.71(8)
O14	1.6(1)	1.6(2)	1.8(1)	0.2(1)	0.84(9)	0.1(1)	1.63(8)
O15	1.3(1)	2.0(2)	1.9(1)	-0.1(1)	0.53(9)	-0.2(1)	1.78(8)
O16	1.7(1)	2.2(2)	2.0(1)	-0.2(1)	0.91(9)	-0.1(1)	1.92(9)
N1	3.2(2)	2.7(2)	3.7(2)	-0.9(2)	1.7(1)	-1.4(2)	3.1(1)
N2	1.9(2)	4.7(3)	5.5(2)	0.4(2)	1.6(2)	1.4(2)	4.0(1)
N3	4.1(2)	4.4(3)	3.5(2)	0.9(2)	1.7(2)	1.2(2)	4.0(2)
C1	1.9(2)	1.7(2)	2.3(2)	0.5(2)	1.2(1)	-0.3(2)	1.9(1)
C2	3.2(2)	1.8(3)	2.9(2)	0.1(2)	1.5(2)	0.3(2)	2.6(1)
C3	5.3(3)	2.0(3)	4.1(2)	-0.9(2)	3.5(2)	-0.5(2)	3.3(2)
C4	2.4(2)	3.4(3)	3.9(3)	-1.5(2)	1.6(2)	-1.5(2)	3.1(2)
C5	2.4(2)	4.9(4)	2.4(2)	-0.8(3)	0.8(2)	-0.5(3)	3.3(2)
C6	2.7(2)	2.9(3)	1.8(2)	-0.4(2)	1.1(1)	-0.1(2)	2.4(1)
C7	3.6(2)	0.9(2)	2.2(2)	0.2(2)	1.1(2)	0.1(2)	2.3(1)
C8	3.6(2)	3.0(3)	2.3(2)	-0.4(3)	1.4(2)	-0.6(2)	2.9(2)
C9	5.6(3)	5.8(4)	2.7(2)	1.2(3)	2.1(2)	-0.8(3)	4.6(2)
C10	5.6(4)	3.2(4)	3.2(3)	0.1(3)	0.3(3)	-0.7(3)	4.6(2)
C11	4.4(3)	2.8(3)	3.5(3)	-1.1(3)	0.2(2)	-0.4(3)	4.1(2)
C12	4.0(3)	2.6(3)	2.9(2)	-0.9(3)	1.4(2)	-0.1(2)	3.2(2)
C13	1.5(2)	2.9(3)	1.6(2)	0.4(2)	0.7(1)	0.7(2)	2.0(1)
C14	2.8(2)	4.0(3)	2.2(2)	-0.8(2)	1.6(1)	-0.4(2)	2.8(1)
C15	3.0(2)	5.3(4)	3.4(2)	-1.6(3)	1.9(2)	-0.4(3)	3.7(2)

Table Ia. Table of General Temperature Factor Expressions - B's (cont.)

Name	B(1,1)	B(2,2)	B(3,3)	B(1,2)	B(1,3)	B(2,3)	Beqv
C16	3.8(3)	4.8(4)	4.2(3)	-2.1(3)	1.8(2)	-0.3(3)	4.3(2)
C17	3.9(3)	3.0(3)	3.8(3)	-1.5(3)	1.7(2)	-1.3(3)	3.5(2)
C18	2.6(2)	3.2(3)	2.3(2)	-0.6(2)	1.2(2)	-0.7(2)	2.6(1)
C19	2.3(2)	1.7(3)	2.4(2)	-0.3(2)	1.5(1)	-0.3(2)	2.0(1)
C20	3.3(3)	3.3(3)	2.5(2)	1.4(2)	0.7(2)	-0.3(2)	3.2(2)
C21	5.6(3)	3.1(3)	3.6(3)	1.1(3)	2.0(2)	-1.0(3)	4.1(2)
C22	3.5(3)	4.4(4)	3.0(2)	-1.4(3)	1.1(2)	-2.1(3)	3.7(2)
C23	2.6(3)	5.7(4)	3.9(3)	-0.9(3)	1.1(2)	-1.9(3)	4.1(2)
C24	1.9(2)	3.9(3)	3.5(2)	-0.3(2)	1.5(2)	-1.1(2)	3.0(2)
C25	1.5(2)	2.2(3)	2.1(2)	-0.6(2)	0.5(1)	0.3(2)	2.0(1)
C26	2.4(2)	3.0(3)	2.5(2)	-0.4(2)	0.6(2)	-0.3(2)	2.8(2)
C27	1.6(2)	4.7(4)	4.0(3)	1.0(3)	1.0(2)	0.9(3)	3.5(2)
C28	3.4(2)	4.7(4)	4.5(2)	1.7(3)	2.8(2)	1.5(3)	3.8(2)
C29	3.8(3)	5.5(4)	4.0(3)	0.9(3)	2.1(2)	-1.0(3)	4.3(2)
C30	2.7(2)	4.3(4)	2.6(2)	-0.1(3)	0.9(2)	-1.3(2)	3.3(2)
C31	1.6(2)	2.1(3)	2.0(2)	-0.2(2)	0.9(1)	-0.2(2)	1.8(1)
C32	2.1(2)	2.8(3)	2.6(2)	-0.5(2)	0.9(2)	0.2(2)	2.6(1)
C33	2.7(2)	4.6(4)	2.3(2)	-0.4(3)	1.2(2)	-0.4(2)	3.1(2)
C34	3.2(2)	3.8(3)	3.3(2)	-0.9(2)	1.9(2)	-1.3(2)	3.2(2)
C35	2.8(2)	2.9(3)	4.7(3)	-0.3(2)	2.2(2)	-1.3(3)	3.3(2)
C36	1.7(2)	3.1(3)	2.6(2)	-0.2(2)	1.0(1)	0.4(2)	2.5(1)
C37	2.2(2)	2.4(3)	2.1(2)	0.1(2)	0.9(2)	-0.2(2)	2.2(1)
C38	4.3(3)	2.7(3)	2.4(2)	0.3(3)	1.6(2)	-0.4(2)	3.1(2)

Table Ia. Table of General Temperature Factor Expressions - B's (cont.)

Name	B(1,1)	B(2,2)	B(3,3)	B(1,2)	B(1,3)	B(2,3)	Beqv
C39	6.3(3)	3.1(3)	3.9(3)	0.2(3)	3.1(2)	-0.4(3)	4.1(2)
C40	6.2(3)	3.7(4)	4.1(3)	-1.4(3)	2.3(2)	-2.5(3)	4.6(2)
C41	4.4(3)	7.2(5)	3.8(3)	-2.1(4)	0.9(2)	-2.2(3)	5.5(2)
C42	2.6(2)	4.8(4)	3.1(3)	-0.5(3)	0.8(2)	-1.9(3)	3.6(2)
C43	2.0(2)	2.4(3)	3.4(2)	0.3(2)	0.6(2)	-1.2(2)	2.8(2)
C44	3.8(3)	8.7(5)	4.0(3)	2.1(3)	2.3(2)	-0.8(3)	5.3(2)
C45	4.7(3)	21(1)	4.4(3)	6.0(4)	1.5(2)	-2.0(5)	10.3(3)
C46	3.7(3)	12.9(6)	10.3(4)	2.6(3)	0.7(3)	-8.3(4)	9.8(3)
C47	2.9(3)	2.7(3)	13.4(6)	1.3(3)	0.9(3)	-2.7(4)	7.2(3)
C48	2.5(3)	1.8(3)	9.5(4)	-0.2(3)	1.8(3)	-0.2(3)	4.9(2)
C49	2.2(2)	2.5(3)	1.6(2)	-0.2(2)	1.2(1)	-0.0(2)	2.0(1)
C50	2.1(2)	3.0(3)	2.5(2)	0.2(2)	0.6(2)	-0.2(2)	2.7(2)
C51	2.6(2)	4.4(4)	2.5(2)	-0.5(3)	0.4(2)	-0.1(3)	3.4(2)
C52	3.8(3)	3.2(3)	3.4(2)	-1.7(3)	1.6(2)	-1.5(3)	3.5(2)
C53	4.1(3)	1.9(3)	4.3(3)	-0.1(3)	1.2(2)	-0.5(3)	3.6(2)
C54	3.2(2)	2.3(3)	3.1(2)	0.4(2)	1.1(2)	0.1(2)	3.0(2)
C55	2.3(2)	2.4(3)	1.3(2)	0.3(2)	0.9(1)	0.3(2)	2.0(1)
C56	2.0(2)	4.0(3)	4.0(2)	-0.0(2)	2.3(1)	-0.1(2)	3.0(2)
C57	3.5(2)	3.7(4)	4.6(3)	-0.1(3)	2.3(2)	0.7(3)	3.7(2)
C58	2.4(2)	6.4(4)	3.5(2)	-0.7(3)	1.8(2)	0.3(3)	3.9(2)
C59	2.4(2)	4.8(4)	3.3(2)	0.9(3)	1.9(1)	0.5(3)	3.3(2)
C60	2.3(2)	2.9(3)	2.5(2)	0.4(2)	1.5(1)	0.2(2)	2.4(1)
C61	1.5(2)	2.2(3)	2.5(2)	0.0(2)	1.0(1)	-0.1(2)	2.1(1)

Table Ia. Table of General Temperature Factor Expressions - B's (cont.)

Name	B(1,1)	B(2,2)	B(3,3)	B(1,2)	B(1,3)	B(2,3)	Beqv
C62	3.3(2)	2.9(3)	2.0(2)	0.3(3)	0.7(2)	-0.3(2)	2.9(2)
C63	3.6(3)	4.7(4)	1.6(2)	0.2(3)	0.4(2)	-0.6(3)	3.6(2)
C64	4.1(3)	4.4(4)	2.9(2)	1.3(3)	1.5(2)	1.1(3)	3.8(2)
C65	6.6(4)	3.4(3)	3.6(3)	2.0(3)	2.2(2)	1.1(3)	4.5(2)
C66	5.2(3)	3.6(3)	2.0(2)	0.9(3)	1.2(2)	-0.3(3)	3.7(2)
C67	1.4(2)	1.9(3)	1.3(2)	-0.1(2)	0.4(1)	-0.2(2)	1.6(1)
C68	2.3(2)	3.2(3)	3.8(3)	-0.1(2)	1.3(2)	0.1(3)	3.1(2)
C69	4.3(3)	2.7(3)	5.3(3)	-0.7(3)	2.8(2)	0.2(3)	3.8(2)
C70	4.7(3)	3.8(3)	3.9(3)	-2.7(3)	2.3(2)	-1.5(3)	4.0(2)
C71	1.9(2)	4.7(4)	3.6(3)	-1.1(3)	0.9(2)	0.2(3)	3.5(2)
C72	2.0(2)	3.9(3)	2.9(2)	-0.7(2)	0.8(2)	-0.2(3)	3.0(2)
C73	6.1(3)	4.8(4)	4.1(3)	2.9(3)	2.8(2)	0.9(3)	4.8(2)
C74	3.4(3)	3.8(3)	2.7(2)	0.7(3)	0.9(2)	1.2(3)	3.5(2)
C75	4.0(3)	8.1(5)	12.0(5)	-4.4(3)	3.7(3)	-5.6(4)	7.9(3)
C76	5.7(3)	3.7(4)	8.3(4)	-2.0(3)	4.2(2)	-1.5(3)	5.5(2)
C77	6.1(4)	6.5(5)	4.5(3)	-0.4(4)	1.2(3)	0.9(4)	6.1(3)
C78	6.0(4)	7.7(6)	4.3(3)	0.1(4)	2.1(3)	1.3(4)	6.0(2)
C79	2.7(3)	5.2(4)	2.0(2)	-0.3(3)	0.1(2)	-0.3(3)	3.6(2)
C80	5.4(3)	4.0(4)	7.1(4)	-0.7(3)	2.9(3)	-0.8(4)	5.4(2)
C81	8.0(4)	5.7(5)	6.7(4)	1.4(4)	4.3(3)	1.2(4)	6.4(3)
C82	4.0(3)	8.6(5)	3.6(3)	-2.6(3)	2.1(2)	-1.5(3)	5.2(2)

The form of the anisotropic thermal parameter is:

$\exp[-0.25(h^2 a^{*2} B(1,1) + k^2 b^{*2} B(2,2) + l^2 c^{*2} B(3,3)' + 2hka^*b^*B(1,2) + 2hla^*c^*B(1,3)$

$+ 2klb^*c^*B(2,3))]$, where a*, b*, and c* are reciprocal lattice constants.

Table II. Positional Parameters and Their Estimated Standard Deviations $[H_2NEt_2]_2[Ti_4O_2(OH)_2(OSiPh_2O)_5((OSiPh_2)_2O)]\cdot PhMe\cdot 2H_2O$

Atom	x	y	z	B(Å^2)
TI1	0.59970(5)	-0.06249(5)	0.23344(5)	1.70(2)
TI2	0.55433(5)	0.06120(5)	0.21830(5)	1.55(2)
SI1	0.46866(9)	-0.21155(6)	0.17774(6)	1.98(4)
SI2	0.58311(8)	0.01327(8)	0.36832(8)	2.00(4)
SI3	0.7627(1)	-0.0600(1)	0.2233(1)	3.94(5)
SI4	0.3923(1)	0.000	0.167	2.06(6)
O1	0.5384(2)	-0.1616(2)	0.2278(2)	2.20(9)
O2	0.4521(2)	-0.1609(2)	0.1262(2)	1.99(9)
O3	0.5663(2)	0.0620(2)	0.3149(2)	1.93(9)
O4	0.5994(2)	-0.2437(2)	0.3261(2)	2.13(9)
O5	0.6858(2)	-0.0636(2)	0.2315(2)	2.9(1)
O6	0.8126(3)	0.000	0.167	4.5(2)
O7	0.4638(2)	0.0529(2)	0.2133(2)	2.14(9)
O8	0.6530(2)	0.0516(2)	0.2105(2)	1.65(8)
O9	0.5179(2)	-0.0445(2)	0.2147(2)	1.57(9)
O10	0.3854(3)	-0.1947(3)	0.9787(3)	6.2(2)
N1	0.2712(5)	-0.1853(5)	1.0269(6)	17.5(3)
C1	0.3884(3)	-0.2659(3)	0.2354(3)	2.5(1)
C2	0.3329(3)	-0.3332(4)	0.2175(4)	3.7(2)
C3	0.2748(4)	-0.3721(5)	0.2618(5)	6.0(3)
C4	0.2722(4)	-0.3424(4)	0.3249(4)	5.5(2)
C5	0.3271(4)	-0.2757(4)	0.3426(4)	4.8(2)
C6	0.3850(3)	-0.2375(4)	0.2994(4)	3.5(2)
C7	0.4913(3)	-0.2689(3)	0.1213(3)	2.5(1)
C8	0.5225(3)	-0.2424(3)	0.0564(3)	3.2(2)
C9	0.5457(4)	-0.2793(4)	0.0146(4)	4.1(2)
C10	0.5368(4)	-0.3440(4)	0.0370(4)	4.7(2)
C11	0.5066(4)	-0.3727(4)	0.1003(4)	4.5(2)
C12	0.4835(4)	-0.3352(3)	0.1431(4)	3.5(2)
C13	0.6643(3)	0.0744(3)	0.4215(3)	2.5(1)
C14	0.6645(3)	0.1237(3)	0.4659(4)	3.7(2)
C15	0.7240(4)	0.1708(4)	0.5043(4)	4.8(2)
C16	0.7849(4)	0.1679(4)	0.4991(4)	5.0(2)
C17	0.7891(4)	0.1197(4)	0.4538(5)	5.3(2)
C18	0.7285(4)	0.0726(4)	0.4144(4)	3.8(2)
C19	0.5022(3)	-0.0370(3)	0.4243(3)	2.6(1)
C20	0.5062(3)	-0.0491(3)	0.4952(3)	3.2(2)
C21	0.4437(4)	-0.0847(4)	0.5351(4)	4.3(2)
C22	0.3774(4)	-0.1082(4)	0.5054(4)	4.7(2)
C23	0.3714(4)	-0.0975(5)	0.4377(4)	5.6(3)
C24	0.4335(4)	-0.0631(4)	0.3967(4)	4.5(2)
C25	0.7525(4)	-0.1460(4)	0.1906(5)	5.4(2)
C26	0.7120(5)	-0.1803(5)	0.1375(7)	11.0(3)
C27	0.7085(5)	-0.2426(6)	0.1079(8)	14.9(4)

Table II. Positional Parameters and Their Estimated Standard Deviations (cont.)

Atom	x	y	z	$B(Å^2)$
C28	0.7469(5)	-0.2699(5)	0.1361(6)	7.5(3)
C29	0.7899(5)	-0.2381(5)	0.1922(6)	9.6(3)
C30	0.7998(5)	-0.1698(4)	0.2223(5)	9.1(2)
C31	0.8131(4)	-0.0360(5)	0.3071(5)	6.7(2)
C32	0.7791(8)	-0.0735(5)	0.3652(5)	10.3(4)
C33	0.8152(7)	-0.0611(6)	0.4308(6)	14.6(4)
C34	0.8822(7)	-0.016(1)	0.4338(8)	24.6(6)
C35	0.9186(8)	0.046(2)	0.3794(8)	29(2)
C36	0.8833(7)	0.020(2)	0.3100(8)	29(2)
C37	0.3712(3)	0.0584(3)	0.1110(3)	2.8(1)
C38	0.3021(4)	-0.1255(4)	0.2433(4)	3.9(2)
C39	0.4112(4)	0.1712(4)	0.0482(4)	5.4(2)
C40	0.3452(4)	0.1502(4)	0.0283(4)	6.3(2)
C41	0.2040(4)	-0.0828(5)	0.2856(5)	5.8(2)
C42	0.2629(4)	-0.0360(4)	0.2430(4)	4.8(2)
C43	0.2630(5)	-0.1359(5)	0.9921(8)	10.7(4)
C44	0.3228(6)	-0.0793(5)	0.9563(5)	8.3(3)
C45	0.199(1)	-0.2395(9)	1.082(1)	35.2(7)
C46	0.2349(7)	-0.2564(8)	1.1007(6)	18.5(5)
C47	0.676(1)	0.000	0.667	10.6(7)
C48	0.7189(9)	0.0075(6)	0.6050(6)	12.6(6)
C49	0.7757(7)	-0.0090(5)	0.7296(7)	10.2(5)
C50	0.815(1)	0.000	0.667	13.9(8)
C51	0.877(2)	0.000	0.667	19(2)
C52	0.602(2)	0.000	0.667	16(2)

Anisotropically refined atoms are given in the form of the isotropic equivalent thermal parameter defined as:

$$(4/3) * [a^2*B(1,1) + b^2*B(2,2) + c^2*B(3,3) + ab(\cos gamma)*B(1,2)$$

$$+ ac(\cos beta)*B(1,3) + bc(\cos alpha)*B(2,3)]$$

Table II. Positional Parameters and Their Estimated Standard Deviations (cont.)

Atom	x	y	z	B(Å^2)
H1	0.7090	0.0840	0.2337	3.5**
H2	0.3332	-0.3537	0.1725	6.0**
H3	0.2354	-0.4190	0.2495	8.0**
H4	0.2324	-0.3695	0.3568	8.0**
H5	0.3257	-0.2553	0.3882	7.0**
H6	0.4243	-0.1892	0.3124	6.0**
H8	0.5262	-0.1977	0.0299	5.0**
H9	0.5696	-0.2591	-0.0297	5.0**
H10	0.5511	-0.3709	0.0076	6.5**
H11	0.5027	-0.4176	0.1159	6.0**
H12	0.4620	-0.3544	0.1876	5.5**
H14	0.6198	0.1248	0.4709	6.0**
H15	0.7214	0.2052	0.5364	7.0**
H16	0.8261	0.1999	0.5270	7.0**
H17	0.8341	0.1189	0.4468	7.0**
H18	0.7315	0.0391	0.3815	6.0**
H20	0.5526	-0.0320	0.5164	5.0**
H21	0.4487	-0.0902	0.5848	6.0**
H22	0.3344	-0.1328	0.5342	7.0**
H23	0.3227	-0.1186	0.4165	7.3**
H24	0.4284	-0.0547	0.3474	6.0**
H38	0.2862	-0.1682	0.2718	6.0**
H39	0.4624	0.2140	0.0390	7.0**
H40	0.3259	0.1649	-0.0106	8.0**
H41	0.1715	-0.1185	0.3195	6.0**
H42	0.2982	-0.0137	0.2800	6.7**
H43	0.5840	0.1543	0.3333	8.0**
H44	0.5820	0.2363	0.3158	8.0**
H45	0.2472	-0.1131	1.0243	12.5**
H46	0.2254	-0.1597	0.9575	12.5**
H47	0.3406	-0.0978	0.9205	10.0**
H48	0.3624	-0.0513	0.9873	10.0**
H49	0.3103	-0.0461	0.9344	10.0**
H50	0.1909	-0.2120	1.1148	38.5**
H51	0.1575	-0.2755	1.0622	38.5**
H52	0.2113	-0.2936	1.1408	20.0**
H53	0.2466	-0.2848	1.0688	20.0**
H54	0.2802	-0.2213	1.1214	20.0**

** -- Atoms included but not refined.

Table IIa. Table of General Temperature Factor Expressions - B's for $[H_2NEt_2]_2[Ti_4O_2(OH)_2(OSiPh_2O)_5((OSiPh_2)_2O)]\cdot PhMe\cdot 2H_2O$

Name	B(1,1)	B(2,2)	B(3,3)	B(1,2)	B(1,3)	B(2,3)	Beqv
TI1	1.91(3)	1.62(3)	1.61(4)	0.90(2)	-0.27(3)	-0.02(3)	1.70(2)
TI2	1.77(3)	1.47(3)	1.39(4)	0.80(2)	0.14(3)	-0.02(3)	1.55(2)
SI1	2.36(5)	1.26(5)	2.03(6)	0.70(4)	-0.12(5)	0.01(5)	1.98(4)
SI2	2.33(5)	2.01(5)	1.41(6)	0.89(4)	-0.15(5)	-0.12(5)	2.00(4)
SI3	3.06(6)	3.79(7)	5.6(1)	2.15(4)	0.35(7)	1.05(7)	3.94(5)
SI4	1.87(7)	2.3(1)	2.16(9)	B(2,2)	-0.13(4)	2B(1,3)	2.06(6)
O1	2.8(1)	1.9(1)	1.9(2)	1.17(9)	-0.0(1)	0.2(1)	2.20(9)
O2	2.2(1)	1.4(1)	2.0(2)	0.7(1)	-0.1(1)	0.0(1)	1.99(9)
O3	2.2(1)	2.0(1)	1.3(1)	0.86(9)	-0.0(1)	-0.2(1)	1.93(9)
O4	2.8(1)	1.8(1)	1.6(2)	1.02(9)	-0.3(1)	0.2(1)	2.13(9)
O5	2.6(1)	3.4(1)	3.5(2)	2.0(1)	-0.3(1)	0.1(1)	2.9(1)
O6	3.5(2)	3.9(4)	6.2(4)	B(2,2)	0.6(2)	2B(1,3)	4.5(2)
O7	2.1(1)	2.2(1)	2.2(2)	1.07(9)	-0.2(1)	-0.2(1)	2.14(9)
O8	1.7(1)	1.3(1)	1.7(1)	0.53(9)	0.2(1)	0.0(1)	1.65(8)
O9	1.7(1)	1.2(1)	1.4(1)	0.43(9)	0.1(1)	0.0(1)	1.57(9)
O10	4.9(2)	6.0(3)	6.4(3)	1.8(2)	-1.9(2)	-2.9(2)	6.2(2)
N1	23.4(5)	20.3(4)	20.0(7)	19.2(3)	14.7(5)	14.6(5)	17.5(3)
C1	2.7(2)	2.1(2)	2.5(3)	1.0(2)	-0.1(2)	0.8(2)	2.5(1)
C2	2.2(3)	3.1(3)	4.0(3)	-0.1(2)	-0.2(3)	0.6(3)	3.7(2)
C3	3.6(3)	4.7(4)	7.1(5)	0.0(3)	-0.8(4)	2.2(4)	6.0(3)
C4	3.6(3)	6.0(3)	6.2(4)	1.9(2)	1.8(3)	3.9(3)	5.5(2)
C5	4.8(3)	6.3(3)	4.0(3)	3.4(2)	1.8(3)	2.0(3)	4.8(2)

Table IIa. Table of General Temperature Factor Expressions - B's (cont.)

Name	B(1,1)	B(2,2)	B(3,3)	B(1,2)	B(1,3)	B(2,3)	Beqv
C6	3.4(3)	3.7(2)	3.4(3)	1.8(2)	0.7(2)	0.7(2)	3.5(2)
C7	2.8(2)	2.5(2)	2.5(3)	1.6(1)	-0.8(2)	-0.5(2)	2.5(1)
C8	3.0(2)	3.4(2)	3.0(3)	1.4(2)	-0.5(2)	-1.1(2)	3.2(2)
C9	3.7(3)	4.8(3)	3.9(3)	2.2(2)	-0.4(3)	-0.7(3)	4.1(2)
C10	4.9(3)	5.9(3)	4.8(3)	3.7(2)	-2.1(3)	-3.1(3)	4.7(2)
C11	6.0(3)	4.1(2)	5.0(4)	3.8(2)	-1.4(3)	-0.9(3)	4.5(2)
C12	4.7(3)	2.5(2)	3.4(3)	1.9(2)	-1.1(2)	-0.6(2)	3.5(2)
C13	3.1(2)	2.6(2)	1.9(2)	1.4(2)	-0.3(2)	0.2(2)	2.5(1)
C14	4.0(3)	3.4(2)	3.9(3)	2.0(2)	-0.7(2)	-1.7(2)	3.7(2)
C15	5.0(3)	4.5(3)	5.5(4)	2.7(2)	-1.4(3)	-2.1(3)	4.8(2)
C16	5.9(4)	3.2(3)	4.8(4)	1.4(2)	-2.2(3)	-1.5(3)	5.0(2)
C17	3.6(3)	5.2(3)	7.0(5)	2.1(2)	-1.7(3)	-0.3(3)	5.3(2)
C18	2.8(2)	3.5(3)	4.6(3)	1.2(2)	-1.5(3)	-1.3(3)	3.8(2)
C19	3.8(2)	2.4(2)	1.9(2)	1.7(2)	0.2(2)	0.2(2)	2.6(1)
C20	3.6(2)	3.7(2)	2.2(3)	1.8(2)	0.3(2)	0.6(2)	3.2(2)
C21	5.6(3)	4.5(3)	2.6(3)	2.4(2)	1.0(3)	1.1(3)	4.3(2)
C22	3.4(3)	5.0(3)	4.8(3)	1.3(2)	2.2(3)	1.8(3)	4.7(2)
C23	3.1(3)	7.7(4)	4.5(4)	1.5(3)	0.4(3)	2.1(4)	5.6(3)
C	3.1(3)	6.0(4)	3.2(3)	1.3(2)	0.0(3)	0.6(3)	4.5(2)
C5	3.7(3)	4.0(3)	8.8(5)	2.2(2)	1.7(3)	0.6(3)	5.4(2)
C26	7.4(3)	8.5(4)	20.2(9)	6.2(2)	-8.0(5)	-8.7(5)	11.0(3)
C27	9.9(4)	14.5(6)	25(1)	9.4(3)	-111(5)	-121(6)	14.9(4)

Table IIa. Table of General Temperature Factor Expressions - B's (cont.)

Name	B(1,1)	B(2,2)	B(3,3)	B(1,2)	B(1,3)	B(2,3)	Beqv
C28	6.1(5)	5.1(4)	10.0(6)	1.8(3)	0.2(5)	-2.0(4)	7.5(3)
C29	15.0(4)	9.0(3)	10.4(7)	10.2(2)	2.4(5)	0.7(4)	9.6(3)
C30	15.2(4)	12.4(3)	7.2(5)	12.5(2)	3.2(4)	2.4(4)	9.1(2)
C31	6.3(3)	10.6(4)	5.9(4)	6.3(2)	-0.1(3)	1.0(4)	6.7(2)
C32	20.0(9)	6.7(4)	4.1(4)	6.6(4)	-0.2(6)	-0.3(4)	10.3(4)
C33	28.0(7)	21.9(6)	5.6(5)	21.2(4)	-2.9(5)	-2.3(5)	14.6(4)
C34	21.8(5)	58(1)	11(1)	32.7(4)	-0.5(6)	2.2(9)	24.6(6)
C35	7.4(8)	53(3)	12(1)	5(2)	-3.8(8)	-9(2)	29(2)
C36	3.9(5)	57(4)	11.6(9)	4(1)	-3.6(6)	-5(2)	29(2)
C37	3.3(2)	3.6(2)	2.5(3)	2.5(1)	-0.5(2)	-0.8(2)	2.8(1)
C38	3.3(3)	3.2(3)	3.5(3)	0.3(2)	-0.4(3)	0.8(3)	3.9(2)
C39	6.7(3)	6.2(3)	5.1(4)	4.5(2)	0.9(3)	2.1(3)	5.4(2)
C40	9.4(3)	9.3(3)	4.1(4)	7.6(2)	-0.8(3)	0.4(3)	6.3(2)
C41	3.1(3)	6.5(4)	6.2(4)	1.2(3)	2.3(3)	-0.6(4)	5.8(2)
C42	2.5(2)	6.4(3)	5.1(4)	1.9(2)	-0.3(3)	-2.3(3)	4.8(2)
C43	4.7(4)	3.8(4)	23(1)	1.4(3)	-1.9(6)	-3.3(6)	10.7(4)
C44	12.5(5)	8.8(5)	5.4(5)	6.7(3)	-2.1(5)	-1.6(4)	8.3(3)
C45	43(1)	10.5(8)	53(2)	13.6(7)	-41.(8)	-12.(9)	35.2(7)
C46	8.0(6)	20.0(9)	14.3(6)	-2.9(7)	5.4(5)	-121(5)	18.5(5)
C47	16(1)	6.8(9)	5.5(7)	B(2,2)	0.6(3)	2B(1,3)	10.6(7)
C48	19(1)	5.9(6)	8.5(7)	2.6(7)	-0.7(8)	-0.7(6)	12.6(6)
C49	11.0(8)	6.2(5)	10.9(8)	2.3(5)	0.7(7)	-0.9(6)	10.2(5)
C50	17(2)	4.4(8)	15(2)	B(2,2)	-1.3(5)	2B(1,3)	13.9(8)
C51	7(2)	5(2)	45(7)	B(2,2)	-3(2)	2B(1,3)	19(2)
C52	13(2)	26(6)	13(3)	B(2,2)	-1(2)	2B(1,3)	16(2)

The form of the anisotropic thermal parameter is:

$\exp[-0.25(h^2 a^{*2} B(1,1) + k^2 b^{*2} B(2,2) + l^2 c^{*2} B(3,3) + 2hka^*b^*B(1,2) + 2hla^*c^*B(1,3)$

$+ 2klb^*c^*B(2,3))]$, where a*,b*, and c* are reciprocal lattice constants.

Table III. Positional Parameters and Their Estimated Standard Deviations for $[H_2NEt_2]_2[V_2O_4(OSiPh_2O)_2]$

Atom	x	y	z	$B(Å^2)$
V1	0.02356(8)	0.11359(5)	0.0849(1)	1.52(2)
SI1	-0.1943(1)	0.02022(9)	-0.0878(2)	1.57(3)
O1	0.0358(3)	0.1894(2)	0.2057(4)	2.13(9)
O2	0.0405(4)	0.1435(2)	-0.0867(5)	2.41(9)
O3	-0.1107(3)	0.0698(2)	0.0558(5)	2.11(8)
O4	-0.1294(3)	-0.0422(2)	-0.1741(4)	1.78(8)
N1	0.0716(5)	0.1769(3)	0.5420(6)	2.7(1)
C1	-0.2948(5)	-0.0340(3)	-0.0037(6)	1.8(1)
C2	-0.3336(5)	-0.0074(3)	0.1275(7)	2.1(1)
C3	-0.4149(5)	-0.0456(4)	0.1780(7)	2.6(1)
C4	-0.4613(5)	-0.1121(3)	0.0984(7)	2.5(1)
C5	-0.4249(6)	-0.1400(3)	-0.0297(8)	2.7(1)
C6	-0.3440(5)	-0.1021(3)	-0.0811(7)	2.0(1)
C7	-0.2726(4)	0.0888(3)	-0.2470(6)	1.7(1)
C8	-0.3487(5)	0.0610(3)	-0.3870(7)	2.2(1)
C9	-0.4112(6)	0.1105(4)	-0.5038(7)	2.9(1)
C10	-0.3993(6)	0.1904(4)	-0.4822(7)	3.0(1)
C11	-0.3259(6)	0.2191(4)	-0.3450(8)	3.3(2)
C12	-0.2650(5)	0.1688(3)	-0.2277(7)	2.4(1)
C13	0.001(1)	0.1075(4)	0.5311(8)	6.5(3)
C14	-0.1165(9)	0.1281(7)	0.463(1)	9.3(3)
C15	0.1911(8)	0.1639(8)	0.606(1)	10.3(3)
C16	0.2604(9)	0.1827(9)	0.538(1)	16.2(4)

Anisotropically refined atoms are given in the form of the isotropic equivalent thermal parameter defined as:

$$(4/3) * [a^2*B(1,1) + b^2*B(2,2) + c^2*B(3,3) + ab(\cos gamma)*B(1,2) + ac(\cos beta)*B(1,3) + bc(\cos alpha)*B(2,3)]$$

Table III. Positional Parameters and Their Estimated Standard Deviations (cont.)

Atom	x	y	z	B(Å^2)
H2	-0.2994	0.0384	0.1859	4.0**
H3	-0.4418	-0.0243	0.2674	5.0**
H4	-0.5178	-0.1396	0.1302	5.0**
H5	-0.4567	-0.1856	-0.0858	4.0**
H6	-0.3173	-0.1231	-0.1731	4.0**
H8	-0.3565	0.0055	-0.4016	4.0**
H9	-0.4617	0.0903	-0.6022	5.0**
H10	-0.4395	0.2249	-0.5660	5.0**
H11	-0.3174	0.2743	-0.3282	5.2**
H12	-0.2190	0.1896	-0.1263	4.0**
H13	0.0194	0.0688	0.4625	9.0**
H14	0.0075	0.0853	0.6367	9.0**
H15	-0.1665	0.0852	0.4518	12.0**
H16	-0.1412	0.1674	0.5272	12.0**
H17	-0.1293	0.1508	0.3530	12.0**
H18	0.2118	0.1877	0.7105	15.0**
H19	0.1987	0.1079	0.6232	15.0**
H20	0.3332	0.1665	0.6005	20.0**
H21	0.2472	0.1561	0.4332	20.0**
H22	0.2603	0.2360	0.5205	20.0**
H23	0.0483	0.2143	0.6116	4.5**
H24	0.0584	0.1993	0.4361	4.5**

** -- Atoms included but not refined.

Table IIIa. Table of General Temperature Factor Expressions - B's for $[H_2NEt_2]_2[V_2O_4(OSiPh_2O)_2]$

Name	B(1,1)	B(2,2)	B(3,3)	B(1,2)	B(1,3)	B(2,3)	Beqv
V1	1.70(4)	1.05(3)	1.59(4)	-0.08(3)	0.04(3)	-0.10(3)	1.52(2)
SI1	1.50(6)	1.18(6)	1.79(6)	-0.02(5)	0.02(5)	0.08(5)	1.57(3)
O1	2.7(2)	1.1(1)	2.1(2)	-0.1(1)	-0.1(1)	-0.2(1)	2.13(9)
O2	3.1(2)	2.3(2)	1.9(1)	0.0(2)	0.7(1)	0.1(1)	2.41(9)
O3	2.2(2)	1.7(2)	2.0(2)	-0.5(1)	-0.1(1)	-0.2(1)	2.11(8)
O4	1.7(1)	1.4(1)	2.1(2)	0.3(1)	0.2(1)	0.1(1)	1.78(8)
N1	4.0(2)	2.4(2)	2.0(2)	1.6(2)	1.3(2)	0.4(2)	2.7(1)
C1	1.9(2)	1.6(2)	1.6(2)	-0.2(2)	-0.2(2)	0.6(2)	1.8(1)
C2	2.3(2)	1.9(2)	2.0(2)	0.3(2)	0.2(2)	0.0(2)	2.1(1)
C3	2.4(2)	2.4(3)	2.9(3)	0.5(2)	0.7(2)	0.6(2)	2.6(1)
C4	1.8(2)	2.0(2)	3.6(3)	-0.3(2)	0.5(2)	0.6(2)	2.5(1)
C5	2.8(3)	1.9(2)	3.1(3)	-0.8(2)	0.3(2)	-0.1(2)	2.7(1)
C6	1.9(2)	2.1(2)	1.8(2)	-0.4(2)	0.3(2)	-0.0(2)	2.0(1)
C7	1.7(2)	1.7(2)	1.8(2)	0.7(2)	0.9(2)	0.4(2)	1.7(1)
C8	2.4(2)	1.8(2)	2.4(2)	0.3(2)	0.6(2)	-0.0(2)	2.2(1)
C9	3.1(3)	3.0(3)	2.1(2)	0.4(3)	0.1(2)	-0.1(2)	2.9(1)
C10	4.1(3)	2.7(3)	2.0(2)	2.0(2)	0.6(2)	0.6(2)	3.0(1)
C11	4.4(3)	1.6(2)	3.5(3)	0.9(2)	0.6(3)	-0.0(2)	3.3(2)
C12	3.1(3)	1.9(2)	2.2(2)	0.5(2)	0.6(2)	0.1(2)	2.4(1)
C13	16.6(7)	1.4(3)	3.0(3)	-1.5(4)	5.2(3)	-0.6(2)	6.5(3)
C14	9.4(5)	13.2(7)	6.4(4)	-8.0(4)	4.3(4)	-4.5(5)	9.3(3)
C15	5.1(4)	21.0(9)	5.1(4)	7.4(5)	1.8(3)	6.7(5)	10.3(3)
C16	3.1(4)	29(1)	14.2(5)	-2.9(6)	-1.8(4)	17.4(5)	16.2(4)

The form of the anisotropic thermal parameter is:

$\exp[-0.25(h^2 a^{*2} B(1,1) + k^2 b^{*2} B(2,2) + l^2 c^{*2} B(3,3) + 2hka^*b^*B(1,2) + 2hla^*c^*B(1,3)$

$+ 2klb^*c^*B(2,3))]$, where a*,b*, and c* are reciprocal lattice constants.

Table IV. Positional Parameters and Their Estimated Standard Deviations for $[H_2NEt_2][VO_2((OSiPh_2)_3O)]$

Atom	x	y	z	B(A2)
V1	0.61049(5)	0.09840(3)	0.62251(3)	2.44(1)
SI1	0.50052(8)	-0.00172(5)	0.77710(5)	2.01(2)
SI2	0.73881(8)	0.02965(5)	0.82803(4)	2.02(2)
SI3	0.66958(8)	0.10073(5)	0.66958(5)	2.41(2)
O1	0.5315(2)	0.0291(1)	0.6913(1)	2.54(5)
O2	0.6161(2)	0.0057(1)	0.8123(1)	2.54(5)
O3	0.8276(2)	0.0680(1)	0.7551(1)	2.79(5)
O4	0.7732(2)	0.0863(1)	0.6245(1)	3.23(6)
O9	0.5548(2)	0.1762(1)	0.6373(2)	4.81(7)
O10	0.5907(2)	0.0935(2)	0.5443(1)	4.36(7)
C1	0.4752(3)	-0.0991(2)	0.7980(2)	2.32(7)
C2	0.5725(3)	-0.1523(2)	0.8028(2)	3.16(8)
C3	0.5521(3)	-0.2241(2)	0.8193(2)	3.71(9)
C4	0.4346(4)	-0.2444(2)	0.8310(2)	3.82(9)
C5	0.3361(3)	-0.1930(2)	0.8257(2)	3.42(9)
C6	0.3571(3)	-0.1210(2)	0.8098(2)	2.69(8)
C7	0.3578(3)	0.0484(2)	0.8175(2)	2.25(7)
C8	0.3015(3)	0.0253(2)	0.8893(2)	3.34(9)

Table IV. Positional Parameters and Their Estimated Standard Deviations (cont.)

Atom	x	y	z	B(A2)
C9	0.1957(4)	0.0613(2)	0.9201(2)	4.1(1)
C10	0.1434(3)	0.1217(2)	0.8784(2)	4.0(1)
C11	0.1963(3)	0.1457(2)	0.8076(2)	3.8(1)
C12	0.3032(3)	0.1090(2)	0.7776(2)	2.92(8)
C13	0.8280(3)	-0.0512(2)	0.8713(2)	2.24(7)
C14	0.7699(3)	-0.1110(2)	0.9125(2)	3.45(9)
C15	0.8350(4)	-0.1700(2)	0.9481(2)	4.5(1)
C16	0.9599(4)	-0.1699(2)	0.9427(2)	4.4(1)
C17	1.0194(3)	-0.1116(2)	0.9036(2)	4.4(1)
C18	0.9548(3)	-0.0525(2)	0.8673(2)	3.50(9)
C19	0.6927(3)	0.0914(2)	0.8901(2)	2.33(7)
C20	0.7782(4)	0.1117(2)	0.9217(2)	4.7(1)
C21	0.7440(4)	0.1554(2)	0.9706(2)	6.1(1)
C22	0.6239(5)	0.1802(2)	0.9885(2)	5.4(1)
C23	0.5376(4)	0.1608(2)	0.9597(2)	5.1(1)
C24	0.5717(3)	0.1162(2)	0.9106(2)	3.91(9)
C25	1.0234(3)	0.0578(2)	0.6353(2)	2.27(7)
C26	1.0489(3)	0.0372(2)	0.5703(2)	3.36(9)

Table IV. Positional Parameters and Their Estimated Standard Deviations (cont.)

Atom	x	y	z	B(A2)
C27	1.1669(3)	0.0115(2)	0.5413(2)	3.9(1)
C28	1.2613(3)	0.0057(2)	0.5774(2)	3.54(9)
C29	1.2385(3)	0.0249(2)	0.6426(2)	3.68(9)
C30	1.1211(3)	0.0507(2)	0.6712(2)	3.12(8)
C31	0.8861(3)	0.1975(2)	0.6571(2)	4.0(1)
C32	0.9084(4)	0.2392(2)	0.5855(3)	6.9(1)
C33	0.9278(5)	0.3134(3)	0.5750(4)	10.5(2)
C34	0.9257(5)	0.3421(3)	0.6332(5)	12.2(3)
C35	0.9085(6)	0.3008(3)	0.7033(4)	11.9(2)
C36	0.8876(5)	0.2277(2)	0.7150(3)	7.5(1)
N1	0.4340(3)	0.3037(2)	0.5758(2)	3.56(7)
C73	0.3018(4)	0.2943(3)	0.6049(2)	5.3(1)
C74	0.2609(4)	0.2352(3)	0.5804(3)	6.6(1)
C75	0.4760(4)	0.3660(2)	0.5936(2)	5.3(1)
C76	0.6106(5)	0.3704(3)	0.5673(3)	8.8(2)
V2	0.38607(5)	0.38515(3)	0.38890(3)	2.36(1)
S14	0.50382(8)	0.48315(5)	0.22869(5)	2.51(2)
S15	0.27798(8)	0.46010(5)	0.16770(5)	2.15(2)

Table IV. Positional Parameters and Their Estimated Standard Deviations (cont.)

Atom	x	y	z	B(Å²)
S16	0.15921(8)	0.35996(5)	0.31600(5)	2.30(2)
O5	0.4721(2)	0.4406(1)	0.3109(1)	3.68(6)
O6	0.4001(2)	0.4628(1)	0.1854(1)	2.97(5)
O7	0.2086(2)	0.4026(1)	0.2341(1)	2.91(5)
O8	0.2640(2)	0.3514(1)	0.3635(1)	3.29(6)
O11	0.4754(2)	0.3169(1)	0.4250(1)	3.59(6)
O12	0.3300(2)	0.4295(1)	0.4494(1)	4.49(7)
C37	0.5294(3)	0.5786(2)	0.2228(2)	2.78(8)
C38	0.6447(3)	0.6032(2)	0.2132(2)	3.63(9)
C39	0.6592(4)	0.6748(2)	0.2072(2)	4.4(1)
C40	0.5599(4)	0.7235(2)	0.2093(2)	5.2(1)
C41	0.4453(4)	0.7016(2)	0.2193(3)	7.1(1)
C42	0.4293(4)	0.6298(2)	0.2265(3)	5.5(1)
C43	0.6534(3)	0.4375(2)	0.1859(2)	2.83(8)
C44	0.7090(3)	0.3757(2)	0.2239(2)	3.56(9)
C45	0.8146(3)	0.3402(2)	0.1919(2)	4.5(1)
C46	0.8675(4)	0.3654(2)	0.1217(3)	5.4(1)
C47	0.8153(4)	0.4273(3)	0.0814(3)	6.0(1)

Table IV. Positional Parameters and Their Estimated Standard Deviations (cont.)

Atom	x	y	z	B(A2)
C48	0.7082(4)	0.4629(2)	0.1143(2)	4.7(1)
C49	0.1699(3)	0.5408(2)	0.1474(2)	2.81(8)
C50	0.2092(5)	0.6097(3)	0.1252(3)	3.2(1)*
C51	0.1253(6)	0.6697(4)	0.1048(4)	4.7(2)*
C52	0.0105(5)	0.6601(3)	0.1073(3)	7.9(2)
C53	-0.0346(6)	0.5892(4)	0.1214(4)	4.7(2)*
C54	0.0463(6)	0.5306(3)	0.1441(3)	3.6(1)*
C55	0.3223(3)	0.4174(2)	0.0897(2)	2.75(8)
C56	0.2296(4)	0.3943(2)	0.0641(2)	4.5(1)
C57	0.2600(5)	0.3596(2)	0.0081(2)	6.2(1)
C58	0.3798(6)	0.3470(2)	-0.0235(2)	7.4(2)
C59	0.4722(5)	0.3698(2)	-0.0002(2)	6.6(1)
C60	0.4432(4)	0.4055(2)	0.0558(2)	4.2(1)
C61	0.0179(3)	0.4102(2)	0.3554(2)	2.69(8)
C62	-0.0938(4)	0.4086(2)	0.3360(2)	5.0(1)
C63	-0.2001(4)	0.4451(3)	0.3642(3)	5.8(1)
C64	-0.1982(4)	0.4834(2)	0.4142(2)	4.6(1)
C65	-0.0894(4)	0.4868(2)	0.4342(2)	4.7(1)

Table IV. Positional Parameters and Their Estimated Standard Deviations (cont.)

Atom	x	y	z	B(A2)
C66	0.0177(3)	0.4505(2)	0.4049(2)	3.85(9)
C67	0.1029(3)	0.2700(2)	0.3113(2)	2.46(8)
C68	0.1046(3)	0.2560(2)	0.2481(2)	3.26(9)
C69	0.0728(4)	0.1900(2)	0.2456(2)	4.2(1)
C70	0.0597(4)	0.1359(2)	0.3062(2)	4.9(1)
C71	0.0785(4)	0.1476(2)	0.3694(2)	5.2(1)
C72	0.1089(4)	0.2140(2)	0.3721(2)	4.0(1)
C81	0.071(1)	0.5578(6)	0.2008(6)	5.8(2)*
C82	0.194(1)	0.5895(6)	0.0858(6)	5.7(3)*
C83	-0.010(1)	0.6212(7)	0.1850(7)	7.1(3)*
C84	0.116(1)	0.6539(6)	0.0707(6)	5.5(3)*
N2	0.5823(3)	0.1821(2)	0.4104(2)	3.83(8)
C77	0.7122(4)	0.1965(2)	0.3762(3)	6.0(1)
C78	0.7679(5)	0.2303(3)	0.4200(3)	8.3(2)
C79	0.5174(4)	0.1500(2)	0.3690(2)	5.5(1)
C80	0.3983(5)	0.1272(4)	0.4098(3)	8.7(2)

Starred atoms were included with isotropic thermal parameters.
The thermal parameter given for anisotropically refined atoms is the isotropic equivalent thermal parameter defined as:
(4/3) * [a2*B(1,1) + b2*B(2,2) + c2*B(3,3) + ab(cos gamma)*B(1,2) + ac(cos beta)*B(1,3) + bc(cos alpha)*B(2,3)]
where a,b,c are real cell parameters, and B(i,j) are anisotropic betas.

Table IVa. Table of General Temperature Factor Expressions - B's for $[H_2NEt_2][VO_2((OSiPh_2)_3O)]$

Name	B(1,1)	B(2,2)	B(3,3)	B(1,2)	B(1,3)	B(2,3)	Beqv
V1	1.80(2)	2.99(2)	2.13(2)	0.05(2)	-0.53(2)	0.15(2)	2.44(1)
SI1	1.79(3)	2.16(3)	2.15(3)	-0.27(3)	-0.55(3)	-0.38(3)	2.01(2)
SI2	1.80(3)	2.25(3)	2.06(3)	-0.21(3)	-0.57(3)	-0.40(3)	2.02(2)
SI3	1.73(4)	2.54(4)	2.55(4)	-0.22(3)	-0.29(3)	0.12(3)	2.41(2)
O1	2.24(9)	2.92(9)	2.31(9)	-0.37(8)	-0.46(7)	-0.22(7)	2.54(5)
O2	2.20(9)	2.75(9)	2.95(9)	-0.30(8)	-0.99(7)	-0.67(7)	2.54(5)
O3	2.48(9)	3.1(1)	2.50(9)	-0.44(8)	-0.36(8)	-0.19(8)	2.79(5)
O4	1.87(9)	4.7(1)	2.74(9)	-0.24(9)	-0.64(8)	-0.01(9)	3.23(6)
O9	3.6(1)	2.8(1)	7.2(2)	0.3(1)	-0.4(1)	-0.4(1)	4.81(7)
O10	3.7(1)	6.8(1)	2.3(1)	-0.9(1)	-1.08(8)	0.1(1)	4.36(7)
C1	2.7(1)	2.5(1)	2.0(1)	-0.1(1)	-0.6(1)	-0.7(1)	2.32(7)
C2	2.7(1)	3.1(1)	3.9(2)	0.0(1)	-1.1(1)	-1.1(1)	3.16(8)
C3	4.1(2)	2.4(1)	4.9(2)	0.3(1)	-2.0(1)	-0.9(1)	3.71(9)
C4	5.2(2)	2.5(1)	4.2(2)	-0.7(1)	-1.5(1)	-0.7(1)	3.82(9)
C5	3.4(2)	3.0(1)	3.9(2)	-1.2(1)	-0.3(1)	-0.9(1)	3.42(9)
C6	2.3(1)	2.8(1)	3.0(1)	-0.7(1)	-0.3(1)	-0.8(1)	2.69(8)
C7	1.9(1)	2.3(1)	2.8(1)	-0.5(1)	-0.6(1)	-0.8(1)	2.25(7)
C8	3.0(2)	3.8(2)	3.2(1)	-0.3(1)	-0.1(1)	-1.1(1)	3.34(9)

Table IVa. Table of General Temperature Factor Expressions - B's (cont.)

Name	B(1,1)	B(2,2)	B(3,3)	B(1,2)	B(1,3)	B(2,3)	Beqv
C9	3.5(2)	4.9(2)	3.7(2)	-0.7(2)	0.5(1)	-1.6(1)	4.1(1)
C10	2.5(2)	4.4(2)	5.5(2)	0.1(1)	-0.1(1)	-2.7(1)	4.0(1)
C11	3.0(2)	3.6(2)	5.1(2)	0.3(1)	-1.0(1)	-1.4(1)	3.8(1)
C12	2.6(1)	3.0(1)	3.2(1)	-0.2(1)	-0.5(1)	-0.7(1)	2.92(8)
C13	2.3(1)	2.4(1)	2.0(1)	-0.0(1)	-0.5(1)	-0.7(1)	2.24(7)
C14	3.3(2)	2.9(2)	4.1(2)	-0.5(1)	-1.4(1)	-0.1(1)	3.45(9)
C15	5.9(2)	2.7(2)	4.7(2)	-0.3(2)	-1.9(2)	0.4(1)	4.5(1)
C16	5.1(2)	3.8(2)	3.8(2)	1.8(2)	-1.7(1)	-0.4(1)	4.4(1)
C17	3.1(2)	5.4(2)	4.1(2)	1.3(2)	-1.0(1)	-0.3(2)	4.4(1)
C18	2.6(2)	4.2(2)	3.2(2)	0.3(1)	-0.6(1)	-0.1(1)	3.50(9)
C19	2.6(1)	2.1(1)	2.2(1)	-0.4(1)	-0.7(1)	-0.1(1)	2.33(7)
C20	4.3(2)	5.0(2)	6.2(2)	0.2(2)	-2.4(1)	-2.9(1)	4.7(1)
C21	7.8(2)	5.4(2)	7.2(2)	0.7(2)	-4.4(2)	-3.7(1)	6.1(1)
C22	9.3(3)	3.5(2)	3.7(2)	0.9(2)	-1.9(2)	-1.6(1)	5.4(1)
C23	5.1(2)	4.4(2)	5.7(2)	-0.0(2)	0.4(2)	-2.5(1)	5.1(1)
C24	3.2(2)	4.0(2)	5.0(2)	-0.3(1)	-0.6(1)	-2.2(1)	3.91(9)
C25	2.0(1)	2.2(1)	2.4(1)	-0.4(1)	-0.4(1)	-0.1(1)	2.27(7)
C26	2.6(1)	4.6(2)	2.9(1)	-0.2(1)	-0.8(1)	-0.8(1)	3.36(9)

Table IVa. Table of General Temperature Factor Expressions - B's (cont.)

Name	B(1,1)	B(2,2)	B(3,3)	B(1,2)	B(1,3)	B(2,3)	Beqv
C27	3.1(2)	5.4(2)	3.2(2)	0.2(2)	-0.3(1)	-1.5(1)	3.9(1)
C28	2.3(1)	3.9(2)	4.1(2)	0.5(1)	-0.5(1)	-0.9(1)	3.54(9)
C29	2.4(1)	4.7(2)	4.2(2)	0.5(1)	-1.3(1)	-1.3(1)	3.68(9)
C30	2.5(1)	4.0(2)	3.2(1)	0.1(1)	-0.9(1)	-1.3(1)	3.12(8)
C31	1.8(1)	2.7(2)	6.3(2)	-0.0(1)	0.3(2)	-0.1(2)	4.0(1)
C32	4.8(2)	4.5(2)	9.2(3)	-1.7(2)	-1.8(2)	3.5(2)	6.9(1)
C33	6.1(3)	4.9(2)	16.7(5)	-1.3(2)	-1.5(3)	4.7(3)	10.5(2)
C34	6.3(3)	3.7(2)	23.4(7)	-0.9(2)	2.5(4)	-1.9(3)	12.2(3)
C35	9.9(4)	5.5(2)	18.8(5)	-2.5(3)	5.3(4)	-6.1(3)	11.9(2)
C36	7.2(3)	4.0(2)	10.6(3)	-1.7(2)	2.6(2)	-3.9(2)	7.5(1)
N1	4.3(1)	3.3(1)	2.9(1)	-0.1(1)	-1.1(1)	-0.1(1)	3.56(7)
C73	3.6(2)	7.0(2)	4.4(2)	0.1(2)	-0.1(2)	-0.4(2)	5.3(1)
C74	4.7(2)	7.5(3)	7.2(3)	-1.8(2)	-1.9(2)	0.2(2)	6.6(1)
C75	5.8(2)	5.1(2)	5.3(2)	0.0(2)	-1.7(2)	-1.5(2)	5.3(1)
C76	8.1(3)	10.7(3)	8.8(3)	-4.7(2)	-0.0(2)	-3.6(2)	8.8(2)
V2	2.39(2)	2.58(2)	2.10(2)	-0.00(2)	-0.74(2)	-0.32(2)	2.36(1)
SI4	2.23(4)	2.55(4)	2.70(4)	-0.57(3)	-0.73(3)	-0.08(3)	2.51(2)
SI5	2.10(4)	2.24(4)	2.04(3)	-0.23(3)	-0.53(3)	-0.19(3)	2.15(2)

Table IVa. Table of General Temperature Factor Expressions - B's (cont.)

Name	B(1,1)	B(2,2)	B(3,3)	B(1,2)	B(1,3)	B(2,3)	Beqv
S16	2.09(4)	2.43(4)	2.24(3)	-0.42(3)	-0.29(3)	-0.26(3)	2.30(2)
O5	3.4(1)	4.2(1)	3.2(1)	-1.29(9)	-0.99(8)	0.47(9)	3.68(6)
O6	2.55(9)	3.2(1)	3.37(9)	-0.64(8)	-1.11(8)	-0.41(8)	2.97(5)
O7	3.0(1)	2.72(9)	2.63(9)	-0.48(8)	-0.31(8)	-0.00(8)	2.91(5)
O8	2.9(1)	4.0(1)	3.0(1)	-0.90(9)	-0.99(8)	-0.18(9)	3.29(6)
O11	3.4(1)	3.5(1)	3.5(1)	0.49(9)	-1.33(9)	0.06(9)	3.59(6)
O12	4.3(1)	5.7(1)	4.1(1)	0.4(1)	-0.8(1)	-2.51(9)	4.49(7)
C35	2.8(1)	2.9(1)	2.6(1)	-0.3(1)	-0.7(1)	-0.4(1)	2.78(8)
C36	3.3(2)	3.5(2)	4.4(2)	-0.8(1)	-0.6(1)	-1.5(1)	3.63(9)
C39	4.5(2)	4.2(2)	4.8(2)	-1.7(1)	-0.2(2)	-1.5(1)	4.4(1)
C40	6.3(2)	3.3(2)	6.5(2)	-1.2(2)	-1.9(2)	-1.1(2)	5.2(1)
C41	5.2(2)	3.1(2)	13.5(3)	1.0(2)	-3.1(2)	-2.4(2)	7.1(1)
C42	3.4(2)	3.6(2)	9.8(3)	-0.1(2)	-1.8(2)	-1.5(2)	5.5(1)
C43	2.4(1)	2.2(1)	4.1(2)	-0.3(1)	-1.0(1)	-0.5(1)	2.83(8)
C44	3.2(2)	2.8(1)	5.0(2)	-0.1(1)	-1.9(1)	-0.6(1)	3.56(9)
C45	3.4(2)	3.0(2)	7.5(2)	0.4(1)	-2.3(1)	-1.4(2)	4.5(1)
C46	2.8(2)	3.9(2)	9.5(3)	-0.1(2)	-0.1(2)	-2.5(2)	5.4(1)
C47	4.4(2)	5.1(2)	7.1(3)	-0.2(2)	1.6(2)	-1.1(2)	6.0(1)

Table IVa. Table of General Temperature Factor Expressions - B's (cont.)

Name	B(1,1)	B(2,2)	B(3,3)	B(1,2)	B(1,3)	B(2,3)	Beqv
C48	3.5(2)	4.0(2)	5.2(2)	0.0(2)	0.6(2)	-0.0(2)	4.7(1)
C49	2.7(1)	2.8(1)	2.4(1)	-0.1(1)	-0.3(1)	0.1(1)	2.81(8)
C52	5.6(2)	6.2(3)	8.8(3)	2.6(2)	-0.4(2)	1.8(3)	7.9(2)
C55	3.8(2)	1.9(1)	2.2(1)	-0.1(1)	-0.7(1)	0.1(1)	2.75(8)
C56	6.9(2)	4.0(2)	3.1(2)	-2.1(2)	-1.5(1)	-0.3(1)	4.5(1)
C57	12.1(3)	3.9(2)	3.7(2)	-2.4(2)	-2.8(2)	-0.6(1)	6.2(1)
C58	16.2(4)	2.7(2)	2.8(2)	0.6(2)	-1.6(2)	-0.9(1)	7.4(2)
C59	9.6(3)	4.9(2)	3.8(2)	2.5(2)	0.1(2)	-1.3(2)	6.6(1)
C60	4.7(2)	4.1(2)	3.0(2)	1.0(2)	-0.1(2)	-0.6(1)	4.2(1)
C61	2.6(1)	2.5(1)	2.9(1)	-0.3(1)	-0.3(1)	-0.5(1)	2.69(8)
C62	3.1(2)	6.6(2)	6.3(2)	0.6(2)	-1.0(2)	-3.8(1)	5.0(1)
C63	3.0(2)	7.7(2)	7.8(2)	1.1(2)	-1.5(2)	-4.2(2)	5.8(1)
C64	4.0(2)	4.0(2)	5.4(2)	1.0(2)	-0.2(2)	-1.5(2)	4.6(1)
C65	4.9(2)	4.5(2)	5.0(2)	0.4(2)	-0.3(2)	-2.4(1)	4.7(1)
C66	3.5(2)	4.2(2)	4.2(2)	-0.0(1)	-0.7(1)	-1.9(1)	3.85(9)
C67	1.7(1)	2.6(1)	2.9(1)	0.1(1)	-0.3(1)	-0.4(1)	2.46(8)
C68	3.4(2)	2.8(1)	3.4(2)	0.1(1)	-0.6(1)	-0.7(1)	3.26(9)
C69	4.9(2)	3.5(2)	4.8(2)	-0.2(1)	-1.1(1)	-1.9(1)	4.2(1)
C70	5.0(2)	3.3(2)	6.7(2)	-0.5(2)	-1.2(2)	-1.4(2)	4.9(1)
C71	6.2(2)	2.8(2)	5.8(2)	-1.2(2)	-1.3(2)	1.1(2)	5.2(1)
C72	4.6(2)	3.6(2)	3.7(2)	-1.1(1)	-1.2(1)	0.4(1)	4.0(1)
N2	4.6(2)	3.4(1)	3.2(1)	0.1(1)	-1.1(1)	-0.1(1)	3.83(8)
C77	5.2(2)	4.5(2)	6.1(2)	0.4(2)	1.5(2)	0.3(2)	6.0(1)
C78	4.1(2)	8.7(3)	11.7(4)	-1.9(2)	-0.7(2)	-1.3(3)	8.3(2)
C79	7.9(2)	5.0(2)	4.1(2)	0.4(2)	-2.8(2)	-1.0(2)	5.5(1)
C80	5.3(2)	14.4(4)	7.5(3)	-2.6(3)	-1.8(2)	-2.8(3)	8.7(2)

The form of the anisotropic temperature factor is:
exp[-0.25(h2a2B(1,1) + k2b2B(2,2) + l2c2B(3,3) + 2hkabB(1,2) + 2hlacB(1,3) + 2klbcB(2,3))] where a,b, and c are reciprocal lattice constants.

Table V. Positional Parameters and Their Estimated Standard Deviations for $[Li(THF)_2]_2[VO((OSiPh_2)_2O)_2]$

Atom	x	y	z	B(A2)
V1	0.000	0.2587(1)	0.000	2.21(4)
SI1	0.0493(2)	0.0848(3)	0.1612(4)	2.72(8)
SI2	-0.0792(2)	0.0852(2)	-0.0039(4)	2.53(8)
SI3	-0.0682(2)	0.4417(2)	-0.0113(4)	2.53(8)
SI4	0.0606(2)	0.4315(2)	0.1489(4)	2.90(9)
O1	0.0545(4)	0.1765(5)	0.1185(9)	3.0(2)
O2	-0.0718(4)	0.1837(5)	-0.0067(8)	2.5(2)
O3	-0.0666(4)	0.3435(5)	-0.0160(8)	2.6(2)
O4	0.0597(4)	0.3360(5)	0.1153(8)	2.5(2)
O5	-0.0025(4)	0.4796(6)	0.0775(9)	3.2(2)
O6	-0.0162(4)	0.0410(6)	0.0895(9)	3.5(2)
O7	0.0202(4)	0.2552(6)	-0.1360(9)	3.3(2)
O8	-0.2127(5)	0.2687(6)	-0.122(1)	4.2(2)*
O9	-0.1529(5)	0.2702(6)	0.179(1)	4.1(2)*
O10	0.1722(5)	0.2493(6)	-0.007(1)	4.1(2)*
O11	0.1971(5)	0.2480(6)	0.289(1)	4.1(2)*
O12	0.627(1)	0.256(1)	0.231(2)	15.6(8)*
O13	0.482(2)	0.176(3)	0.638(4)	14(1)*
C1	0.0545(6)	0.0764(9)	0.348(1)	3.2(3)

Table V. Positional Parameters and Their Estimated Standard Deviations (cont.)

Atom	x	y	z	B(A2)
C2	0.0434(8)	0.147(1)	0.420(1)	4.5(4)
C3	0.0454(9)	0.144(1)	0.550(2)	6.9(6)
C4	0.0588(8)	0.071(2)	0.619(2)	7.5(6)
C5	0.0682(8)	0.004(1)	0.550(2)	6.8(5)
C6	0.0655(7)	0.004(1)	0.412(2)	5.0(4)
C7	0.1159(7)	0.0211(9)	0.117(1)	3.4(3)
C8	0.1060(8)	-0.0235(9)	-0.002(1)	4.1(4)
C9	0.1558(8)	-0.063(1)	-0.047(2)	5.4(5)
C10	0.2187(7)	-0.054(1)	0.028(2)	5.6(5)
C11	0.2295(7)	-0.010(1)	0.149(2)	4.5(4)
C12	0.1754(7)	0.0253(9)	0.183(2)	4.1(4)
C13	-0.0887(6)	0.0380(8)	-0.170(1)	3.3(3)
C14	-0.0870(6)	0.082(1)	-0.284(1)	4.0(4)
C15	-0.0980(7)	0.043(1)	-0.407(1)	4.6(4)
C16	-0.1032(7)	-0.044(1)	-0.413(2)	5.0(4)
C17	-0.1035(8)	-0.085(1)	-0.303(2)	4.3(4)
C18	-0.0992(7)	-0.051(1)	-0.183(2)	4.3(4)
C19	-0.1498(6)	0.0541(9)	0.068(1)	2.9(3)
C20	-0.1452(7)	0.024(1)	0.201(1)	4.2(4)

Table V. Positional Parameters and Their Estimated Standard Deviations (cont.)

Atom	x	y	z	B(A2)
C21	-0.1986(8)	0.004(1)	0.249(2)	5.7(4)
C22	-0.2612(7)	0.012(1)	0.173(2)	4.6(4)
C23	-0.2657(7)	0.041(1)	0.039(1)	4.1(4)
C24	-0.2109(7)	0.063(1)	-0.006(1)	4.1(4)
C25	-0.1358(6)	0.4781(8)	0.061(1)	2.8(3)
C26	-0.1989(7)	0.473(1)	-0.020(2)	4.8(4)
C27	-0.2512(7)	0.499(1)	0.039(1)	4.1(4)
C28	-0.2438(8)	0.525(1)	0.164(1)	5.3(5)
C29	-0.1819(7)	0.531(1)	0.247(2)	6.0(5)
C30	-0.1297(8)	0.508(1)	0.192(2)	5.0(4)
C31	-0.0757(6)	0.4880(9)	-0.181(1)	2.9(3)
C32	-0.0873(7)	0.5740(9)	-0.195(2)	4.6(4)
C33	-0.0919(8)	0.610(1)	-0.314(2)	5.3(4)
C34	-0.0837(8)	0.564(1)	-0.426(2)	5.9(5)
C35	-0.0767(8)	0.483(1)	-0.414(2)	4.7(4)
C36	-0.0710(7)	0.441(1)	-0.293(1)	4.0(4)
C37	0.1314(6)	0.4851(9)	0.099(1)	3.7(3)
C38	0.1919(6)	0.468(1)	0.169(2)	4.0(4)
C39	0.2459(7)	0.5005(9)	0.122(2)	4.4(4)

Table V. Positional Parameters and Their Estimated Standard Deviations (cont.)

Atom	x	y	z	B(A2)
C40	0.2363(7)	0.542(1)	0.005(1)	4.0(4)
C41	0.1761(8)	0.558(1)	-0.068(2)	5.1(4)
C42	0.1230(7)	0.529(1)	-0.027(2)	4.1(4)
C43	0.0683(6)	0.4455(9)	0.333(1)	3.8(4)
C44	0.0733(7)	0.528(1)	0.383(2)	6.0(4)
C45	0.0795(9)	0.538(1)	0.524(2)	6.8(5)
C46	0.0773(8)	0.468(2)	0.599(2)	8.4(7)
C47	0.071(1)	0.392(2)	0.551(2)	7.9(7)
C48	0.0678(8)	0.383(1)	0.418(2)	5.1(4)
C49	-0.280(1)	0.274(1)	-0.090(2)	6.5(5)*
C50	-0.316(2)	0.300(2)	-0.226(3)	5.5(8)*
C50'	-0.320(2)	0.231(2)	-0.235(4)	5.0(9)*
C51	-0.2856(9)	0.257(1)	-0.318(2)	5.9(4)*
C52	-0.2154(8)	0.261(1)	-0.265(2)	4.6(4)*
C53	-0.095(1)	0.273(1)	0.288(2)	7.7(6)*
C54	-0.116(1)	0.266(1)	0.414(2)	8.5(6)*
C55	-0.213(1)	0.261(1)	0.235(2)	7.7(5)*
C56	-0.187(1)	0.247(1)	0.379(2)	8.3(6)*
C57	0.176(1)	0.175(1)	-0.080(2)	7.3(5)*

Table V. Positional Parameters and Their Estimated Standard Deviations (cont.)

Atom	x	y	z	B(A2)
C58	0.217(1)	0.193(2)	-0.186(3)	10.0(7)*
C59	0.214(1)	0.279(2)	-0.194(3)	9.0(7)*
C60	0.1739(9)	0.314(1)	-0.093(2)	5.5(4)*
C61	0.263(1)	0.249(1)	0.258(2)	7.0(5)*
C62	0.304(1)	0.255(1)	0.394(2)	8.8(6)*
C63	0.269(1)	0.212(1)	0.488(2)	7.2(5)*
C64	0.2013(9)	0.235(1)	0.435(2)	6.2(5)*
C65	0.584(2)	0.273(2)	0.342(4)	15(1)*
C66	0.527(2)	0.214(2)	0.282(4)	14(1)*
C67	0.526(1)	0.222(2)	0.118(3)	11.2(8)*
C68	0.595(2)	0.229(2)	0.101(3)	11.9(9)*
C69	0.463(2)	0.304(3)	0.654(5)	8(1)*
C70	0.428(3)	0.258(3)	0.762(5)	10(1)*
C71	0.444(3)	0.162(4)	0.728(6)	12(2)*
C72	0.497(2)	0.250(3)	0.600(5)	8(1)*
LI1	0.126(1)	0.253(1)	0.140(2)	3.4(5)
LI2	-0.132(1)	0.266(2)	0.003(2)	3.0(5)

Starred atoms were included with isotropic thermal parameters.
The thermal parameter given for anisotropically refined atoms is the isotropic equivalent thermal parameter defined as:
(4/3) * [a2*B(1,1) + b2*B(2,2) + c2*B(3,3) + ab(cos gamma)*B(1,2) + ac(cos beta)*B(1,3) + bc(cos alpha)*B(2,3)]
where a,b,c are real cell parameters, and B(i,j) are anisotropic betas.

Table Va. Table of General Temperature Factor Expressions - B's for $[Li(THF)_2]_2[VO((OSiPh_2)_2O)_2]$

Name	B(1,1)	B(2,2)	B(3,3)	B(1,2)	B(1,3)	B(2,3)	Beqv
V1	1.16(7)	3.5(1)	2.01(7)	0.00(9)	0.34(6)	-0.0(1)	2.21(4)
SI1	1.7(1)	3.8(2)	2.6(2)	0.0(1)	0.1(1)	0.8(2)	2.72(8)
SI2	1.6(1)	3.5(2)	2.4(2)	-0.1(1)	-0.0(1)	0.6(2)	2.53(8)
SI3	1.6(1)	3.3(2)	2.6(2)	0.1(1)	0.1(1)	0.1(2)	2.53(8)
SI4	2.2(1)	2.9(2)	3.6(2)	-0.1(1)	0.3(1)	-0.6(2)	2.90(9)
O1	2.2(4)	2.6(4)	4.4(5)	0.1(3)	0.6(3)	-0.3(4)	3.0(2)
O2	1.7(3)	3.4(4)	2.3(4)	-0.0(4)	-0.1(3)	0.5(4)	2.5(2)
O3	1.5(3)	3.8(4)	2.4(4)	0.1(3)	-0.0(3)	0.4(4)	2.6(2)
O4	1.9(3)	3.3(4)	2.2(4)	-0.1(3)	-0.0(3)	-0.3(3)	2.5(2)
O5	2.4(4)	4.2(4)	2.9(4)	0.6(4)	0.3(3)	-0.2(4)	3.2(2)
O6	2.6(4)	3.8(4)	3.8(5)	-1.0(4)	-0.0(4)	0.5(4)	3.5(2)
O7	2.2(4)	4.7(5)	2.8(4)	-0.2(4)	-0.2(3)	0.3(4)	3.3(2)
C1	2.0(5)	4.9(8)	3.1(6)	-0.3(5)	0.9(5)	1.1(6)	3.2(3)
C2	4.2(7)	6.6(9)	2.5(7)	-1.5(7)	0.5(6)	-0.7(7)	4.5(4)
C3	4.3(8)	9(1)	8(1)	-2.4(8)	1.1(8)	-0(1)	6.9(6)
C4	2.9(7)	14(2)	5.2(9)	-1(1)	0.6(7)	-1(1)	7.5(6)
C5	3.1(7)	10(1)	7(1)	-1.2(8)	1.1(7)	4.3(9)	6.8(5)
C6	1.7(6)	9(1)	4.0(7)	0.1(7)	0.2(5)	3.0(7)	5.0(4)
C7	2.8(6)	3.3(7)	4.1(7)	0.3(5)	0.9(5)	2.4(5)	3.4(3)

Table Va. Table of General Temperature Factor Expressions - B's (cont.)

Name	B(1,1)	B(2,2)	B(3,3)	B(1,2)	B(1,3)	B(2,3)	Beqv
C8	5.7(9)	4.3(7)	1.7(6)	-1.5(7)	-1.1(6)	Ø.4(6)	4.1(4)
C9	4.2(7)	7(1)	5.8(9)	-Ø.3(8)	1.6(7)	-1.3(8)	5.4(5)
C1Ø	3.3(7)	7(1)	6.7(9)	Ø.8(7)	2.3(6)	1.7(8)	5.6(5)
C11	3.5(6)	4.6(8)	5.6(8)	1.1(6)	1.6(6)	Ø.7(7)	4.5(4)
C12	3.9(7)	3.Ø(7)	5.5(8)	Ø.4(6)	1.5(6)	Ø.4(6)	4.1(4)
C13	1.5(5)	3.1(6)	5.7(7)	Ø.7(5)	2.Ø(4)	1.2(6)	3.3(3)
C14	2.Ø(6)	7.Ø(9)	2.9(7)	Ø.5(6)	Ø.2(5)	Ø.1(7)	4.Ø(4)
C15	3.4(7)	8(1)	2.8(7)	Ø.5(7)	Ø.5(6)	-Ø.6(7)	4.6(4)
C16	3.1(7)	8(1)	3.8(8)	1.5(7)	-Ø.8(6)	-2.Ø(7)	5.Ø(4)
C17	4.4(7)	4.9(8)	3.2(7)	1.6(7)	-Ø.3(6)	-Ø.8(6)	4.3(4)
C18	3.1(7)	6.4(9)	3.2(7)	Ø.4(7)	Ø.1(6)	-Ø.9(7)	4.3(4)
C19	2.6(6)	4.7(7)	1.3(5)	-1.2(6)	-Ø.4(5)	Ø.2(5)	2.9(3)
C2Ø	3.7(7)	5.9(9)	2.8(7)	-Ø.6(7)	Ø.2(6)	Ø.Ø(7)	4.2(4)
C21	5.8(8)	7(1)	5.Ø(7)	Ø.3(8)	3.5(6)	2.4(7)	5.7(4)
C22	3.6(7)	4.7(8)	5.6(8)	Ø.4(6)	1.3(6)	-Ø.5(7)	4.6(4)
C23	2.2(6)	6.8(9)	3.2(7)	-1.6(6)	Ø.1(5)	Ø.3(7)	4.1(4)
C24	3.1(6)	6.6(9)	2.8(7)	Ø.2(7)	Ø.8(5)	-Ø.1(7)	4.1(4)
C25	2.1(5)	2.6(6)	3.9(6)	-Ø.5(5)	1.Ø(5)	-1.6(5)	2.8(3)
C26	1.5(6)	5.5(9)	7(1)	Ø.1(6)	-Ø.3(6)	1.4(8)	4.8(4)

Table Va. Table of General Temperature Factor Expressions - B's (cont.)

Name	B(1,1)	B(2,2)	B(3,3)	B(1,2)	B(1,3)	B(2,3)	Beqv
C27	2.2(6)	6.7(9)	3.2(7)	1.5(6)	-0.3(5)	0.7(7)	4.1(4)
C28	4.2(7)	9(1)	2.7(7)	1.1(8)	0.3(6)	0.2(8)	5.3(5)
C29	2.5(7)	12(1)	3.7(8)	-0.1(8)	0.9(6)	-1.5(9)	6.0(5)
C30	3.7(7)	8(1)	3.7(8)	1.0(7)	0.2(6)	-0.8(8)	5.0(4)
C31	1.6(5)	5.1(7)	1.8(6)	-0.8(5)	-0.1(5)	-0.4(6)	2.9(3)
C32	4.3(7)	3.9(7)	5.6(8)	-0.7(6)	1.2(6)	2.5(6)	4.6(4)
C33	4.9(8)	5.4(9)	4.9(8)	-1.4(7)	-1.1(7)	2.1(7)	5.3(4)
C34	3.8(7)	8(1)	5.7(9)	-0.3(8)	0.4(7)	1.4(9)	5.9(5)
C35	3.2(7)	6.9(9)	3.4(7)	-0.6(7)	-0.6(6)	1.5(7)	4.7(4)
C36	2.6(6)	7.1(9)	2.4(6)	-1.1(6)	0.7(5)	0.6(6)	4.0(4)
C37	2.8(6)	4.2(7)	4.5(7)	-1.6(6)	1.4(5)	-2.4(6)	3.7(3)
C38	1.4(5)	5.5(8)	5.0(8)	-0.8(6)	0.2(5)	-2.7(6)	4.0(4)
C39	4.3(7)	3.8(8)	5.8(8)	-1.1(6)	2.4(6)	-1.8(7)	4.4(4)
C40	3.4(7)	4.8(8)	3.9(7)	-0.3(6)	0.7(6)	-1.1(6)	4.0(4)
C41	4.9(8)	4.6(9)	6.0(9)	0.3(7)	1.4(7)	-0.9(7)	5.1(4)
C42	2.7(6)	5.4(8)	4.3(7)	-0.4(6)	1.3(5)	-0.0(7)	4.1(4)
C43	2.4(6)	4.2(7)	4.9(7)	0.0(6)	1.1(5)	-1.8(6)	3.8(4)
C44	4.9(7)	7(1)	7.9(8)	-0.6(7)	4.6(5)	-3.4(7)	6.0(4)
C45	5.6(9)	9(1)	6.5(9)	-0.9(9)	1.9(7)	-4.6(8)	6.8(5)
C46	2.4(7)	18(2)	4.4(9)	1(1)	0.6(7)	-1(1)	8.4(7)
C47	6(1)	12(2)	5(1)	0(1)	0.4(9)	-0(1)	7.9(7)
C48	5.7(9)	7(1)	2.2(7)	1.4(8)	0.4(6)	1.2(7)	5.1(4)
L11	3(1)	2(1)	4(1)	0.3(9)	0.3(9)	-0(1)	3.4(5)
L12	2.5(9)	5(1)	1.8(8)	-0.8(9)	0.5(7)	-0.0(9)	3.0(5)

The form of the anisotropic temperature factor is:
exp[-0.25(h2a2B(1,1) + k2b2B(2,2) + l2c2B(3,3) + 2hkabB(1,2) + 2hlacB(1,3) + 2klbcB(2,3))] where a,b, and c are reciprocal lattice constants.

LAWRENCE BERKELEY LABORATORY
TECHNICAL INFORMATION DEPARTMENT
UNIVERSITY OF CALIFORNIA
BERKELEY, CALIFORNIA 94720